Aus der Arbeitsgruppe Antigenpräsentation & T/NK-Zell-Aktivierung
Klinische Kooperationseinheit Angewandte Tumorimmunität
(Leiter: Prof. Dr. med. Dirk Jäger)
Deutsches Krebsforschungszentrum
(Wissenschaftlicher Vorstand: Prof. Dr. med. Michael Baumann)

Use of bispecific antibodies to improve transendothelial migration of T cells towards tumor cells

Inauguraldissertation
zur Erlangung des Doctor scientiarum humanarum (Dr. sc. hum.)
an der Medizinischen Fakultät Heidelberg der
Ruprecht-Karls-Universität

vorgelegt von
Márcia Figueiredo Gonçalves, M.Sc.
aus
Quiaios, Portugal

2021

Dekan: Prof. Dr. med. Hans-Georg Kräusslich

Doktorvater: Priv. Doz. Dr. med. Frank Momburg

To all cancer fighters

To my family

TABLE OF CONTENTS

ABBREVIATIONS

AMP	Ampicillin
ANG	Angiopoietin
anti- / α-	Monoclonal mAb specific for ("anti") an indicated antigen
APC	Antigen presenting cells
- APC	Conjugated to allophycocyanin
BiMAb	Bispecific monoclonal antibody
BSA	Bovine serum albumin
°C	Degree Celsius
CAR	Chimeric antigen receptor
CCL	C-C motif chemokine ligand
CCR	C-C motif chemokine receptor
CD	Cluster of differentiation
cDNA	Complementary DNA
CH	Constant heavy chain domain
CHO	Chinese hamster ovary cells
CHO-S	CHO cells growing in suspension
CLA	cutaneous lymphocyte-associated antigen
CLEVER	vascular endothelial receptor
CSC	cancer stem cells
CTL	Cytotoxic T cell
CTLA-4	Cytotoxic T lymphocyte-associated protein 4
CXCR	C-X-C motif chemokine receptor
Da / kDa	Dalton / kilo dalton
DC	Dendritic cell
ddH_2O	Double distilled laboratory-grade water
DKFZ	German Cancer Research Center, Heidelberg
DMSO	Dimethylsulfoxid
DNA	Deoxyribonucleic acid
DPBS	Dulbecco's phosphate-buffered saline
DTT	Dithiothreitol
EC	Endothelial cells
EDTA	Ethylenediaminetetraacetic
ELISA	Enzyme-linked immunosorbent assay
EPC	Endothelial progenitor cells
FACS	Fluorescence activated cell sorting
FBS / FCS	Fetal bovine serum / calf serum
Fc	Fragment crystallizable
Fig.	Figure
g / mg / µg / ng	gram / milligram / microgram / nanogram
gMFI	geometric mean fluorescence intensity
GPCR	G protein-coupled receptor
Gy	Gray (1 Gy = 1 Joule / kg)
Gzm B	Granzyme B
h	Hour
HBMEC-60	human immortalized bone marrow endothelial cells
HC	Heavy chain
HEK	Human embryonic kidney cells
HGF	Hepatocyte growth factor
HIF1	Hypoxia inducible factor 1
HLA	Human leucocyte antigen
HRP	Horseradish peroxidase
HT	Hypoxanthine and thymidine
HUVEC	human umbilical vein endothelial cells
IA	Intussusceptive angiogenesis
ICAM1	Intercellular Adhesion Molecule 1
ICB	Immune checkpoint blocking therapy
ICI	Immune checkpoint inhibitor
IFN	Interferon
Ig / IgG	Immunoglobulin G
Ii	Invariant chain (CD74)
IKK	Inhibitor of κB kinase
IL	Interleukin
ITIM	Immune receptor tyrosine-based inhibitory motifs
KDR	Kinase insert domain receptor
L / mL / µL	Liter / milliliter / microliter
LAG-3	Lymphocyte activation gene-3
LC	Light chain
LDS	Lithium dodecyl sulphate
LFA-1	Lymphocyte function associated antigen 1
LPLC	Low-pressure liquid chromatography
LPS	Lipopolysaccharide
M / mM / µM	Molar / millimolar / micromolar
m / nm	Meter / nanometer
mAb	Monoclonal antibody
MACS	Magnet activated cell sorting
MadCAM1	Vascular Addressin Cell Adhesion Molecule 1
MCF-7	Michigan Cancer Foundation-7, breast cancer cell line
MDSC	Myeloid-derived suppressor cells
MFI	Median fluorescent intensity
MHC-I / -II	Major histocompatibility complex class I / II
min	Minute
MMP	Matrix metalloproteinase
MW	Molecular weight
NF-κB	nuclear factor kappa-light-chain-enhancer of activated B cells
NK	Natural killer cells
NO	Nitric oxide
NRPs	Neuropilins
PAMP	pathogen-associated molecular pattern
PBL	peripheral blood lymphocytes
PBMC	Peripheral blood mononuclear cells

PBS	Phosphate buffered saline
PD-1	Programmed cell death protein-1
PD-L1	PD-ligand 1
PDGF	Platelet-derived growth factor
PDGFR	Platelet-derived growth factor receptor
PE	Phycoerythrin
PECAM1	Platelet endothelial cell adhesion molecule 1
PEI	Polyethyleneimine
PHD1-3	Prolyl hydroxylase domain proteins 1-3
PlGF	Placenta growth factor
PNAd	Peripheral node addressin
PSGL-1	P- selectin glycoprotein ligand-1
Ref.	Reference
RNA	Ribonucleic acid
rpm	Rounds per minute
RPMI-60	Roswell Park Memorial Institute
RT	Room temperature (i.e., 21–24°C)
SA	Sprouting angiogenesis
SAv	Streptavidin
scFv	Single-chain variable fragment
SDS-PAGE	Sodium dodecyl sulfate–polyacrylamide gel electrophoresis
TAA	Tumor-associated antigens
TAMs	Tumor-associated macrophages
TCR	T cell receptor
TGE	Transient gene expression
TGF-β	Transforming growth factor beta
Th	T helper cell
TIE	Tyrosine Kinase with Immunoglobulin Like And EGF Like Domains
TIGIT	T cell immunoreceptor with immunoglobulin and ITIM domains
TIL	Tumor infiltrating lymphocytes
TIM3	T cell immunoglobulin and mucin domain-containing protein3
TKIs	Tyrosine kinase inhibitors
TMB	3,3',5,5'-Tetramethylbenzidine
TME	Tumor microenvironment
TNF	Tumor necrosis factor
TNFR	Tumor necrosis factor receptor
Treg	T regulatory cell
v/v	Volume/volume
VCAM1	Vascular cell adhesion molecule 1
VEGF	Vascular endothelial growth factors
VEGFR	Vascular endothelial growth factor receptor
VLA-4	Very late antigen 4
VPA	Valproic acid sodium salt
w/v	Weight/volume
WPBs	Weibel-Palade bodie

LIST OF FIGURES

LIST OF TABLES

1 INTRODUCTION

The interaction between tumor cells and the surrounding microenvironment is recognized as a key player in the development and progression of cancer. The tumor microenvironment includes blood vessels, lymphatic vasculature, stroma, and resident immune cells or recruited from the periphery, and each of them has an essential role in tumor regulation.

1.1 THE CANCER IMMUNITY CYCLE

Although cancerous and infectious diseases are entirely distinct, significant aspects such as the immune response and features of terminal events during disease progression are highly analogous following the (cancer) immunity cycle steps demonstrated in **Fig. 1.1** (Rolston 2017).

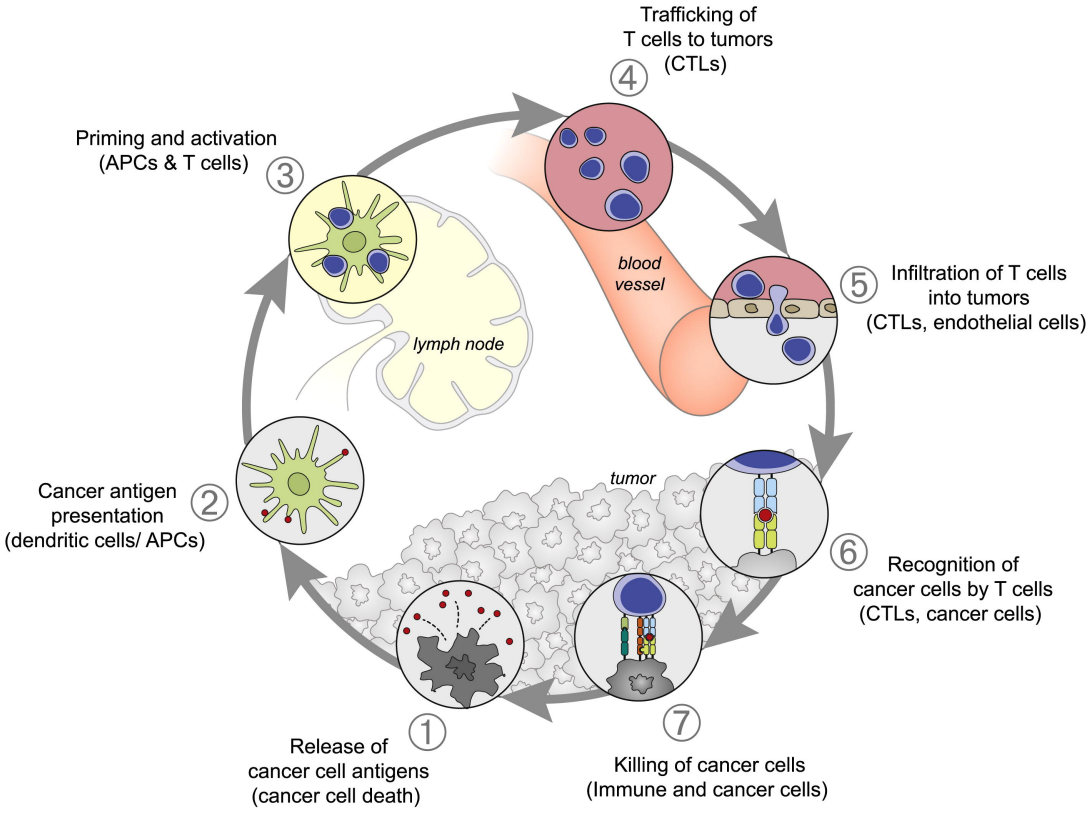

Figure 1.1 Stimulatory and inhibitory factors in the cancer-immunity cycle. The cycle starts with the release of antigens from the cancer cells and ends with the killing of cancer cells described in the following sections. Figure from Chen and Mellman 2013.

1.1.1 Release of neoantigens and uptake (1 & 2)

For the anti-tumor immune response to be effective in killing cancer cells, a series of stepwise events must be initiated and allowed to progress and expand successively.

Like pathogen-associated molecular pattern (PAMPs) on infectious agents such as bacteria, also cancerous tissue provides contact points for the immune system, i.e., via genetic and cellular alterations upon transformation.

Accordingly, the cancer immunity cycle (**Fig. 1.1**) is initiated by the release of tumor antigens as a result of immunogenic tumor cell death. Tumor-specific antigens comprise cancer-testis antigens or tumor neoantigens derived from mutations (Lim et al. 2018). Released tumor antigens are then captured, processed, and presented by antigen-presenting cells (APCs) belonging to the innate immunity, such as dendritic cells (DCs) or macrophages which reside in the tumor microenvironment (Step 2). Subsequently, the phagocytes traffic to the draining lymph node where additionally soluble tumor antigens arrive.

1.1.2 T cell priming, activation and differentiation (3)

Effective priming and activation of T cells (Step 3) with specificity against the initially released tumor antigen requires three major signals (Eggermont et al. 2014) as shown in **Fig. 1.2.**

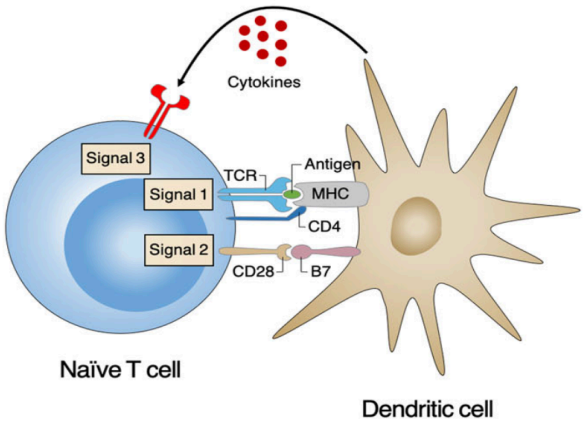

Figure 1.2 Antigen-specific T cell activation. The first signal is antigen-specific and mediated by T cell receptor (TCR) recognition of peptides presented by major histocompatibility complex (MHC) molecules. Signal 1 together with signal 2 delivered by co-stimulatory and/or co-inhibitory receptors as well cytokine receptor-derived signals (signal 3) converge into the decision of T cell activation associated with the induction of T cell proliferation, differentiation, and effector functions. Figure adapted from Lee et al. 2020.

1.1.2.1 T cell priming/activation – signal 1

In the lymph nodes, T cell priming is initiated by presentation of the processed tumor antigens via major histocompatibility complex I and II (MHC I and MHC II) on APCs with the matching T cell receptor (TCR) on the T cells, which confers specificity to the adaptive response (Chen and Mellman 2013). Upon non-covalent binding of the TCRαβ heterodimer to CD3 complex components (including CD3γ, CD3δ, CD3ε and, CD3ζ) and initiation of a kinase-mediated signaling cascade, the activating signal is transmitted from the cell membrane to the nucleus triggering downstream events (Dong et al. 2019).

Depending on the original source of the antigen, two classical antigen-presentation pathways can be distinguished. Cytosolic proteins are primarily presented by MHC-I molecules to $CD8^+$ T cells, whereas MHC-II molecules are destined to present exogenous antigens to $CD4^+$ T cells, which have been internalized by professional APC (Blum et al. 2013; Roche and Furuta 2015). Exceptionally, exogenous antigens can also be presented by MHC-I molecules – a process called cross-presentation (Kurts et al. 2010) – as well as cytosolic antigens via autophagy-related mechanisms presented by MHC-II molecules (Crotzer and Blum 2010).

1.1.2.2 T cell co-stimulation/co-inhibition – signal 2

The second signal, summed up in **Fig. 1.3**, is highly regulated by co-ligation of co-stimulatory receptors and co-inhibitory immune checkpoint molecules on T cells and APCs (Chen and Mellman 2013).

The interaction of CD28 homodimer with its ligands B7-1 (CD80) or B7-2 (CD86) on APCs is one of the most studied co-stimulatory signaling events (Boomer and Green 2010), resulting in an increased T cell survival and proliferation capacity, which is mediated mostly due to increased IL-2 expression. Other molecules belonging to the tumor necrosis factor receptor (TNFR) family, such as OX40 (CD134) or 4-1BB (CD137), also provide co-stimulation upon engagement with their ligands OX40L and 4-1BBL, respectively. However, unlike CD28, which is constitutively expressed by most resting T cells, OX40 and 4-1BB are up-regulated after initial T cell activation (Chen and Flies 2013; Ward-Kavanagh et al. 2016).

Besides co-stimulatory molecules also multiple inhibitory molecules have been described, which play an essential role in dampening an immune response and preventing autoimmune disorders. However, during cancer progression, T cell-inhibitory receptors, hereafter referred to as “checkpoints”, represent a major hurdle for an effective immune response against malignant cells. The most prominent inhibitory molecules are CTLA-4/CD154 (cytotoxic T lymphocyte-associated protein 4) and PD-1 (programmed cell death protein-1). CTLA-4 is

generally up-regulated upon T cell activation as well as constantly expressed by so-called $CD4^+$ T regulatory cells and competes with higher affinity with the co-stimulatory receptor CD28 for binding to the same ligands B7-1 (CD80) and B7-2 (CD86). PD-1 in contrast is considered to be induced in T cells upon chronic antigen stimulation and reduced $CD4^+$ T cell-mediated help. PD-1 binds to its ligand PD-L1 (PD-ligand 1/B7-H1/CD274) as well as PD-L2 (B7-H2/CD273), which are expressed by activated T cells and are up-regulated in peripheral tissues upon exposure to inflammatory cytokines such as IFN-γ.

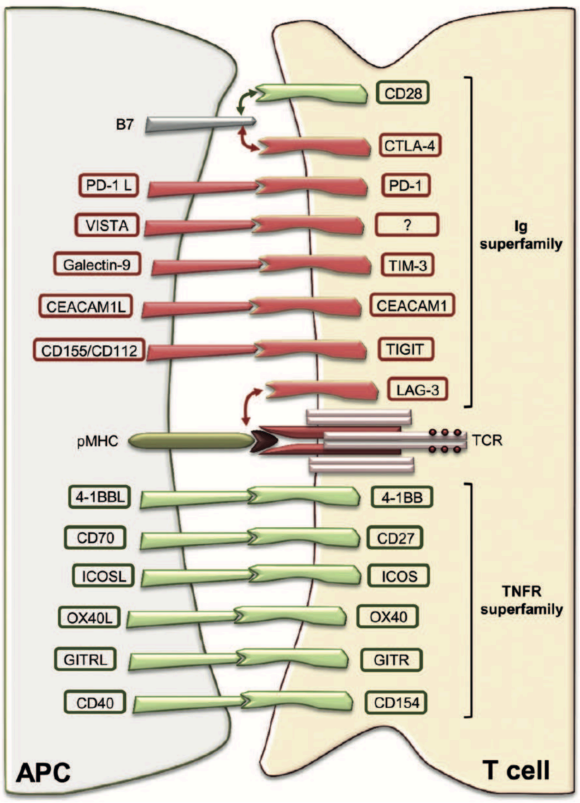

Figure 1.3 Co-regulation of immune synapse. Inhibitory (red) and stimulatory (green) interactions between APC and T cell during immune synapse formation. Adapted from Finetti and Baldari 2018.

1.1.2.3 Inflammatory cytokines – signal 3

The third signal is provided by pro- or anti-inflammatory cytokines that drive T cell differentiation and contribute to T cell survival and proliferation (Curtsinger and Mescher 2010).

Particularly for naïve $CD8^+$ T cells it has been described that the presence of IL-12 and type I interferons is required to initiate full $CD8^+$ T cell differentiation into polyfunctional cytotoxic $CD8^+$ T cells (CTL). Both IL-12 and type I interferons are provided by mature DC or by CD40-dependent interaction with $CD4^+$ T helper cells (Curtsinger and Mescher 2010). Moreover, the cytokine environment at the time of antigen-encounter plays a pivotal role in determining the effector function of naïve $CD4^+$ T cell populations.

1.1.2.4 T cell differentiation

CD4⁺ T cells

CD4⁺ T cells play a versatile and essential role in shaping adaptive and local innate immune responses through their secretion of defined sets of cytokines as well as by cell-cell contacts providing stimulatory or inhibitory signals for the interacting partner cell. Upon priming and activation, naïve CD4⁺ T cells differentiate into specific effector subtypes depending on the cytokines present in the microenvironment as well as specific transcription factors (Zhu et al. 2010) as described in **Fig. 1.4**.

Every CD4⁺ T cells subtype plays a particular role in the clearance of pathogens, maintaining tolerance against "self" and eradication of malignant cells. Briefly, IFN-γ secreted by Th1 cells triggers immune responses against intracellular pathogens as well as tumor cells; Th2 cells are strong mediators of immune responses against extracellular parasites, including helminths, and are involved in allergy/asthma/IgE responses against through IL-4, IL-5 and IL-13; Th17 cell-produced IL-17A, IL-17F and IL-22 recruit and activate neutrophils during immune responses against extracellular bacteria and fungi; iT_{reg} are responsible for maintaining self-tolerance as well as regulating/suppressing immune responses by IL-10 and TGF-β production (Jiang and Dong 2013). In addition also direct cytolytic activity of CD4⁺ T helper cells has been observed in certain tumor contexts that might contribute to tumor control (Borst et al. 2018; Kreiter et al. 2015; Quezada et al. 2010).

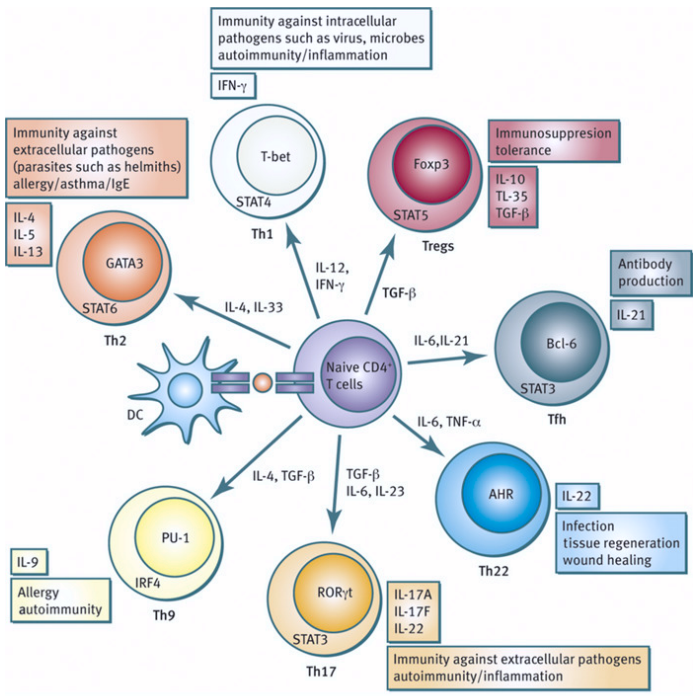

Figure 1.4 CD4⁺ T cell subsets. Naive CD4⁺T cells differentiate into Th1, Th2, Th9, Th17, Th22, follicular T-helper (Tfh) cells, and CD4⁺ regulatory T cells (Treg) after antigen-specific stimulation by (DCs) under environmental cytokines. These CD4⁺ T cell subsets produce distinct sets of cytokines that contribute to adaptive immunity, including the clearance of pathogens, control of autoimmunity, immune homeostasis, and immune responses again tumors. Figure from Jiang and Dong 2013.

$CD8^+$ T cells

The successful priming of naïve $CD8^+$ T cells within secondary lymphoid organs is accompanied by profound changes in their migration capacity, overall gene expression profile and metabolism, which leads to the acquisition of effector functions (Farber et al. 2014; Halle et al. 2017; Zhang and Bevan 2011). Unlike $CD4^+$ T cells, antigen-experienced $CD8^+$ T cells are typically not subdivided into subsets that fulfill completely distinct functions and are usually considered as cytotoxic T cells (CTL).

A key effector function of CTL is the antigen-dependent and cell-to-cell contact-mediated cytolysis of most notably virus-infected and malignant cells that display the cognate peptide antigen on MHC-I. CTLs that encounter their target cell may start the production and secretion of soluble cytokines including IFN-γ, TNF-α and IL-2 (Zhang and Bevan 2011).

1.1.2.5 Phenotype of activated T cells

Upon T cell activation, numerous cell surface markers are induced or up-regulated, each at a different stage during the activation process. These molecules include receptor proteins, co-stimulatory molecules, adhesion molecules, chemokine receptors, and MHC class II molecules (**Fig. 1.5**).

Examples of up-regulated receptor proteins observed on proliferating lymphocytes include CD25 (interleukin-2 receptor) and CD69. The earliest activation marker is CD69, an inducible cell surface glycoprotein expressed upon activation via the TCR or the IL-2 receptor (CD25), and plays a role in the proliferation and survival of activated T lymphocytes (Cambiaggi et al. 1992; López-Cabrera et al. 1993). Its expression increases in a time-dependent way between 3-12 hours, remaining elevated until 24 hours and diminishing thereafter (Reddy et al. 2004).

CD25 is the alpha chain of the trimeric IL-2 receptor and the most prominent cellular activation marker. Regulatory and resting memory T cells constitutively express CD25. After 24 hours of the TCR/CD3 complex stimulation, IL-2 receptor is up-regulated and remains elevated for a few days (Jackson et al. 1990; Reddy et al. 2004). It plays a key role in lymphocyte activation and further IL-2 production which is vital for T cell survival, expansion, and function.

Co-stimulatory molecules can either belong to the immunoglobulin G (IgG) superfamily, the tumor necrosis factor–tumor necrosis factor receptor (TNF–TNFR) family, or the TIM (type 1 transmembrane glycoprotein) family (**Fig. 1.3**). CD28 belongs to the IgG superfamily and is constitutively expressed on naïve and activated T cells. Other molecules such as OX40 (CD134) or 4-1BB (CD137) belong to the tumor necrosis factor receptor (TNFR) family and

are up-regulated only after initial T cell activation (Chen and Flies 2013; Ward-Kavanagh et al. 2016).

During T cell exhaustion a variety of inhibitory receptors are up-regulated, like CTLA-4, PD-1, lymphocyte activation gene 3 protein (LAG-3), T cell immunoreceptor with immunoglobulin and ITIM domains (TIGIT), T cell immunoglobulin and mucin domain-containing protein 3 (TIM3) suppressing T cell effector function (Manieri et al. 2017; Wherry 2011).

Adhesion molecules like selectins ligands and integrins are also up-regulated in activated T cells mediating the extraversion of alloreactive T cells from the lymph nodes into the inflamed tissue (see section 1.1.3). The selectin ligand P-selectin glycoprotein ligand-1 (PSGL-1) is a glycoprotein that binds to P-selectin (platelets) or to E-selectin (endothelial cells) (Kappelmayer and Nagy 2017). The integrin family include lymphocyte function-associated antigen 1 (LFA-1, αLβ2, CD11a/CD18) that binds to the intercellular adhesion molecule family (ICAM1,-2,-3,-4,-5), and the very late antigen 4 (VLA-4, α4β1, CD49d/CD29) a ligand for endothelial vascular cell adhesion molecule 1 (VCAM1) (Harjunpää et al. 2019).

The chemokine superfamily constitutes a group of structurally related cytokines that play pivotal roles in inflammatory and immunological responses by recruiting selective types of leukocytes. Chemokine receptors, such as CXCR3 and CCR5, are strongly up-regulated in activated T cells (Groom and Luster 2011; Liu et al. 2005; Tan and Zhou 2005). MHC class II molecules expressed on activated T cells include all isotypes (HLA-DR, HLA-DQ, and HLA-DP) and are up-regulated only after 3–5 days (Holling et al. 2004).

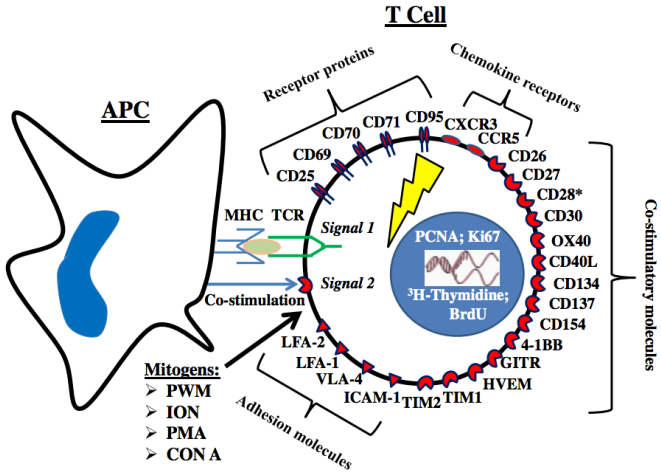

Figure 1.5 T cell activation and proliferation markers. Upon T cell activation different receptor proteins, chemokine receptors, co-stimulatory molecules and adhesion molecules are up-regulated (*constitutively expressed). Figure from Shipkova and Wieland 2012.

1.1.3 T cell trafficking and transendothelial migration (4 & 5)

Once tumor-reactive T cells of the adaptive immunity are efficiently primed and activated, they traffic towards the tumor site (Step 4) as a result of recruitment via inflammatory chemokines (Slaney et al. 2014).

Activated T cells infiltrate the tumor bed by passing its vascular endothelium via transendothelial migration (Step 5). Migration of leukocytes like effector T cells from the blood circulation into the periphery represents one of the most important critical steps of anti-tumor immunity which requires sequential interactions between homing receptors on the immune cell that are up-regulated during effector differentiation in the lymph node, and matching ligands on vascular endothelial cells (**Fig. 1.6.**).

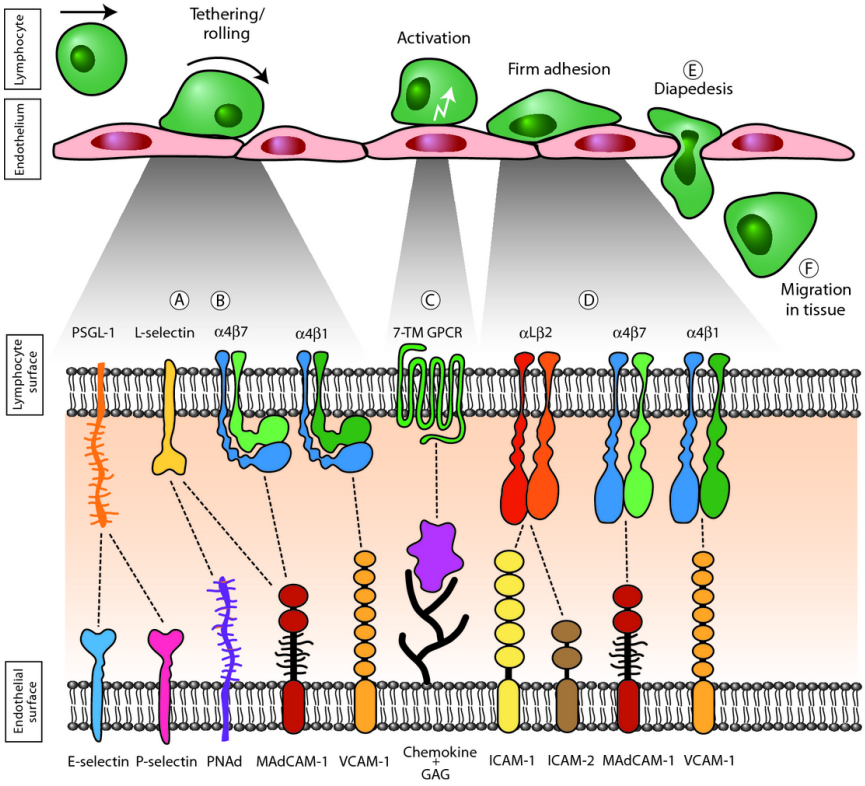

Figure 1.6 Transendothelial Migration a multistep cascade. Tissue-specific homing involves a multistep adhesion cascade between vascular endothelium and effector leukocytes on the luminal surface of the endothelial cells. (A, B) Upon correct initial loose interactions/'tethering', involving PSGL-1, L-selectin and α4 integrins on the lymphocytes with E- and P-selectin, PNAd, MAdCAM1 and VCAM1 on the endothelial cells, the lymphocyte is slowed down, and rolls along the endothelium. (C) The chemokine receptors of the rolling lymphocyte bind chemokines on the endothelium and intracellular signal cascades trigger conformational change in the β2 and/or α4 integrins on lymphocytes (D) which induces strong binding of respective endothelial receptors (ICAM1, ICAM2, VCAM1 and MAdCAM1). Consequently, firm adhesion and arrest of the lymphocyte occurs. (E) The lymphocyte undergoes diapedesis and (F) the migrating cell uses integrins to adhere to various extracellular matrix molecules (i.e. collagen fibers, laminin and fibronectin) as well as is guided by chemoattractants for further tissue localization. Figure from Marsal and Agace 2012.

Initial transient adhesion includes engagement and slow rolling of leukocytes on the apical surface of the vascular endothelium (A & B), followed by chemokine-mediated activation and high affinity conformation of integrins (C) on the endothelium which in turn leads to firm adhesion (D), diapedesis through the blood vessel wall (E) and migration into the underlying tissue (F) (Marsal and Agace 2012).

Up-regulation of individual homing receptors on effector $CD8^+$ T cells depends on the properties of the priming DC, as well as the location and stromal composition of the respective lymph node. Both in turn are subject to their local environment from which three major effector CD8 T cell populations can be generated expressing tissue-specific markers involved in the initiation of slow rolling, as shown on **Table 1.1** (Masopust and Schenkel 2013). For example, T cells activated by gut-associated DC or within gut-associated lymph nodes, express α4β7 integrin and the chemokine receptor CCR9, whereas T cells primed within skin-associated lymph nodes up-regulate E-selectin ligand (ESL), P-selectin ligand (PSL) and CCR10. Further, T cells activated in mediastinal lymph nodes or spleen express α4β1 without ESL or α4β7 co-expression and another subpopulation of CD8 T cells up-regulates homing receptors independently from the site of priming (Ferguson and Engelhard 2010; Peske et al. 2015b). By contrast, broad expression of chemokine receptors permits sensing and characterization of different inflammation-induced chemokines for further immobilization and tissue infiltration.

Expression of matching vascular ligands is similarly variable and depends on localization and inflammatory status of the underlying tissue thereby allowing tissue-selective T cell trafficking. For instance, expression of E- and P-selectin on skin vasculature facilitates slow rolling via ESL^+ and PSL^+ effector leukocytes and respective protein expression is enhanced by various inflammatory stimuli such as proinflammatory cytokines (IL-1β, TNF-α, IFN-γ) lipopolysaccharide (LPS), thrombin or irradiation (Brinkman et al. 2013; Zarbock et al. 2011).

Furthermore, chemokines secreted by endothelial cells induce selective T cell adhesion and are up-regulated upon inflammation in multiple different tissues. CXCL9, 10 and 11, ligands for CXCR3, are induced by IFN-γ, whereas ligands for CCR5 (CCL3, 4 and 5) are produced upon virus and bacterial endotoxin response (Tsai et al. 2013) MAdCAM-1, the major ligand for $\alpha4\beta7$ on the endothelium, is constitutively expressed at low levels on gut-associated tissue also enhanced by proinflammatory cytokines. Initial low affinity $\alpha4\beta7$-MAdCAM-1 interaction induces slow rolling of leukocytes, while subsequent CCR9-CCL25 engagement triggers high affinity $\alpha4\beta7$ or LFA-1 conformation for firm adhesion (Chen et al. 2003).

Additional vascular ligands like VCAM1 are expressed in a more ubiquitous manner among different tissues which promote T cell transmigration into various inflammatory sites. α4β1-

VCAM1 interaction facilitates T cell trafficking into brain and lung but also skin and gut. Additionally, α4β1-VCAM1 binding does not only support slow-rolling but also firm adhesion without need of chemokine-induced activation (Kenyon et al. 2009).

Table 1.1 Overview of molecules involved in TEM of different immune cell subtypes.

Adapted from Wettschureck et al. 2019.

CLA, cutaneous lymphocyte-associated antigen; ICAM1, intercellular adhesion molecule 1; MAdCAM 1, mucosal addressin cell adhesion molecule 1; PECAM-1, platelet endothelial cell adhesion molecule; PLN, peripheral lymph node; PNAd, peripheral node addressin; PP/MLN, Peyer's patches/mesenteric lymph nodes; PSGL-1, P- selectin glycoprotein ligand-1; VCAM1, vascular cell adhesion molecule 1.

Cell type	Region	Capture & rolling		Integrin activation		Arrest/firm adhesion	
		Leukocyte	Endothelium	Leukocyte	Endothelium	Leukocyte	Endothelium
Homeostatic trafficking							
Naive T cells	PLN	L-Selectin	PNAd	CCR7	CCL21, CCL19	αLβ2 (LFA-1)	ICAM-1
	PP/MLN	L-Selectin α4β7	MAdCAM-1 MAdCAM-1	CCR7	CCL21, CCL19	αLβ2 (LFA-1) α4β7	ICAM-1 MAdCAM-1
Inflammatory trafficking							
All leukocytes	All	PSGL1	P-Selectin			αLβ2 (LFA-1)	ICAM-1
Effector T cells	Gut	α4β7	MAdCAM-1	CCR9	CCL25	α4β7	MAdCAM-1
	Skin	CLA, CD43	E-selectin	CCR4, CCR10	CCL17, CCL27	α4β1 (VLA-4)	VCAM-1
Monocyte	All	α4β1 (VLA-4)	VCAM1	CCR2	CCL2, CCL7	αMβ2 (Mac-1) α4β1 (VLA-4)	ICAM-1/-2 VCAM-1
Neutrophils	All	ESL-1, CD44	E-selectin	CXCR2	CXCL1, CXCL2	αMβ2 (Mac-1)	ICAM-1/-2

1.1.4 Cancer recognition and elimination (6 & 7)

At the tumor site, tumor cell death is elicited by cytotoxic tumor-reactive CD8 T cells (CTLs) upon formation of an immunological synapse between tumor and tumor-reactive T cell (Step 6 + 7) (Dustin and Long 2010). CTL cytotoxicity is driven by secretion of death-inducing effector molecules such as granzyme B, perforin and Fas ligand (FasL) as well as the release of pro-inflammatory cytokines like interferon-γ (IFN-γ) or tumor necrosis factor- α (TNF-α). In addition, tumor-reactive CD4 T cells secrete stimulatory cytokines via tumor antigen recognition on APCs (Halle et al. 2017). Final cancer cell killing releases additional tumor-associated antigens which enhance breadth and depth of the specific anti-tumor response (Chen and Mellman 2013).

Nevertheless, in a substantial proportion of cancer patients the cancer immunity cycle does not function optimally and on the way from immune-mediated recognition and elimination, cancer cells are able to interfere with the ongoing anti-tumor immunity. Manipulation and inhibition of important key processes allow immune evasion thereby favoring cancer progression. Besides tumor-mediated immune suppression, tumor infiltration of potent

activated T cells may be hindered by the tumor microenvironment thereby impeding final effector function in the tumor bed (Motz and Coukos 2013).

Consequently, targeting of immune effector cells to the tumor endothelium represents an important subdiscipline in the field of tumor immunology that the underlying study will focus on.

1.2 Prognostic Significance of Immune Cell Infiltration in Tumors

Previous studies have demonstrated a correlation between the presence of tumor-infiltrating lymphocytes (TILs) in most solid tumor types and progression-free survival as well as overall patient survival (Jass, 1986; Zhang et al. 2003; Galon et al. 2006; Anraku et al. 2008; Fridman et al. 2012; Hwang et al. 2012; Peske, Woods and Engelhard 2015; Sepesi et al. 2017; Chen et al. 2018; Idos et al. 2020).

These findings suggest a central role of T cells in tumor immunity further supported by the robust responses of some patients to high-dose interleukin-2 (IL-2) as well as to the adoptive transfer of autologous ex vivo expanded TILs (TIL therapy) (Restifo et al. 2012; Rosenberg et al. 2011).

Furthermore, checkpoint blockade therapy with monoclonal antibodies (mAbs) targeting cytotoxic T lymphocyte-associated protein 4 (CLTA-4), programmed cell death protein 1 (PD-1) and its ligand (PD-L1), has enabled T cell-mediated tumor regression for a range of malignancies (Hodi et al. 2010; Powles et al. 2014; Ansell et al. 2015; Brahmer et al. 2015; Le et al. 2015; Motzer et al. 2015) and its responses are greatly correlated to the presence of $CD8^+$ TILs (Tumeh et al. 2014).

In so-called hot tumors, besides $CD8^+$ T cells (CTLs), other tumor-infiltrating cells like natural killer (NK) cells and Th1 phenotypic interferon γ (IFN-γ) producing $CD4^+$ T cells are also linked to positive prognosis (Fridman et al. 2012). However, tumor-infiltrating cells such as those of myeloid origin like neutrophils, macrophages and myeloid-derived suppressor cells (MDSCs) and regulatory T cells (T_{reg}) are mostly associated with negative prognosis (Fridman et al. 2012) as well as tumors that are completely devoid of immune infiltrate, often referred to as cold tumors (Chen and Mellman 2013; Kim and Chen 2016).

Since multiple immune cell subsets are present in the tumor microenvironment at the same time, their relative representation is important to balance positive and negative influences on anti-tumor immunity. For instance, the ratio between $CD8^+$ T cells and regulatory T cells or total $CD4^+$ T cells has been shown to be prognostically relevant in various cancers (Anraku et

al. 2008; Gao et al. 2020; Wang et al. 2020). Yet, cytotoxic T cells are only associated with positive clinical outcomes if they can execute their effector function, i.e., being in an actively proliferating or IFNγ and granzyme producing state (Galon et al. 2013). Interestingly, also the exact intratumoral localization and density of $CD8^+$ lymphocytes alter their prognostic meaning. The presence in both the tumor center and the invasive front is associated with better outcome than localization at either site only (Erdag et al. 2012).

Even patients with similar tumor histology show great heterogeneity in overall T cell representation and distribution which indicates that fundamental processes controlling effector cell infiltration into and migration within cancerous tissue varies between patients and evidence shows that the individuality of the tumor microenvironment itself has remarkable impact.

1.3 TUMOR MICROENVIRONMENT - DETERMINANTS OF TUMOR T CELL INFILTRATION

For an effective host immune response, tumor cells need to be recognized as foreign and the immune effector cells must be able to infiltrate the tumor to destroy it. Tumor genomes contain many mutations that leads to altered proteins products which can be detected by the host immune system during surveillance leading to a systemic tumor-specific immune response. However, as part of its strong adaptive profile, tumors develop mechanisms to overcome this immune response in order to grow and eventually metastasize.

The overall representation of effector T cells in tumors is determined by various factors and central processes. At the site of the tumor-draining lymph node, cold, poorly immunogenic tumors (Peske et al. 2015; Yu et al. 2005) may diminish effector T cell infiltration due to a paucity of tumor antigens.

Similarly, poor T cell infiltration into tumors can result from impaired DC maturation and trafficking (**Fig. 1.7.** upper panel). One possible reason is impaired type I IFN signaling which normally is induced by tumor DNA and is required for DC-mediated antigen-specific anti-tumor $CD8^+$ T cell response via the STING cytosolic DNA sensing pathway. Defects in respective pathways restrict DC activation and subsequent T cell priming (Deng et al. 2014; Woo et al. 2014). Similar findings have been reported for murine tumor responses to anti-CTLA-4 (cytotoxic T lymphocyte-associated protein 4) or anti-PD-1/PD-L1 (programmed cell death (ligand) 1), which are associated with pre-existing CD8 T cell infiltration but also related to mutational burden, thereby linking T cell representation and tumor antigenicity (Snyder et al. 2014) (**Fig. 1.7.** lower right panel).

In addition, there is ample evidence that the tumor vasculature limits infiltration of $CD8^+$ T cells into cancerous tissue, a phenomenon called endothelial cell anergy. Tumors with poor T cell representation show active down-regulation of cognate ligands of leukocyte homing receptors on the tumor vasculature (**Fig. 1.7.** lower left panel), thus limiting extravasation of potent effector cells. Furthermore, tumor endothelial cells can express surface ligands that do not match immune cell receptors for transendothelial migration (Kupper and Fuhlbrigge 2004). In general, hypoxia in solid tumors hinders proper immune cell infiltration as it dysregulates angiogenesis in the tumor microenvironment which leads to tortuous and leaky blood vessels promoting irregular blood flow and increased interstitial pressure in cancer tissues (Chung et al. 2010). Within this context, the high-level production of vascular endothelial cell growth factors (VEGF) and basic fibroblast growth factors (FGF) by tumor and stromal cells like TAMs (tumor-associated macrophages) plays a major role (Peske et al. 2015).

Even if some T cells can successfully home and extravasate through tumor endothelium, further challenges can be faced to both their function and survival in the tumor bed. Tumor cells can up-regulate inhibitory receptors like PD-L1 and secrete molecules including IL-10 and TGF-β, that can directly block T cell function and/or recruit and activate immunosuppressive immune cells, including T_{reg}s, MDSCs, TAMs, and tumor-associated neutrophils (TANs).

In sum, all mechanisms alone or in combination allow cancer to escape host immune surveillance and to render endothelial cells unresponsive to inflammatory activation which may also explain the resistance of some solid tumors to anti-tumor immune checkpoint blockade (Bellone and Elia 2017). Therefore, crossing the abnormal endothelial barrier in solid tumors remains a major hurdle for endogenous or adoptively transferred tumor-specific CTLs which must be overcome in order to promote direct contact with their targets, hence effective anti-tumor immunity.

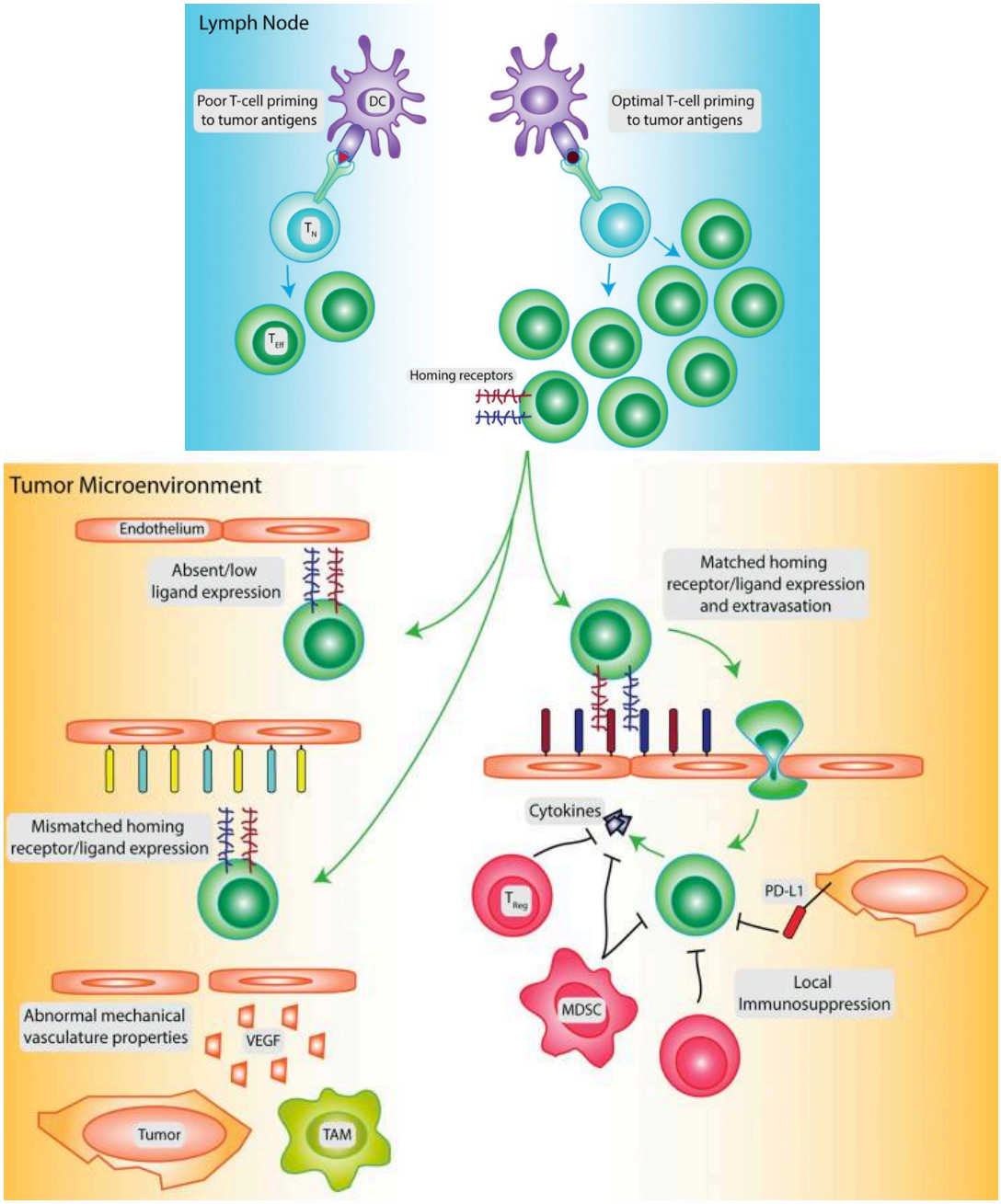

Figure 1.7 Factors controlling CD8 T cell presence in tumors. Initial T cell priming to tumor neoantigens may be hindered by reduced tumor antigenicity as well as poor DC trafficking and maturation. Furthermore, the tumor vasculature can decrease expression of ligands needed for T cell homing or express ligands for homing receptors not recognized by the T cells. Additionally, dysregulated angiogenesis poorly supports CD8 T cell infiltration. Figure adapted from Peske et al. 2015.

1.3.1 Tumor endothelium activation profile

In non-inflamed tissue, endothelial cells (EC) are in a quiescent state. EC are connected through tight junctions, allowing a stable blood flow. In response to extracellular stimuli, for example pro-inflammatory cytokine TNF-α, IL-1β, and toll-like receptor ligand lipopolysaccharide (LPS), EC are activated and mediate vascular permeability and leukocyte recruitment cascades. Two types of endothelial activation have been described.

Type I activation is a rapid response without transduction of new gene expression and is mediated by GPCR (G protein-coupled receptor) signaling. Upon activation, P-selectin is released to the cell surface via exocytosis of Weibel-Palade bodies (WPBs) (Rondaij et al. 2006). P-selectin is capable of capturing leukocytes and activating signaling to integrins that mediate leukocyte diapedesis.

Type II activation is a delayed but sustained response with de novo gene expression in endothelial cells (Pober and Sessa 2007). After cytokines such as TNF-α and IL-1 bind to their receptor TNFR1 and IL1-R1 respectively, the inhibitor of κB kinase (IKK) complex is activated and phosphorylates inhibitor of κB (IκB), which is subsequently tagged for ubiquitination and degradation by the proteasome. IκB degradation releases the NF-κB subunits p50 and p65 (also known as RelA) allowing them to translocate to the nucleus and to induce the transcription of a set of genes including chemokines and adhesion molecules such as E-selectin, intercellular adhesion molecule 1 (ICAM1) and vascular cell adhesion molecule 1 (VCAM1). Both chemokines and adhesion molecules are important mediators of the leukocyte recruitment process. This pathway is called the canonical NF-κB pathway. However, other cytokines and pro-inflammatory stimuli (i.e., CD40L and lymphotoxin β receptor (LTβR)) also stimulate a similar pathway through activating the homologous subunits of NF-κB, namely p52, RelB and c-Rel (the p52 and RelB complex are also named the NF-κB2 complex) via the non-canonical NF-κB pathway.

In tumors, pro-angiogenic signaling can result in endothelial cell anergy, poor response to pro-inflammatory signaling, decreased regulation of adhesion molecules and chemokines essential for arrest and migration of leukocytes (Klein 2018; Wu et al. 2015). More specifically, tumor endothelial cell anergy occurs mainly through insufficient expression or functionality of adhesion molecules as E-selectin, ICAM1, ICAM2 and VCAM1. Down-regulation or ineffective clustering of adhesion molecules modulates tumor T cell infiltration (Afanasiev et al. 2013; Bouzin et al. 2007; Buckanovich et al. 2008; Clark et al. 2008; Enarsson et al. 2006; Griffioen et al. 1996; Madhavan et al. 2002; Piali et al. 1995; Weishaupt et al. 2007; Yoong et al. 1998) is related with the presence of high angiogenic factors levels such as basic fibroblast growth

factor (bFGF) and vascular endothelial growth factor (VEGF) in the tumor microenvironment (Dirkx et al. 2003; Griffioen et al. 1996). Even though pro-inflammatory cytokines like TNF-α are abundant in many cancers, pro-angiogenic factors can reverse endothelial activation (Mauge et al. 2014). Other suggested mechanisms for reduced adhesion molecule/integrin interactions in tumors include the presence of nitric oxide (NO) (Gehad et al. 2012). Interestingly, another aspect of tumor endothelial regulation of tumor immunity is the preferential recruitment of specific immunosuppressive leukocyte subsets, as T_{reg}, through up-regulation of selective adhesion molecules such as vascular endothelial receptor-1 (CLEVER-1) (Mauge et al. 2014).

Integrins and integrin ligands therefore play important roles in several immune system functions, especially in immune cell migration and activation. In fact, cell adhesion molecules have been shown to play both positive and negative roles in anti-tumor immunity.

For example, in order for T_{reg} to exert their suppressive function, it is crucial that they migrate to the site of inflammation. T_{reg} express high levels of cell adhesion molecules including ICAM1, L-selectin, P-selectin, and VLA-4 (Kohm et al. 2002). Furthermore, some adhesion molecules, particularly β2-integrins, also play a key role in regulatory T cells development and function (Haasken et al. 2011; Marski et al. 2005; Wang et al. 2008; Wohler et al. 2009).

The expression of integrin on tumor cells has been connected with tumor progression and metastasis due to increased proliferation, survival, migration and invasion of the malignant cells (Desgrosellier and Cheresh 2010). Moreover, on tumor-associated vasculature, aberrant VCAM1 expression has also been observed on many types of tumor cells such as breast, renal, colorectal cancer and gastric carcinoma cells (Dai et al. 2020; Schlesinger and Bendas 2015; Wu 2007). High levels of VCAM1an ICAM1 on malignant cells has been associated with metastases, recruitment of tumor-associated monocytes and macrophages and poor prognosis in several cancers like melanoma, breast, lung and oral cancers (Johnson et al. 1989; Lin et al. 2006; Schröder et al. 2011; Usami et al. 2013). Besides some human myeloma cells have been shown to express various adhesion molecules including LFA-1, VLA-4, CD44, and ICAM1 (Ahsmann et al. 1992; Tatsumi et al. 1996; Vacca et al. 1995) and adhesion molecules like LFA-1 and VLA-4 have also been associated with drug resistance in multiple myeloma patients (Di Marzo et al. 2016). E-selectin increased expression on tumor endothelium and the presence of soluble E-selectin is also known to mediate cancer extravasation (Kang et al. 2016; Zhong et al. 2014).

In conclusion, adhesion molecules play an important role in the function of the immune system both in health and disease. During cancer progression, adhesion molecules mediate essential functions in almost every step of the anti-tumor response cascade, including tumor antigen uptake, activation of tumor-specific T cells, leukocyte trafficking into the tumor site and tumor cell killing. Nevertheless, malignant cells can also use cell adhesion molecule pathways to support tumor growth. Expression of various integrins on tumor cells promotes tumor cell proliferation, survival and metastases. However, increased secretion of angiogenic molecules causes down-regulation of adhesion molecules on tumor-associated blood vessels and consequently avoids immune effector cell infiltration into the tumor. Tumor cells also recruit regulatory cells such as T_{reg} and MDSC which express high levels of integrins allowing them to reach the tumor site. The main cell adhesion molecule-mediated events promoting tumor growth are listed in **Table 1.2**.

Besides affecting leukocyte recruitment, tumor endothelial cells can also influence immune cell functions. Tumor endothelial cells can present increased expression of T cell activation inhibitory molecules such as programmed death-ligand (PD-L) 1, FasL, TNF-related apoptosis-inducing ligand (TRAIL), T-cell immunoglobulin domain and mucin domain (TIM3), B7-H3, B7-H4, IL-6, Prostaglandin E (PGE) 2, IL-10 and TGF-β (Maishi et al. 2019; Nagl et al. 2020; Zonneville et al. 2018). Receptors involved in angiogenesis, like TIE2 (Mazzieri et al. 2011; Willam et al. 2000) and VEGFR2 (Lian et al. 2019; Smith et al. 2010) are also up-regulated in tumor endothelium.

Table 1.2 Adhesion molecule-mediated events promoting tumor growth.

Adapted from Harjunpää et al. 2019

Type of tumor	Adhesion molecule-mediated mechanisms operating in the tumor microenvironment	Consequence for tumor progression	Ref.
Solid	Increased secretion of angiogenic factors by the tumor cells reduces the expression of various adhesion molecules including ICAM1/2, VCAM1 and E-selectin in tumor-associated endothelial cells	Leukocytes in blood are unable to extravasate to the tumor site (endothelial anergy)	(Dirkx et al. 2003; Griffioen et al. 1996; Klein 2018; Tromp et al. 2000; Wu et al. 2015)
	Dying tumor cells become opsonized with iC3b	DCs interact with dying tumor cells via β2-integrins Mac-1 and CD11c/CD18 leading to suppression of DC activation and tolerance	(Skoberne et al. 2006; Verbovetski et al. 2002)
	High expression of adhesion molecules including ICAM1, VLA-4 and L-selectin on Tregs	Affects T_{reg} trafficking possibly enabling them to reach the tumor site where they suppress effector T cells leading to tumor evasion of the immune system	(Kohm et al. 2002)
	High expression of VLA-4 and CD11b on myeloid cells	Myeloid cells are able to reach the tumor site and promote angiogenesis and tumor growth	(Arnaout 1990; Jin et al. 2006; Palmen et al. 1995; Zhang et al. 2015)
	Expression of various integrins including αVβ3, ICAM1 and VCAM1 on tumor cells	Increase in tumor cell proliferation, survival and invasion, recruitment of tumor-associated macrophages (TAMs) which allows evasion of the immune system	(Brooks et al. 1995; Desgrosellier et al. 2009; Huveneers et al. 2007; Johnson et al. 1989; Lin et al. 2006; McCabe et al. 2007; Schlesinger and Bendas 2015; Schröder et al. 2011; Takayama et al. 2005; Uhm et al. 1999; Usami et al. 2013; Wu 2007)
	Expression of MUC-1 on tumor cells, which is able to bind to ICAM1 in endothelial cells	Tumor cells are able to cross the endothelial barrier, which promotes metastasis	(Nath and Mukherjee 2014; Roland et al. 2007)
Hematological	Up-regulation of LFA-1/VLA-4 expression on tumor cells which are able to bind to ICAM1/VCAM1 in endothelial cells	Tumor cells are able to cross the endothelial barrier and migrate to lymphoid tissues to receive more proliferation and survival signals promoting tumor progression	(Ahsmann et al. 1992; Burger and Gribben 2014; Gattei et al. 2008; Hartmann et al. 2009; Lúcio et al. 1998; Riches et al. 2014; Shanafelt et al. 2008; Tatsumi et al. 1996; Vacca et al. 1995)

1.4 TUMOR VASCULATURE

1.4.1 Blood vessel formation

Blood vessels, orderly arranged in arteries, veins, and capillaries, together with the blood and heart formed the cardiovascular system, the first functional organ during vertebrate development (Swift and Weinstein 2009). Tissue oxygenation, nutrient supply, bioactive molecule distribution and immune cell mobility to distal sites in the body are the main blood vessels functions (Potente et al. 2011).

Vasculogenesis is the process of *de novo* vessel formation and occurs during embryogenesis by mesoderm-derived endothelial precursors, called angioblasts (Swift and Weinstein 2009). The growth of new blood vessels from pre-existing ones occurs through angiogenesis (Risau 1997). Angiogenesis typically starts from the capillaries and plays an important role in tumor growth, maintenance and metastasis.

Subsequently, the newly formed vessels, either through vasculogenesis or angiogenesis, need to mature to ensure the integrity of the new vessel channel (Potente et al. 2011). The vessel maturation reflects higher states of organization of the vessel wall as well as the vascular network. The vessel wall is composed of endothelial cells (EC, the foundation of blood vessels), recruited mural cells (pericytes or vascular smooth muscle cells) and ECM.

During adulthood, the endothelial cells are quiescent and under physiologic conditions new blood vessel formation rarely takes place, for example, in wound healing, female menstrual cycle, and placenta generation (Schmidt and Carmeliet 2011). However, EC retain the capacity to respond in pro-angiogenic signals when required, for example in pathologic conditions like tumor formation (Potente et al. 2011).

1.4.2 Tumor blood vessel formation

In fact, tumors rely on a blood supply for maintained tumor cell survival and induction of dysregulated angiogenesis is one of the hallmarks of cancer, stimulated by multiple factors like inflammation and hypoxia (low oxygen tension) present in the tumor microenvironment (Hanahan and Weinberg 2011). Blood vessel formation in tumors can be triggered by several cellular processes (**Fig. 1.8**) like: Sprouting angiogenesis (SA); intussusceptive angiogenesis (IA, vessel splitting or non-SA); vasculogenesis and recruitment of endothelial progenitor cells; vascular mimicry and trans-differentiation of cancer stem cells.

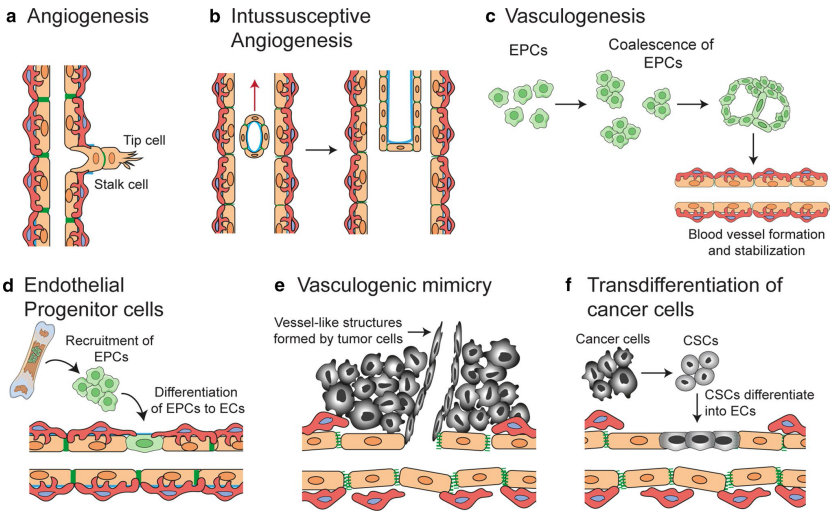

Figure 1.8 Mechanisms of blood vessel formation. Neo-vascularization in normal tissues and tumors can occur through one or more of the following mechanisms: Sprouting angiogenesis: consists in formation and outgrowth of tip cells that can fuse with an existing vessel or newly formed. b Intussusceptive angiogenesis: *de novo* vasculature formation from a pre-existing vessel. c Vasculogenesis: embryo neo-vascularization from endothelial progenitor cells that proliferate and form new vessels. d Recruitment of circulating endothelial progenitor cells. e Vascular mimicry: a matrix-embedded fluid-conducting meshwork formed by tumor cells. f Trans-differentiation of cancer stem cells (CSC): neo-vascularization through differentiation of CSCs to endothelial cells. Figure from Lugano, Ramachandran and Dimberg, 2020.

SA which accounts for a considerable amount of vessel formation refers to the process of vessel sprouting from pre-existing blood vessels triggered by pro-angiogenic factor gradients (like VEGF) inducing EC activation and morphology changes with an invasive character, forming filopodia and start exploring the adjacent microenvironment in search of guidance. The cells of the leading edge are called tip cells and differ from the following cells, namely stalk cells. Stalk cells are more proliferative, they form fewer filopodia and generate tubes with the lumen. However, the tip/stalk cell fate is not permanent since it is a highly dynamic and transient state mainly regulated by Notch signaling (Hellström et al. 2007). The tip cells are responsible for vessel dividing through anastomosis with other tip cells creating vessel loops. Finally, blood flow and vessel maturation need to occur to ensure the integrity of the new vessel channel (Potente et al. 2011).

The process known as “intussusception” (IA) is a less studied neo-angiogenesis mechanism where new vessels arise from splitting of pre-existing ones without the need of sprouting. During this process endothelial walls of the opposite side of a vessel extend towards each other creating an intraluminal pillar, which is perforated and thus forms two lumens. Then pericytes and myofibroblasts support the pillar by generating ECM. Several pillars fuse together and create two capillaries from the initial one. Intussusceptive angiogenesis is quicker

than sprouting angiogenesis (De Spiegelaere et al. 2012). The molecular mechanisms involved in IA are not completely understood but is known to be influenced by growth factors like VEGF, PDGF and erythropoietin (Crivellato et al. 2004; Hellström et al. 1999; Wilting et al. 1996). IA have been observed in various tumor types including melanoma, colorectal cancer, glioma and mammary tumors contributing to tumor growth by increasing the complexity and number of microvascular structures within the tumor (Djonov et al. 2001; Nico et al. 2010; Patan et al. 1996; Ribatti et al. 2005).

De novo blood vessel formation in the embryo starting through endothelial progenitor cells (EPCs) differentiation and association is known as vasculogenesis (Risau et al. 1988; Risau and Lemmon 1988). EPCs can be derived from hematopoietic stem cells, myeloid cells, circulating mature endothelial cells or other circulating progenitor cells (Chopra et al. 2018; Urbich and Dimmeler 2004). EPCs are recruited from the bone marrow to places of injury due to the presence of growth factors, cytokines and hypoxia-related signaling pathways. There, they differentiate into mature endothelial cells and incorporate themselves into sites of active neovascularization (Asahara et al. 1997; Reale et al. 2016). However, vasculogenesis was also observed in adults during capillary formation post-ischemia (Asahara et al. 1997) or in tumors as an alternative mechanism for neovascularization (Bussolati et al. 2011). In tumors, specifically, this process is initiated by crosstalk between tumor cells and EPCs or bone marrow-derived hematopoietic cells, initiating the formation of new vessels boosting tumor growth (Ahn et al. 2010; Greenfield et al. 2010) due to the presence of VEGF, chemokines CCL2, CCL5, CXCL12 (also known as SDF-1) (Chang et al. 2007) and adiponectin (Chang et al. 2007; Nakamura et al. 2009; Spring et al. 2005) in the tumor microenvironment. In preclinical glioma models, the revascularization that occurs during glioma recurrence after irradiation is mediated by vasculogenesis and not angiogenesis (Kioi et al. 2010).

Aggressively growing tumor cells can also form vessel-like structures without contribution of endothelial cells through vascular mimicry. Vascular mimicry has been reported in some tumor types including melanoma (Maniotis et al. 1999), glioma (Ricci-Vitiani et al. 2010), head and neck cancer (Upile et al. 2011), lung cancer (Williamson et al. 2016), colorectal cancer (Baeten et al. 2009) and prostate cancer (Sharma et al. 2002) and has been related with poor prognosis (Baeten et al. 2009; Li et al. 2010). In gliomas, for example, increased vascular mimicry has been reported following anti-angiogenic therapy (Angara et al. 2017), maybe as an alternative neovascularization process. However, due to a lack of techniques that can be used to distinguish vascular mimicry from normal endothelial cell lining clearly, investigation of this process is still difficult.

Trans-differentiation of cancer stem cells to endothelial cells and vascular smooth muscle-like cells resulting in neovascularization has been reported in several tumor types (Alvero et al. 2009; Bussolati et al. 2009; Mei et al. 2017; Ricci-Vitiani et al. 2010; Wang et al. 2010), although with somewhat controversial results. Some studies reported the fact that tumor endothelial cells can harbor similar somatic mutations as the malignant cells, indicating a neoplastic origin (Ricci-Vitiani et al. 2010; Wang et al. 2010) but not in others (Kulla et al. 2003; Rodriguez et al. 2012). A later study using lineage-specific fluorescent reporters even demonstrated that glioma cancer stem cells can differentiate into pericytes and that specific depletion of pericytes disrupted tumor vessels and tumor growth (Cheng et al. 2013).

A common feature of all these processes is the quick and dysregulated tumor blood vessel formation due to the persistence of pro-angiogenic factors in the tumor microenvironment leading to morphological and functional deficiency on networks maturation and division. Malformed vessels poorly organized are characterized by the heterogeneous vessel caliber size, disrupted EC junctions, pericytes partially detached from EC and an uneven basement membrane (Baluk et al. 2003; Baluk et al. 2005; McDonald and Baluk 2005; Morikawa et al. 2002). As a consequence of abnormal tumor vascular network, the blood flow within the tumor parenchyma is uneven, vessel permeability is enhanced, and interstitial fluid pressure is increased leading to hypoxia and increased vessel fragility (Abramsson et al. 2002; Bennewith and Durand 2004; Hashizume et al. 2000) (**Fig. 1.9**). The efficacy of cancer therapies is also negatively affected since compression of tumor vessels and poor vascular perfusion hamper drug delivery (Padera et al. 2004).

Importantly, tumor-infiltrating inflammatory cells such as TAMs and myeloid-derived suppressor cells (MDSCs) may also induce the angiogenic switch by secreting multiple pro-angiogenic factors (Gao et al. 2008; Murdoch et al. 2008). In pathophysiological conditions, wounds attract immune cells that need to reach the injured site through blood vessel extravasation. As inflammation continues, vessels become more permeable and secrete chemoattractants for the immune cells. Leukocyte recruitment is a multistep process orchestrated by activated endothelial cells, as discussed in section 1.1.3.

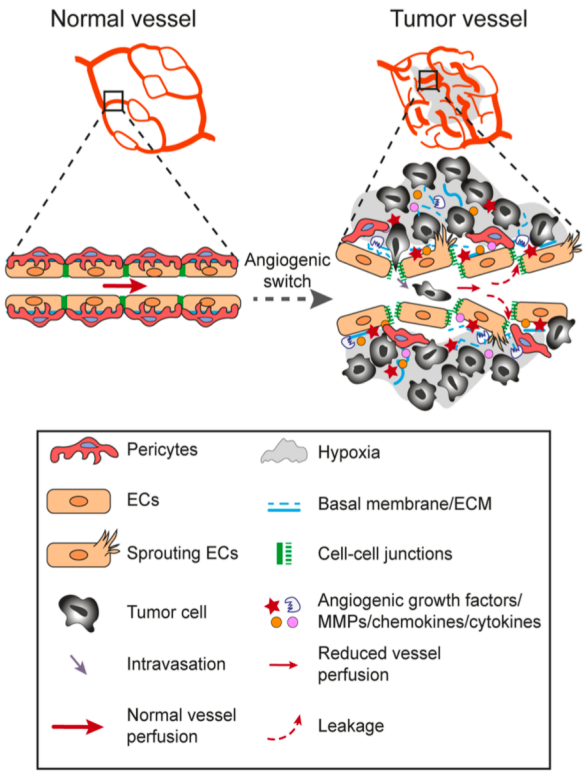

Figure 1.9 Morphological and functional differences between normal and tumor vessels. In healthy tissue, a regularly patterned and functioning vasculature is formed. Endothelial cells, basal membrane and pericytes are tightly connected by strong cell-cell junctions. In established tumors, the vasculature, as well as the endothelium and vessel wall, exhibit structural and functional abnormalities including loose associations with EC and variable thickness, leading to regions of severe hypoxia in response to persistent and imbalanced expression of angiogenic factors and inhibitors. Tumor vessels are characterized by reduced blood flow, EC sprouting, disruption of EC junctions, loss of pericytes coverage. Figure from Lugano, Ramachandran and Dimberg, 2020.

1.4.3 Molecular regulation of tumor angiogenesis

Hypoxia is one of the predominant stimuli inducing tumor angiogenesis. When oxygen supply in the tissue is too low to satisfy a high proliferation of tumor cells, ICA;1 (HIF-1) is up-regulated. HIF-1, a heterodimeric protein, consists of the oxygen level-regulated HIF-1α subunit and the stably expressed HIF-1β. HIF-1α is regulated by oxygen-sensing prolyl hydroxylase domain proteins 1-3 (PHD1–3). In normoxia, PHDs use oxygen to hydroxylate HIF-1α, thereby targeting it for proteasomal degradation. Oxygen sensors become inactive in hypoxic conditions, allowing HIF-1α to escape degradation and regulate the expression of angiogenesis, proliferation and glycolytic metabolism-related molecules such as VEGF and GLUT-1 (Fong 2009; Forsythe et al. 1996; Greer et al. 2012; Span and Bussink 2015).

Many pro-angiogenic factors have been identified, including acidic fibroblast growth factor (FGF), hepatocyte growth factor (HGF), TGF-α, TGF-β, epidermal growth factor (EGF), tumor necrosis factor α (TNF-α), angiogenin, interleukin 8 (IL-8) and angiopoietins (Ferrara et al. 2003; Yadav et al. 2015). These factors are often expressed simultaneously, effectively co-operating at different stages of tumor angiogenesis.

During tumor angiogenesis, as shown in **Fig. 1.10**, VEGF is produced and secreted by tumor cells and surrounding stroma in response to hypoxia via the PHD2/HIF pathway or due up-regulation by oncogenic activation (like PI3K), inflammatory cytokines. VEGF-A may also be

derived from tumor-infiltrating myeloid cells, pericytes, or released from the extracellular matrix and acts primarily via VEGFR2 on ECs (Goel et al. 2011). VEGF-mediated cell invasion is promoted by the expression of MMP (matrix metalloproteinase) which degrade the basal membrane and extracellular matrix allowing migration of endothelial cells and the formation of capillary sprouts (Jiang and Liu 2009; Van Hinsbergh and Koolwijk 2008). VEGF-A is associated with tumor progression, increased vessel density, invasiveness, metastasis and tumor recurrence and is up-regulated during hypoxia (Apte et al. 2019; Ferrara 2004). Except for the cognate VEGFRs, co-receptors of VEGF as NRPs (NRP1 and NRP2) and integrins have been identified. Based on expression patterns, NRP1 has been associated as a co-receptor of VEGFR1/2, whereas NRP2 is a co-receptor of VEGFR3. Integrins such as αvβ3 orchestrate cell-matrix adhesion by specific ECM bindings, are mediators of VEGFR2 activity (Koch and Claesson-Welsh 2012).

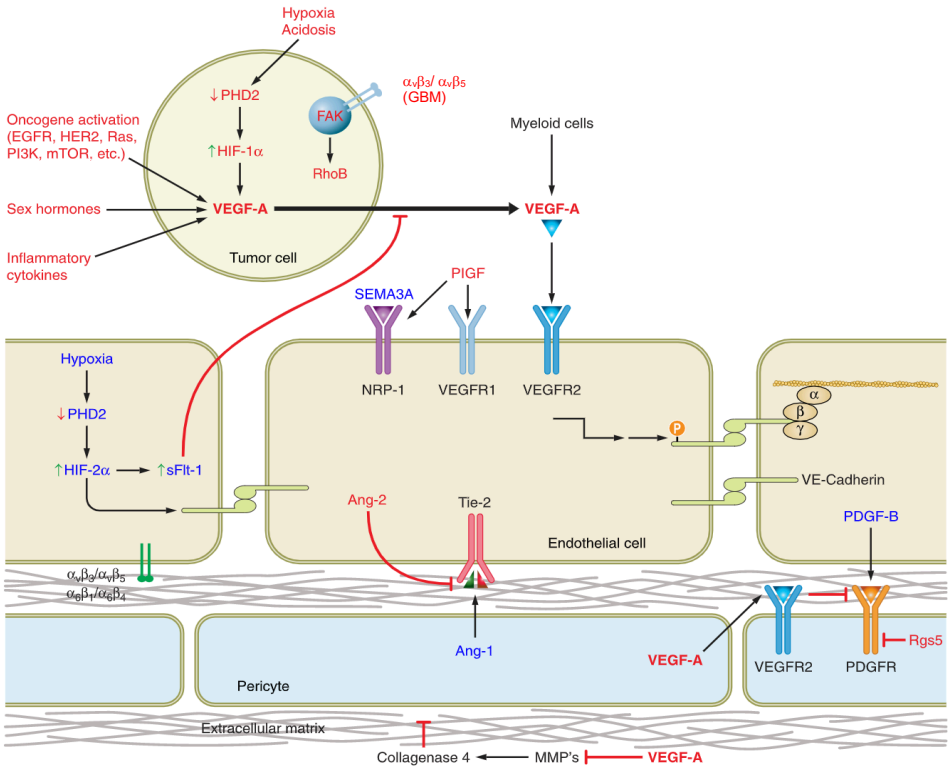

Figure 1.10 Molecular regulation of tumor angiogenesis. This schematic diagram depicts a tumor cell, endothelial cell, surrounding pericytes, and the extracellular matrix. Molecules that lead to characteristic vessel abnormalities are in red, and those that promote the normalization phenotype are in blue. The principal angiogenic molecule responsible for vascular abnormalities is VEGF-A. Other mediators of the abnormal vessel phenotype shown include Ang-2 (acting on the TIE2 receptor), Rgs5 (which inhibits PDGFR-mediated pericyte recruitment), and tumor cell integrins (in the case of GBM). Factors that may restore tumor vessels toward a more normal phenotype include Ang-1 (derived primarily from perivascular cells and acting on TIE2), SEMA3A and PDGF-B. Figure adapted from Goel et al. 2011.

1.4.3.1 Vascular endothelial growth factors (VEGF) and respective receptors (VEGFR)

VEGFs are considered as central molecules for blood and lymphatic vessel biology during development as well as adulthood. VEGF(A) was the first identified member of the VEGF family, originally identified as vascular permeability factor (VPF), one of the most potent inducers of angiogenesis (Koch and Claesson-Welsh 2012). VEGF-A belongs to the VEGF family of growth factors composed of five members, VEGF(A-D) and the placenta growth factor PlGF (Ferrara et al. 2003). VEGF-A has been acknowledged as the key regulator of the main blood vessel functions throughout development. VEGF-B and PlGF also stimulate angiogenesis in normal tissues, but their activities are limited compared to VEGF-A (De Falco 2012; Scotney et al. 2002). VEGF-C and VEGF-D mainly regulate lymphatic angiogenesis.

VEGFs are the ligands of a family of receptor tyrosine kinases (RTKs), namely vascular growth factor receptor 1, 2 and 3 (VEGFR1, VEGFR2 and VEGFR3), that like other RTKs, consist of an extracellular ligand-binding region, a transmembrane part and an intracellular tyrosine kinase domain (Shibuya and Claesson-Welsh 2006) (**Fig. 1.11)**. Traditionally upon ligand-binding, VEGFRs homodimerize but studies have shown that heterodimerization is also possible (Domigan et al. 2015). Receptor dimerization enables activation and autophosphorylation of certain tyrosine residues leading to differential intracellular signaling cascades and multifunctional role of the receptor throughout vessel development and pathophysiology. VEGFR1 (or Flt1, in mice), up-regulated by hypoxia through HIF-1 activation, binds VEGF-A, VEGF-B and PlGF. VEGFR1 and its soluble version are considered negative regulators of VEGFR2 by binding VEGF-A with higher affinity. Under specific conditions, it has been implicated to mediate mitogenic signals and it also has a role in hematopoiesis (Ferrara et al. 2003). VEGFR2 (or KDR in humans and Flk-1 in mice) is the major receptor of VEGF-A but it can also bind VEGF-C and VEGF-D (with implication for lymphatics). VEGFR2 can also be found as soluble molecule. VEGFR2 is an endothelial cell signaling transducer with multiple effects in angiogenesis, differentiation, migration and tube formation (Shaik et al. 2020). VEGFR3 binds VEGF-C and VEGF-D and these interactions are critical for lymphatic endothelial cells but are also essential for angiogenesis (Dumont et al. 1998; Koch and Claesson-Welsh 2012).

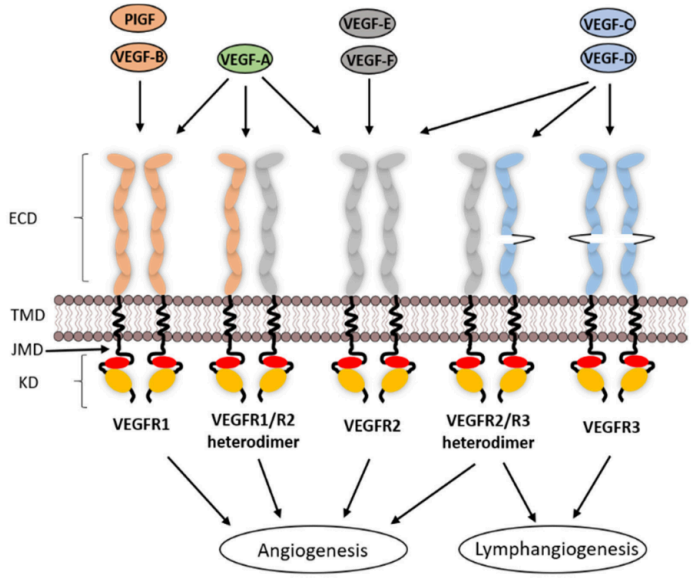

Figure 1.11 Schematic representation of vascular endothelial growth factor receptor (VEGFR) organization and ligand specificity. All vascular endothelial growth factors (VEGFs) bind to three receptor tyrosine kinases (RTKs), VEGFR1, VEGFR2 and VEGFR3. VEGFRs contain an extracellular domain (ECD), transmembrane domain (TMD) and a cytoplasmic domain which is further divided into juxtamembrane domain (JMD) and kinase domain (KD) and form homo- and heterodimers upon ligand binding. Figure from Shaik et al. 2020.

1.4.3.2 Angiopoietin-1/-2/ and TIE2 interactions

The angiopoietin-TIE2 pathway plays a key role in regulating both physiological and pathological angiogenesis (Huang et al. 2010; Suri et al. 1996). TIE2 is a tyrosine kinase receptor originally found in the membrane of EC and hematopoietic precursor (Dumont et al. 1992), that has later been described to be expressed in other cells, such as tumor cells, pericyte precursors, and specific monocytic populations (Gabrusiewicz et al. 2014; Lee et al. 2006; Martin et al. 2008). TIE2 signaling is initiated after binding to angiopoietins, leading to a dynamic role in vessel formation, maintenance, and permeability (**Fig. 1.10**). Thus, Ang-1 stimulation of TIE2 tightens endothelial junctions resulting in blood vessel stabilization while Ang-2 has been shown to induce vessel destabilization, pericytes detachment, vessel sprouting and angiogenesis (Reiss et al. 2009). Increased ANG2 expression has been observed in activated endothelial cells during inflammation and in tumor-associated vessels of several human cancers in response to hypoxia and VEGF (Shim et al. 2007). Moreover, up-regulation of Ang-2 in glioblastoma has been associated with reduced efficacy of anti-VEGF treatment and increased therapy resistance (Chae et al. 2010). TIE2-Ang signaling pathway

Regarding dual inhibition of Ang-2/VEGFR2, preclinical studies have demonstrated beneficial effects impairing tumor growth, prolonging vessel normalization and blocking macrophage recruitment and thereby improving survival of glioma-bearing mice (Kloepper et al. 2016; Peterson et al. 2016). Co-targeting of Ang-2/VEGFR2 is also effective in other murine tumor models (Koh et al. 2010; Tetreault et al. 2017; Wu et al. 2016).

1.5 CANCER THERAPIES

1.5.1 Anti-angiogenic therapies

The idea of targeting angiogenesis was raised by Judah Folkman in the 1970s, with the aim to limit tumor growth by inhibiting tumor angiogenesis and thereby prolonging patient survival (Sherwood et al. 1971). After this initial suggestion, many anti-angiogenic targets have been identified and multiple anti-angiogenic strategies have been developed, including monoclonal antibodies (Reinacher-Schick et al. 2008), tyrosine kinase inhibitors (TKIs) (Gotink and Verheul 2010), fusion proteins binding to pro-angiogenic factors (Van Cutsem et al. 2012), aptamers (Bates et al. 2009), vaccines (Wagner et al. 2015), oncolytic viruses (Tysome et al. 2013) or endogenous anti-angiogenic inhibitors (e.g., endostatin) (Abdollahi et al. 2005). FDA-approved drugs with anti-angiogenic effects are summed up in **Table 1.3**.

Table 1.3 FDA-approved drugs with anti-angiogenic effect

Adapted from Al-Abd et al. 2017.

Drug	Target molecule(s)	Tumor type	References
Monoclonal antibodies			
Bevacizumab (Avastin)	VEGF-A	Colorectal cancer, non-small cell lung cancer, cervical cancer, ovarian cancer, renal cell carcinoma, glioblastoma	(Ferrara et al. 2006; Kazazi-Hyseni et al. 2010)
Ramucirumab (Cyramza)	VEGFR2	gastric or gastro-esophageal junction cancers, colorectal cancer, hepatocellular carcinoma, non-small-cell lung carcinoma	(Al-Halafi 2014; Arrieta et al. 2017)
Cetuximab	EGFR	Squamous cell carcinoma of the head and neck, colorectal cancer	(Bonner et al. 2006; Heinemann et al. 2014)
Panitumumab	EGFR	Colorectal cancer	(Price et al. 2014)
Necitumumab	EGFR	Squamous non-small-cell lung cancer	(Thatcher et al. 2015)
Trastuzumab	HER2	HER2-positive breast cancer, HER2-positive advanced gastric or gastro-esophageal junction cancer	(Bang et al. 2010; Gianni et al. 2014)
Pertuzumab	HER2	HER2-positive breast cancer	(Hurvitz et al. 2018)
Tyrosine kinase receptors (TKRs)			
Sunitinib (Sutent)	VEGFR1, VEGFR2, VEGFR3, PDGFRβ, FLT3	Metastatic renal cell carcinoma (mRCC) and gastrointestinal stromal tumor (GIST)	(Roskoski 2007; Wilhelm et al. 2004)
Sorafenib (Nexavar)	VEGFR2, PDGFR, c-kit, Raf-1, B-Raf	Advanced renal cell carcinoma, advanced hepatocellular carcinoma	(Berretta et al. 2016; Escudier et al. 2016)
Cabozantinib (Cabometyx)	VEGFR2, MET, RET	Advanced renal cell carcinoma	(Grülich 2014; Sonpavde and Hutson 2007)
Pazopanib (GW78603)	VEGFR1, VEGFR2, VEGFR3, PDGFR-α, PDGFR-β and c-kit	Renal cell carcinoma	(Jain et al. 2015)
Ponatinib (AP24534)	VEGFR2, FGFR-1, FGFR-2, FGFR-3, PDGFR-α	Chronic myeloid leukemia	(Rey et al. 2015)

Regorafenib (BAY 73-4506)	VEGFR1, VEGFR2, VEGFR3, FGFR-1, FGFR-2, PDGFR-α, PDGFR-β, KIT, TIE2, TrkA	Metastatic colorectal cancer (mCRC), gastrointestinal stromal tumors (GIST) and hepatocellular carcinoma	(Hu-Lowe et al. 2008; Omata et al. 2017)
Axitinib	VEGFR1, VEGFR2, VEGFR3, PDGFRβ, c-Kit	Renal cell carcinoma	(Hewett et al. 2018)
Lenvatinib (E7080)	VEGFR1, VEGFR2, VEGFR3, PDGFR-α, FGFR-1, FGFR-2, FGFR-3, FGFR-4, KIT and RET	Radioactive iodine (RAI)-refractory thyroid cancer	(Kawalec et al. 2016; Ton et al. 2013)
Vandetanib (ZD6474)	VEGFR2, VEGFR3, EGFR, RET FGFR-1, FGFR2, FGFR3,	Locally advanced and metastatic medullary thyroid cancer	(Fala 2015)
Nintedanib (BIBF 1120)	VEGFR1, VEGFR2, VEGFR3, PDGFR-α, PDGFR-β and FLT3	Idiopathic pulmonary fibrosis (IPF)	(Roskoski 2007)
Imatinib	PDGFR, c-Kit, Abl	Gastrointestinal stroma tumor, myeloid leukemia, philadelphia chromosome-positive acute lymphoblastic leukemia	(DeMatteo et al. 2009; Druker et al. 2006; Fielding et al. 2014)
Gefitinib	EGFR	Non-small cell lung cancer	(Kim et al. 2008)
Erlotinib	EGFR	Non-small cell lung cancer, pancreatic adenocarcinoma	(Lee et al. 2012; Moore et al. 2007)
Neratinib	EGFR, HER2	HER2 positive breast cancer	(Martin et al. 2017)
Lapatinib	EGFR, HER2	HER2 positive breast cancer	(Baselga et al. 2012)
Afatinib	EGFR, HER2	Non-small cell lung cancer	(Sequist et al. 2013)
Receptor fusion proteins			
Ziv-aflibercept (VEGF trap)	VEGF-A, VEGF-B, PlGF	Colorectal cancer	(Tabernero et al. 2014)
Immunomodulatory agents			
Thalidomide	TNF-α, ILs, IFNs, VEGF, bFGF	Multiple myeloma	(Rajkumar et al. 2002)
Lenalidomide	TNF-α, ILs, IFNs, VEGF, bFGF	Multiple myeloma	(Rajkumar et al. 2010)
mTOR inhibitor			
Everolimus	mTOR	Renal cell carcinoma, breast cancer, pancreatic cancer, gastrointestinal cancer, lung neuroendocrine tumor, subependymal giant cell astrocytoma	(Motzer et al. 2008)

The first FDA (The Food and Drug Administration) approved anti-angiogenic therapy for cancer was Bevacizumab (Avastin®), a humanized monoclonal antibody neutralizing VEGF-A mainly used for metastatic colorectal cancer in combination with chemotherapy (Vasudev and Reynolds 2014). Today bevacizumab is used as first- and second-line treatment for metastatic colorectal cancer, advanced non-small cell lung cancer, breast cancer, renal cell carcinoma and glioblastoma, and significantly increases progression-free survival when combined with chemotherapy (Van Meter and Kim 2010).

Ramucirumab is a fully-humanized IgG1 monoclonal antibody, FDA approved in 2014, that binds to the extracellular domain of VEGFR2 and has an antagonist effect. In several cancers like non-small cell lung cancer (NSCLC), gastric cancer (GC), colorectal cancer, and bladder cancer has been described as a potent anti-angiogenic agent (Fuchs et al. 2014; Garon et al. 2014; Jayson et al. 2016; Petrylak et al. 2017; Wilke et al. 2014). (Tada et al. 2018) showed that $CD8^+$ T cell infiltration and PD-L1 expression were induced by Ramucirumab-containing therapies and also reported a decrease in TIL, effector T_{reg} cells and PD-1 expression by $CD8^+$ T cells after the treatment.

1.5.1.1 Tyrosine kinase inhibitors (TKIs)

The tyrosine kinase inhibitors represent another important class of anti-angiogenic drugs. Unlike bevacizumab and other monoclonal antibodies, TKIs are small hydrophobic molecules that can enter the cell cytoplasm and interfere with the intracellular signaling domain of the targeted kinase or other molecules (Gotink and Verheul 2010). Most TKIs act by competing with ATP for binding to the kinase domain and have the ability to target multiple different kinases hence blocking several signaling pathways simultaneously (Gotink and Verheul 2010). It is likely that this multi-targeted character of TKIs is the reason why they have stronger efficacy as single agents than monoclonal antibodies. For example, TKIs that simultaneously target VEGFRs and platelet-derived growth factor receptors (PDGFRs) affect endothelial cells as well as pericytes (Erber et al. 2004). Increased toxicity in combination therapies with chemotherapy is an important parameter (Moserle et al. 2014).

1.5.1.2 Resistance to anti-angiogenic therapy and future directions

Although therapeutic intervention blocking the VEGF/VEGFR2 pathway has proven to be successful in limiting disease progression in a number of different clinical settings, there is an obvious need for an improved response due to therapy resistance which can explain the variable responses in different types of cancer. Resistance can be classified into intrinsic resistance, observed from the beginning of the therapy, and acquired resistance, observed after an initial positive response to therapy (Bergers and Hanahan 2008). Numerous mechanisms have been proposed for anti-angiogenic therapy resistance such as: up--regulation of alternative pro-angiogenic factors, direct effect of hypoxia stimulating tumor invasion and metastasis, vascular mimicry and the contribution of stromal cells , EPC and pro-angiogenic myeloid cells (Bergers and Hanahan 2008; Zarrin et al. 2017). VEGF-VEGFR2 activation can promote the accumulation of immature dendritic cells, myeloid-derived suppressor cells, and regulatory T cells (Treg) and can inhibit the migration of T lymphocytes but these effects can be reversed by anti-angiogenic reagents (Terme et al. 2013; Voron et al. 2014; Voron et al. 2015; Wallin et al. 2016; Yuan et al. 2014).

Adverse effects to anti-angiogenic therapies are explained by the fact that VEGF and the other targeted signaling pathways are not tumor-specific, thus they could exert systemic effects. The spectrum of side effects are hypertension, impaired wound healing, gastrointestinal perforation, thrombosis, proteinuria and occasional bleedings (Vasudev and Reynolds 2014). However, the most important side effect due to anti-angiogenic therapies is the promotion of tumor aggressiveness leading to increased invasion and metastases (Ebos et al. 2009; Pàez-Ribes et al. 2009). Even though there is no consistency in the literature, mainly due to different study settings, anti-angiogenic therapies (both monoclonal antibodies and TKIs) have been associated with increased tumor dissemination in preclinical and several clinical studies (Vasudev and Reynolds 2014).

The vessel normalization hypothesis was introduced by Rakesh Jain in 2001 and suggested an alternative mechanism through which anti-angiogenic therapy has anti-cancer potential. He claimed that anti-angiogenic therapies, instead of destroying, could normalize the tumor vasculature and further restore its architecture and functionality. The 'vessel normalization window' could offer the possibility of enhanced chemotherapy delivery to deeper tumor sites and increased tissue oxygenation (Huang et al. 2013; Jain 2005). This theory has been used to explain why the combination of bevacizumab or ramucirumab with chemotherapy has proven more effective in the clinical setting (Jayson et al. 2012). However contradictory evidence have been reported (Moserle et al. 2014). The treatment scheduling in order to gain the full potential of vessel normalization has been suggested as a crucial factor. In parallel, other studies have shown that anti-angiogenic therapy works at least partly through enhanced immune cell infiltration, by altering the anergic tumor endothelial phenotype leading to improved endothelial-immune cell interactions (Dings et al. 2011; Dirkx et al. 2006; Griffioen et al. 1999).

Evidence supporting that vessel normalization can improve cancer therapy has been reported in mouse models. These studies show that by improving tumor vessel perfusion and oxygenation, the efficacy of conventional therapies such as radiotherapy, chemotherapy and immunotherapy can be improved and metastatic dissemination can be lower (Carmeliet and Jain 2011; Jayson et al. 2012; Mazzone et al. 2009). Evidence that supports the idea that vessel normalization occurs in response to anti-angiogenic therapy has also been obtained from clinical studies.

1.5.2 Cancer Immunotherapy

In cancer immunotherapy the activation of the host's immune system is focused on generating an immunological response in the TME and eliminating tumor cells. An antibody targeting the cytotoxic T lymphocyte antigen 4 (CTLA-4) was the first immune checkpoint inhibitor (ICI) by the Food and Drug Administration in 2011 (Hodi et al. 2010; Xi Liu et al. 2020). So far, six more ICIs have been approved by the FDA, exclusively targeting the T cell co-inhibitory programmed cell death protein 1 (PD-1)/programmed cell death ligand 1 (PD-L1) signaling pathway (Beaver et al. 2017; Davis and Patel 2019), with clinical indications across 19 different cancer types (Twomey and Zhang 2021). While there is great potential in ICIs, only a small patient population achieve a durable response to monotherapy. However, new targets for checkpoint blockade are arising, including lymphocyte activation gene 3 (LAG-3), T cell immunoglobulin 3 (TIM3), V-domain immunoglobulin suppressor of T cell activation (VISTA), B7-H3 and T cell immunoreceptor with immunoglobulin and immunoreceptor tyrosine-based inhibitory motif domains (TIGIT), as adjuvant cancer drugs (Burugu et al. 2018; Donini et al. 2018; Marin-Acevedo et al. 2018).

Table 1.4 ICI - FDA approved.
Information from Twomey and Zhang 2021.

ICI - FDA approved	
anti-CTLA-4	ipilimumab
anti-PD-1	pembrolizumab
	nivolumab
	cemiplimab
anti-PD-L1	atezolizumab
	durvalumab
	avelumab

Further therapy approaches next to ICB are tumor-antigen vaccination-based (Sahin and Türeci 2018) and adoptive T cell transfer-based therapies. In case of cell-based therapies tumor-infiltrating lymphocytes are isolated, expanded and re-infused to boost anti-tumor response. Alternatively, chimeric antigen receptor (CAR) technology is used to modify T cell specificity for specific surface expressed tumor antigens (Kershaw et al. 2013; Rosenberg and Restifo 2015). These cell-based therapy approaches utilize the cytotoxic function of $CD8^+$ T cells to eliminate tumor cells. $CD8^+$ T cell activation can be achieved as well by non-cell based approaches, using bispecific antibodies to crosslink tumor cells and T cells.

1.5.2.1 Bispecific Antibodies

In contrast to a monoclonal antibody with one antigen specificity, a bispecific antibody (BsAb) has two antigen specificities by combining the features of two conventional monoclonal antibodies within one molecule. The binding of two antigens or epitopes simultaneously can be used for crosslinking. In tumor therapy this feature facilitates BsAb the specific recruitment of T cells to the tumor cells. That means the BsAb binds on the one side of the T cell, e.g., by targeting CD3ε chain and on the other side a tumor-associated antigen (TAA). The crosslinking of T cell and tumor cells can lead to T cell activation and improved tumor killing (Brinkmann and Kontermann 2017; Choi et al. 2011; Dhimolea and Reichert 2012; Kontermann 2012). So far, BsAb can be synthesized by three different methods. In case of chemical conjugation, two antibodies are synthesized with chemical crosslinkers which subsequently fuse in a chemical reaction to form one BsAb. In the quadroma technology two hybridoma cell lines must undergo somatic fusion to receive BsAbs. In the third method, called genetic engineering of BsAb, BsAb are generated by recombinant DNA technology (Chames and Baty 2009).

BsAb which are generated by genetic engineering are subdivided into IgG-like BsAb or non-IgG-like BsAb. A normal monovalent IgG like antibody consists of a light chain being subdivided into two Ig-like domains and a heavy chain that comprises four Ig-like domains. The heavy and the light chain bind to each other to form a pair that dimerize with a second pair to form an antibody (**see Fig. 1.12A**) (Suurs et al. 2019). The antibody is divided into Fc region (tail), the hinge region (connection site of both chain pairs) and Fab regions (binding site). The Fc region triggers effector function of the immune system, such as target cell killing (Scott et al. 2012; Suurs et al. 2019). Formats for IgG-like BsAb can be crossMab, ortho-Fab IgG, DVD-Ig, “knob into hole” IgG, two in one IgG, IgG-single chain variable fragment (scFv) and scFv2-Fv (Kontermann and Brinkmann 2015). A common feature of these formats is a relatively large size, a high similarity to conventional antibodies and a long serum half-live which is enabled by, e.g., FcRn (neonatal Fc receptor)-mediated recycling. In comparison, non-IgG like BsAbs are smaller. Therefore, these constructs have advantages for therapeutic usage due to improved tissue penetrating, tumor-infiltrating properties, however, have a short serum half-life (Fan et al. 2015; Kontermann and Brinkmann 2015; Mitragotri et al. 2014). Non-IgG like BsAb are received by cloning of two variable parental monoclonal antibody domains connected by a linker. Possible formats for non-IgG like antibody cloning are tandem scFvs, dual affinity retargeting molecules (DARTs), diabody format, dock-and-lock (DNL), single-chain diabodies, tandem diabodies, bispecific T cell engagers (BiTE) and nanobodies (Fan et al. 2015). A summary of already approved or in clinical trials tested BsAb, IgG-like or non-IgG like is shown in **Fig. 1.12B**.

The tandem single-chain variable fragments (scFvs) format is composed of two scFvs which are connected by a 3-11 amino acid long linker, such as a glycine serine repeat motif (Chames and Baty 2009; Schumacher et al. 2014). One single scFvs is made up by the variable regions (VH and VL) which are connected to each other by a flexible peptide linker. The structure of a tandem scFv can be described as: VLa-linker1-VHa-linker2-VHb-linker3-VLb (a and b indicate the origin from different parenteral monoclonal antibodies) (Löffler et al. 2000). The length of linkers 1 and 3 defines the folding of each scFv. In comparison the flexibility of the connected scFvs is characterized by linker 2. In case of a too-long linker 2 antigen binding is permitted because of high rotation flexibility. A very short linker 2 prevents intra-chain but not inter-chain interactions of the corresponding scFvs. To achieve flexible and strong target interacting tandem scFvs, linker lengths and types must be optimized (May and Glode 2016).

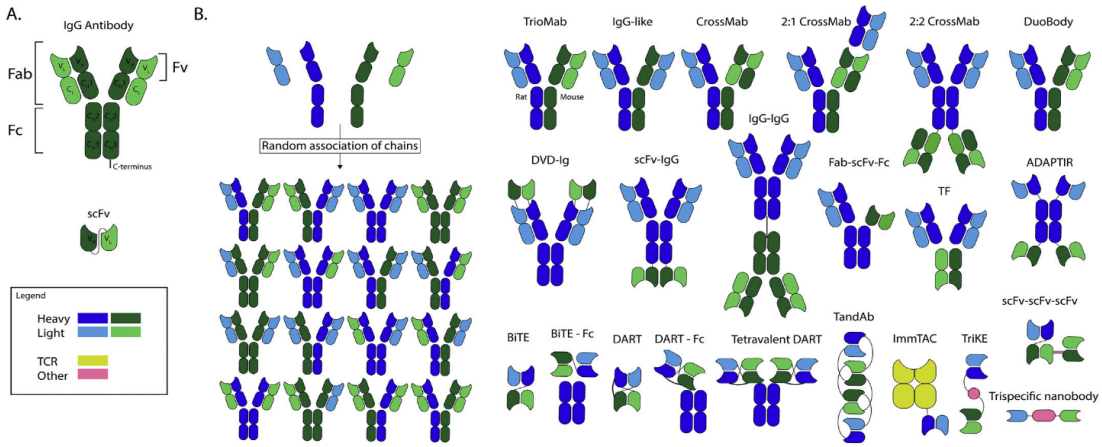

Figure 1.12 IgG Antibody structure and BsAb formats. A) Structure of IgG antibody and scFv Fragment. **B)** Already approved or in clinical trials tested BsAb formats for cancer immunotherapy. Adapted from Suurs et al. 2019.

1.5.3 Combination therapy

The rationale of combining anti-angiogenic therapy with immunotherapy lies in the interconnected biology of tumor blood vessels and tumor-infiltrating leukocytes. Vessel normalization, up-regulation of adhesion molecules and enhanced blood flow are some of the benefits that anti-angiogenic therapies can offer and facilitate a more permissive microenvironment leading to improved leukocyte tumor extravasation. In parallel, therapies targeting pro-angiogenic factors can create a less immunosuppressive TME.

Interestingly, anti-angiogenic therapies have been associated with direct immunomodulatory effects (Finke et al. 2008; Ko et al. 2009; Roland et al. 2009). Additionally, tumor immunotherapy is dependent on effective leukocyte migration and activation to the tumor sites. So far, this combination has shown positive results in various therapeutic settings (Hodi et al.

2014; Ramjiawan et al. 2017; Wallin et al. 2016). For instance, combination of anti-VEGF and adoptive T cell transfer in murine melanoma increased T cell tumor infiltration and led to increased survival (Shrimali et al. 2010). Anti-VEGF has also been combined with anti-CD40 *in vivo* leading to survival and reduced angiogenesis (Selvaraj et al. 2014). An antibody targeting both VEGF-A and Angiopoietin-2, which is another important pro-angiogenic factor in the TME, showed improved responses *in vivo* in many preclinical models and it was also combined with PD-1 inhibition (Schmittnaegel et al. 2017). Sunitinib treatment combined with vaccine-based immunotherapy enhanced $CD8^+$ T cell responses, and reduced the recruitment of MDSC and T_{reg} cells in the tumor microenvironment and reduced tumor growth (Bose et al. 2011). Notably, sunitinib is capable of decreasing MDSC and T_{reg} aside from its role in modulating the tumor vasculature (Finke et al. 2008; Ko et al. 2009).

A combination of CTLA-4 blockade (ipilimumab) and VEGF inhibition (bevacizumab) can be safely administered and reveals that VEGF-A blockade influences inflammation, lymphocyte trafficking, and immune regulation. This provides a basis for further investigating the double role of angiogenic factors in blood vessel formation and immune regulation as well as future combinations of anti-angiogenesis agents and immune checkpoint blockade (Hodi et al. 2014).

Although the combination of anti-angiogenesis and anti-tumor immune activation shows promise for treating solid tumors, the use of bispecific antibodies has pharmaco-economic advantages and also provides the advantage of blocking both pathways simultaneously from the beginning of therapy, and may thus avoid tumor escape mechanisms.

Some studies have demonstrated the efficacy of bispecific antibodies strategy. A heterodimeric Fc-based bispecific antibody simultaneously targeting VEGFR2 and c-MET, efficiently inhibited the downstream signaling and tube formation stimulated by the two receptors in human endothelial cells, and exhibited more potent anti-tumor (Choi et al. 2013). Tetravalent bispecific antibody (Ang-2-VEGF-TAvi6) binding VEGF-A with two arms based on bevacizumab (Avastin®) abrogated angiogenesis completely in the cornea micro pocket assay (Scheuer et al. 2016). Bispecific antibody anti-VEGFR2–MICA (JZC01), targeted vascular endothelial growth factor receptor 2 (VEGFR2) and inhibited tumorigenesis by blocking the VEGFR2 signaling pathway. Additionally, it increased the infiltration and activation of NK and $CD8^+$ T cells in the tumor microenvironment, promoting the release of IFN-γ and engaging activated lymphocytes to lysis of VEGFR2-expressing tumor cells and effectively reducing the tumor vascular density.

Given the success in preclinical models, anti-angiogenic therapy in combination with adoptive cell therapy may offer another promising therapy for the treatment of cancer.

1.6 AIMS OF THE STUDY

As targeting of reactive cytotoxic cells to the tumor microenvironment appears to be essential for successful immune-mediated tumor eradication, it seems desirable to develop new strategies leading to tumor vessel activation that consequently can increase the transendothelial migration of effector T cells into the tumor.

We hypothesized that tumor endothelial cell activation could be facilitated indirectly by T cell activation *in situ.* As a first approach, VEGFR2-binding bifunctional protein constructs were used to deliver cytokines to vascular endothelial cells. In a second approach, we studied tetravalent bispecific monoclonal antibodies (BiMAbs) in the $(scFv\text{-}Fc\text{-}scFv)_2$ format that bind to VEGFR2 or TIE2 endothelial cell (EC) growth factor receptors on one side, and the stimulatory/co-stimulatory T cell molecules CD3ε or CD28 on the other. VEGFR2 and TIE2 serve as examples for receptors that are selectively expressed by the growing tumor neovasculature. Local CD3ε-mediated T cell activation would lead to the release of cytokines like TNF-α and IFN-γ that in turn activate endothelial cells to express adhesion molecules for improved transmigration. Antibody-mediated blocking of VEGF binding to VEGFR2 could concomitantly exert anti-angiogenic effects and lead to tumor vasculature normalization. As a consequence of HUVEC activation, due to treatment with self-made stimulatory and co-stimulatory bispecific antibodies, adhesion molecules like E-selectin and VCAM1 can be up-regulated and were also used as a targeting point for BiMAbs that will bind $CD8^+$ T cells to prioritize the migration of these cytotoxic T cells into the tumor bed.

Enforced targeting of immune effector cells (cytotoxic T cells, NK cells) to tumor-associated endothelial cells tissues using bispecific constructs would facilitate an improved cytolytic response against tumors. We reason that the improvement of T-cell binding to growing endothelial cells and subsequent infiltration towards the tumor is critical for the development of novel combinatorial strategies conferring improved patient response rates to immunotherapy.

1st approach – Direct EC activation - VEGFR2-binding bifunctional protein constructs were used to deliver cytokines to vascular endothelial cells.

⇒ **αVEGFR2xFc-mIgG2a-rhIL-1β** and **αVEGFR2xFc-mIgG2a-rhTNFα**

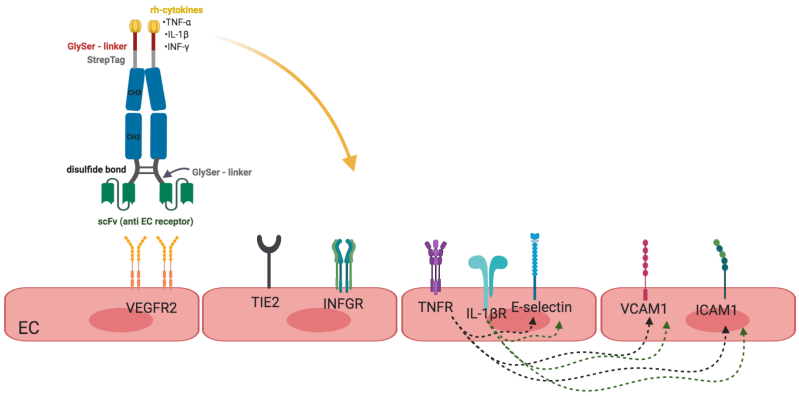

2nd approach - Indirect EC activation - Tetravalent bispecific monoclonal antibodies (BiMAbs)

⇒ **αVEGFR2xFc-hIgG1-αCD3 and αTIE2xFc-hIgG1-αCD28**

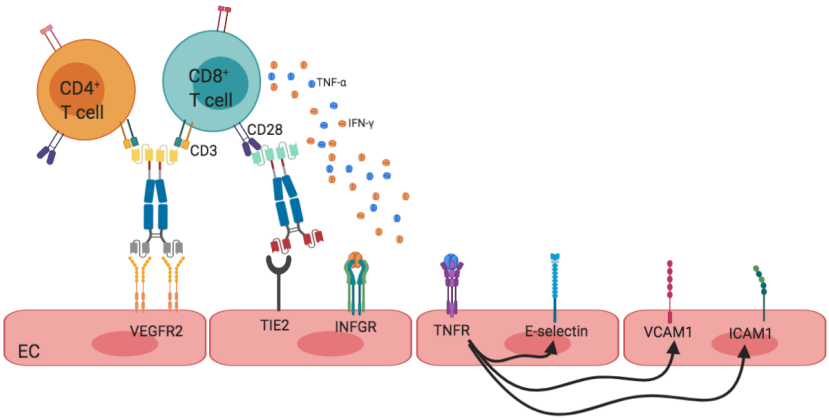

⇒ Targeting of CD8+ T cell to the tumor

VEGFR2xFc-hIgG1-αCD3 and αTIE2xFc-hIgG1-αCD28 plus αEC-hIgG1-αCD8

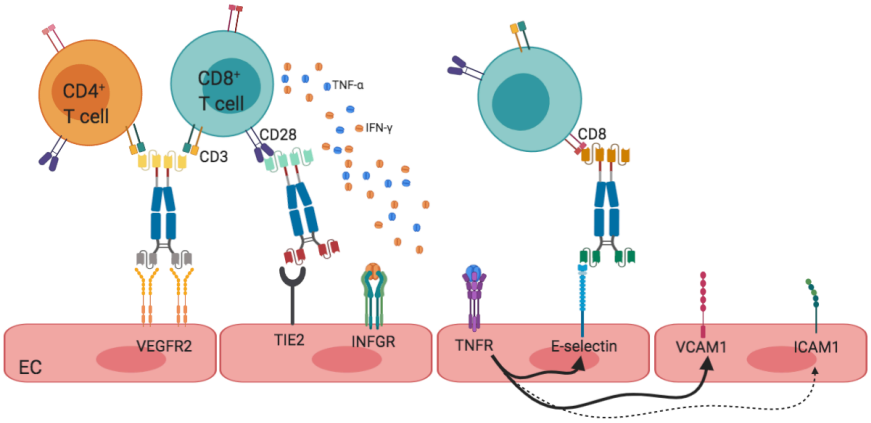

2 MATERIALS AND METHODS

2.1 MATERIALS

2.1.1 Cell lines and primary cells

Name	Origin	Supplier
FreeStyle™ CHO-S	Chinese hamster ovarian cells (CHO)	Thermo Scientific
HBMEC-60	Human bone marrow endothelial cell line	Sanquin, Amsterdam
HUVEC	Human umbilical vein endothelial cells	Promocell, Heidelberg
MCF-7	Human breast adenocarcinoma cell line	DKFZ, Heidelberg
PBMC	Human buffy coats obtained from blood donations of healthy volunteers	Blutbank, Heidelberg/Mannheim Deutsches Rotes Kreuz

2.1.2 Cell culture media, supplements and reagents

Product	Supplier
Antibiotic antifungal (100X) (Anti-Anti)	Gibco
Biocoll separating solution • *1.077 g/mL, isotonic solution*	Biochrom
Cell dissociation solution PBS based - enzyme-free	Millipore
Dulbecco's phosphate buffered saline (1x) (DPBS) • *Without calcium chloride and magnesium chloride, pH 7.2*	Sigma Aldrich
Endothelial cell growth medium 2 (ECGM2) • *Fetal calf serum: 0.02 ml/ml* • *Epidermal growth factor (recombinant human): 5 ng/ml* • *Basic fibroblast growth factor (recombinant human): 10 ng/ml* • *Insulin-like growth factor (R3 IGF-1): 20 ng/ml* • *Vascular endothelial growth factor 165 (recombinant human): 0.5 ng/ml* • *Ascorbic acid: 1 µg/ml* • *Heparin: 22.5 µg/ml* • *Hydrocortisone: 0.2 µg/ml*	Promocell
Fetal bovine serum (FBS) • *heat-inactivated at 56 °C for 30 minutes*	Biochrom
GlutaMAX™ -I (100X), *200 mM*	Gibco
HT media supplement (50×) Hybri-Max™ • *Hypoxanthine 6.8 mg* • *Thymidine 1.94 mg*	Sigma Aldrich

PBS (Phosphate buffered saline)	Sigma Aldrich
Penicillin/Streptomycin-Solution (P/S) • *10,000 U Penicillin, 10,000 µg/ml Straptomycin*	Sigma Aldrich
PowerCHO-2 CD medium (chemically defined) • *HEPES, 1x Pluronic® F-68 without L-glutamine, HT, phenol red* • *8 mM GlutaMAXTM (L-alanyl-L-glutamine dipeptide)* • *1x HT Media Supplement Hybridmax™ (2 vials / 1L)* *13.6 mg/L hypoxanthine, 3.9 mg/L thymidine* • *0.5x Antibiotic Antimycotic solution (Anti-Anti)* *50 units/mL penicillin; 0.05 mg/mL streptomycin; 0.1 µg/mL amphotericin B*	Lonza
ProCHO-4 transfection medium • *HEPES, 1x Pluronic® F-68 without L-glutamine, HT, phenol red* • *4 mM GlutaMAX™ (L-alanyl-L-glutamine dipeptide)* • *1x HT Media Supplement Hybridmax™ (2 vials / 1L)* *13.6 mg/L hypoxanthine, 3.9 mg/L thymidine* • *0.5x Antibiotic Antimycotic solution (Anti-Anti)* *50 units/mL penicillin; 0.05 mg/mL streptomycin; 0.1 µg/mL amphotericin B*	Lonza
RPMI medium 1640 (1x) (Roswell park memorial institute) • *Without L-glutamine, phenol red* • *10% (v/v) Heat-inactivated fetal bovine serum (FBS)* • *2 mM GlutaMAXTM (L-alanyl-L-glutamine dipeptide)* • *100 Units/mL penicillin and 0.1 mg/mL streptomycin (Pen-Strep)*	Gibco
Trypsin-EDTA (1x) 0.05%	Gibco
Trypan blue solution 0.5% (w/v)	Biochrom

2.1.3 Magnetic cell sorting (MACS)

Product	Supplier
MACS multi stand LS columns Pan T cell isolation kit, human Quadro MACS magnet	Miltenyi Biotech

2.1.4 Commercial recombinant human cytokines and stimulation antibodies

Cytokines	Final Concentration	Supplier	Appl.
Anti-CD3 (OKT3)	5 ng/ml	Homemade	T cell stimulation
Anti-CD28 (9.3)	100 ng/ml	Homemade	T cell stimulation
Human IL-2	20 U/ml	Miltenyi Biotech	Culture maintenance
Human IL-12	2 ng/ml	Biolegend	PBMC stimulation
Human IL-1β	20 ng/ml	Biolegend	EC stimulation
Human TNF-α	10 ng/ml	Biolegend	EC stimulation
Human TNF-α	1:50	Biolegend	ELISA
Human NF-γ	1:100	Biolegend	ELISA

2.1.5 Reagents for bacteria transformation, plasmid purification, protein expression purification and quantification

Product	Supplier
Chemically competent *Escherichia coli* • *strain XL-1 Blue*	Agilent
Ethidium bromide	Carl Roth
InstantBlue™ Coomassie protein staining solution	Expedeon
LB medium, pH 7.0 • *1000 mL ddH_2O* • *10 g peptone from casein, tryptic digest* • *5 g yeast extract ultrapure* • *5 g NaCl*	 Sigma Aldrich Gerbu Carl Roth
LB AMP medium • *LB medium* • *0.1 mg/mL ampicillin*	Sigma Aldrich
LB AMP agar plates • *1000 ml LB medium, pH 7.0* • *15 g Agar-Agar* • *1 mL ampicillin (100 mg/mL stock)*	 Roth Sigma Aldrich
Nuclease-free water	Thermo Scientific
QIAGEN gel extraction kit	QIAGEN

QIAGEN plasmid Maxi kit	QIAGEN
QIAGEN miniprep kit	QIAGEN
RunBlue™ prestained dual color marker	Expedeon
RunBlue™ TEO-Tricine SDS-Precast Gels ▪ *10%, 10x10 cm, 12 well* ▪ *10%, 10x10 cm, 17 well*	Expedeon
Strep-Tactin® Superflow ® high capacity resin • *50% suspension*	IBA Lifesciences
Valproic acid sodium salt (VPA) • *500 mM VPA in ddH20 stock solution was always prepared freshly and 0.22 µm sterile filtrated prior usage.*	Sigma-Aldrich
25 kDa-Linear polyethyleneimine (PEI) • *Briefly, 100 mg PEI in 100 mL ddH_2O [1 mg/mL] was stirred at pH 2.0 for 3 hours until PEI was completely dissolved, followed by pH 7.0 neutralization and 0.22 µm sterile filtration. 5 mL PEI aliquots were stored at -80°C and thaw directly before its usage for transfection.*	Polysciences

2.1.6 Antibodies for flow cytometry

2.1.6.1 Immune cell markers

Marker	Clone	Isotype	Conjugate	Final Conc. (µg/ml)	Supplier	Appl.
CD3	UCHT1	mIgG1	APC/Cy7	1	BioLegend	FACS
CD3	HIT3a	mIgG2a	AF488	1	BioLegend	FACS
CD3	HIT3a	mIgG2a	PerCp/Cy5.5	1	BioLegend	FACS
CD4	OKT4	mIgG2b	BV510	1	BioLegend	FACS
CD4	RPA-T4	mIgG1	AF488	1	BioLegend	FACS
CD4	RPA-T4	mIgG1	PE	1	BioLegend	FACS
CD8	RPA-T8	mIgG1	V450	1	BD Biosciences	FACS
CD8	SK1	mIgG1	Pacific blue	1	BioLegend	FACS
CD8	SK1	mIgG1	APC	1	BioLegend	FACS
CD19	HIB19	mIgG1	PerCp/Cy5.5	1	BioLegend	FACS
CD19	HIB19	mIgG1	AF647	1	BioLegend	FACS
CD19	HIB19	mIgG1	BV510	0.5	BioLegend	FACS
CD14	HCD14	mIgG1	PerCp/Cy5.5	1	BioLegend	FACS
CD14	HCD14	mIgG1	BV510	0.5	BioLegend	FACS
CD56	HCD56	mIgG1	BV510	0.5	BioLegend	FACS
CD335 (NKp46)	9E2	mIgG1	PE/Cy7	1	BioLegend	FACS

CD25	BC96	mIgG1	AF488	1	BioLegend	FACS
CD25	BC96	mIgG1	PerCp/Cy5.5	1	BioLegend	FACS
CD25	M-A251	mIgG1	AF488	1	BioLegend	FACS
CD25	B696	mIgG1	APC/Cy7	1	BioLegend	FACS
CD28	CD28.2	mIgG1	PE/Cy7	1.5	BioLegend	FACS
CD69	FN50	mIgG1	PE	1	BioLegend	FACS
CD69	FN50	mIgG1	PE/Cy7	1	BioLegend	FACS
4-1BB	4B4-1	mIgG1	PE	1	BioLegend	FACS
4-1BB	4B4-1	mIgG1	PE/Cy7	1	BioLegend	FACS
4-1BB	4B4-1	mIgG1	PerCpCy5.5	1	BioLegend	FACS
CD49d (ITGα4)	9F10	mIgG1	PE	1	BioLegend	FACS
CD44 (ITGβ1)	TS2/16	mIgG1	PE	1	BioLegend	FACS
CD18 (ITGβ2)	TS1/18	mIgG1	PE	1	BioLegend	FACS
CD162 (PSGL-1)	KPL-1	mIgG1	PE	1	BioLegend	FACS
CD183 (CXCR3)	G025H7	mIgG1	APC	1	BioLegend	FACS
CD184 (CXCR4)	12G5	mIgG2a	APC	1	BioLegend	FACS
CD279 (PD-1)	EH12.2H7	mIgG1	APC	1	BioLegend	FACS
CD366 (TIM3)	F38-2E2	mIgG1	APC	1	BioLegend	FACS
TIGIT (VSTM3)	A15153G	mIgG2a	PE	1	BioLegend	FACS

2.1.6.2 Endothelial cell markers

Marker	**Clone**	**Isotype**	**Conjugate**	**Final Conc. (μg/μl)**	**Supplier**	**Appl.**
CD105	43A3	mIgG1	PE/Cy7	0.5	BioLegend	FACS
CD105	43A3	mIgG1	PerCpCy5.5	0.5	BioLegend	FACS
CD62E (E-selectin)	HAE-1f	mIgG1	PE	1	BioLegend	FACS
CD106 (VCAM1)	STA	mIgG1	APC	1	BioLegend	FACS
CD54 (ICAM1)	HA58	mIgG1	APC	0.2	BioLegend	FACS
CD309 (VEGFR2)	7D4-6	mIgG1	APC	1	BioLegend	FACS
CD202B (TIE2)	33.1(Ab33)	mIgG1	PE	1	BioLegend	FACS
CD274 (PD-L1)	29E.2A3	mIgG2b	PE	1	BioLegend	FACS
CD273 (PD-L2)	24F.10C12	mIgG2a	PE	1	BioLegend	FACS

2.1.6.3 Isotype Controls

Isotype Controls	Conjugate	Supplier	Appl.
mIgG1	APC	BioLegend	FACS
mIgG1	PE	BioLegend	FACS
mIgG2a	PE	BioLegend	FACS
mIgG2b	PE	BioLegend	FACS

2.1.6.4 Secondary Antibodies

Antibody	Clone	Isotype	Conjugate	Dilution	Supplier	Appl.
Anti-human IgG1	AD2	mIgG2a	PE	1:200	BioLegend	FACS
Anti-mouse-IgG2a	10G7	goat IgG	PE	1:200	BioLegend	FACS

2.1.7 Dyes and reagents for flow cytometry

Product	Dilution	Supplier	Appl.
Precision counting beads	1:10	BioLegend	Cell counting
Propidium iodide (PI)	1:2500	BioLegend	Live/dead
Sandoglobulin	1:15	CSL Behring	Fc blocking
TruStain (human)	1:50	BioLegend	Fc blocking
Zombie Aqua fixable viability kit	1:300	BioLegend	Live/dead

2.1.8 ELISA antibodies and reagents

Product		Conjugate	Con. (µg/µl)	Supplier
Human-IFN-γ	Capture antibody	-	2.5	BioLegend
	Detection antibody	Biotin	0.5	BioLegend
	Recombinant human cytokine	-	1:100	BioLegend
Human-TNF-α	Capture antibody	-	5	BioLegend
	Detection antibody	Biotin	1	BioLegend
	Recombinant human cytokine	-	1:100	BioLegend
Streptavidin - HRP	Peroxidase, SAv-HRP		1:2500	BioLegend
TMB Substrate Set	3, 3', 5, 5' tetramethyl benzidine	-	-	BioLegend

2.1.9 Cytotoxicity Assay

Product	Supplier
CyQUANT™ LDH Cytotoxicity Assay kit	Invitrogen

2.1.10 Buffer and solutions

Buffer	Ingredients	Supplier	App.
Coating Buffer, pH 9.6	0.05 M carbonate-bicarbonate buffer	Sigma Aldrich	ELISA
Blocking Solution, pH 7.4	DPBS (1x) w/o $MgCl_2$ $CaCl_2$	Sigma Aldrich	
	0.05% (v/v) Tween-20	Sigma Aldrich	
	2.5% (w/v) BSA (Bovine serum albumin, fraction V)	PAA	
Sample Buffer, pH 7.4	DPBS (1x) w/o $MgCl_2$ $CaCl_2$	Sigma Aldrich	
	0.05% (v/v) Tween-20	Sigma Aldrich	
	0.5% (w/v) BSA (Bovine serum albumin, fraction V)	PAA	
Stop Solution	1 M H_2SO_4	Carl Roth	
Washing buffer, pH 7.2	DPBS (1x), pH7.2, no $MgCl_2$ $CaCl_2$	Sigma Aldrich	
	0.5% (w/v) BSA (Bovine serum albumin, fraction V)	PAA	
FACS Buffer	DPBS w/o $MgCl_2$ $CaCl_2$	Sigma Aldrich	FACS
	1% BSA (Bovine serum albumin, fraction V)	PAA	
	2 mM EDTA (Ethylenediamine tetraacetic acid)	Sigma Aldrich	
	0.05% NaN3 (Sodium Azide)	Sigma Aldrich	
MACS Buffer	DPBS w/o $MgCl_2$ $CaCl_2$	Sigma Aldrich	T cell isolation
	0.5% BSA (Bovine serum albumin, fraction V)	PAA	
	2 mM EDTA (Ethylenediamine tetraacetic acid)	Sigma Aldrich	
Strep-Tactin elution buffer	• 1x PBS, pH 7.4 (self-prepared) • 5 mM Desthioiotin	IBA Lifesciences	Protein purification
Sample Buffer	• RunBlue™ LDS Sample Buffer – TEO-Tricine 4x • 40 mM dithiothreitol (DTT) for reducing conditions	Expedeon Sigma-Aldrich	SDS-PAGE

2.1.11 Reagents for Transmigration assay

Product	Supplier
Fibronectin 1% (human)	Sigma Aldrich
FITC-Dextran (3-5 kDa)	Sigma Aldrich

2.1.12 Plastic and consumables

Product	Supplier
Cell Culture Flasks (25, 75 and 150 cm^2) • Vented closure, cell culture-treated	TPP
Cell culture plates (6, 24 and 96-well) • Flat-bottom	TPP
Corning® erlenmeyer cell culture flask (125, 250 and 500 mL) • Erlenmeyer flask with vent cap, polycarbonate	Sigma-Aldrich
Eppendorf Tubes (1.5 and 2 mL)	Eppendorf
FACS tubes	BD Biosciences
Falcon™ conical 15 and 50 mL tubes • Polypropylene	BD Biosciences
Microplate 96 Well, Black, Non-Binding	Greiner Bio-One
Nunc™ 96-well Microwell™ Maxisorp™ flat-bottom plate	Thermo Scientific
Nunc™ 96-well polypropylene V-bottom plate	Thermo Scientific
Pipette tips	Starlab
Serological pipettes	Falcon
Slide-A-lyzer™ dialysis cassettes, 20 kda mwco, 3 ml	Thermo Scientific
Transwell Inserts • 24-well hanging inserts, 5 μm pore size, PET)	Millipore

2.1.13 Equipment

Devices	Manufector
Axiovert 40 C inverted phase contrast microscope	Zeiss
Azure Imager c400-600 (In-gel fluorescence)	Azure biosystems
Brand® counting chamber (improved Neubauer chamber)	Sigma-Aldrich
Cassettes with occlusion lever (Pressure lever) • *Material: POM-C*	Ismatec
Electrophoresis chamber (SDS-PAGE) – mini cell	Thermo Scientififc
Eppendorf™ Innova™ 44 Incubator Shaker	Eppendorf
Flow cytometer, BD FACS Canto™ II	BD Biosciences
Floor standing centrifuge - ROTANTA 460 RC	Hettich
Fluorescence Reader, Fluoroskan ascent FL	Thermo Scientific
Gammacell 40 Exactor	Theratonics
Heating shaker	

HeracellTM240i CO_2 incubator with stainless steel chamber	Thermo Scientific
INFORS HT Minitron, CO2 incubator • *Integrated orbital shaker with 50 mm shaking diameter* • *plate heat exchanger, 1.5 KW*	INFORS HT Wutke
Inverted laboratory microscope leica DM IL LED	LEICA
Laminar flow hood - HERAsafe® HS/HSP	Heraeus
Low-pressure liquid chromatography columns • *Luer Lock inlet and outlet fittings, non-jacketed, polyethylene bed supports.*	Sigma-Aldrich
MaxQ™2000 benchtop orbital shaker CO2 resistant • 19 mm shaking diameter	Thermo Scientific
Megafuge 2.0R	Heraeus
Microcentrifuge Fresco 17	Heraeus
Multilable plate reader, Multiskan EX	Thermo Scientific
Nano Drop	
PTC-200 thermal cycler	MJ Research
Peristaltic Pump - REGLO digital MS-4/6-100 • *4 channels, 6 rolls, 0.002 – 43 mL/min*	Ismatec
pH-Meter 766	Knick
Pipetboy	INTEGRA
Pipettes	Thermo Scientific
Saint-Gobain TygonTM LMT-55 Tubing • *3.17 mm inner diameter, wall: 0.86 mm, length 38.1 mm* • *Material: Tygon R3607* • *Three stop configuration, black and white*	Fisher Scientific

2.1.14 Software

Software	Manufector
Biorender (trial version)	Biorender
FACSDIVA v.6.1.2	BD
FlowJo v.10.1	Treestar
Graph Pad Prism 7	GraphPad Software Inc.
Mendeley	Elsevier B.V.
Microsoft Office 2018	Microsoft Corporation

2.2 METHODS

2.2.1 Isolation of peripheral blood mononuclear cells (PBMC)

Human peripheral blood mononuclear cells (PBMC) were freshly isolated in every experiment from blood of healthy donors by density gradient centrifugation. Therefore, 15 ml of Biocoll separating solution was added to 50 ml Falcon tubes under sterile conditions. Blood was diluted in DPBS and gently pipetted on the prepared Biocoll. The PBMC were then separated from the rest of the blood cells by centrifugation at 1800 rpm for 25 minutes (without break).

After centrifugation, blood components were separated and four phases are distinguishable: erythrocytes (present as pellet), followed by Ficoll, a white layer of PBMC at the interface and right the majority of the platelets and the plasma layer at the top. PBMC were collected and washed three times with DPBS. The washing steps were performed at 800 rpm for 15 min, 10 min and 5 min to completely remove residual Ficoll medium. For cell counting, cells were diluted in trypan blue (1:100) for live-dead discrimination and placed in a Neubauer counting chamber.

2.2.2 Purification of CD3+ T cells with Magnetic cell sorting (MACS)

Partially purified PBL (peripheral blood lymphocytes) were obtained by routine overnight culture of PBMC, once most of the monocytes have settled down and remained adherent to the flask. T cells were freshly isolated in every experiment from PBL using MACS isolation. $CD3^+$ T cells were purified by negative selection using the pan-T cell isolation kit to obtain “untouched” cells, according to manufacturer’s instructions. Briefly, PBL were resuspended in cold MACS buffer (see table.) and incubated with biotin-antibody cocktail for 5 min at 4 °C.

After antibody-labelling, cells were incubated with MicroBead cocktail for 10 min at 4 °C and applied onto the column. After collecting the flow-through, that contained the unlabeled cells representing the enriched T cells, the column was washed with MACS buffer and the effluent was also collected. The sort was performed on a MACS MultiStand with Quadro MACS magnet using MS columns.

$CD3^+$ T cells were usually used directly after isolation, otherwise, were cultured in RPMI-1640 medium supplemented with 10% heat-inactivated fetal bovine serum (iFBS), 1% penicillin/streptomycin and 2 mM GlutaMAX^{TM} solution in the presence of 20 U/mL of IL-2, at 37 °C and 5% CO_2.

2.2.3 Cell Culture

PBMC were cultured with a final concentration of $2x10^6$ cells/ml in RPMI-1640 medium supplemented with 10% heat-inactivated fetal bovine serum (iFBS), 1% penicillin/streptomycin and 2 mM GlutaMAX™ solution. 20 U/ml of IL-2 was added to maintain T cell survival and PBMC culture was kept at 37 °C and 5% CO_2.

Primary human umbilical vein endothelial cells (HUVEC) and human immortalized bone marrow endothelial cells (HBMEC-60) were cultured in endothelial cell growth medium 2 (ECGM2), supplemented with 10% heat-inactivated fetal bovine serum (iFBS) and 1% penicillin/streptomycin at 37 °C in a 5% CO_2 atmosphere. The cells were split when confluency was 80-90% and used until passage 5 (HUVEC) or passage 20 (HBMEC-60). Adherent cells were detached using cell dissociation buffer (PBS based).
MCF-7 were cultured in RPMI-1640 medium supplemented with 10% heat-inactivated fetal bovine serum (iFBS), 1% penicillin/streptomycin and 2 mM GlutaMAX™ solution, at 37 °C and 5% CO_2.

FreestyleTM CHO-S cells (CHO-S) were cultured routinely in 500 mL round-bottom glass bottles filled with 100 mL PowerCHO-2CD medium supplemented with 8 mM GlutaMAXTM, 0.5x Anti-Anti and 1x HT at 37 °C, 130 rpm with a 19 mm shaking diameter in a humidified 8% CO2 atmosphere. CHO-S were cultured until a density of $4x10^6$ cells/mL was reached and were subsequently either 1:10 diluted for subculture or directly processed for transfection as described in section 2.2.4.

2.2.4 Cloning, expression and purification of VEGFR2 antibody-cytokine fusion proteins and BiMAbs

All constructs used in this study were designed and kindly provided by PD Dr. Frank Momburg (DKFZ). Cloning strategies were developed by PD Dr. Frank Momburg and carried out by Nadja Bulbuc (DKFZ). Individual protein sequences are shown in the Appendix section. Fully assembled expression vectors were confirmed by DNA sequencing prior subsequent protein production. The expression and purification methods used in this study were optimized by Marten Mayer (DKFZ) and carried out by Susanne Knabe (DKFZ).

2.2.4.1 Cloning of anti-VEGFR2 scFv-Fc fusion protein

To construct the anti-VEGFR2 scFv-Fc fusion protein, a synthetic cDNA fragment comprising anti-VEGFR2 scFv (variable VH and VL regions of KDR-1121, ramucirumab) was ordered from BioCat GmbH (for sequences see appendix).

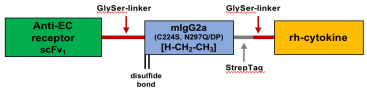

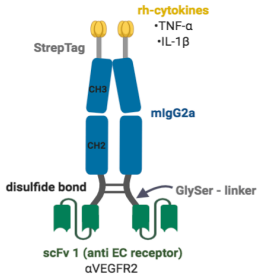

The synthetic cDNA was first cloned at the 3' end of an IL-2 ER leader sequence in pBluescript KSII+ cut using restriction sites at the 5' and 3' ends and subsequently cloned into an appropriately cut pcDNA3.1(–) expression vector already containing a mouse IgG2a hinge-CH2-CH3 fragment. A $(G_4S)_3$ linker separated the scFv sequence from the hinge region and the Fc portion. The 2 intermolecular disulfide bridges of the hinge region lead to homodimerization of the construct. To avoid aberrant disulfide bridge formation in the absence of Ig light chain, the mutation C224S was introduced. To reduce Fc receptor binding the glycan mutation N297Q was introduced. At the C-terminal end of the CH3 domain a was cloned that was used for Strep-Tactin affinity purification.

VEGFR2 antibody-cytokine fusion were generated by cloning a DNA fragment comprising a recombinant human cytokines, IL-1β or TNF-α were cloned without their original ER leader sequences after the Strep tag-II sequence.

2.2.4.2 Cloning of monoclonal single-chain bispesific antibodies

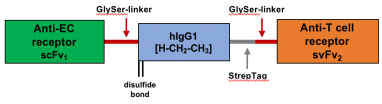

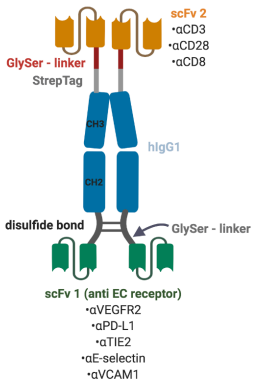

In tetravalent bispecific antibodies a second T-cell activating scFv (anti-CD3ε antibody OKT3), a T-cell co-stimulatory scFv (anti-CD28 antibody 9.3), or a CD8-binding scFv (OKT8) were added after a short Gly_4 linker.

cDNAs encoding scFv antibodies with EC specificities (anti-TIE2, anti-VCAM1, anti-E-selectin) or with specificity for PD-L1 were cloned at the N-terminal end of bispecific antibodies similar to the anti-VEGFR2 scFv described above, however, preceded by an IgGκ ER leader sequence.

After ligations, minipreps were analyzed by restriction enzyme analysis. Positive clone sequences were confirmed by Sanger DNA sequencing.

2.2.4.3 Plasmid amplification and purification procedure

For plasmid amplification chemocompetent bacteria were transformed by standard heat-shock procedure. Briefly, 1 µg plasmid DNA was added to thaw bacterial stocks (10 µL bacteria + 40 µL H20) and subsequently incubated for 20 min on ice. Next, a 90 sec heat-shock at 42 °C was performed followed by a 5 min incubation step on ice. Transformed bacteria were plated onto LB AMP agar plates and incubated at 37 °C overnight. Next, 100 mL LB AMP medium-based liquid bacterial cultures were prepared using scraped bacteria from the agar plate. Liquid cultures were incubated overnight at 180 rpm at 37 °C. Finally, plasmids were purified using the QIAGEN Plasmid Maxi preparation kit according to the manufacturer's protocol. Plasmid concentration was measured at 260nm (A260) and 280nm (A280) absorbance. Only plasmid preparations with A260/A280 ratios between 1.87 and 1.92 were used for subsequent mammalian cell-based protein productions.

2.2.4.4 PEI-based transfection procedure for large-scale 100 mL CHO-S TGE batches

Transient gene expression (TGE) for protein production on the basis of the CHO-S/ProCHO4/PEI system was performed and optimized as described previously by (Rajendra et al. 2011; Rajendra et al. 2012; Wulhfard et al. 2008; Wulhfard et al. 2010). FreeStyle^{TM} CHO-S were routinely cultivated in complete PowerCHO-2 CD medium as described in Section 2.1.2. One day prior to transfection (day -1), when CHO-S cells reached a density of $4x10^6$ cells/mL, CHO-S were splitted to a final density of $2x10^6$ cells/mL using fresh complete PowerCHO-2 CD (8 mM GlutaMAX). On the transfection day (day 0), cells were centrifuged and resuspended in complete ProCHO-4 (4 mM GlutaMAX) (Rajendra et al. 2012) at a cell density of $3x10^6$ cells/mL. For a default large-scale protein production always 100 mL cell suspension were seeded in 500 mL autoclaved round-bottom glass bottles. Transfections were performed by sequential addition of 25 kDa-linear PEI [2.5 µg/$1x10^6$ cells] and plasmid DNA [maximal 0.625 µg/$1x10^6$ cells] directly to the cell suspension (Rajendra et al. 2011). The transfected cultures were maintained for 6 h at 37 °C, 130 rpm with a 19 mm shaking diameter in a humidified 8% CO_2 atmosphere. 6 h after transfection, dissolved valproic acid (VPA) was added to the transfected culture to a final concentration of 1 mM (Wulhfard et al. 2010). Subsequently, the culture was maintained for 6 days under hypothermic conditions at 32°C (Wulhfard et al. 2008), 5% CO_2 and 100 rpm (50 mm shaking diameter) prior harvest.

2.2.4.5 Mouse/human IgG-titter quantification ELISA

6 days after CHO-S transfection, the cell supernatant was collected and cleared from cells by two successive centrifugation steps: (1) 10 min at 1500 rpm, 4 °C and (2) at 4000 rpm for 30 min, 4 °C. To validate successful secretion and production of a vector of interest prior affinity-chromatography, anti-mouse-IgG-Fc or anti-human-IgG-Fc sandwich ELISA (described in 2.2.6) were performed depending on the Fc-fusion protein's design.

Unconjugated anti-human IgG-Fc or anti-mouse IgG-Fc capture antibodies (polyclonal goat serum) was diluted to a final concentration of 5 µg/mL in coating buffer (pH 9.6). 100 µL/well diluted capture antibody was transferred to a 96-well MaxiSorb ELISA plate. The plate was sealed and incubated at 37 °C for 45 min. After the incubation, the plate was washed three times using 200 µL/well PBS-T washing buffer. Unspecific protein interactions were blocked by adding 100 µL/well of PBS-T + 2.5% BSA blocking solution followed by an incubation at 37 °C for 45 min and one timing washing.

Affinity-chromatography purified disulfide-trapped single-chain trimer-based pMHC-I-mIgG2a-Fc or pMHC-I-hIgG1-Fc constructs with known concentrations were used for standard-curve-based IgG-Fc quantification of fresh TGE-derived supernatants. Samples (cleared TGE supernatants, diluted 1:100–1:900) and standard (in the range of 900 ng/mL – 1 ng/mL) were diluted in PBST + 0.5% BSA sample buffer and 100 µL/well were transferred in duplicates to the coated and blocked MaxiSorb ELISA plate. Samples and standard were incubated for 45 min at RT. The plate was washed three times as described before, followed by the addition of 100 µL/well of anti-human IgG-Fc-peroxidase or anti-mouse IgG-Fc-peroxidase detection antibodies diluted in sample buffer and incubation at RT for 45 min. After washing, TMB peroxidase substrate was added (100 µL/well) and incubated for 5 min – 15 min until the standard became clearly visible. Finally, the reaction was stopped by addition of TMB stop solution (1 M H_2SO_4) and absorbance was measured at 450 nm and 540 nm using a microplate reader.

2.2.4.6 Strep-tag II / Strep-Tactin resin column-based purification

Cleared TGE cell culture supernatants of Strep-tag proteins were purified using the Strep-Tactin-based purification system according to the manufacture's protocol and previously described by (270) with minor modifications. Briefly, a LPLC column with an inner diameter (I.D.) of 0.7 cm or 1.5 cm was filled with a column-bed volume (CV) of 0.5 mL or 1.5 mL Strep-Tactin Superflow high-capacity resin, respectively, depending on the anticipated protein yield and TGE culture volume. If the expected protein yield determined by ELISA exceeded 2 mg or the overall TGE culture volume exceeded 250 mL, a CV of 2 mL Strep-Tactin resin and a 1.5

cm I.D. LPLC column was selected. Cleared supernatants were supplemented with 0.1 volume of 10x PBS pH 7.4 prior purification. Strep-Tactin resin filled columns were equilibrated two times with 5 CV 1x PBS pH 7.4 followed by loading of cleared and biotin-masked TGE supernatants at a flowrate of 1.5–2.5 mL/min at RT using a peristaltic pump. Next, the column was washed by gravity flow using two times 5 CV 1x PBS pH 7.4. Elution of purified proteins was performed at a flowrate of 1.5 mL/min using 5 CV

PBS pH 7.4 supplemented with 5 mM desthiobiotin. 0.25–0.5 mL elution fractions were separately collected, and protein concentration was measured at 280 nm absorbance. The highest protein fractions were pooled and dialyzed in PBS 7.4 to remove the excess of desthiobiotin. Finally, all purified and dialyzed proteins were analyzed by SDS-PAGE according to Section 2.5.4. Strep-Tactin resin-filled columns were recycled afterwards according to the manufacture's protocol using buffer R and buffer W and were only reused for productions of the same protein.

Before functionality testing, protein concentration was determined by NanoDrop and the correct protein size was confirmed by reducing and non-reducing 10% SDS-PAGE.

2.2.4.7 SDS-PAGE analysis procedure

All SDS-PAGE analysis was performed using the RunBlueTM Teo-Tricine precast gel system (Expedeon) according to the manufacture's protocol. For reducing conditions protein samples were combined with LDS sample buffer and a final concentration of 10 mM DTT and were heated at 70 °C for 10 min prior to loading onto the SDS-PAGE. Electrophoresis was performed at RT at 140 V for 90 minutes. SDS-PAGE gels were stained at RT using the InstantBlueTM Coomassie staining solution for 3-4 h at constant orbital shaking. After the incubation, the staining solution was removed and replaced by ddH_2O followed by an overnight incubation for destaining. Usually, 2.5 µg of dialyzed protein sample was loaded per lane.

2.2.5 Flow cytometry

Flow cytometric acquisition was performed on a BD FACS Canto II with BD FACSDiva software. After voltage adjustments with single stained untreated cells, automatic compensation was obtained. Data was further analyzed with the FlowJo v.10 software.

2.2.5.1 Characterization of activated T cells

For cell surface staining of human lymphocytes from healthy donors, PBMC treated with 5 ng/ml of the T-cell stimulatory αCD3ε mAb OKT3, either alone or in combination with 100 ng/ml αCD28 antibody for co-stimulation, or with 2 ng/ml recombinant human IL-12 for 3 days. As a control, PBMC were also kept in culture for 3 days only in the presence of IL-2 (20 U/ml).

After the treatment, PBMC were washed DPBS, and transferred into a 96 well V-bottom plate (around $1x10^6$ cells/well) and blocked with Sandoglobulin (1:15 dilution in DPBS) for 15 minutes at 4 °C. Sandoglobulin® contains human immunoglobulins, thus used to block Fc receptors on immune cells. After centrifugation (1500 rpm, 3 minutes at 4 °C), immune cells were stained for lineage markers (NKp46, CD19, CD3, CD4 and CD8) and the T cell activation marker (CD25). Simultaneously, PBMC were also stained for T cell surface markers important for transendothelial migration (PSGL-1; ITGA4; ITGB1; ITGB2; CXCR3; CXCR4), T cell inhibitory receptors (TIGIT; TIM3; PD-1) as well as with the respective isotype controls for 30 minutes at 4 °C in the dark. The dilution for fluorochrome conjugated primary antibodies is shown in ***2.1.6.1***. Subsequently, cells were washed twice using FACS buffer and the pellets were resuspended FACS buffer with PI (1:2500 dilution) for live and dead discrimination and transferred to FACS tubes.

For flow cytometry analysis, 50,000 events were acquired from target population selection in FSC-A vs. SSC-A. After doublet exclusion, live $CD3^+CD4^+$ and $CD3^+CD8^+$ populations were evaluated.

2.2.5.2 Activation profile of endothelial cell surface markers

Endothelial cell (HUVEC and HBMEC) activation was either done by cytokine stimulation to induce surface marker expression simulating intratumorally inflammation, or by gamma irradiation to mimic radiation therapy. Before both stimulations, EC cells were seeded overnight in a T75 flask. For cytokine stimulation, human recombinant IL-1β (20 ng/mL) and/or TNF-α (10 ng/mL) were added to the cells and left overnight. Gamma irradiation (output 0.911 Gy/min) was performed at room temperature (RT) with different doses, 5 Gy and 10 Gy, applied once. After treatment, cells were kept at 37 °C in a 5% CO_2 atmosphere and further investigated after overnight incubation. Sham-irradiated (0 Gy) and unstimulated samples were kept under standard culture conditions (see above).

Surface marker expression of activated ECs was studied by flow cytometry. To this end, cells were harvested and washed with DPBS. EC were transferred into a 96 well V-bottom plate (around $1x10^6$ cells/well) and incubated with ZombieAqua (1:300 dilution in DPBS) for 10 min

at RT in the dark, for live and dead discrimination. To stop the reaction, FACS buffer (se ***2.1.10***) was added to the samples and after centrifugation (1500 rpm, 3 minutes at 4°C) EC were stained with fluorochrome-labeled primary antibodies as well as with the respective isotype controls for 30 minutes at 4 °C kept from light (see ***2.1.6.2***). Subsequently, cells were washed twice with FACS buffer and the pellets were resuspended in FACS buffer and transferred to FACS tubes. For flow cytometry analysis, 10000 events were acquired from live cells.

Table 2.1 Purified constructs.

* Protein sequences of purified constructs are shown at annex section.

Constructs	Concentration for Functional Assays	Concentration for binding confirmation
αVEGFR2 x mIgG2aFc	x	1 μg/ml
α*VEGFR2 x mIgG2aFc x hIL-1*β	20 ng/ml, 3.3-fold and 10-fold	1 or 10 μg/ml
α*VEGFR2 x mIgG2aFc x TNF-*α	10 ng/ml, 3.3-fold and 10-fold	1 or 10 μg/ml
αVEGFR2 x hIgG1Fc	0.5 nM	5 μg/ml
α*VEGFR2 x hIgG1 x* α*CD3*ε	0.5 nM	5 μg/ml
α*VEGFR2 x hIgG1Fc x* α*CD28*	1.0 nM	5 μg/ml
αTIE2 x hIgG1Fc x αCD28	1.0 nM	5 μg/ml
αPD-L1 x hIgG1Fc x αCD28	1.0 nM	5 μg/ml
αE-selectin x hIgG1Fc	1.0 nM	5 μg/ml
αE-selectin x hIgG1Fc x αCD8	1.0 nM	5 μg/ml
αVCAM1 x hIgG1Fc	1.0 nM	5 μg/ml
αVCAM1 x hIgG1Fc x αCD8	1.0 nM	5 μg/ml
αTIE2 x hIgG1Fc	1.0 nM	5 μg/ml
αTIE2 x hIgG1Fc x αCD8	1.0 nM	5 μg/ml

2.2.5.3 Binding of purified bispecific constructs to target cells

To assess binding efficiency of purified bispecific constructs, either cytokine-activated HUVEC (as described above on ***2.2.5.2***) or isolated PBMC, were transferred into a 96 well V-bottom plate (around $1x10^6$ cells/well) and incubated with ZombieAqua (as described in 2.2.5.2). After centrifugation (1500 rpm, 3 minutes at 4 °C), cells were incubated with constructs shown on **table 1**, for 20 minutes at 4°C. After two washing steps with FACS buffer, EC were stained with a secondary antibody, goat-anti-mouse-IgG2a or mouse-anti-human-IgG1 (1:200 dilution in FACS buffer) fluorochrome-labeled with PE, for 20 minutes at 4 °C kept from light. After two washing steps with FACS buffer cells were transferred to FACS tubes. For flow cytometry analysis, 10000 events were acquired from live cells.

2.2.5.4 Activation capacity of purified αVEGFR2-cytokine fusion proteins for HUVEC

In order to study if αVEGFR2-cytokine fusion proteins could activate EC and be as effective as commercial cytokines in up-regulating adhesion molecules expression, HUVEC were stimulated overnight with αVEGFR2 scFv-Fc-hIL-1β and/or αVEGFR2 scFv-Fc-hTNF-α and respective commercial recombinant human cytokines rhIL-1β (20 ng/ml) and rhTNF-α (10 ng/ml). Produced constructs were used at the same molarity as commercial cytokines (1x) and further titrated up (3.3-fold and 10-fold higher concentrated). After incubation, cells were collected, washed with DPBS and transferred to 96-well plate. ZombieAqua staining was performed as described in 2.2.5.2 for live and dead discrimination. After centrifugation (1500 rpm, 3 minutes at 4 °C), HUVEC were stained for adhesion molecules, E-selectin, ICAM1 and VCAM1, as well as with the respective isotype controls for 30 minutes at 4 °C kept from light (concentrations shown in ***2.1.6.2***). After washing, cells were collected into FACS tubed, and HUVEC activation was assessed by flow cytometry. 10,000 events were acquired from live cells.

2.2.5.5 T-cell binding to HUVEC in the presence of purified αVEGFR2-cytokine fusion proteins

To test if purified αVEGFR2-cytokine fusion proteins purified constructs have an impact on T-cell binding to HUVEC, purified $CD3^+$ T cells (described in 2.2.2) were co-cultured with endothelial cells. HUVEC were seeded at a density of $5x10^4$ cells per well into a 24 well cell culture plate and cultured in supplemented medium (EC complete medium) at 37 °C and 5% CO_2. After 24 hours and the formation of a confluent monolayer, HUVEC were treated with the respective αVEGFR2-cytokine fusion proteins (see ***2.2.5.3*** **- Table 1**) and $1x10^6$ isolated $CD3^+$ T cells were added on top. After 24 h co-culture, non-adherent cells were aspirated, and the wells were carefully washed 2x with DPBS.

After washing away unbound T cells, bound T cells and ECs were detached with cell dissociation buffer and washed with DPBS. Cells were further transferred to 96-well plate and incubated with Zombie Aqua (1:300 dilution in DPBS) for life/dead discrimination for 10 minutes at room temperature (RT) in the dark, and further blocked with TruStain FcX Fc receptor blocking solution (1:50 dilution in FACS buffer) for 10 minutes at RT.

After blocking, cells were washed twice with FACS buffer (2.1.10) and $CD3^+$ T cells were stained with linage marker antibodies (CD3, CD4, CD8) for 30 minutes at 4 °C in the dark.

After washing (2x), cells were collected into FACS tubed and counting beads were added to assess T cell binding by flow cytometry. 10000 events were acquired from live $CD3^+$ cells.

2.2.5.6 In vitro biological activities of bispecific antibodies

To test the biological activity of purified constructs, human purified $CD3^+$ T cells (described in 2.2.2) were co-cultured with endothelial cells. HUVEC were seeded at a density of $5x10^4$ cells per well into a 24 well cell culture plate and cultured in supplemented medium (EC complete medium) at 37 °C and 5% CO_2. After 24 hours and the formation of a confluent monolayer, HUVEC were treated with the respective bispecific antibodies (***2.2.5.3*** **- Table 1**) and $1x10^6$ isolated $CD3^+$ T cells were added on top. After 24 h co-culture, non-adherent cells were aspirated, and the wells were carefully washed 2x with DPBS.

After washing away unbound T cells, bound T cells and ECs were detached with cell dissociation buffer and washed with DPBS. Cells were further transferred to 96-well plate and incubated with Zombie Aqua (1:300 dilution in DPBS) for life/dead discrimination for 10 minutes at room temperature (RT) in the dark, and further blocked with TruStain Fc receptor blocking solution (1:50 dilution in FACS buffer) for 10 minutes at RT.

After blocking, cells were washed twice with FACS buffer (see ***2.1.10***) and $CD3^+$ T cells were stained with linage marker antibodies (CD3, CD4, CD8), CD28, as well as activation marker antibodies (4-1BB, CD69 and CD25) and HUVEC with anti-CD105, activation marker antibodies (E-selectin, ICAM1, VCAM1) and antibodies recognizing EC receptors (VEGFR2 and TIE2), for 30 minutes at 4 °C in the dark.

After washing (2x), cells were collected into FACS tubed, and cell activation status was assessed by flow cytometry. Counting beads were used to evaluate T cell binding to HUVEC. 10000 events were acquired from live cells.

Bound cells count

$$\left(\frac{Cell\ count \times Precision\ Count\ Beads\ volume}{Precision\ Count\ Beads \times Cell\ volume} \times Precision\ Count\ Beads\ Concentration\right) \times Sample\ volume$$

Percentage of bound cells

$$\frac{Bound\ cells\ count}{Input\ Cells\ count} \times 100$$

2.2.6 Enzyme-linked Immunosorbent Assay (ELISA)

The cytokine levels (TNF-α and INF-γ) in supernatants of T cells and HUVEC co-cultures (***2.2.5.5***) were determined by sandwich ELISA using kit from BioLegend (***2.1.8***). The capture antibody was resuspended in coating buffer (***2.1.10***) and added to the 96-well ELISA plate overnight (ON) at 4 °C. After washing (***2.1.10***) the wells were blocked with blocking buffer (***2.1.10***) for 45 minutes at 37 °C. After three washing steps, samples were diluted with sample buffer (***2.1.10***) and transferred, in duplicate, to each well. Depending on the type of cytokine measured, the sample dilution was adjusted (TNF-α 1:5 dilution, IFN-γ 1:10 dilution). Human cytokine standards were diluted 1:2 (8 dilutions in duplicate) in sample buffer to make the standard curve. After 90 minutes incubation at RT and 3 washing steps, detection antibody diluted in sample buffer was added to each well (***2.1.8***) for 60 minutes at RT. After washing 3 times, streptavidin-HRP (***2.1.8***) was added and incubated at RT for 20 minutes. After 3x washing, substrate solution (***2.1.8***) was added for 10 minutes at RT and the reaction was stopped by the addition of stop solution (***2.1.8***). Absorbance was assessed using a spectrophotometer (450/540 nm) and the final concentrations were determined using the standards.

2.2.7 Transwell migration assay

Targeting of T cells to and through ECs via produced bifunctional proteins constructs was investigated by a migration assay under sterile conditions. One day before transmigration analysis, transwell inserts (0.5 µm pore size, 6.5 mm diameter, polyester membrane) were coated with 15 µg/cm2 human fibronectin in 1x PBS for 1 h followed by 10 min drying at RT. After washing the insert in 1x PBS, $2.5x10^4$ ECs/well were seeded in the upper well using 200 µL EC complete medium II, while the lower well was supplied with fresh EC complete medium. Attachment and growth to 100 % confluence took place after 48 h at standard culture conditions. After confirming the quality of the monolayer using the dextran permeability assay (described below), bifunctional constructs were diluted in EC medium (supplemented with 1% FBS) and added to the upper well followed by $1x10^6$/well $CD3^+$ isolated T cells. Transmigration took place for 24 h at 37 °C and 5 % CO_2 under static conditions. The number of viable transmigrated T cells in the down well was determined by flow cytometry using counting beads according to the respective manufacturer's instructions. T cell activation status was studied by FACS using activation markers (4-1BB, CD69 and CD25 (***2.1.6.1***). Immune staining was performed as described on ***2.2.5.6.***

Migrated cells count

$$\left(\frac{Cell\ count \times Precision\ Count\ Beads\ volume}{Precision\ Count\ Beads \times Cell\ volume} \times Precision\ Count\ Beads\ Concentration\right) \times Sample\ volume$$

Percentage of migration

$$\frac{Binding\ cell\ count}{Input\ Cell\ count} \times 100$$

2.2.8 Dextran permeability assay

Prior the transmigration assay, permeability of endothelial cell layers was tested by applying 100 µg/mL FITC-dextran solution (diluted with EC growth medium II) to the upper well. After 1h at 37 °C, medium from the lower well was collected and dextran concentration was determined in duplicates measuring excitation at 485 nm and emission at 538 nm using the Fluoroskan Ascent FL (ThermoFisher Scientific). Dextran diffusion was quantified using standard curve.

2.2.9 Killing assay

Migrated $CD3^+$ T cells cytotoxic capacity was evaluated by lactate dehydrogenase (LDH) quantification of supernatants from the co-culture with tumor MCF-7. $1x10^4$ MCF-7 were seeded in a 96-well plate, 24 h prior to the co-culture. Migrated T cells (from the transwell migration assay) were collected from the bottom well and transferred onto pre-cultured MCF-7 for 24 h, alone, or in the presence of an additional bispecific antibody (αHER2xhIgG1xαCD3ε,1 nM). This BiMAb can crosslink with migrated T cells via αCD3ε and with MCF-7 via HER2, leading to an additional stimulation of T cells and tumor cell targeting (Warwas et al. 2021). Binding confirmation of αHER2xhIgG1xαCD3ε to T cells and concentration optimization for LDH assay were performed by Karsten Warwas (DKFZ) .

Migrated T cell cytotoxicity capacity was studied using the CyQUANT LDH Cytotoxicity Assay kit, according to the manufacturer's instructions. Briefly, the supernatants from T-cell/MCF-7 co-cultures were transferred to a 96-well plate and substrate mix solution (from the kit) was added on top for 30 minutes in the dark at RT. To stop the reaction, stop solution was added and the plate fluorescence was measured with an ELISA plate reader (Multiskan EX) at 492 nm and 620 nm. The respective controls were also included. Percent cytotoxicity was quantified using the formula:

$$\% \text{ Cytotoxicity} = \left[\frac{\text{Compound-treated LDH activity} - \text{Spontaneous LDH activity}}{\text{Maximum LDH activity} - \text{Spontaneous LDH activity}} \right] \times 100$$

2.2.10 Statistical analysis

Statistical analyses were performed using GraphPad Prism 7. All the data are expressed as mean ± SEM. Significant differences ($P < 0.05$) between means of data sets were assessed by one-way ANOVA with Tukey's test. Significant differences compared to the controls are marked by asterisks (*, $P < 0.05$; **, $P < 0.01$; ***, $P < 0.001$) and significant differences between treatments are marked by hashtags ($^{\#}$, $P < 0.05$; $^{\#\#}$, $P < 0.01$; $^{\#\#\#}$, $P < 0.001$).

3 RESULTS

3.1 CHARACTERIZATION OF T CELL SURFACE MARKERS UPON ACTIVATION

As a consequence of T cell activation, there is a change in the expression of surface adhesion molecules, and only lymphocytes expressing the appropriate set of homing molecules can make contact with activated vasculature, undergo the full adhesion cascade, and exit from the bloodstream to the target tissue.

Priming and activation of T cells start in the lymph nodes when T cells encounter APCs that secret IL-12 and can present via MHC pathogen or cancer-derived peptides recognized by the specific T-cell receptor (TCR). However, in immunologically "cold" tumors, the infiltration of T cells is poor, and because of the commonly suppressive tumor microenvironment, T cell activation is not effective.

In order to overcome this problem, we aimed at using bispecific constructs to specifically target T cells to the tumor vasculature and activate them *in situ* after antibody-mediated crosslinking with tumor endothelial cells.

To mimic T cell activation and find the best conditions for optimal expression of adhesion molecules, PBMC were stimulated with IL-12 and/or αCD3ε (OKT3 - a monoclonal antibody that binds to CD3ε, a molecule associated with the TCR complex) and/or αCD28 antibodies to mimic co-stimulation. 20 U/ml of IL-2 was added to maintain T cell survival. After three days of culture, the cells were harvested. After staining with fluorochrome-labeled antibodies, the activation profile of $CD4^+$ (**Fig. 3.1**) and $CD8^+$ (**Fig. 3.2**) T cell subpopulations, gated from live $CD3^+$ cells (**Fig. 3.1A)** was analyzed using flow cytometry. Surface markers contributing to lymphocyte tethering/rolling (PSGL-1), chemotaxis (CXCR3), adhesion, and migration (integrins α4, β1, and β2) (**Fig. 3.1B and Fig. 3.2A**) as well as checkpoint receptors (TIGIT, TIM3, and PD-1) (**Fig. 3.1C and Fig. 3.2B**) were investigated on both subpopulations.

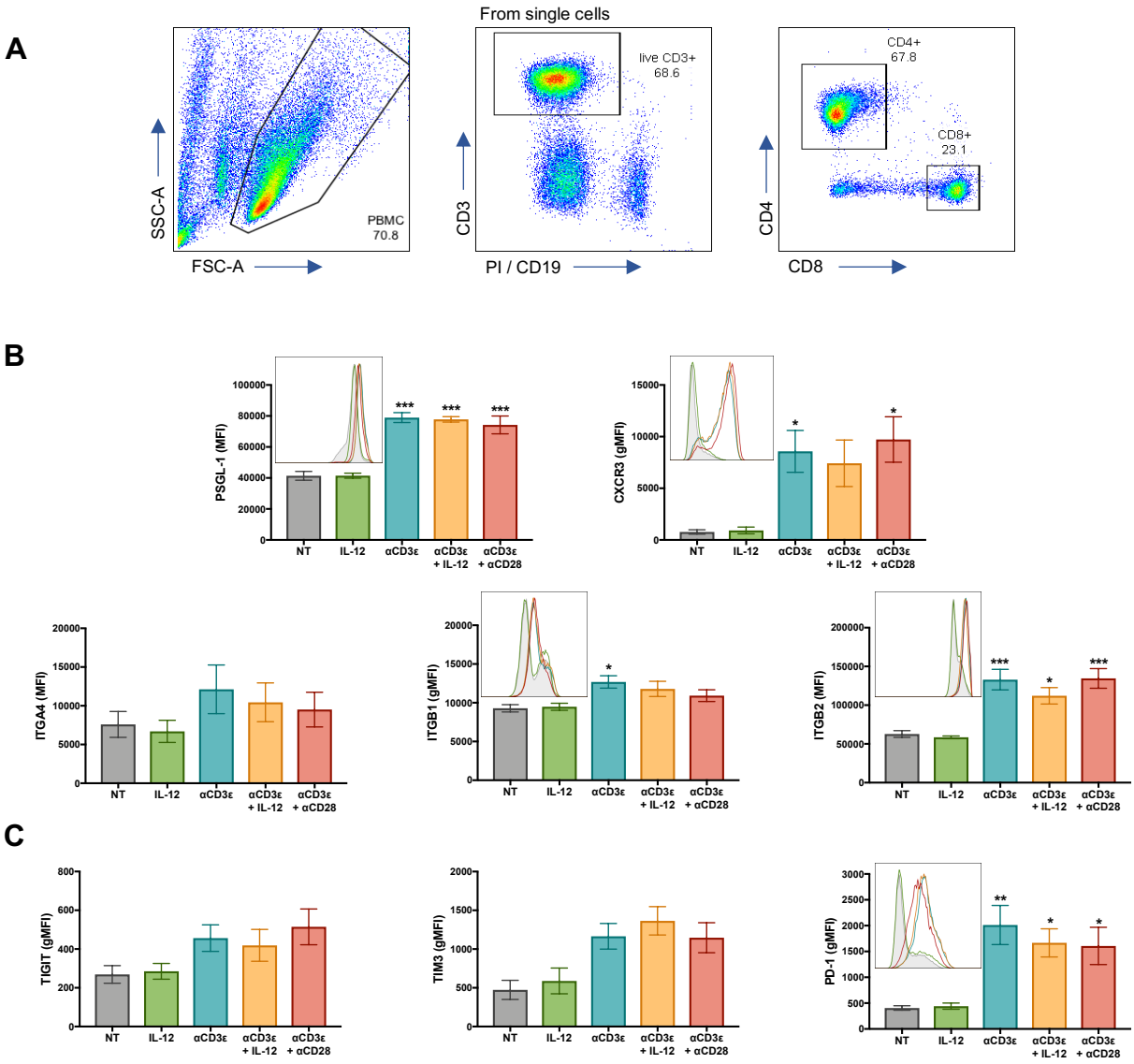

Figure 3.1 CD4+ T cell activation profile. PBMC were isolated from the blood of healthy donors and treated with rhIL-12 (2 ng/ml) and/or αCD3ε (5 ng/ml) and/or αCD28 (100 ng/ml). 20 U/ml of rhIL-2 was added to the culture for T cell survival. After 3 days, the cells were harvested, and surface markers expression was analyzed by flow cytometry. **(A)** Gating scheme of evaluated T cell subpopulations. Graphs represent the expression levels (MFI or gMFI) of **(B)** adhesion molecules (PSGL-1, ITGA4, ITGB1, and ITGB2) and chemokine receptor 3 (CXCR3), and **(C)** inhibitory receptors (TIGIT, TIM3, and PD-1). Data is presented as mean ± SEM of 4-5 independent experiments. Significant differences compared to the control (NT, treated with rhIL-2 only) are marked by asterisks (*, $P < 0.05$; **, $P < 0.01$; ***, $P < 0.001$). Histograms illustrate one representative staining.

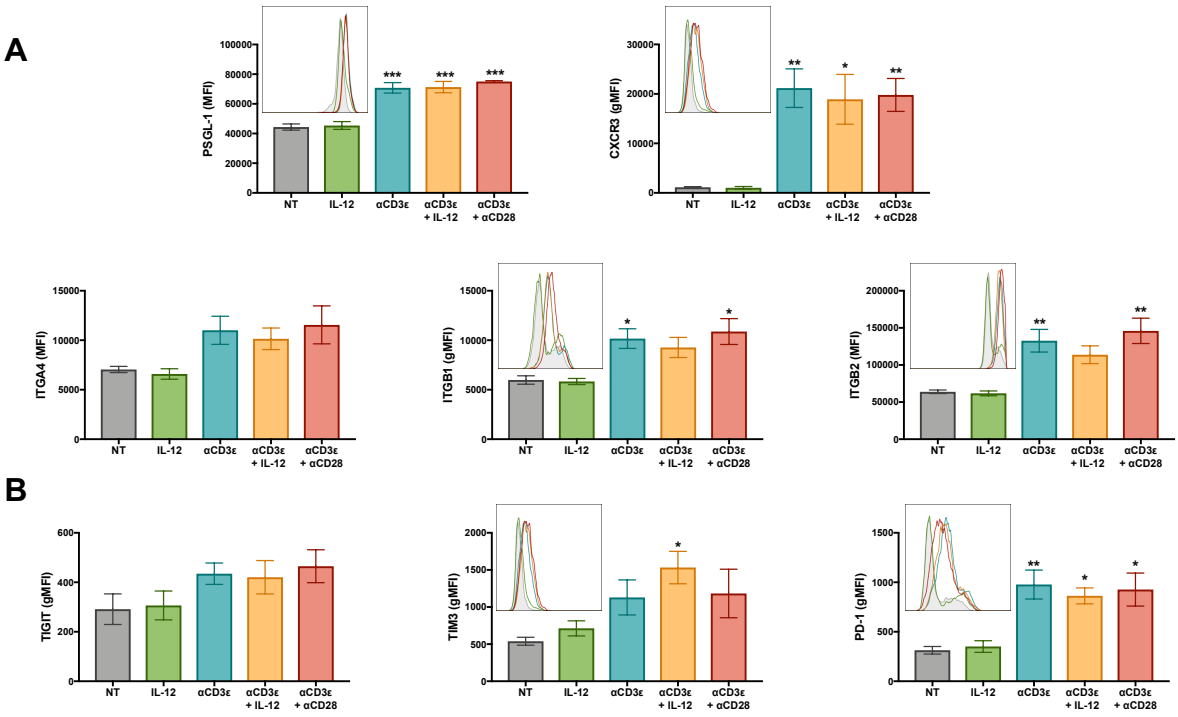

Figure 3.2 CD8+ T cell activation profile. PBMC were isolated from the blood of healthy donors and treated with rhIL-12 (2 ng/ml) and/or αCD3ε (5 ng/ml) and/or αCD28 (100 ng/ml). 20 U/ml of rhIL-2 was added to the culture for basic T cell survival. After 3 days, the cells were harvested, and surface marker expression was analyzed by flow cytometry. Graphs represent the expression levels (MFI and gMFI) of **(A)** adhesion molecules (PSGL-1, ITGA4, ITGB1, and ITGB2) and chemokine receptor 3 (CXCR3), and **(B)** inhibitory receptors (TIGIT, TIM3, and PD-1). Data is presented as mean ± SEM of 4-5 independent experiments. Significant differences compared to the control (NT) are marked by asterisks (*, $P < 0.05$; **, $P < 0.01$; ***, $P < 0.001$). Histograms illustrate one representative staining.

The homing receptors PSGL-1, Integrin β1, Integrin β2, and the chemokine receptor CXCR3 showed significant up-regulation on both T cell populations ($CD4^+$ and $CD8^+$) with αCD3ε stimulation. Integrin α4 did not show a significant increase even though there was a tendency to be also up-regulated in the presence of the αCD3ε antibody. The same treatment increased the levels of the inhibitory checkpoint receptor PD-1 as well. In general, αCD28 co-stimulation did not improve the expression of these receptors, and IL-12 could even attenuate the αCD3ε effect. TIM3 levels significantly increased in the presence of αCD3ε and IL-12 stimulation only on the $CD8^+$ T cell population, while TIGIT levels did not change substantially, although a tendency for TIGIT up-regulation was observed. Taken together, the data suggests that T cell activation via αCD3ε is sufficient to get the required expression pattern of molecules crucial for vascular adhesion and transmigration, although it led to a concomitant PD-1 up-regulation.

The expression of the activation marker CD25 was also evaluated for both $CD4^+$ and $CD8^+$ T cell populations upon each stimulation (**Fig. 3.3A**). Co-expression of CD25 allowed the evaluation of the expression of the relevant receptors in both activated ($CD25^+$) and non-activated ($CD25^-$) cells inside the $CD4^+$ (**Fig. 3.3B**) and $CD8^+$ (**Fig. 3.3C**) T cell populations.

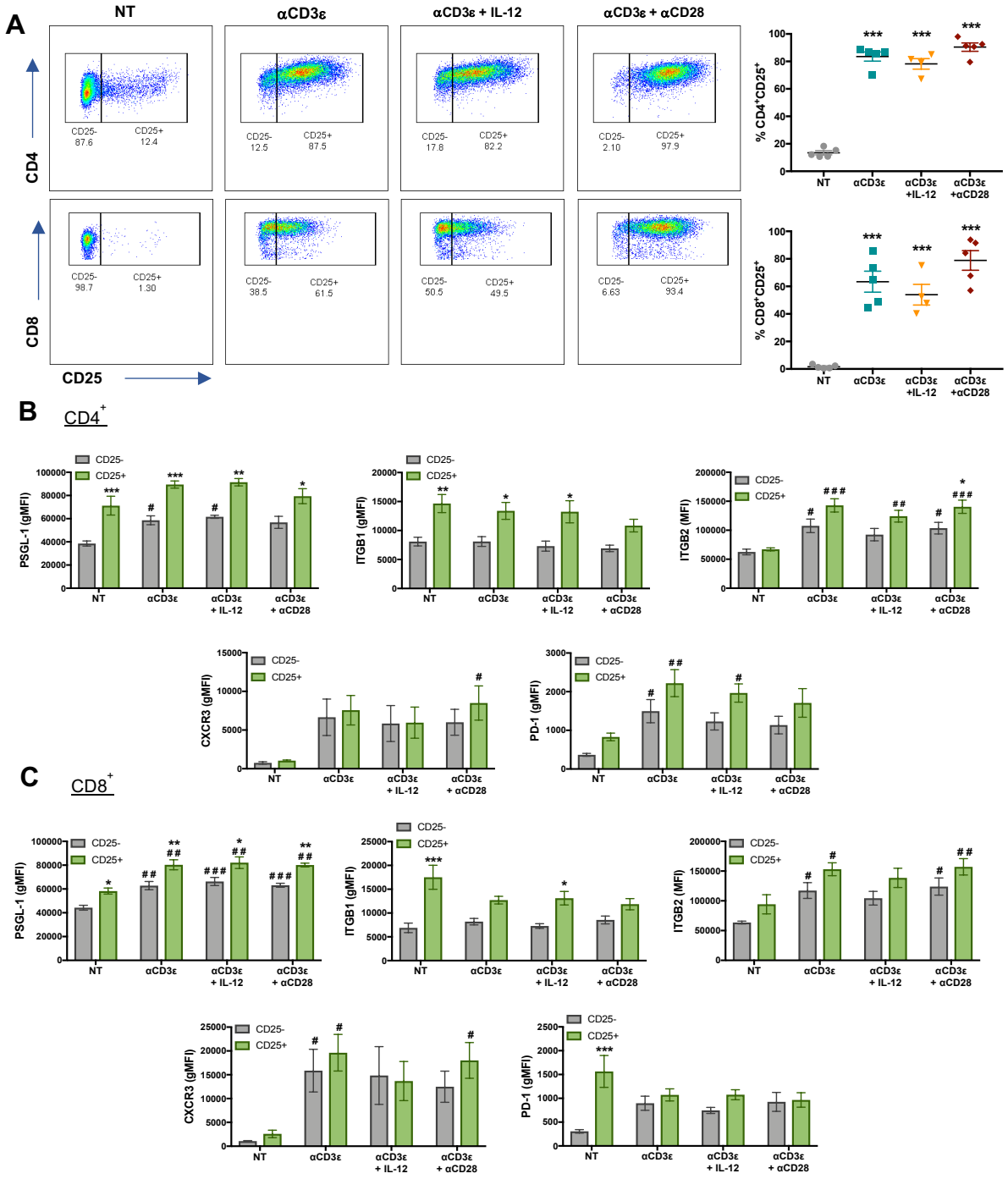

Figure 3.3 Expression of homing receptors and PD-1 in gated CD25$^+$ and CD25$^-$ T cell populations. PBMC were isolated from the blood of healthy donors and treated with rhIL-12 (2 ng/ml) and/or αCD3ε (5 ng/ml) and/or αCD28 (100 ng/ml). After 3 days the cells were harvested, and surface marker expression was analyzed by flow cytometry. **(A)** Dot-plot on the left side illustrating a representative experiment showing CD25 expression among different treatments (NT; αCD3ε ± IL-12; αCD3ε ± αCD28) and on the right side the respective quantification of % CD25$^+$ expressing cells on CD4$^+$ and CD8$^+$ T cells. Graphs showing the expression levels (MFI and gMFI) of adhesion molecules, CXCR3 and PD-1 on non-activated (CD25$^-$) vs activated (CD25$^+$) on **(B)** CD4$^+$ and on **(C)** CD8$^+$ T cells. Data is presented as mean ± SEM, n=4-5 independent experiments. Significant differences compared to the control (NT) of the same subpopulation are marked by hashtags (#, P < 0.05; ##, P < 0.01; ###, P < 0.001). Significant changes in the CD25$^+$ population compared to the CD25$^-$ in the same treatment are marked by asterisks (*, P < 0.05; **, P < 0.01; ***, P < 0.001).

After stimulation with αCD3ε antibody, $CD4^+$ T cells significantly increased the frequency of $CD25^+$ cells up to 80% and $CD8^+$ T cells up to 60%. The addition of co-stimulation with αCD28 further increases activated $CD4^+$ T cells up to 90% and $CD8^+$ T cells up to 80% (**Fig. 3.3A**).

For $CD4^+$ T cells (**Fig. 3.3B**), PSGL-1 expression as well as ITGB1 expression was significantly higher on activated cells ($CD25^+$) compared with non-activated cells ($CD25^-$) both untreated and upon stimulation. The treatment with αCD3ε alone or combined with IL-12 increased the amount of PSGL-1, but not ITGB1. ITGB2 levels were significantly increased only on activated $CD4^+$ T cells upon combined αCD3ε and αCD28 stimulation, compared to non-activated $CD4^+$ T cells. However, in the $CD25^+CD4^+$ T cell subpopulation, ITGB2 expression was augmented upon all treatments compared to the control (NT), as well as in the $CD25^-CD4^+$ T cell subpopulation, with exception of plus αCD28 stimulation. The chemokine receptor CXCR3 tended to be up-regulated on both subpopulations, non-activated, and activated $CD4^+$ T cells after all treatments, mainly with αCD3ε plus αCD28. PD-1 levels were not significantly different between $CD25^-$ and $CD25^+CD4^+$ T cells among conditions, although a tendency was observed for higher PD-1 expression in $CD25^+$ cells. However, in both subpopulations, PD-1 levels increased after αCD3ε treatment compared to non-treated cells, and in $CD25^+$ $CD4^+$ T cells also after αCD3ε and IL-12 stimulation.

The expression levels of PSGL-1 on activated $CD8^+$ T cells (**Fig. 3.3C**) were significantly higher than on non-activated cells ($CD25^-$) in both untreated and treated conditions. PSGL-1 expression increased on both $CD8^+$ T cell subpopulations after stimulation when compared with cells that were not stimulated. ITGB1 levels are significantly higher on untreated activated $CD8^+$ T cells than on $CD8^+CD25^-$ T cells but this difference is attenuated upon treatment, with the exception of the αCD3ε plus IL-12 condition. Regarding ITGB2 expression on $CD8^+$ T cell subpopulations, there were no significant differences between $CD25^-$ and activated cells, although after αCD3ε treatment, alone or together with CD28 co-stimulation, both subpopulations showed high levels of ITGB2 compared to non-treated cells. CXCR3 showed similar behavior with an evident up-regulation of CXCR3 upon activation of $CD8^+$ T cells. PD-1 expression did not show differences between $CD25^-$ and $CD25^+$ after stimulation, only on non-treated $CD8^+$ cells $CD25^+$ cells expressed significantly higher levels of PD-1.

Overall, αCD3ε antibody showed promising results on both activating T cells and enhancing receptor expression involved in their recruitment and migration. Although the combination with αCD28 co-stimulation did not significantly enhance homing receptors expression, it increased overall activation of both $CD4^+$ and $CD8^+$ T cells. As such, both stimuli will be used as part of the bispecific antibodies to recruit and activate T cells.

3.2 ACTIVATION PROFILE OF ENDOTHELIAL CELL SURFACE MARKERS

3.2.1 Effect of γ-radiation on endothelial cell surface regulation

Radiation therapy is a standard treatment in cancer patients, which does not only affect malignant tumor cells but also surrounding cells of the tumor stroma including tumor-associated fibroblasts, endothelial cells of the tumor neovasculature and tumor-infiltrating lymphocytes and macrophages. Previously studies showed that ionizing radiation can compromise endothelial cell integrity, and thereby increase permeability, tumor metastasis and angiogenesis.

To assess the effect of γ-radiation on endothelial cell surface markers, HUVEC were exposed to γ-radiation at different doses (5 Gy and 10 Gy, applied once) (**Fig. 3.4**). Adhesion molecules (**Fig. 3.4A**), angiogenic receptors (**Fig. 3.4B**), and PD-1 ligands (**Fig. 3.4C**) were analyzed on HUVEC 24h after γ-radiation treatment

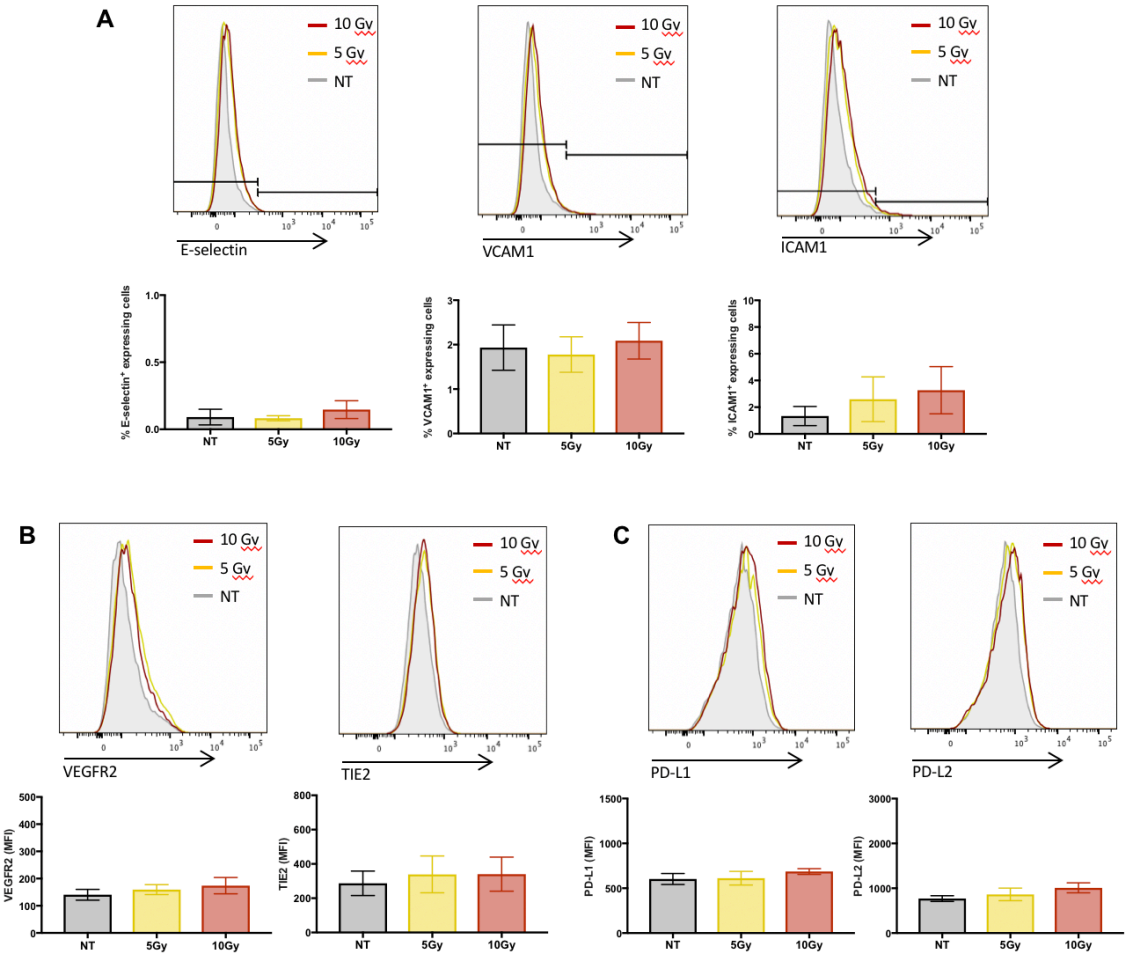

Figure 3.4 Effect of γ-radiation on HUVEC. (A) Expression of adhesion molecules involved in lymphocyte adhesion and transmigration (E-selectin, ICAM1, VCAM1), **(B)** endothelial cell growth (VEGFR2, TIE2), as well as **(C)** T cell inhibition (PD-L1, PD-L2), were analyzed on HUVEC exposed to one-time γ-radiation with different doses (5 Gy and 10 Gy). Data is presented as mean ± SEM, n=4-5 independent experiments. Histograms show one representative staining.

Results suggest that HUVEC were not affected by γ-radiation, at least after 24 h none of the studied markers showed significant changes.

The effect of irradiation was also analyzed on HBMEC-60 (**Fig. 3.5**). Consistently with HUVEC results, adhesion molecules were not induced (data not shown) on irradiated-HBMEC after 24 h, however, VEGFR2 (**Fig. 3.5A**) and PD-L1 (**Fig. 3.5B**) expression were up-regulated on HBMEC-60 exposed to 10 Gy of γ-radiation, compared to the control cells.

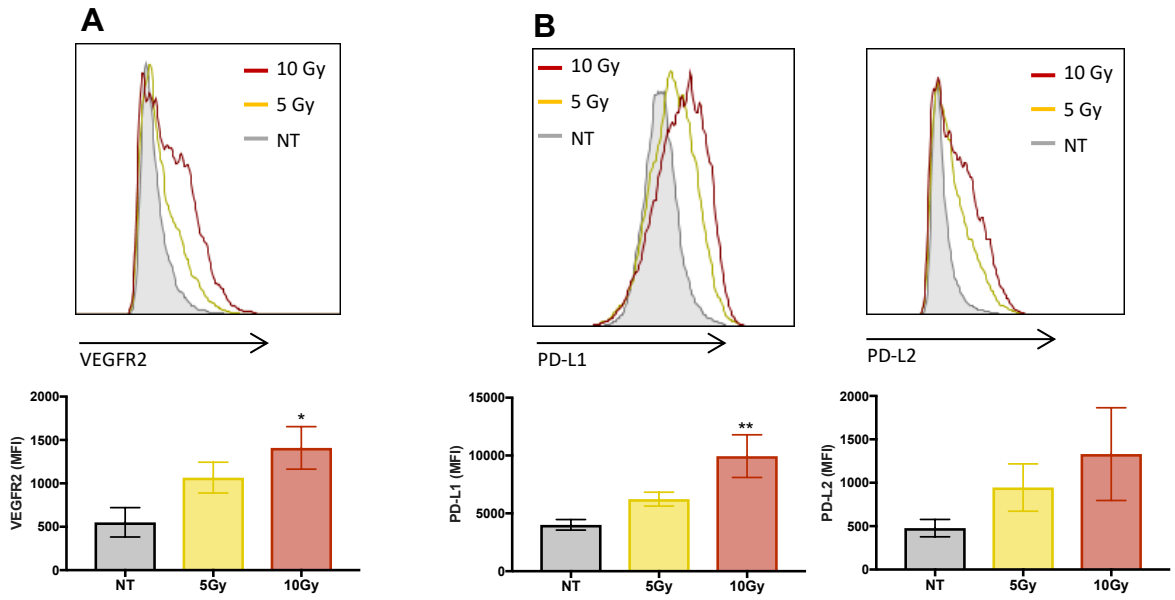

Figure 3.5 Effect of γ-radiation on HBMEC-60. (A) Expression of molecules involved in endothelial cell growth (VEGFR2) and **(B)** T cell inhibition (PD-L1, PD-L2), were analyzed on HBMEC-60 exposed to one-time γ-radiation with different doses (5 Gy and 10 Gy). Data is presented as mean ± SEM, n=3-5 independent experiments. Significant differences compared to the control (NT) are marked by asterisks (*, $P < 0.05$; **, $P < 0.01$). Histograms show one representative staining.

3.2.2 Cytokine-regulated expression of endothelial surface markers

Endothelial cells play a central role in the inflammatory reaction. In the resting stage, endothelial cells do not recruit lymphocytes (Ley and Reutershan 2006) because gene transcription and *de novo* synthesis of proteins such as adhesion molecules (E-selectin, VCAM1 and ICAM1), cytokines and chemokines are mainly suppressed. The secretion of pro-inflammatory cytokines (TNF-α and IL-1β) by inflamed tissues activates the endothelium leading to morphological and functional changes. The expression of adhesion molecules is induced in the activated endothelium, resulting in T cell recruitment. Furthermore, PD-L1 and PD-L2 expression on EC cells are also known to be influenced by pro-inflammatory cytokines (Boghozian et al. 2013) and consequently lead to the inhibition of adhering T cells via PD-1 interaction. Besides endothelium-T cell interaction, angiogenesis is another event that is related to EC activation.

To study endothelial cell surface markers' regulation, as part of their functional response during inflammation, and find a relevant EC target to be used in T cell-targeting bispecific constructs, environmental conditions were simulated by the pro-inflammatory cytokines IL-1β and/or TNF-α in order to induce EC activation. Adhesion molecule expression (**Fig. 3.6A**), angiogenic receptors (**Fig. 3.6B**), and inhibitory ligands for checkpoint receptors (**Fig. 3.6C**) were analyzed on HUVEC after overnight stimulation using flow cytometry.

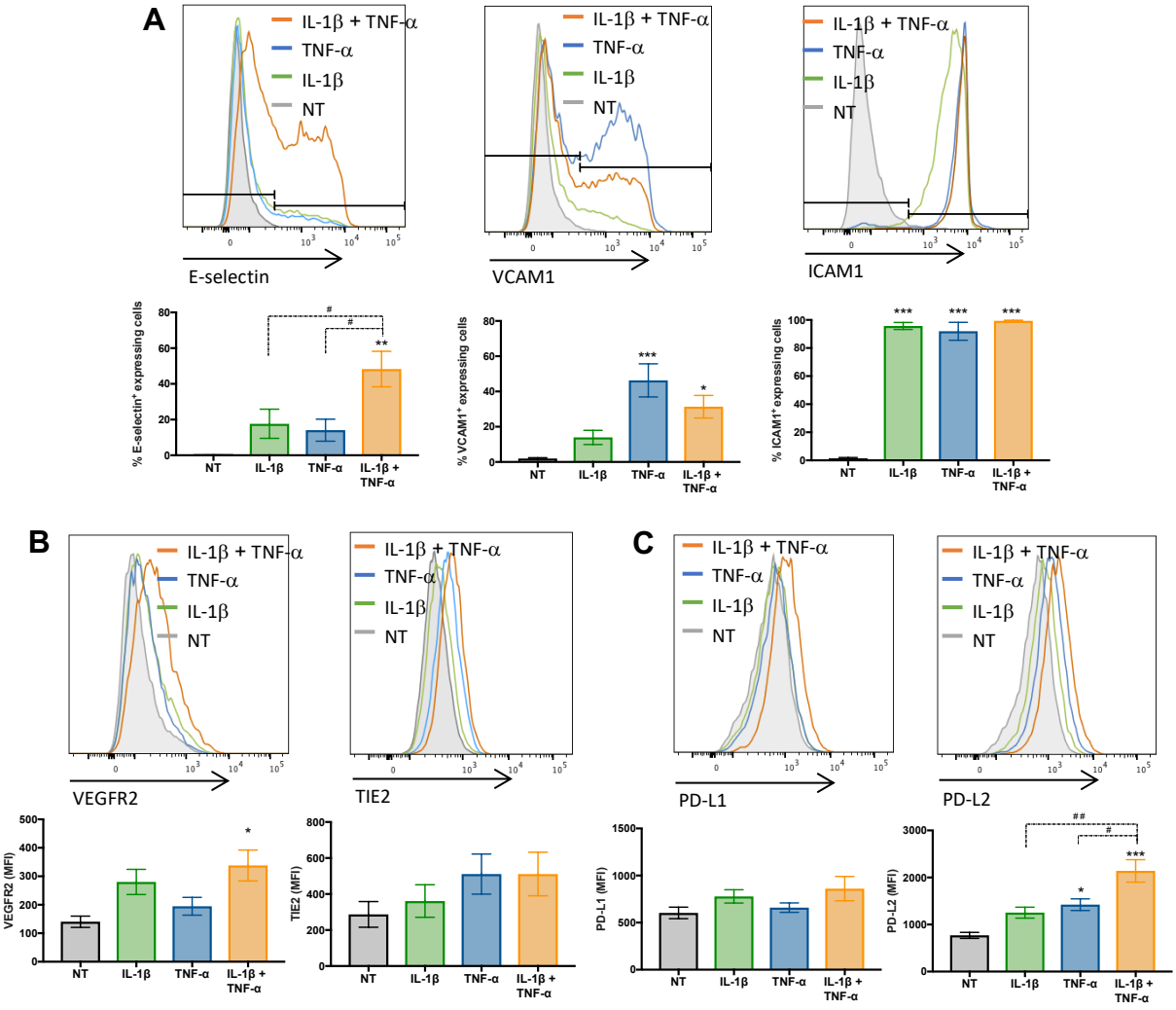

Figure 3.6 Endothelial cell profile upon cytokine activation. HUVEC activation was investigated after overnight stimulation with pro-inflammatory cytokines, IL-1β (20 ng/ml) or/and TNF-α (10 ng/ml). Graphs represent the expression levels (MFI or % of positive expressing cells) of **(A)** EC adhesion molecules involved in lymphocyte adhesion and transmigration (E-selectin, ICAM1, VCAM1), **(B)** endothelial cell growth (VEGFR2, TIE2), as well as **(C)** T cell immune checkpoint blockade (PD-L1, PD-L2). Data is presented as mean ± SEM, n=4-5 independent experiments. Significant differences compared to the control (NT) are marked by asterisks (*, $P < 0.05$; **, $P < 0.01$; ***, $P < 0.001$) and significant differences between treatments are marked by hashtags (#, $P < 0.05$; ##, $P < 0.01$). Histograms show one representative staining.

Expression of E-selectin, VCAM1 and ICAM1 was barely detectable above background levels in the basal unstimulated state (**Fig. 3.6A**). When HUVEC were treated with IL-1β or TNF-α alone, E-selectin expression was only slightly induced, but both cytokines added together had a synergistic effect and E-selectin expressing cells reached a frequency of 50%. VCAM1 was also only slightly induced on IL-1 β-stimulated HUVEC but, in contrast to E-selectin, VCAM1 expression was mostly TNF-α-dependent that increased the percentage of $VCAM1^+$ cells up to 50%. The combination treatment also increased the number of HUVEC expressing VCAM1 (30%), but less effectively when compared with TNF-α alone. ICAM1 induction was sensitive to all cytokine treatments and after overnight stimulation between 90-100% of HUVEC expressed ICAM1.

Regarding angiogenic receptor expression (**Fig. 3.6B**), VEGFR2 and TIE2 both had a basal expression but with different intensities. VEGFR2 expression was lower on non-treated HUVEC than TIE2, however, VEGFR2 was significantly up-regulated by double stimulation (IL-1β and TNF-α) while TIE2 did not show significant changes yet with a clear tendency to become up-regulated by TNF-α or the combination of IL-1β and TNF-α.

Surface markers involved in checkpoint signaling like PD-L1 and PD-L2 (**Fig. 3.6C**), were constitutively expressed by HUVEC with similar intensities. PD-L1 expression was not significantly affected by pro-inflammatory cytokine stimulation whereas PD-L2 was up-regulated by TNF-α and further boosted by the presence of IL-1β.

All of the previous EC surface markers, except TIE2, were also studied on the immortalized HBMEC-60 cell line (**Fig. 3.7**). Only the regulation of E-selectin and ICAM1 was cytokine-dependent although in a different manner compared to HUVEC (**Fig. 3.7A**). E-selectin was up-regulated by all treatments, especially by IL-1β, while ICAM1, that showed a high constitutive expression, was significantly up-regulated only after stimulation with both cytokines. VCAM1 expression was not at all inducible on HBMEC-60, which can limit transmigration studies. VEGFR2 (**Fig. 3.7B**), PD-L1 and PD-L2 (**Fig. 3.7C**) are constitutively expressed by HBMEC-60 at higher levels than on HUVEC, however, were not significantly affect by cytokine-stimulation.

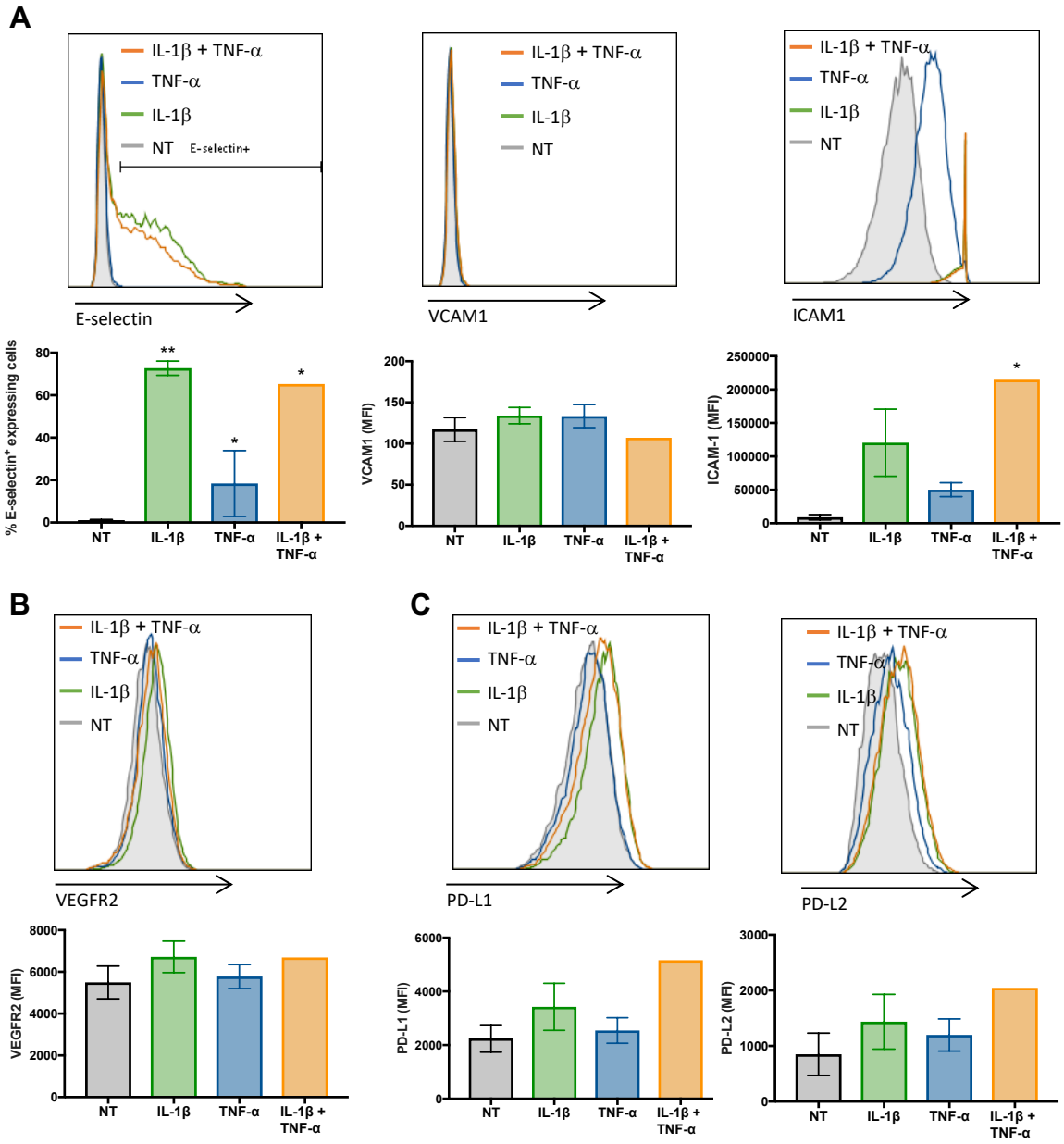

Figure 3.7 Regulation of surface markers on HBMEC-60 upon cytokine-activation. HBMEC cell line was overnight stimulated with pro-inflammatory cytokines, IL-1β (20 ng/ml) or/and TNF-α (10 ng/ml). Graphs represent the expression levels (MFI or % of expressing cells) of EC surface markers **(A)** involved in lymphocyte adhesion and transmigration (E-selectin, ICAM1, VCAM1), **(B)** endothelial cell growth (VEGFR2), as well as **(C)** T cell immune checkpoint blockade (PD-L1, PD-L2). Data is presented as mean ± SEM, n=1-5 independent experiments. Significant differences compared to the control (NT) are marked by asterisks (*, P < 0.05; **, P < 0.01).

In general, pro-inflammatory cytokine stimulation proved to be effective for adhesion molecules induction in two endothelial cell lines *in vitro*, which is important for T cell transmigration. However, on tumor endothelium *in vivo*, the microenvironment is rather immunosuppressive, inhibiting adhesion molecules expression and hampering T cell infiltration. Thus, the use of bispecific fusion proteins carrying pro-inflammatory cytokines (IL-1β and TNF-α) might represent a promising strategy to stimulate tumor EC directly *in situ*.

We conclude that specific antibodies bearing cytokine fusion proteins and targeting VEGFR2/TIE2 might represent a promising therapeutic approach since these receptors are highly expressed by the tumor endothelium.

3.3 TUMOR VASCULATURE NORMALIZATION AND *IN SITU* ACTIVATION USING αVEGFR2 ANTIBODY-CYTOKINE FUSION PROTEINS IMPROVE T CELL BINDING.

Dysregulation of angiogenesis is a hallmark of malignant tumors (Hanahan and Weinberg 2011). The tumor microenvironment is characterized by an excess of proangiogenic factors, like VEGF, secreted by tumor cells and tumor-associated stromal cells. VEGF binds to VEGFR2, expressed tumor endothelial cells, creating an imbalance of pro- and anti-angiogenic signaling. Consequently, new blood vessel formation is uncontrolled and disorganized resulting in hyperpermeable vessels with high fluid pressure, irregular blood flow and low oxygenation. The abnormal vasculature together with a suppressive microenvironment feed tumor progression and reduce the efficacy of cancer therapy such as chemotherapy, radiotherapy and immunotherapy.

Therefore, targeting the angiogenesis process can have a positive impact on tumor regression and can also improve the delivery and efficacy of exogenously administered therapeutics, radiotherapy and infiltration of effector immune cells.

3.3.1 Endothelial cell activation using VEGFR2 antibody-cytokine fusion proteins

It has been shown that anti-angiogenic therapy targeting the VEGF receptor induce "vascular normalization" improving tumor perfusion (Tong et al. 2004; Winkler et al. 2004). One of the anti-angiogenic biologic agents in clinical use is ramucirumab, a fully human IgG1 monoclonal antibody that selectively inhibits VEGFR2 and blocks the signaling pathways in ECs that mediate angiogenesis. A ramucirumab sequence-based single-chain (scFv) antibody was used as part of the VEGFR2 antibody-cytokine fusion protein, as described in Material and Methods, to target tumor endothelium and deliver pro-inflammatory cytokines *in situ*.

To confirm the binding of the specific antibodies, activated HUVEC were incubated with αVEGFR2 scFv-Fc antibody and αVEGFR2 scFv-Fc-cytokine fusion proteins and stained with a secondary antibody (goat-anti-mouse-IgG2a-PE) (**Fig. 3.8**).

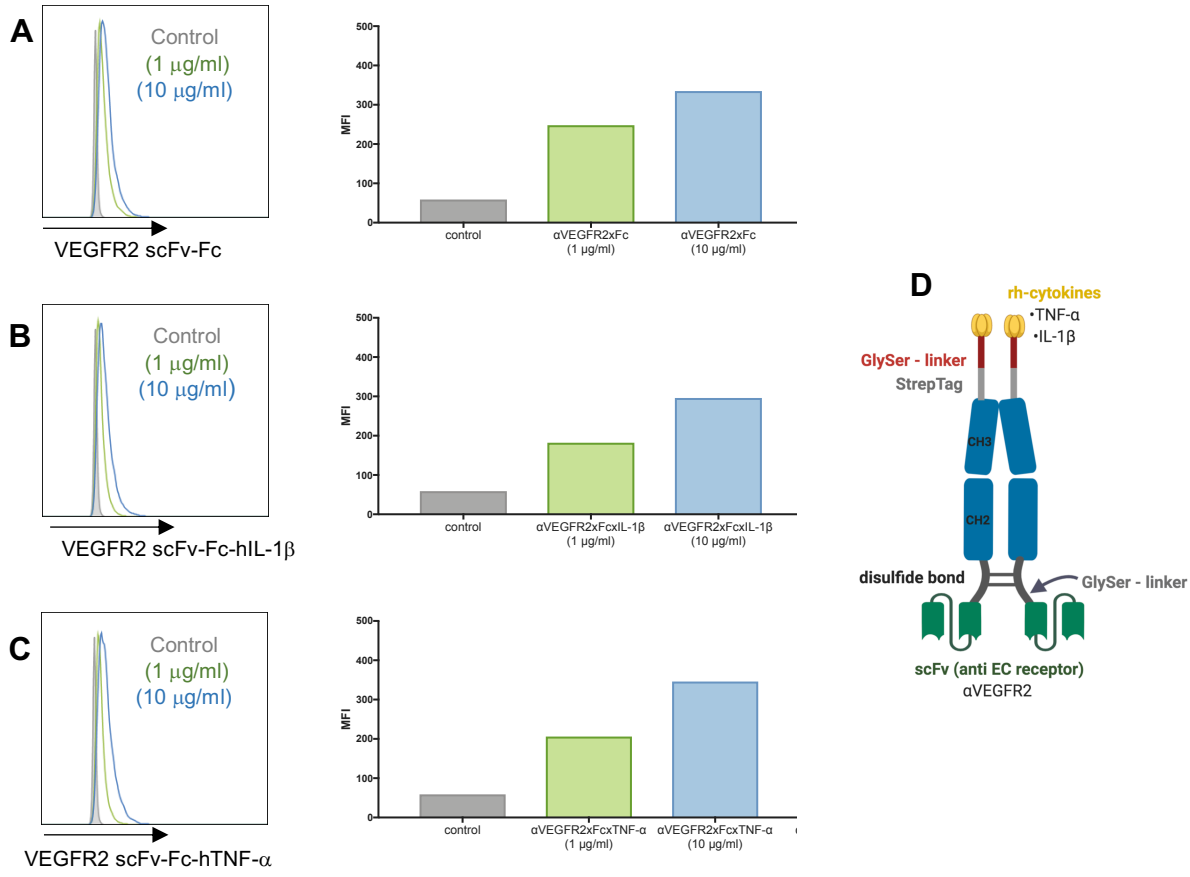

Figure 3.8 Efficiency of the produced αVEGFR2 constructs to bind to HUVEC. HUVEC were pre-stimulated overnight with IL-1β (20 ng/ml) and TNF-α (10 ng/ml) for enhanced expression of VEGFR2. HUVEC were then collected, washed and incubated with two different concentrations (1 μg/ml and 10 μg/ml) of each construct for 15 min on ice. **(A)** αVEGFR2 scFv-Fc antibody, **(B)** αVEGFR2 scFv-Fc-hIL-1β and **(C)** αVEGFR2 scFv-Fc-hTNF-α binding was detected by goat-anti-mouse-IgG2a-PE secondary antibody (also used alone as control – grey line/bar). **(D)** VEGFR2 antibody-cytokine fusion protein structure.

The produced constructs were able to bind to VEGFR2 expressed by HUVEC, confirming the functional structure of the αVEGFR2 single-chain antibody.

The activation capacity of the antibody-cytokine fusion proteins was also studied (**Fig. 3.9**). As shown in previous results, cytokine-mediated activation of endothelium can induce adhesion molecules expression. In order to test whether αVEGFR2-cytokine fusion proteins could induce endothelial cell activation, HUVEC were stimulated with different concentration of purified αVEGFR2 scFv-Fc-hIL-1β and/or αVEGFR2 scFv-Fc-hTNF-α proteins and, for comparison, with a respective commercial recombinant human cytokines. αVEGFR2 scFv-Fc was used as a negative control.

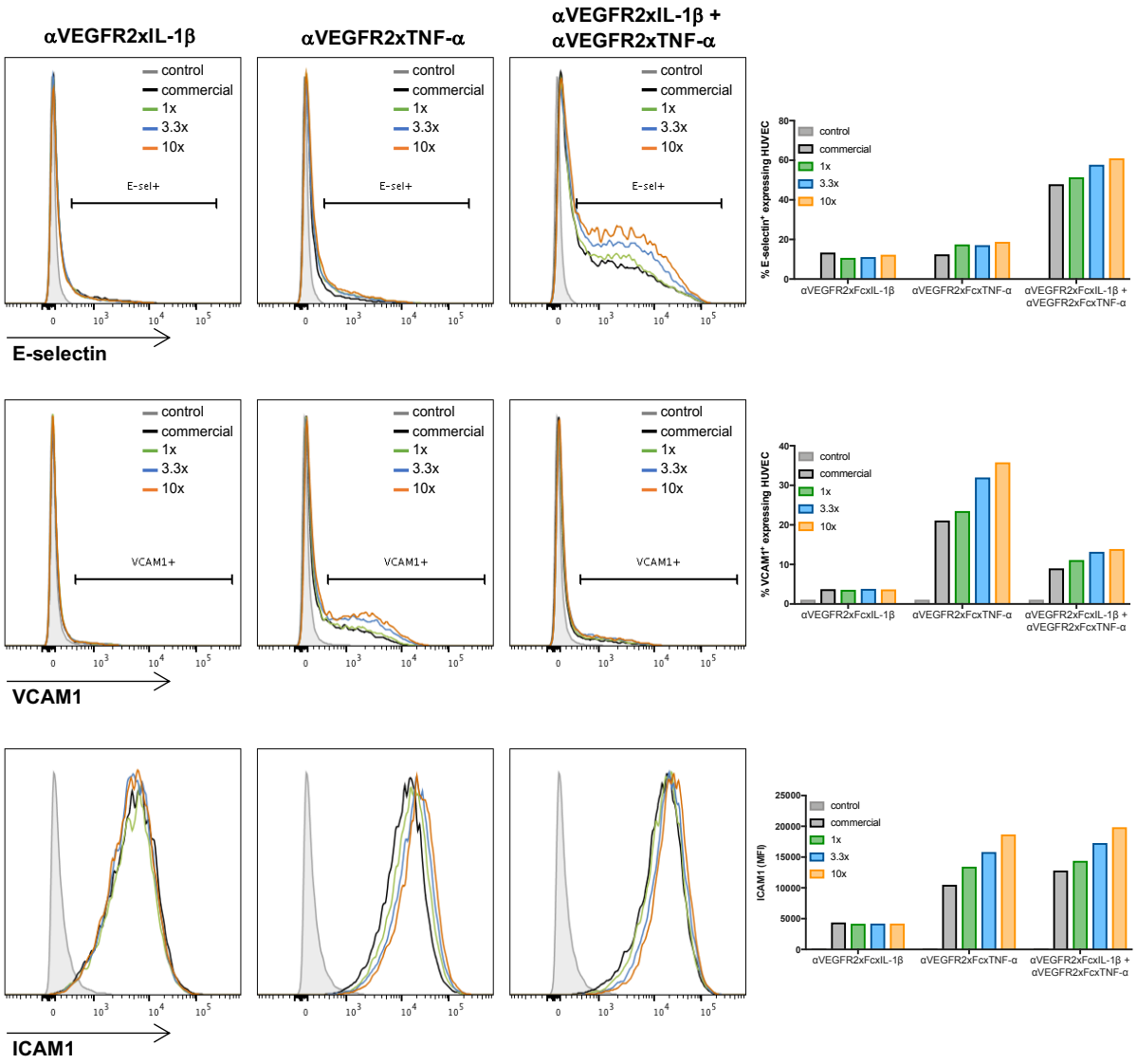

Figure 3.9 Titration of antibody-cytokine fusion proteins. HUVEC were stimulated overnight with αVEGFR2 scFv-Fc-hIL-1β and/or αVEGFR2 scFv-Fc-hTNF-α or respective commercial recombinant human cytokines rhIL-1β (20 ng/ml) and rhTNF-α (10 ng/ml). Produced constructs were used at the same molarity as commercial cytokines (1x) and further titrated up (3.3-fold and 10-fold higher concentrated). Histograms representing expression levels (frequency of positive cells or MFI) of adhesion molecules (E-selectin, ICAM1 and VCAM1). αVEGFR2 scFv-Fc was used as a negative control (grey line/bar).

EC activation profile after stimulation with αVEGFR2 scFv-Fc-hIL-1β and/or αVEGFR2 scFv-Fc-hTNF-α is consistent with previous results obtained with commercial cytokines (**Fig. 3.6**). The adhesion marker induction was dose dependent. E-selectin induction was effective when HUVEC were incubated with both antibody-cytokine fusion proteins, αVEGFR2 scFv-Fc-hIL-1β and αVEGFR2 scFv-Fc-hTNF-α. ICAM1 up-regulation was also slightly more prominent with both fusion proteins, but αVEGFR2 scFv-Fc-hTNF-α was playing a major role. The induction of VCAM1 on HUVEC was clearly observed when HUVEC were stimulated with the αVEGFR2 scFv-Fc-hTNF-α construct, while the αVEGFR2 scFv-Fc-hIL-1β fusion protein had

an inhibitory effect in combination with the former. Taken together, both antibody-cytokine fusion proteins were able to efficiently promote an activated status of HUVEC.

T cell binding increases after EC stimulation with αVEGFR2 antibody-cytokine fusion proteins

Activated endothelial cells undergo morphological and functional changes to recruit T cells to inflamed tissues. E-selectin expressed by activated EC is an adhesion molecule involved in the early steps of the transmigration cascade making loose interactions with T cells. After T cell activation, intracellular activating signal induces a conformational change in integrins on the lymphocyte surface and after ICAM1 and VCAM1 engagement, firm adhesion and transmigration occurs.

Since VEGFR2 antibody-cytokine fusion proteins induced EC activation and up-regulation of adhesion molecules it can be expected that T cell binding is influenced. To study that, activated and non-activated T cells were co-cultured overnight with HUVEC, in the presence of the antibody-cytokine fusion proteins produced. After washing, adherent cells were collected, and T cell binding was assessed by flow cytometry (**Fig. 3.10**).

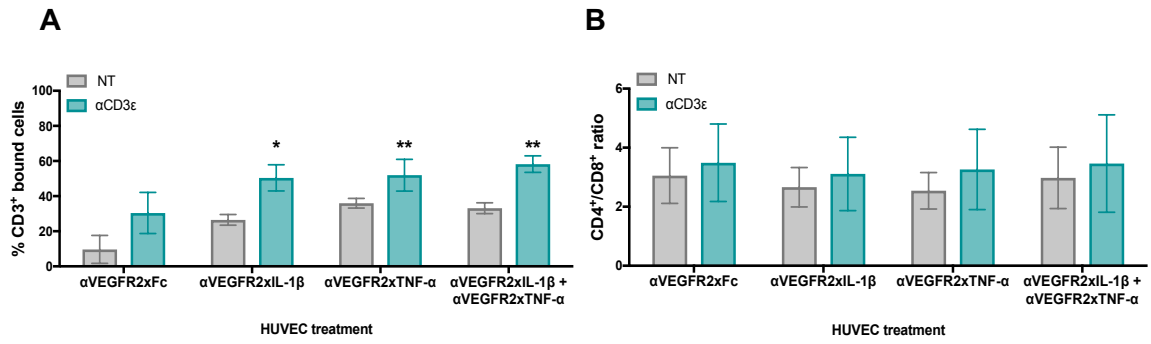

Figure 3.10 T cell binding is influenced by αVEGFR2 antibody-cytokine fusion proteins. T cells were treated with αCD3ε (5 ng/ml) for 3 days or left untreated before co-culture with HUVEC. αVEGFR2 scFv-Fc, αVEGFR2 scFv-Fc-hIL-1β and/or αVEGFR2 scFv-Fc-hTNF-α constructs were added to the co-culture and left overnight. After washing, adherent cells were collected, and T cell binding was assessed by flow cytometry. **(A)** Percentage of $CD3^+$ bound T cells are shown in part. **(B)** $CD4^+/CD8^+$ ratio of $CD3^+$ bound T cells. Data is presented as mean of 3 independent experiments ± SEM. Significant differences compared to the control (NT/αVEGFR2-Fc; first grey bar) are marked by asterisks (*, $P < 0.05$; **, $P < 0.01$).

T cell or HUVEC activation alone was not able to increase T cell binding in a statistically significant manner. Just after the co-activation of both cells, T cells were able to bind more efficiently to HUVEC (**Fig. 3.10A**). Activated $CD3^+$ T cells showed a significantly increased binding to HUVEC in the presence of αVEGFR2 scFv-Fc-hIL-1β (40%) and αVEGFR2 scFv-Fc-hTNF-α (40%), especially when combined (60%), compared to non-treated T cells

co-cultured with non-treated HUVEC. However, the ratio between $CD4^+$ and $CD8^+$ of the bound $CD3^+$ cells did not change after T cell activation, staying around one $CD8^+$ to three $CD4^+$ T cells (**Fig. 3.10B**).

Although αVEGFR2 antibody-cytokine fusion proteins performed well in activating EC and consequently increasing T cell binding *in vitro*, IL-1β and TNF-α could bind *in vivo* to their receptors on other cells leading to adverse effects. Also, T cell binding to endothelium occurs as a consequence of EC activation which can limit T cell infiltration *in vivo.* On the other hand, αVEGFR2 antibody-cytokine fusion proteins might be advantageous if one considers a two-step scenario with a first activation of $VEGFR2^+$ tumor neovasculature and enhanced T cell binding and extravasation as the second step.

3.4 DIRECT TARGETING OF T CELLS TO TUMOR ENDOTHELIUM USING BISPECIFIC ANTIBODIES INDUCES T CELL ACTIVATION AND SUBSEQUENT EC ACTIVATION

3.4.1 Binding confirmation and titration of the produced bispecific antibodies

To overcome a potential problem of T cell binding as a secondary event acquired after EC activation, bispecific antibodies were engineered to target and activate T cells directly at the tumor endothelium.

A αVEGFR2-hIgG1-$Fc_{Aglycan}$-OKT3 bispecific antibody was built to bind T cells via CD3ε, inducing activation, and at the same time bind tumor endothelium via VEGFR2 and blocking VEGF binding to this angiogenic receptor. To boost T cell activation and increase T cell binding to EC, a αTIE2-hIgG1-$Fc_{Aglycan}$-9.3 (αCD28) and αPD-L1-hIgG1-$Fc_{Aglycan}$-9.3 (αCD28) bispecific antibodies were included in further studies as well. With the same principle as the construct described before, αCD28 single chain antibody will bind to T cells, giving a co-stimulatory signaling via αCD28 molecule, and αTIE2 or αPD-L1 single chain antibodies will bind to TIE2 and PD-L1 receptor on EC. The TIE2 pathway is very important for angiogenesis regulation, especially on tumors vessels. Angiopoietin-2 (Ang-2) is known to be highly up-regulated in tumors and is one of the TIE2 ligands, playing a role in vessel destabilization. For this reason, using a blocking αTIE2 antibody could prevent Ang-2 binding to TIE2, helping tumor vessel normalization. PD-L1 is expressed on the surface of tumor cells and it can bind to PD-1 on the surface of activated T cells and B cells. The binding of PD-L1 to PD-1 leads to an immunosuppressive effect and allows the tumor to evade immune destruction (Swaika et al. 2015). Endothelial cells also expressed PD-L1 which can also limit T cell activation as well as compromise the blocking of PD-L1 on tumor cells by check point inhibition immunotherapy. For these reasons PD-L1 seems to be a very good target on EC too.

To confirm the binding of produced constructs, isolated CD3⁺ T cells were incubated with purified αVEGFR2-Fc-αCD3ε, αTIE2-Fc-αCD28, αVEGFR2-Fc-αCD28 and αPD-L1-Fc-αCD28 bispecific monoclonal antibodies (BiMAbs) and stained with a secondary antibody (goat-anti-human-IgG1-PE) (**Fig. 3.11**). The binding of the bispecific antibodies to activated HUVEC was also evaluated by flow cytometry. (**Fig. 3.12**).

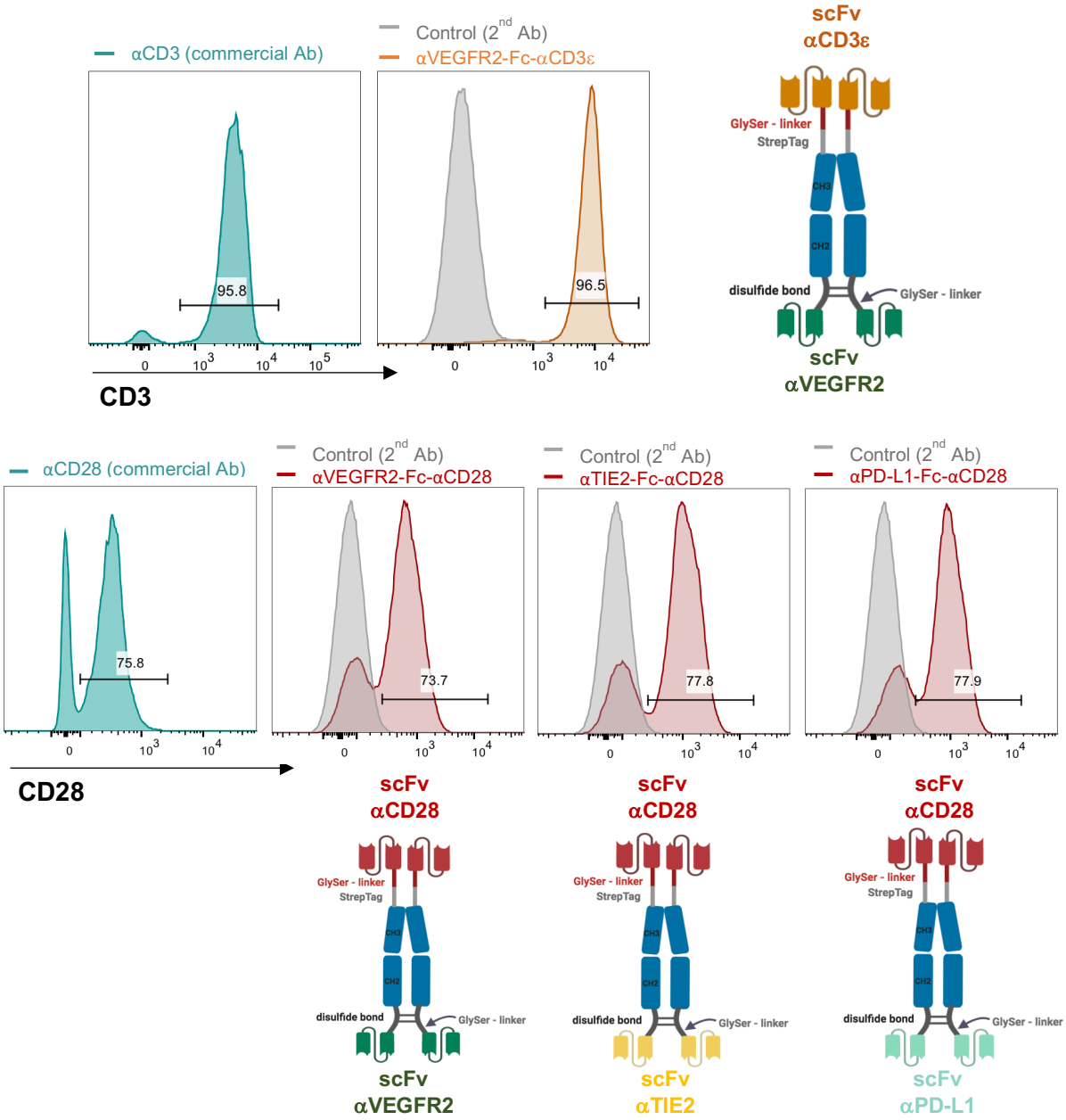

Figure 3.11 Binding of produced BiMAbs to CD3⁺ T cells. Freshly isolated T cells were incubated with 5 μg/ml of produced constructs (αVEGFR2-Fc-αCD3ε, αTIE2-Fc-αCD28, αPD-L1-Fc-αCD28) for 20 min on ice. Binding was detected by goat-anti-human-IgG1-PE secondary antibody (also used alone as negative control). αCD28 and αCD3 commercial antibodies were used as a positive control (1 μg/ml).

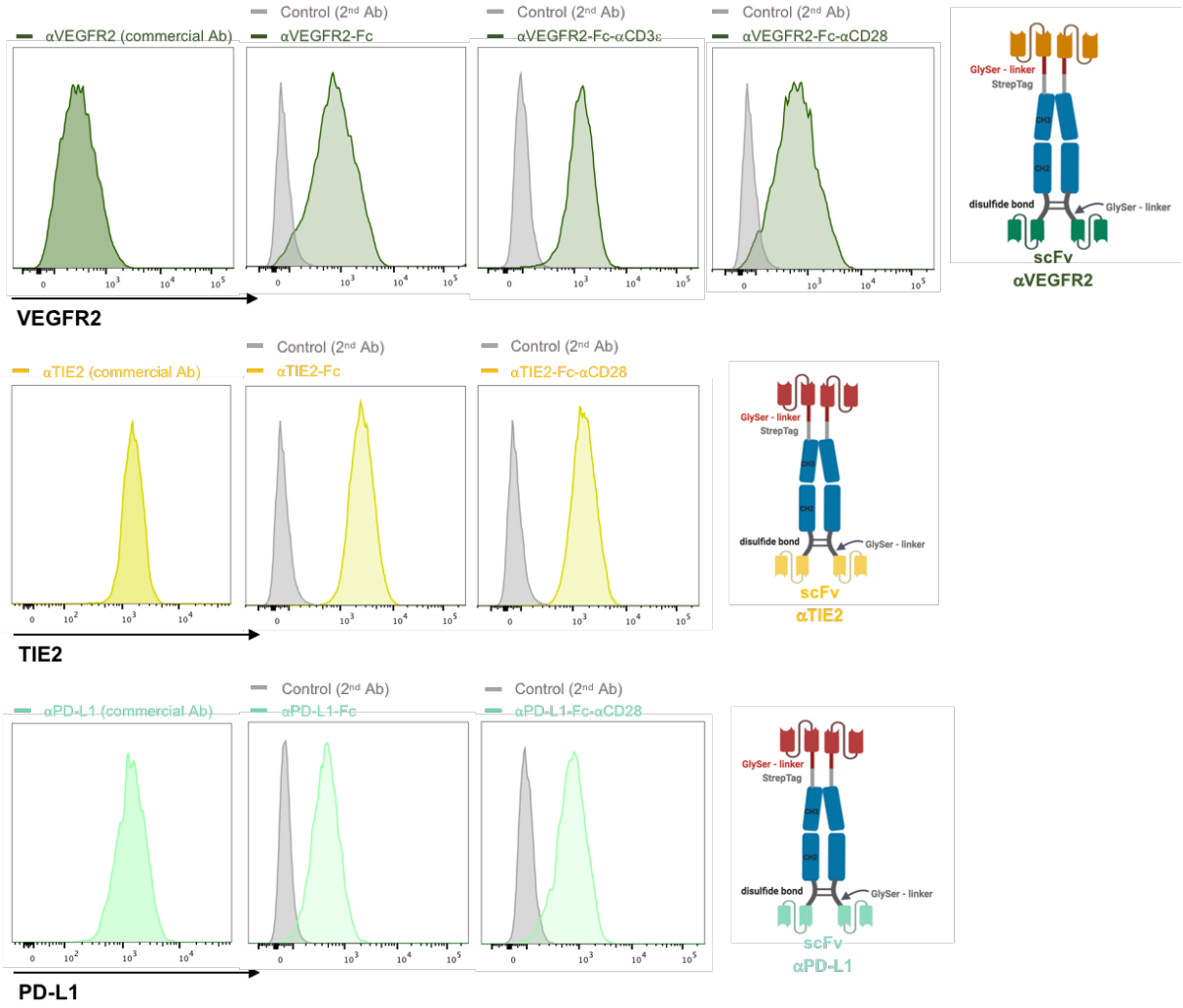

Figure 3.12 Binding of produced BiMAbs to endothelial cells. HUVEC were pre-stimulated overnight with IL-1β (20 ng/ml) and TNF-α (10 ng/ml) for enhanced expression of VEGFR2, TIE2 and PD-L1. HUVEC were then collected, washed and incubated with 5 μg/ml of each construct for 20 min on ice (αVEGFR2-Fc-αCD3ε; αVEGFR2 scFv-Fc-αCD28; αTIE2 scFv-Fc-αCD28; αPD-L1 scFv-Fc-αCD28, and respective Fc controls). Binding was detected by goat-anti-human-IgG1-PE secondary antibody (also used alone as negative control). αVEGFR2, αTIE2 and αPD-L1 commercial antibodies were used as a positive control (1 μg/ml).

After binding confirmation, BiMAbs were titrated in order to determine the best concentration for an optimal T cell activation profile. T cells were culture or co-cultured with HUVEC in the presence of αVEGFR2-Fc-αCD3ε, and/or αTIE2-Fc-αCD28, and/or αPD-L1-Fc-αCD28 for 24 hours. CD25 and 4-1BB expression was evaluated on both T cell $CD4^+$ (**Fig. 3.13A**) and $CD8^+$ subpopulations (**Fig. 3.13B**) as an early and late activation marker respectively.

A

αTIE2 x Fc x αCD28

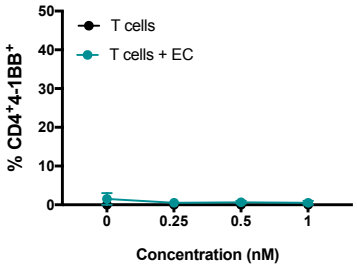

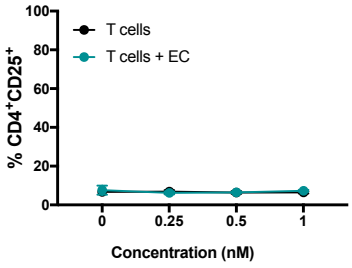

αPD-L1 x Fc x αCD28

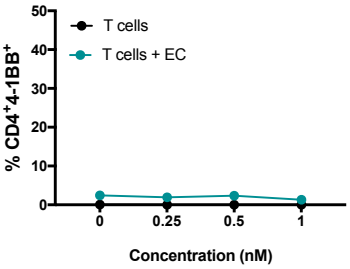

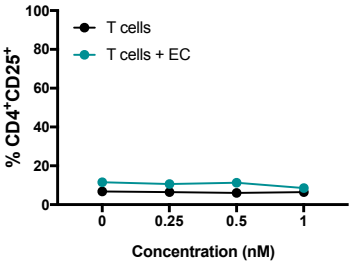

αVEGFR2 x Fc x αCD3ε

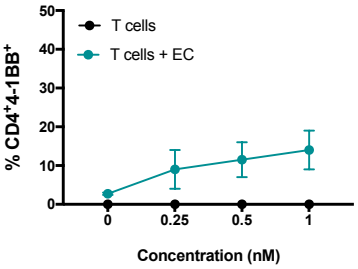

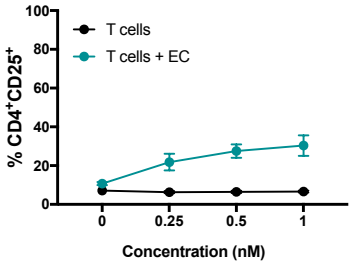

αVEGFR2 x Fc x αCD3ε + αTIE2 x Fc x αCD28

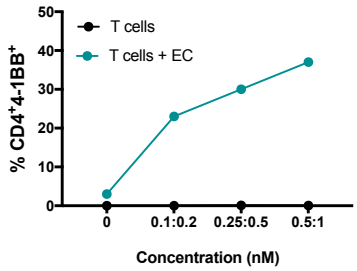

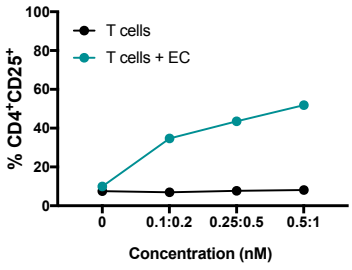

αVEGFR2 x Fc x αCD3ε + αPD-L1x Fc x αCD28

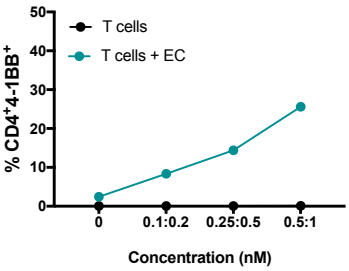

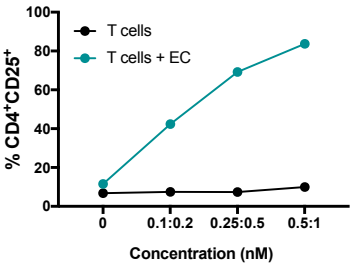

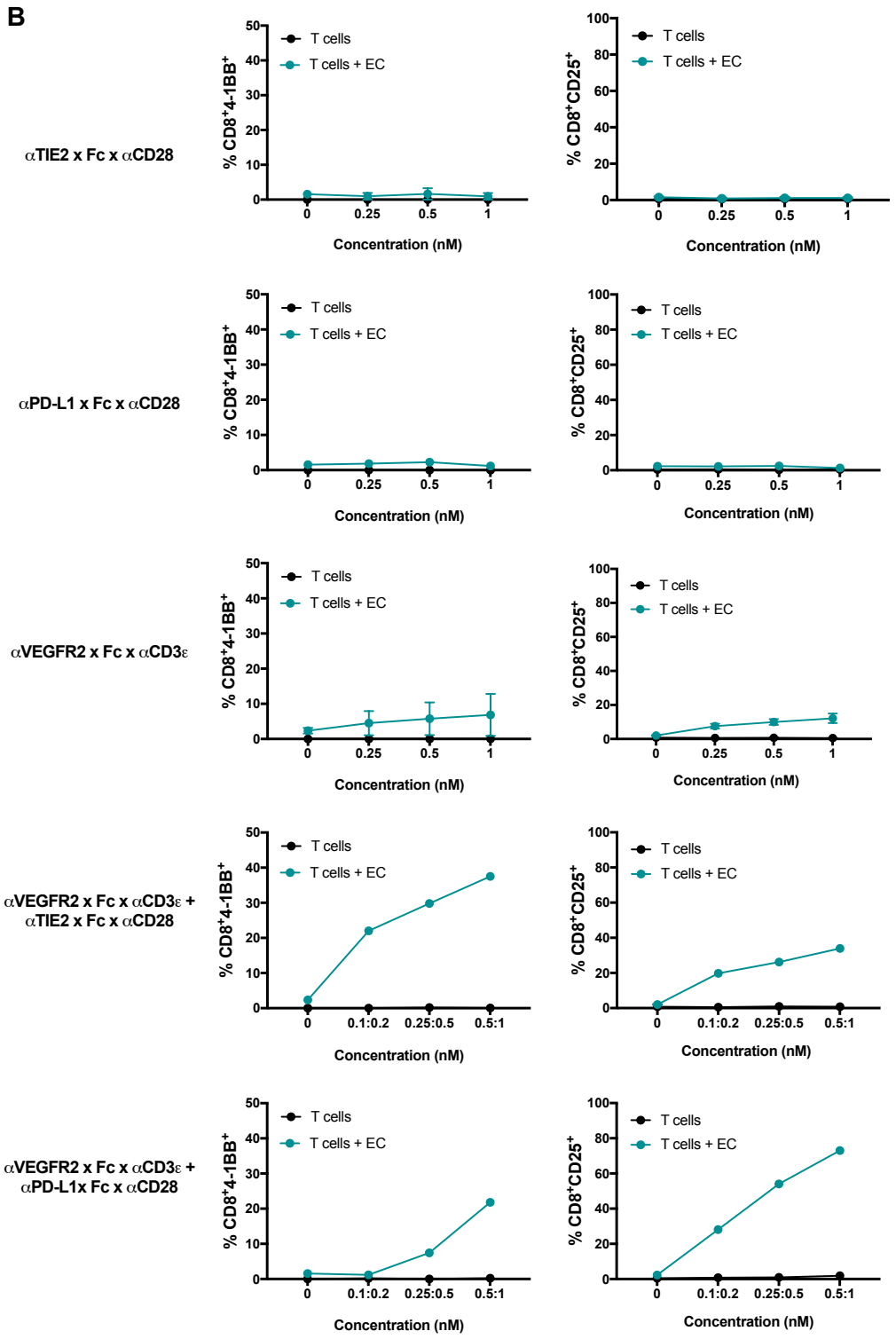

Figure 3.13 Titration of produced bispecific antibodies to achieve optimal T cell activation. Freshly isolated T cells alone or co-cultured with HUVEC in the presence of purified bispecific antibodies, αVEGFR2-Fc-αCD3ε, and/or αTIE2-Fc-αCD28, and/or αPD-L1-Fc-αCD28 for 24 hours. Cells were collected and evaluated by flow cytometry. **(A)** $CD4^+$ and **(B)** $CD8^+$ T cell activation was characterized by the expression levels of 4-1BB and CD25. Data is presented as mean ± SEM, n=1-3 independent experiments.

The αTIE2-Fc-αCD28 and αPD-L1-Fc-αCD28 bispecific antibodies alone did not influence T cell activation, as expected since CD28 works as a co-stimulatory molecule depending on a simultaneous activation by TCR complex/CD3 triggering. Interestingly, αVEGFR2-Fc-αCD3ε bispecific antibody after CD3ε crosslinking was able to induce activation on both T cell subpopulations $CD4^+$ and $CD8^+$ (**Fig. 3.13**), only in the presence of HUVEC after VEGFR2 engagement. This is a very important finding regarding safety since the αVEGFR2-Fc-αCD3ε construct needs crosslinking on both targets to trigger T cell activation.

In the presence of αVEGFR2-Fc-αCD3ε, it is possible to observe 4-1BB and CD25 up--regulation on $CD4^+$ and $CD8^+$ T cells in a dose-dependent fashion. T cell activation was further boosted when T cells were simultaneously co-stimulated with αTIE2-Fc-αCD28 or with αPD-L1-Fc-αCD28.

The best activation profile on both T cell subpopulations was achieved in the presence of 0.5 nM αCD3ε (stimulatory) BiMAb in combination with 1 nM αCD28 of the (co-stimulatory) BiMAbs. Of note, T cell co-stimulation could also be achieved by targeting VEGFR2 or TIE2 with 2 BiMAbs harboring αCD3ε scFv and αCD28 scFv, respectively but showed less T cell activation capacity (data not shown).

3.4.2 αVEGFR2-Fc-αCD3ε alone or in combination with and αTIE2-Fc-αCD28 or αPD-L1-Fc-αCD28 bispecific antibodies induce T cell activation after crosslinking with HUVEC

To confirm the previous findings and to quantify the activation status of T cells, isolated $CD3^+$ cells were kept in culture or were co-culture with HUVEC, in the presence of αVEGFR2-Fc-αCD3ε (0.5 nM) alone or together with αTIE2-Fc-αCD28 (1 nM) or with αPD-L1-Fc-αCD28 for 24 h. Cells were collected, stained, and analyzed by flow cytometry. Cell surface activation markers such as 4-1BB, CD69 and CD25 were evaluated on $CD4^+$ (**Fig. 3.14A**), and $CD8^+$ (**Fig. 3.14B**) T cell subpopulations. CD3 levels on live cells and CD28 levels on $CD3^+$ cells from the co-culture were analyzed in order to confirm αVEGFR2-Fc-αCD3ε and αTIE2-Fc-αCD28 engagement (**Fig. 3.14C**). Cytokine secretion was assessed by sandwich ELISA to quantify the levels of IFN-γ and TNF-α, as described in Material and Methods **(2.2.6**).

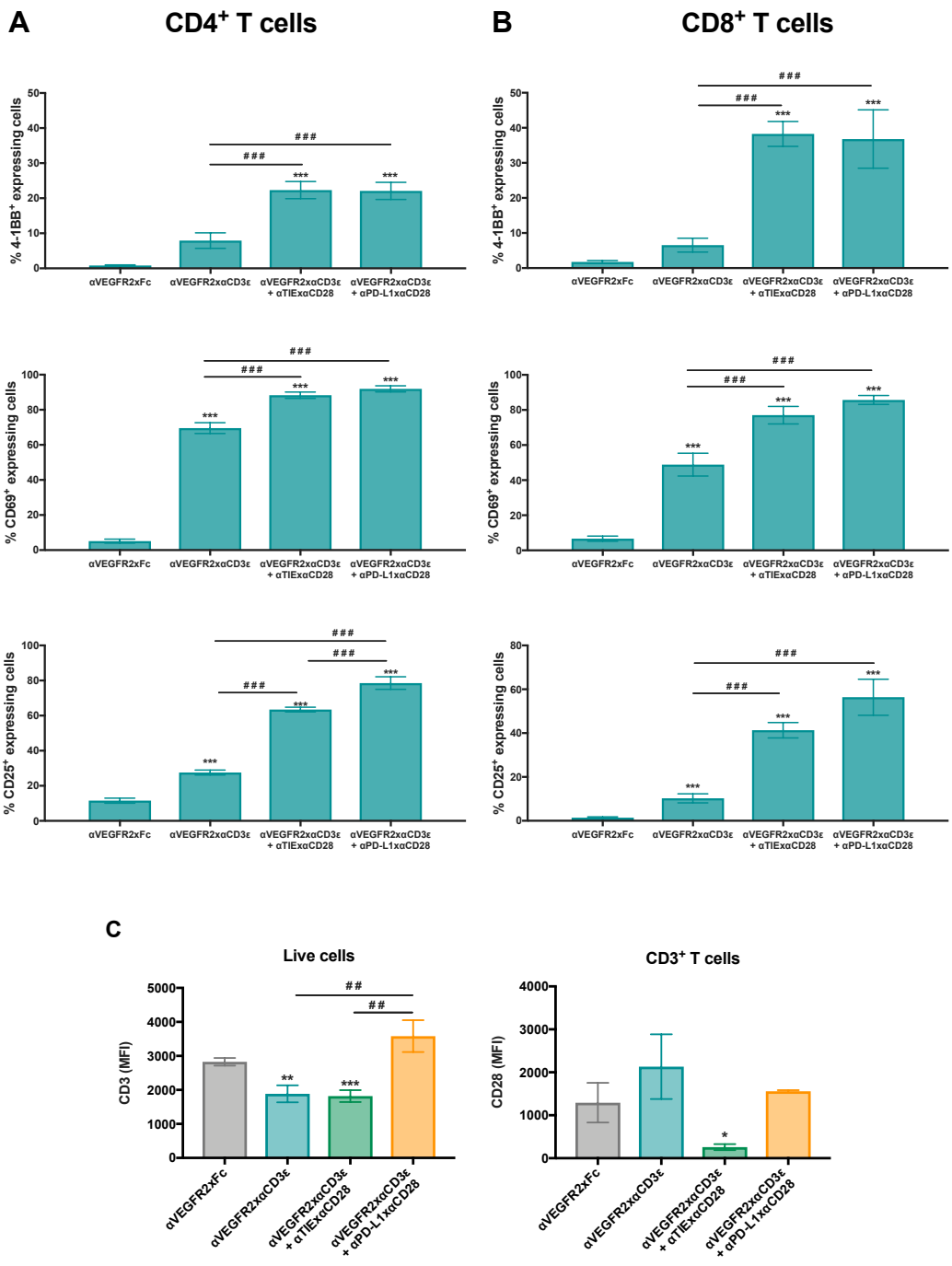

Figure 3.14 T cell activation induced by αVEGFR2-Fc-αCD3ε alone or in combination with and αTIE2-Fc-αCD28 or αPD-L1-Fc-αCD28 antibodies. T cells were co-cultured with HUVEC or left alone overnight with or without bispecific antibodies (αVEGFR2-Fc-αCD3ε (0.5 nM) alone or in combination with αTIE2-Fc-αCD28 or αPD-L1-Fc-αCD28 (1 nM)). After washing, cells were collected, and T cell activation was analyzed by flow cytometry. The induction of early (4-1BB and CD69) and late (CD25) activation surface markers was studied on both T cell subpopulations, $CD4^+$ T cells (**A**) and $CD8^+$ T cells (**B**). CD3 and CD28 regulation was evaluated on live cells or on $CD3^+$ T cells, respectively (**C**) from the co-culture, to confirm the engagement of the bispecific constructs. Data is presented as mean ± SEM from 9-12 independent experiments. Significant differences compared to the control (αVEGFR2-Fc) are marked by asterisks (*, $P < 0.05$; **, $P < 0.01$; ***, $P < 0.001$) and significant differences between treatments are marked by hashtags ($^{\#\#}$, $P < 0.01$; $^{\#\#\#}$, $P < 0.001$).

Interestingly, αVEGFR2-Fc-αCD3ε, αTIE2-Fc-αCD28, and αPD-L1-Fc-αCD28 did not induce 4-1BB, CD69 expression, or up-regulating CD25 on T cells that had no contact with HUVEC, indicating the specificity and safety of those BiMAbs (data not shown). Even though αVEGFR2-Fc-OKT3 crosslinks the CD3ε receptor on T cells, there was no binding of αVEGFR2 antibody, and no T cell activation was observed.

On the other hand, the αVEGFR2-Fc-αCD3ε bispecific antibody successfully stimulated T cells co-cultured with HUVEC, leading to a significant increase of CD69 (~70%) and CD25 (~30%) levels on $CD4^+$ and $CD8^+$ T cell subpopulations. Co-stimulation with αTIE2-Fc-αCD28 or with αPD-L1-Fc-αCD28 resulted in a strong synergistic effect regarding T cell activation, significantly increasing the levels of expression of all activation markers on both T cell populations compared to the single treatment with αVEGFR2-Fc-αCD3ε (**Fig. 3.14A/B**).

Live T cells from the co-culture showed a decrease in CD3 expression (MFI ~50% reduced) after stimulation with αVEGFR2-Fc-αCD3ε, which indicates a successful binding of the αCD3ε single-chain antibody leading to blocking or modulation of the epitope of the commercial αCD3ε antibody used for staining. However, in the presence of αPD-L1-Fc-αCD28 CD3 expression seems to be restored. $CD3^+$ T cells from the co-culture treated with αTIE2-Fc-αCD28 also showed downmodulation of the CD28 antigen, which decreased αCD28 staining (**Fig. 3.14C**).

To further confirm T cell activation, cytokine secretion (TNF-α and IFN-γ) was assessed by sandwich ELISA (**Fig. 3.15**), as described in Material and Methods.

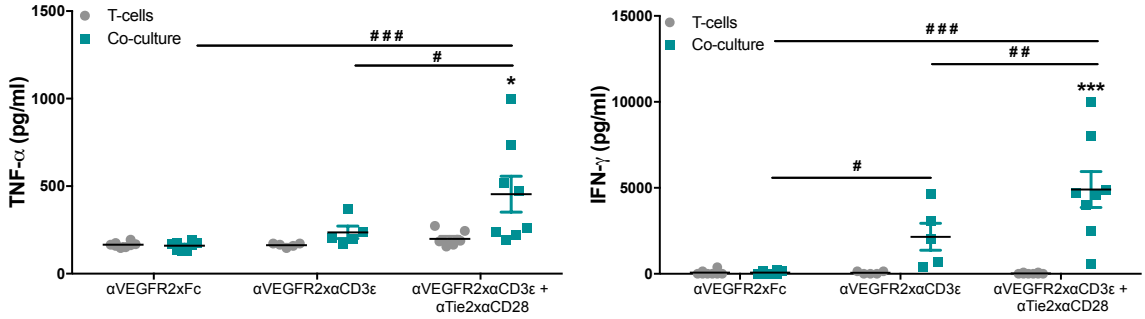

Figure 3.15 T cell cytokine secretion after stimulation with αVEGFR2-Fc-αCD3ε and αTIE2-Fc-αCD28 bispecific antibodies. T cells were co-cultured with HUVEC or left alone overnight with or without αVEGFR2-Fc-αCD3ε (0.5 nM) and αTIE2-Fc-αCD28 (1 nM). Supernatants were collected and analyzed by sandwich ELISA. Graphs are representing the quantification of TNF-α and IFN-γ (pg/ml). Data is presented as mean ± SEM from 5-8 independent experiments. Significant differences compared to the control (αVEGFR2-Fc) are marked by asterisks (*, $P < 0.05$; ***, $P < 0.001$) and significant differences between treatments are marked by hashtags ($^{\#}$, $P < 0.05$; $^{\#\#}$, $P < 0.01$; $^{\#\#\#}$, $P < 0.001$).

T cells co-cultured with HUVEC in the presence of αVEGFR2-Fc-αCD3ε produced measurable amounts of TNF-α slightly above background. When αTIE2-Fc-αCD28 is additionally present in the co-culture, a marked increase in TNF-α secretion is observed (~500 pg/ml), either compared to control or with a single treatment. IFN-γ secretion was more abundantly secreted and significantly higher in the presence of αVEGFR2-Fc-αCD3ε (~2150 pg/ml) compared to the control. IFN-γ secretion detected in the supernatant from T cells co-stimulated with αTIE2-Fc-αCD28 was two times higher (~5000 pg/ml) compared to the single treatment with αVEGFR2-Fc-αCD3ε.

Together, these observations confirmed the capacity of the produced bispecific antibodies αVEGFR2-Fc-αCD3ε and αTIE2-Fc-αCD28 to induce a successful T cell activation upon crosslinking both targets on each cell. This activation resulted in TNF-α and IFN-γ secretion, which can have an impact on HUVEC activation.

Further experiments will be performed with αPD-L1-Fc-αCD28 to compare both co-stimulation BiMAbs regarding cytokine secretion.

3.4.3 EC activation as a consequence of local T cell activation promoted by bispecific constructs

In parallel to T cell analysis, HUVEC were also collected after co-culture and evaluated by flow cytometry. CD105, also known as endoglin, was used to gate EC on the FACS analysis. The expression of EC activation markers, such as E-selectin, VCAM1, and ICAM1 was evaluated (**Fig. 3.16**)

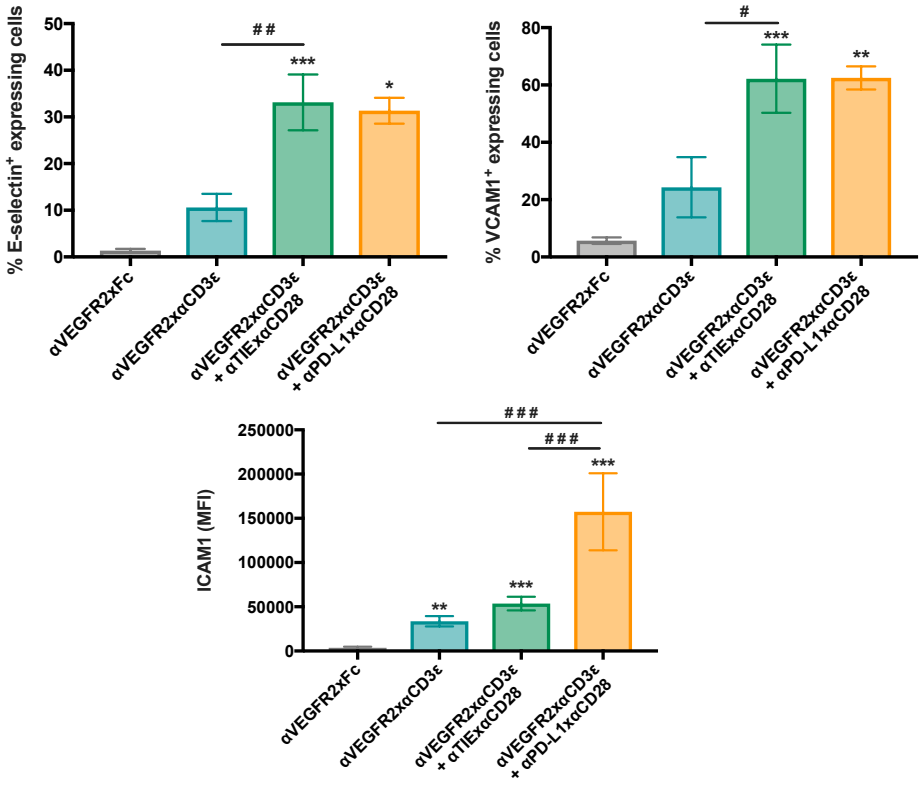

Figure 3.16 HUVEC activation profile after T cell *in situ* activation. T cells were co-cultured with HUVEC overnight with or without bispecific antibodies (αVEGFR2-Fc-αCD3ε (0.5 nM), αTIE2-Fc-αCD28 and αPD-L1-Fc-αCD28 (1 nM)). After washing, cells were collected and HUVEC activation status was analyzed by flow cytometry. The induction of adhesion molecules on HUVEC surfaces was evaluated. Data is presented as mean ± SEM from 9-12 independent experiments. Significant differences compared to the control (no BiMAbs) are marked by asterisks (*, P < 0.05; **, P < 0.01; ***, P < 0.001) and significant differences between treatments are marked by hashtags (#, P < 0.05; ##, P < 0.01; ###, P < 0.001).

HUVEC activation was effectively achieved in the presence of αVEGFR2-Fc-αCD3ε with αTIE2-Fc-αCD28 or with αPD-L1-Fc-αCD28. The activation profile was consistent with T cell activation and cytokine secretion. In the presence of αVEGFR2-Fc-αCD3ε, ICAM1 was inducible, whereas VCAM1 and E-selectin expression was dependent of co-stimulation with αTIE2-Fc-αCD28 or αPD-L1-Fc-αCD28 bispecific antibody. ICAM1 up-regulation was also more effective in the presence of co-stimulatory antibodies, specially αPD-L1-Fc-αCD28.

Previous results showed that supernatants from the co-culture with both bispecific antibodies had higher amounts of TNF-α which can directly influence HUVEC activation (**Fig. 3.15**).

To study whether HUVEC activation could be achieved indirectly through the presence of secreted factors by activated T cells, supernatants from all conditions of T-cell/HUVEC co-culture (24 h) were collected and transferred to pre-seeded HUVEC (**Fig. 3.17**). Supernatants from co-culture (48 h) with OKT3 antibody were also used for comparison.

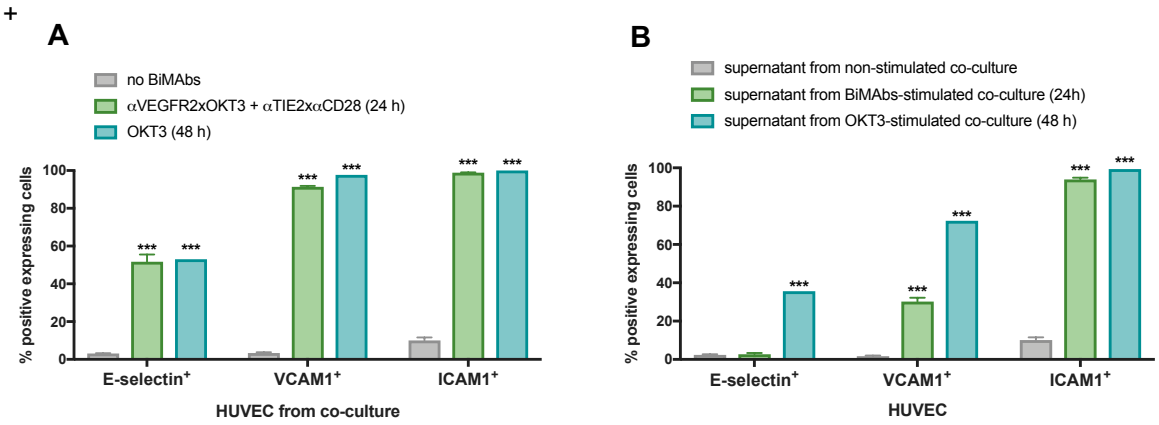

Figure 3.17 Activation of HUVEC promoted by soluble factors secreted by activated T cells. T cells were co-cultured with HUVEC with or without bispecific antibodies (αVEGFR2-Fc-αCD3ε (0.5 nM) and αTIE2-Fc-αCD28 (1 nM)) for 24 h, or with commercial OKT3 antibody (5 ng/ml) for 48 h. After washing, cells were collected, and **(A)** HUVEC activation status was analyzed by flow cytometry. **(B)** Supernatants from T-cell/HUVEC co-cultured were collected and transfer into unstimulated HUVEC for 24 h. The induction of adhesion molecules on HUVEC surface was evaluated by flow cytometry. Data is presented as mean ± SEM from 1-3 independent experiments. Significant differences compared to the respective control (grey bars - no BiMAbs) are marked by asterisks (***, $P < 0.001$).

HUVEC activation is inducible by soluble factors **(Fig. 3.17B)** as an effect of local T cell activation promoted by the bispecific antibodies.

This is an important finding that can be crucial to improve T cell transendothelial migration towards tumors with low levels of T cell infiltrates. Furthermore, once HUVEC activation is reached, induced EC markers like E-selectin, VCAM1, or ICAM1 could also be used as targets to augment the migration of cytotoxic T cells towards tumor endothelium.

However, neutralizing assays need to be performed to find the exact cytokine panel responsible for HUVEC activation.

3.5 T CELL TRANSENDOTHELIAL MIGRATION INCREASED BY THE PRESENCE OF BISPECIFIC ANTIBODIES

So far, self-produced BiMAbs have proven to induce activation of both T cells and EC. However, the T cell transmigration cascade is a complex process that depends not only on the expression of suitable homing receptors but also on the success of the dynamic interaction between both cells.

3.5.1 Transwell experiment optimizations

The influence of αVEGFR2-Fc-αCD3ε and αTIE2-Fc-αCD28 bispecific antibodies on T cell transendothelial migration was analyzed using a transwell assay as described in Materials and Methods. For this purpose, HUVEC were seeded in transwell inserts, pre-coated with 1% of human fibronectin at 15 µg/cm^{2,} and grown until confluency. To optimize HUVEC monolayer growth in 48 h, different seeding numbers were tested (**Fig. 3.18**). HUVEC monolayer permeability was evaluated by FITC-dextran (3-5 kDa) permeability test. FITC-dextran is added to the upper chamber, and after one h, molecules that pass through the endothelial cell monolayer will be detected in the lower chamber using a fluorescence reader. The FITC-dextran migration rate is proportional to the monolayer's permeability. Results suggest that 2.5x10^4 HUVEC were the optimal seeding number to reach the tightest monolayer after 48 h since the percentage of FITC-Dextran found in the lower chamber was close to zero.

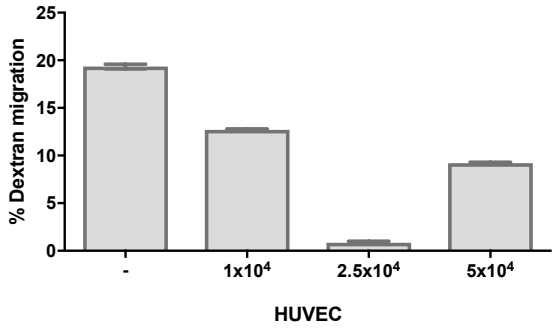

Figure 3.18 Optimization of HUVEC monolayer for transwell assay. Transwell inserts were coated with 1% of human fibronectin at 15 µg/cm^2. HUVEC were seeded on coated inserts at different densities (1x10^4, 2.5x10^4 and 5x10^4) and left for 48 h until a confluent monolayer was achieved. HUVEC monolayer permeability was evaluated by the presence of FITC-dextran (3-5 kDa) in the supernatant from the down-chamber using a fluorescence reader. Data is presented as mean ± SEM of technical triplicates.

After confirmation of the tightness of the HUVEC monolayer, isolated CD3$^+$ T cells were added to the upper chamber in a ratio of 1 EC to 10 T cells, together with bispecific antibodies. Different concentrations of αVEGFR2-Fc-αCD3ε and αTIE2-Fc-αCD28 were tested to find the best conditions for CD3$^+$ T cell optimal migration (**Fig. 3.19**).

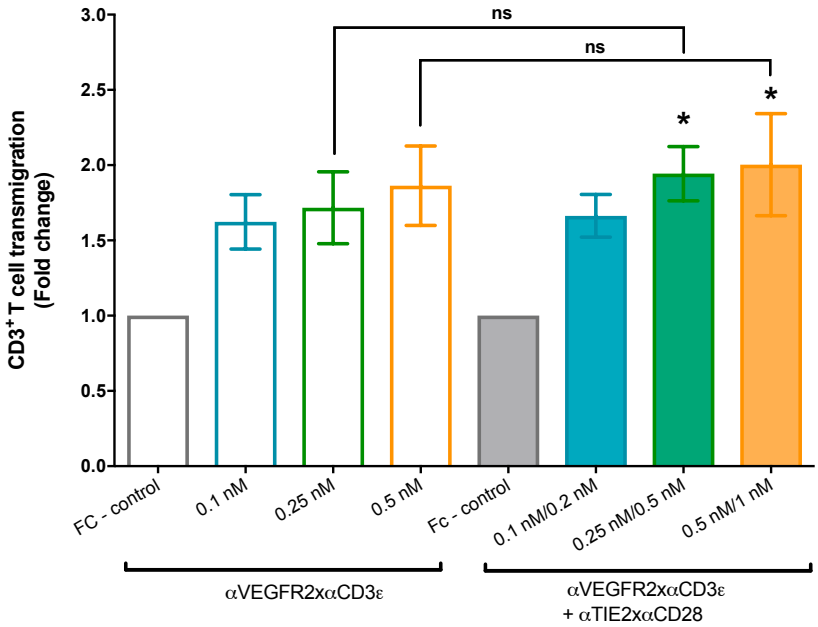

Figure 3.19 Titration of bispecific antibody concentrations for optimal T cell migration. Transwell inserts were coated with 1% of human fibronectin at 15 µg/cm^{2,} and 2.5x10^4 HUVEC were seeded and left for 48 h until reaching a confluent monolayer. Isolated CD3$^+$ T cells were added to the upper chamber, in a ratio of 1 EC to 10 T cells, together with (αVEGFR2-Fc-αCD3ε (0.1-0.5 nM) and αTIE2-Fc-αCD28 (0.2-1 nM). After 24 h, migrated T cells were collected from the lower chamber and quantified by flow cytometry using counting beads. Graph representing fold change of CD3$^+$ T cell migration through endothelial cell monolayer. Data is presented as mean ± SEM of 3 independent experiments. Significant differences compared to the respective Fc control are marked by asterisks (*, P < 0.05). **NS**, non-significant changes between stimulation and stimulation plus co-stimulation BiMAbs.

Even though there was a tendency for the αVEGFR2-Fc-αCD3ε BiMAb to increase CD3$^+$ T cell migration at a higher concentration (0.5 nM) through the HUVEC monolayer, the combination with αTIE2-Fc-αCD28 seemed to be slightly more efficient, also at higher concentrations (0.25/0.5 nM and 0.5/1 nM), improving CD3$^+$ T cell migration for the double compared to the respective monospecific scFv-Fc control.

3.5.2 The efficiency of T cell transendothelial migration is increased in the presence of αVEGFR2-Fc-αCD3ε

To further evaluate the impact of purified BiMAbs on T cell transendothelial migration, transwell experiments were repeated using either 0.5 nM of αVEGFR2-Fc-αCD3ε or a combination with 1 nM of αTIE2-Fc-αCD28 or 1 nM of αPD-L1-Fc-αCD28. Migrated CD3$^+$ cells were collected from the down-well and quantified by flow cytometry using counting beads (**Fig. 3.20**).

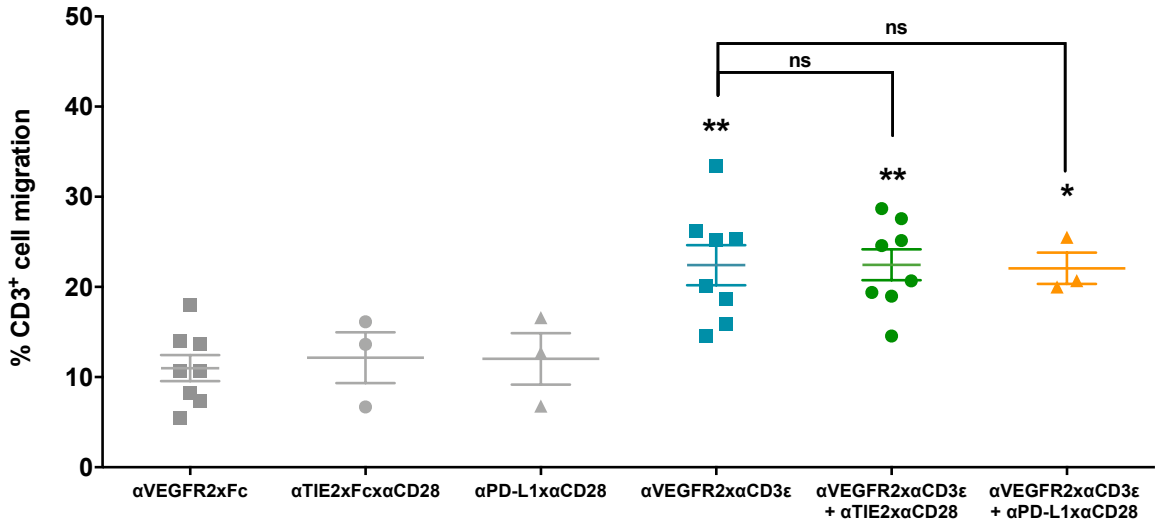

Figure 3.20 T cell migration is increased by αVEGFR2-Fc-αCD3ε treatment alone or together with αTIE2-Fc-αCD28 or αPD-L1-Fc-αCD28 co-stimulation. Transwell inserts were coated with 1% of human fibronectin at 15 µg/cm^{2,} and 2.5x10^4 HUVEC were seeded and left for 48 h until reaching a confluent monolayer. Isolated CD3$^+$ T cells were added to the upper chamber, in a ratio of 1 EC to 10 T cells, together with αVEGFR2-Fc-αCD3ε (0,5 nM), αTIE2-Fc-αCD28 (1 nM), αPD-L1-Fc-αCD28 (1 nM) or respective controls. After 24 h, migrated CD3$^+$ T cells were collected from the lower chamber and quantified by flow cytometry using counting beads. The figure indicates the percentage of transmigrated CD3$^+$ T cells from CD3$^+$ T cells added to the upper well (1x10^6). Data is presented as mean ± SEM from 3-9 independent experiments. Significant differences compared to the respective Fc control are marked by asterisks (*, P < 0.05; **, P < 0.01). **ns**, non-significant changes between stimulation and stimulation plus co-stimulation BiMAbs.

Before starting the transwell assay, HUVEC monolayer permeability was always assessed by the FITC-dextran permeability test. Although dextran diffusion was always close to zero (data not shown), indicating a tight HUVEC monolayer, the results show that 10% of T cells were able to migrate through HUVEC in the presence of Fc control antibodies. This finding can be explained by the fact that there is no flow applied in this model, and T cells, due to gravity, will make contact with HUVEC which can lead to unspecific T cell migration.

Nevertheless, in the presence of αVEGFR2-Fc-αCD3ε, T cell migration doubled compared to the respective control, however is no further increased by co-stimulation.

To confirm an activated phenotype of transmigrated CD4$^+$ and CD8$^+$ T cells after the co-culture with stimulatory or stimulatory and co-stimulatory BiMAbs, activation markers CD69, CD25 and 4-1BB were evaluated (**Fig. 3.21**).

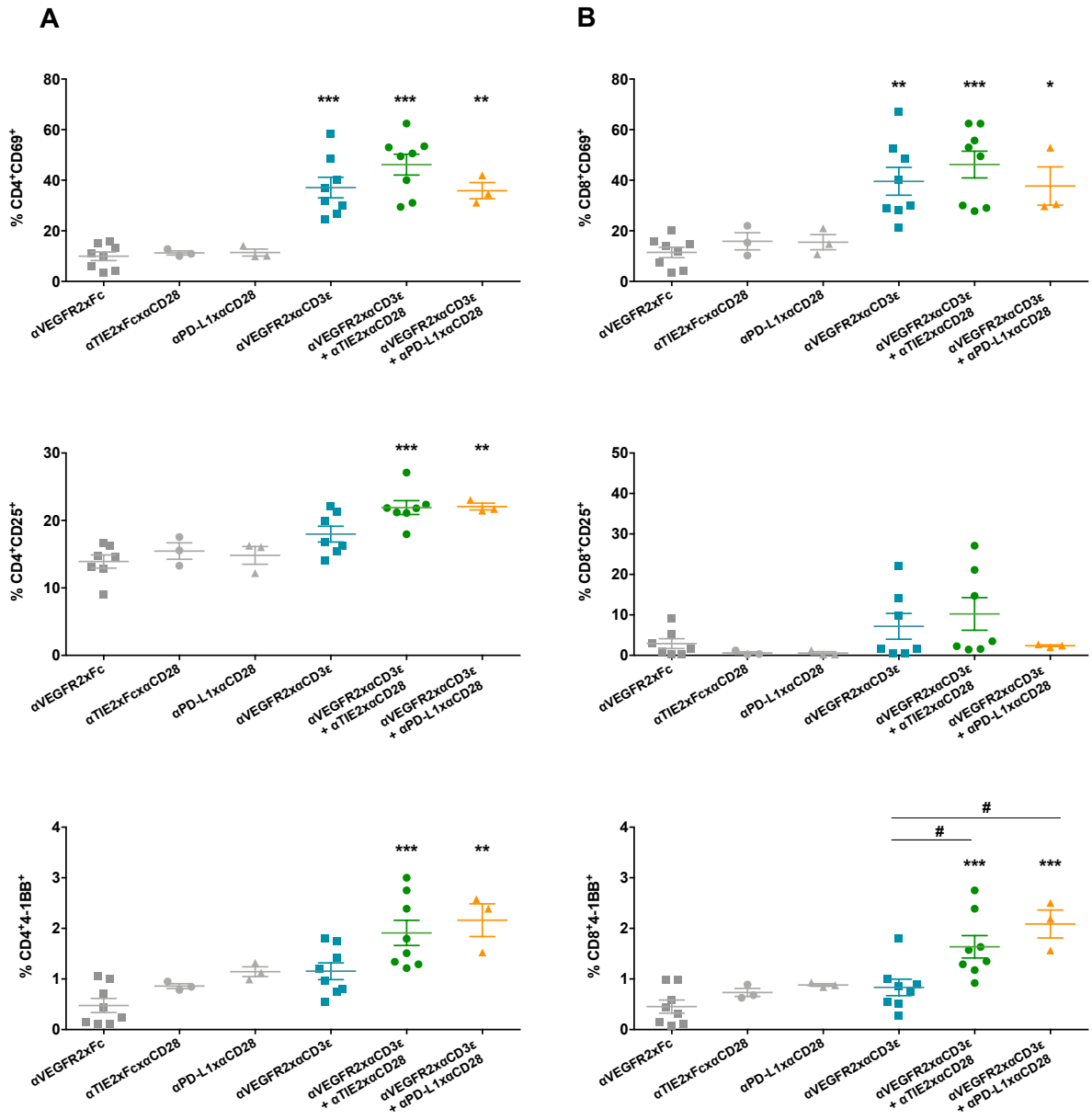

Figure 3.21 Migration capacity is related to the T cell activation status. Transwell inserts were coated with 1% of human fibronectin at 15 µg/cm^2 and 2.5x10^4 HUVEC were seeded and left for 48 h until reaching a confluent monolayer. Isolated CD3$^+$ T cells were added to the upper chamber, in a ratio of 1 EC to 10 T cells, together with αVEGFR2-Fc-αCD3ε (0.5 nM), αTIE2-Fc-αCD28 and αPD-L1-Fc-αCD28 (1 nM) or respective Fc controls. After 24 h, migrated CD3$^+$ T cells were collected from the lower chamber and the activation profile was characterized by flow cytometry. The induction of early (CD69) and late (4-1BB and CD25) activation surface markers was studied on both T cell subpopulations, CD4$^+$ T cells **(A)** and CD8$^+$ T cells **(B)** that had migrated. Data is presented as mean ± SEM from 5 independent experiments. Significant differences compared to the respective monospecific scFv-Fc control are marked by asterisks (*, P < 0.05; **, P < 0.01; ***, P < 0.001) and significant differences between treatments are marked by hashtags ($^{\#}$, P < 0.05).

The activation of migrated T cells was observed when αVEGFR2-Fc-αCD3ε and αTIE2-Fc-αCD28 or αPD-L1-Fc-αCD28 bispecific antibodies were present. 4-1BB up-regulation was mainly dependent on the co-stimulatory bispecific antibodies in both T cell subpopulations.

CD69 was the most sensitive marker to the stimulation with αVEGFR2-Fc-αCD3ε showing a similar pattern of expression on $CD4^+$ and $CD8^+$ T cells and co-stimulatory bispecific antibodies did not showed a synergistic effect for this activation marker.

CD25 expression on $CD4^+$ T cells was dependent of co-stimulation. $CD4^+$ T cells have a baseline expression of ~15% $CD25^+$ cells that could be increased (up to 25%) in the presence of both BiMAbs. On $CD8^+$ T cells, CD25 was slightly inducible by αVEGFR2-Fc-αCD3ε alone (~10%) or in combination with αTIE2-Fc-αCD28 (~15%).

In general, the T cell activation status of migrated T cells was lower than in T cells derived from co-culture experiments (**Fig. 3.14**) although still enough to improve T cell migration trough HUVEC monolayer as suggested by **Fig. 3.20.**

HUVEC from the transmigraton assay were also collected in order to assess their activation profile by flow cytometry (**Fig. 3.22**).

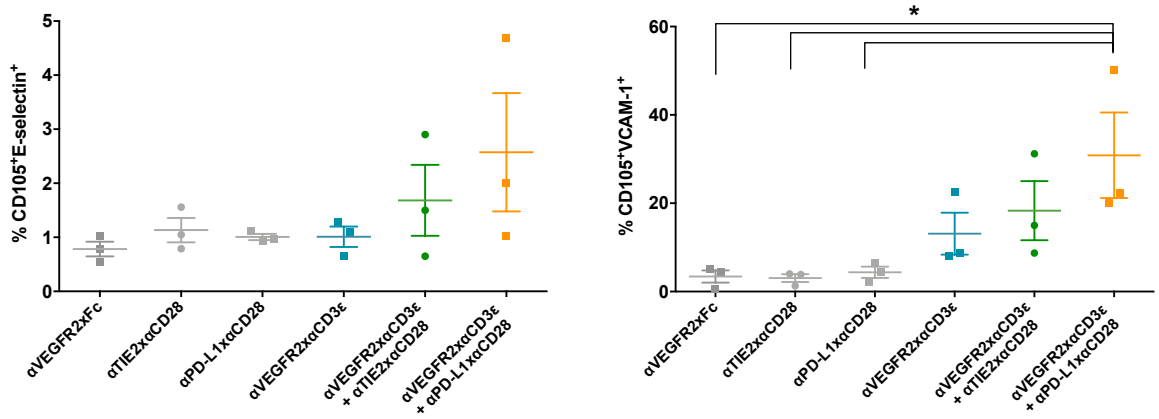

Figure 3.22 HUVEC activation profile after T cell activation and transmigration. After transmigration for 24 h in the presence of αVEGFR2-Fc-αCD3ε (0.5 nM) and/or together with αTIE2-Fc-αCD28 (1 nM) and/or with αPD-L1-Fc-αCD28 (1 nM), HUVEC from the transwell insert were collected and the activation status was assessed by flow cytometry. The induction of E-selectin and VCAM1 on HUVEC ($CD105^+$ cells) is represented in the graphs. Data is presented as mean ± SEM from 3 independent experiments. Significant differences compared to the controls (grey dots) are marked by asterisks (*, $P < 0.05$).

The expression of E-selection on HUVEC after transmigration assay was poorly affected, although in the presence of both bispecific antibodies, stimulatory and co-stimulatory, showed a little increase. VCAM1 expression showed the same regulation as E-selectin but in the presence of αVEGFR2-Fc-αCD3ε with αPD-L1-Fc-αCD28, up-regulation of VCAM1 levels were significant higher compare to the controls.

However EC activation was not successfully achieved compared to the same treatments on previous co-culture experiments (**Fig. 3.16**).

3.5.3 Using αCD8 bispecific antibodies to prioritize cytotoxic T cell migration

The presence of produced bispecific antibodies was effectively improving $CD3^+$ T cell migration through HUVEC monolayer. However, regarding tumor killing, cytotoxic T cells ($CD8^+$) play a major role, as suggested by several studies have reported a positive correlation between $CD8^+$ T cell tumor infiltration and better response and prognosis in several types of cancers (Gooden et al. 2011; Kim and Ahmed 2010; Kmiecik et al. 2013; Tumeh et al. 2014).

In order to preferentially induce the migration of cytotoxic T cells, bispecific antibodies targeting CD8 receptor were produced. Taking advantage of the fact that αVEGFR2-Fc-OKT3 and αTIE2-Fc-αCD28 bispecific antibodies were inducing HUVEC activation and consequently up-regulating homing receptors, E-selectin and VCAM1 were used as a target on HUVEC as well as TIE2 (control) that is constitutively expressed. Therefore, bispecific antibodies incorporating the scFv of the anti-CD8 antibody OKT8 with αE-selectin, αVCAM1, and αTIE2 were generated.

To confirm the binding of produced constructs, isolated $CD3^+$ T cells were incubated with purified αE-selectin-Fc-αCD8, αVCAM1-Fc-αCD8, and αTIE2-Fc-αCD8 bispecific monoclonal antibodies (BiMAbs) and stained with a secondary antibody (goat-anti-human-IgG1-PE) (**Fig. 3.23**). The binding of the αCD8 bispecific antibodies to activated HUVEC was also evaluated by flow cytometry (**Fig. 3.24**).

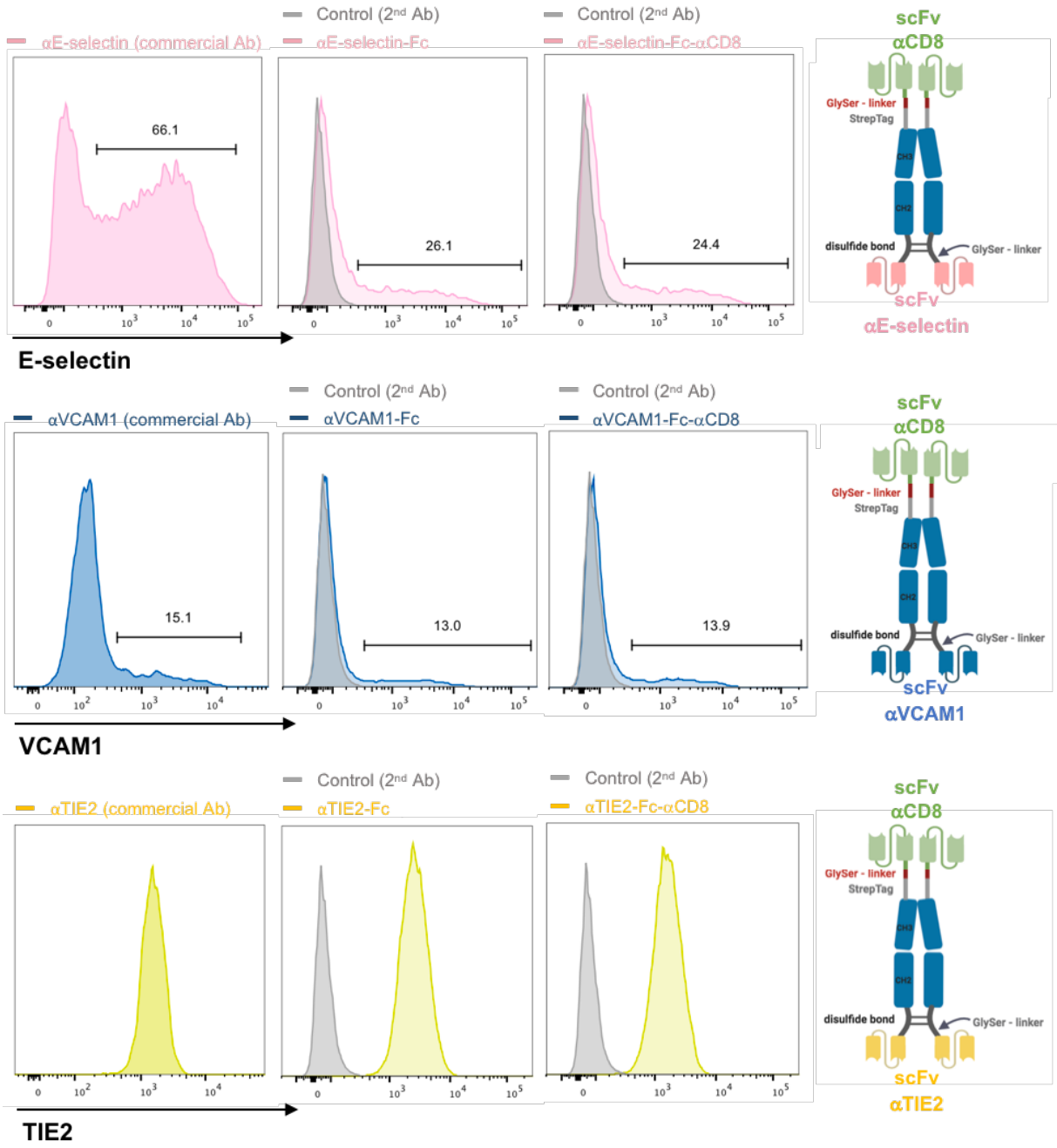

Figure 3.23 Binding of self-produced BiMAbs to endothelial cells. HUVEC were pre-stimulated overnight with IL-1β (20 ng/ml) and TNF-α (10 ng/ml) for enhanced expression of E-selectin, VCAM1 and TIE2. HUVEC were then collected, washed and incubated with 5 μg/ml of each construct for 20 min on ice (αE-selectin-Fc-αCD8, αVCAM1-Fc-αCD8, αTIE2-Fc-αCD8 and respective Fc controls). Binding was detected by goat-anti-human-IgG1-PE secondary antibody (also used alone as negative control). αE-selectin, αVCAM1 and αTIE2 commercial antibodies were used as a positive control (1 μg/ml).

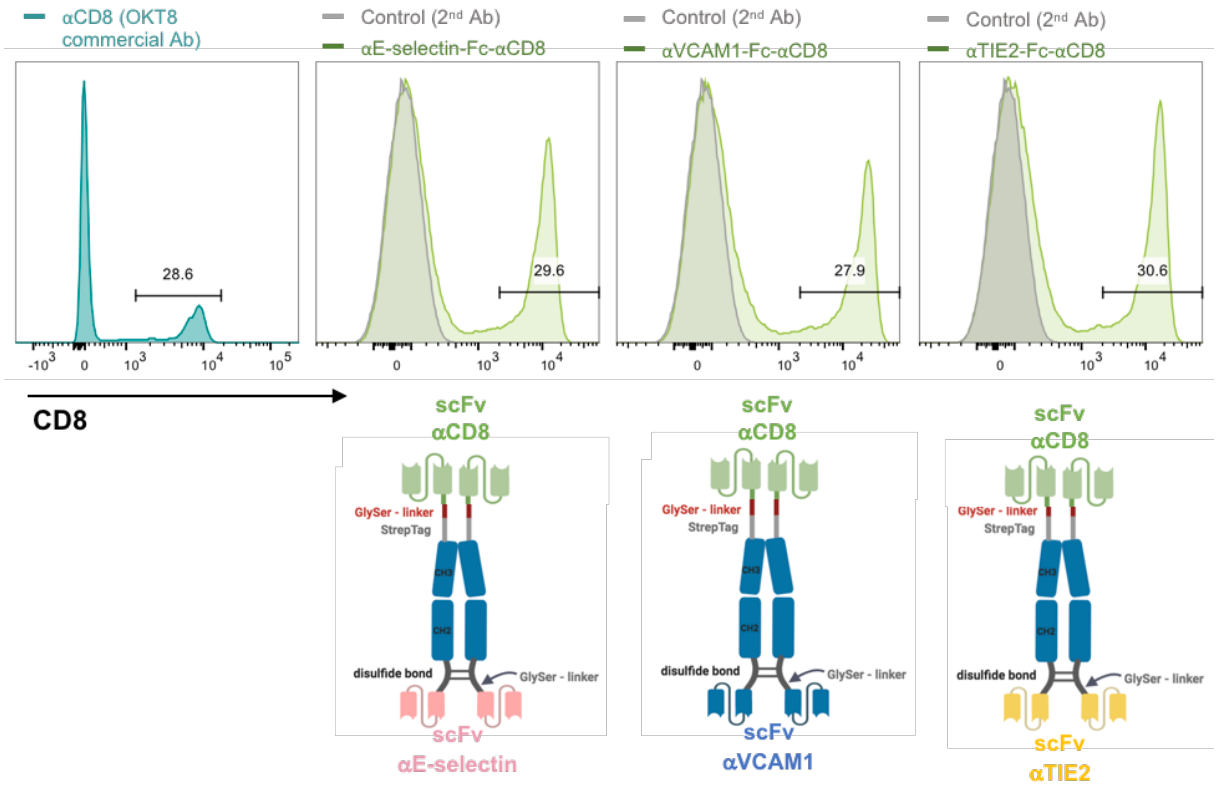

Figure 3.24 Confirmation of binding of αCD8 bispecific antibodies to CD8⁺ T cells. Freshly isolated T cells were incubated with 5 μg/ml of produced constructs (αE-selectin-Fc-αCD8, αVCAM1-Fc-αCD8, αTIE2-Fc-αCD8) for 20 min on ice. Binding was detected by goat-anti-human-IgG1-PE secondary antibody (also used alone as negative control). αCD8 (OKT8) commercial antibody was used as a positive control (1 μg/ml).

After successful binding of self-made BiMAbs, to confirm the enhanced binding of CD8⁺ T cells to pre-activated EC in the presence of αCD8-BiMAbs, an experiment under static conditions has been conducted.

Isolated CD3⁺ cells were co-culture with HUVEC, in the presence of αVEGFR2-Fc-αCD3 (0.5 nM) alone or together with αTIE2-Fc-αCD28 (1 nM) or with αPD-L1-Fc-αCD28 (1 nM) for 24 h.

Simultaneously, αE-selectin-Fc-αCD28, αVCAM1-Fc-αCD28, and αTIE2-Fc-αCD28 (1nM) bispecific antibodies were also included. After washing, adherent cells were collected, and CD3⁺CD8⁺ binding was assessed by flow cytometry using counting beads (**Fig. 3.25**).

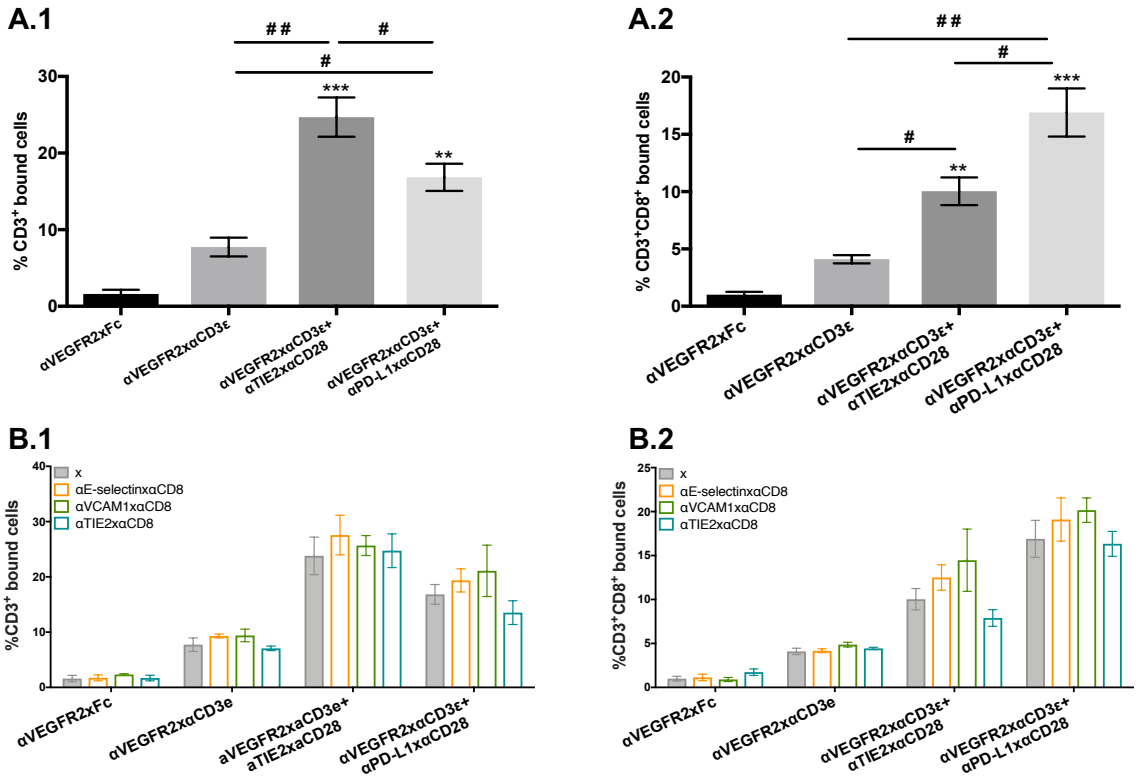

Figure 3.25 Static binding assay of $CD3^+$ and $CD3^+CD8^+$ T cells in the presence self-made BiMAbs. T-cells were co-cultured with HUVEC overnight with stimulatory and co-stimulatory bispecific antibodies (αVEGFR2-Fc-αCD3ε (0.5 nM) alone or together with αTIE2-Fc-αCD28 (1 nM) or with αPD-L1-Fc-αCD28 (1 nM)). αVEGFR2-Fc (0.5 nM) antibody was used as a control. Simultaneously, αE-selectin-Fc-αCD8, αVCAM1-Fc-αCD8 and αTIE2-Fc-αCD8 (1 nM) bispecific antibodies were also included. After washing, adherent cells were collected and binding cells were evaluated by flow cytometry. **(A)** Binding efficiency among stimulatory conditions (**1**.$CD3^+$ T cells; **2**.CD3+$CD8^+$ T cells). **(B)** Binding efficiency among stimulatory conditions in the presence of αCD8 BiMAbs (**1**.$CD3^+$ T cells; **2**.$CD3^+CD8^+$ T cells). Data is presented as mean ± SEM from 3 independent experiments. Significant differences compared to the control (grey bar) are marked by asterisks (*, P < 0.05; **, P < 0.01; ***, P < 0.001) and significant differences between treatments are marked by hashtags (#, P < 0.05; ##, P < 0.01; ###, P < 0.001).

T cell binding is influenced by its activation status. The treatment with αVEGFR2-Fc-αCD3ε together with αTIE2-Fc-αCD28 or with αPD-L1-Fc-αCD28 improved the binding of $CD3^+$ and $CD8^+$ T cells to HUVEC, matching the activation results shown on **Fig. 3.14.** However, αCD8 constructs did not show significant benefits in prioritizing cytotoxic T cell binding.

A migration assay was also performed with the same stimulatory conditions to study if $CD8^+$ T cell migration could be enhanced by the presence of αCD28 constructs in a more dynamic system. $CD8^+$ T cell migration was quantified by flow cytometry using counting beads (**Fig. 3.26**).

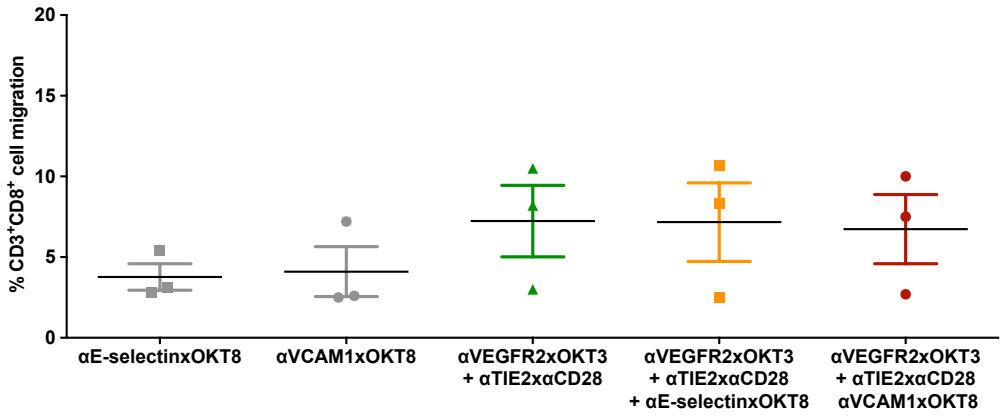

Figure 3.26 Migration of cytotoxic T cells through HUVEC in the presence of αCD8 antibodies. Transwell inserts were coated with 1% of human fibronectin at 15 µg/$cm^{2,}$ and $2.5x10^4$ HUVEC were seeded and left for 48 h until reaching a confluent monolayer. Isolated $CD3^+$ T cells were added to the upper chamber, in a ratio of 1 EC to 10 T cells, together with αVEGFR2-Fc-αCD3ε (0.5 nM) and αTIE2-Fc-αCD28 (1 nM) combined either with αE-selectin-Fc-αCD8 (1 nM) or αVCAM1-Fc-αCD8 (1 nM). αE-selectin-Fc-αCD8 (1 nM) or αVCAM1-Fc-αCD8 (1 nM) were also used alone as a control. After 24 h, migrated $CD3^+$ T cells were collected from the lower chamber and quantified by flow cytometry using counting beads. The figure indicates percentage of transmigrated $CD3^+CD8^+$ T cells from $CD3^+CD8^+$ T cells added to upper well. Data is presented as mean ± SEM for 3 independent experiments.

The percentage of $CD3^+CD8^+$ T cells slightly increased in the presence of αVEGFR2-Fc-αCD3ε and αTIE2-Fc-αCD28 but the addition of αE-selectin-Fc-αCD8 and αVCAM1-Fc-αCD8 did not further enhanced $CD8^+$ frequency on transmigrated T cells.

3.5.4 Cytotoxic capacity of migrated BiMAb-treated T cells towards tumor cells

T cells migration was effectively increased by self-produced stimulatory and co-stimulatory bispecific antibodies even though αCD8 constructs were not sufficient to prioritize $CD8^+$ T cell migration.

Nevertheless, the influence of αVEGFR2-Fc-αCD3ε and αTIE2-Fc-αCD28 on T cell killing capacity towards tumor cells was not expected since these constructs do not target tumor cells.

For BiMAb-treated migrated cells to be able to kill tumor cells, 1 nM of αHER2xhIgG1xαCD3ε was additionally added to the co-culture of migrated cells (collected from down wells of transmigration assay) and MCF-7 for 24 h. αHER2xhIgG1xαCD3ε can crosslink with migrated

T cells via CD3ε and with MCF-7 via HER2, leading to an additional stimulation of T cells and tumor cell targeting.

To study the impact of bispecifific antibodies, used to improve T cell transmigration, on the killing capacity of migrated $CD3^+$ T cells in the presence of αHER2xhIgG1xαCD3ε, supernatants from the co-culture with tumor MCF-7 were collected and cytotoxic capacity was quantified by lactate dehydrogenase (LDH) released.

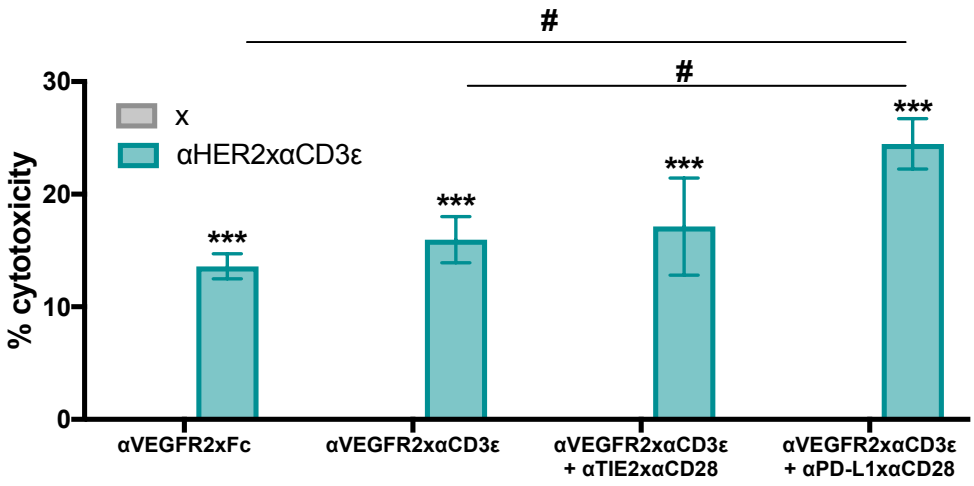

Figure 3.27 The cytotoxic capacity of BiMAb-treated migrated CD3+ T cells in the presence of αHER2xhIgG1xαCD3ε. MCF-7 were seeded in a 96-well plate, 24 h prior to the co-culture. Migrated T cells (from the transwell migration assay) were collected from the bottom well and transferred onto pre-cultured MCF-7 for 24 h, only pre-treated with αVEGFR2-Fc-αCD3ε ± αTIE2-Fc-αCD28 or ± αPD-L1-Fc-αCD28, or in the presence of an additional bispecific antibody αHER2xhIgG1xαCD3ε (1 nM). Migrated $CD3^+$ T cells cytotoxic capacity was evaluated by lactate dehydrogenase (LDH) quantification of supernatants from the co-culture with tumor MCF-7. Data is presented as mean ± SEM from 3 independent experiments. Significant differences compared to the control (grey bar) are marked by asterisks (***, $P < 0.001$) and significant differences between treatments are marked by hashtags (#, $P < 0.05$).

As expected, $CD3^+$ T cells treated with αVEGFR2-Fc-αCD3ε ± αTIE2-Fc-αCD28 or ± αPD-L1-Fc-αCD28 during the transmigration assay do not show the ability to kill MCF-7. Yet αHER2xhIgG1xαCD3ε effect was not compromised by VEGFR2-Fc-αCD3ε treatment. Indeed, αHER2xhIgG1xαCD3ε effect was further improved on migrated cells pre-treated with VEGFR2-Fc-αCD3ε and αPD-L1-Fc-αCD28.

4 DISCUSSION

4.1 T CELL STIMULATION INDUCES KEY MOLECULES FOR TRANSENDOTHELIAL MIGRATION

Cellular adhesion plays an essential role in immune cell functions since T cell subsets circulate between tissues, draining lymph nodes and peripheral blood (Brown et al. 2010; Collins et al. 2016; Gebhardt et al. 2011). Alterations in adhesion molecule patterns regulate each cell population's functional behavior and dynamics, a process modulated by different activation signals. Regarding T cells, cellular adhesion is preferentially driven by several groups of molecules, including integrins (e.g., ITGA4, ITGB1, and ITGB2), ligands for selectins such as PSGL-1 (Harjunpää et al. 2019), cadherins, and chemokine receptors (e.g., CCR9, CXCR3).

To have a better understanding of how T cell activation can influence the modulation of surface molecules involved in transmigration and checkpoint inhibition, PBMC were isolated from healthy donors and stimulated for three days using rhIL-12 alone or using αCD3ε alone or in combination with rhIL-12 or and/or αCD28 in the presence of rhIL-2. Analysis of surface molecules on activated peripheral blood T cells revealed a similar signature of adhesion molecules on both $CD4^+$ and $CD8^+$ T cell subsets. **Figs. 3.1-3.2** shows a substantial PSGL-1 up-regulation after αCD3ε stimulation, but the combination treatment of αCD3ε with rhIL-12 and αCD28 kept PSGL-1 expression levels without a synergistic effect. PSGL-1 is expressed by most lymphocytes, however, only after T cell activation, in a functionally glycosylated form (Carlow et al. 2005; Tinoco et al. 2017). CXCR3 expression was mainly up-regulated by αCD3ε treatment with no further improvement by the addition of αCD28 co-stimulation.

Integrins are not constitutively active and able to bind ligands. Instead, their activity is regulated through a process called inside-out signaling, originated by other cell surface receptors (Gahmberg et al. 2009). For instance, TCR engagement or chemokine exposure initiates signaling cascades that induce a conformational change in both integrin subunits of LFA-1 (ITGAL/ITGB2) or VLA-4 (ITGA4/ITGB1), yielding an active form that substantially increases ligand affinity (Harjunpää et al. 2019).

As shown in **Figs. 3.1-3.2**, the basal expression level of β2 integrin (part of LFA-1) on T cells was 10x higher than α4 and β1 integrins (VLA-4) levels, but both β integrins were further up-regulated upon T cell activation, as previously described by others (Hynes 1992; Park et al. 1998). Besides its role in T cell transmigration, the LFA-1/ICAM1 interaction is also responsible for sustained T cell–APC adhesion (Morgan et al. 2001). VLA-4 is reportedly up-regulated on activated T cells localized at the site of inflammation (Laffón et al. 1991; Rose et al. 2002), which was simulated by αCD3-mediated protein kinase C (PKC) activation (Vassilopoulos et al. 1995; Zhu et al. 2015). Combination treatment with αCD28 did not increase integrin expression levels compared with αCD3ε treatment alone.

Checkpoint inhibitor molecules (TIGIT, TIM3, and PD-1) that are potentially affected by T cell activation were also studied. PD-1 expression was induced on both $CD4^+$ and $CD8^+$ T cells upon αCD3ε stimulation, which was in accordance with the literature (Keir et al. 2008). A clear tendency of $CD4^+$ and $CD8^+$ T cells to up-regulate the checkpoint inhibitors TIGIT and TIM3 was also observed but without statistical significance.

Moreover, CD25, an important cellular activation marker, was evaluated upon T cell activation. CD25 was up-regulated within 24 hours of stimulation of the TCR/CD3 complex, remaining elevated for a few days, as previously described (Jackson et al. 1990; Reddy et al. 2004). $CD4^+$ T cells have a baseline expression of CD25, unlike CD8 T cells. Still, CD25 expression was up-regulated after αCD3ε stimulation on both T cell subpopulations, with the highest levels achieved using αCD3ε in combination with αCD28 (**Fig. 3.3.A**).

The expression levels of PSGL-1, ITGB1, ITGB2, CXCR3 and PD-1 were also separately analyzed on $CD4^+CD25^+$ and $CD8^+CD25^+$ subpopulations. In particular, PSGL-1 and ITGB1 were elevated in $CD4^+CD25^+$ and $CD8^+CD25^+$ subpopulations compared with $CD25^-$ T cell subpopulations, while the other markers showed up-regulation independent of CD25 expression (**Fig. 3.3.B/C**).

Although αCD28 treatment did not augment the effect of αCD3ε stimulation in up-regulating integrins, PSGL-1, CXCR3, and inhibitory molecules on T cells (**Figs. 3.1, 3.2**), the activation status of T cells were slightly higher with the combination treatment. CD28-mediated signals have been reported to enhance the signal intensity of T cell activation through the T cell receptor (TCR), leading to the increased production of cytokines such as interleukin-2 (IL-2) and expression of the IL-2 receptor (CD25) (Boomer and Green 2010; Chen and Mellman 2013; Yamada-Ohnishi et al. 2004).

IL-12 was also expected to give an activation boost as the third signal for T cell activation (Curtsinger and Mescher 2010). Contrarily, IL-12 mainly attenuated the effect of αCD3ε treatment on adhesion molecules expression and did not have an additive effect on T cell activation after αCD3ε stimulation regarding CD25 expression. Only TIM3 expression on $CD8^+$ T cells increased when rhIL-12 was combined with αCD3ε.

Taken these observations into account is possible to conclude that expression levels of T cell surface adhesion molecules were mainly positively modulated by αCD3ε treatment. Regarding the activation status of T cells, it was predominantly influenced by αCD3ε, leading to very high CD25 expression levels. Probably due to the strong T cell activation by the αCD3ε antibody OKT3 alone, αCD28-mediated co-stimulatory effects were not visible under the assay conditions used herein.

4.2 EC ACTIVATION WAS MAINLY DEPENDENT ON PRO-INFLAMMATORY CYTOKINES, IL-1β AND TNF-α

For effective T cell transendothelial migration, not only the T cell activation status matters, with endothelial cells being major participants and regulators of an inflammatory process (de Visser and Coussens 2006). Abnormalities of endothelial cells on tumor vessels, such as reduced expression of homing receptors and deregulated angiogenesis, can result in the dysfunctional extravasation of leukocytes into tumors. Moreover, the EC phenotype needs to match T cell surface receptors for successful binding and migration (Kupper and Fuhlbrigge 2004; Lugano et al. 2020; Peske et al. 2015b; Yu et al. 2005).

To mimic adhesion molecule up-regulation on endothelial cells (HUVEC and HBMEC-60) as part of their functionality during viral infection and sterile inflammation, the prototypic pro-inflammatory cytokines IL-1β and TNF-α were added in a targeted approach using anti-VEGFR2–cytokine fusion proteins in order to evoke EC activation in vitro (**Figs. 3.6-3.7**). The impact of ionizing radiation (γ-radiation) on EC activation was also assessed in this work to mimic the effect of radiation cancer treatments on tumor EC (**Figs. 3.4-3.5**). Radiation can activate and damage rapidly dividing cells, such as microvascular endothelial cells, which have the capability of self-renewal, proliferation, and differentiation (Baskar et al. 2014; Himburg et al. 2016; Kim et al. 2019). Although ionizing radiation induces cell death, during DNA repairing mechanisms, a multi-protein complex so-called inflammasome is formed and can either directly lead to activation of the caspase-1, a protease required for IL-1β and IL-18 maturation and secretion, or indirectly recruits the inflammasome caspase recruitment domain, resulting in processing of inactive pro-inflammatory cytokines to their bio-active forms interleukins (IL-1β, IL-18) (Rodriguez et al. 2018; Stoecklein et al. 2015; West and Barnett 2011). Prolonged activation of the inflammasome signaling also mediates the release of other inflammatory intermediaries such TNF-α (Schroder and Tschopp 2010).

In this line, up-regulation of adhesion molecules was expected either after cytokine treatment or γ-radiation. Hallahan et al. and Gaugler et al. irradiated HUVECs and observed up-regulation of E-selectin and ICAM1 but not VCAM1 after various doses of IR (1-10 Gy) (Gaugler et al. 1997; Hallahan et al. 1996). Others exposed epidermal keratinocytes and dermal microvascular ECs to 6 Gy and found that IR triggered surface expression of ICAM1 on these cells within 24 h, independent of *de novo* protein synthesis (Behrends et al. 1994). Although cytokine-related activation was observed on HUVEC and HBMEC-60, leading to increased levels of adhesion molecules, γ-radiation was not that successful achieved since E-selectin, VCAM1, and ICAM1 were not inducible (**Fig. 3.4-3.5**) at least after 24 h.

Besides adhesion molecules regulation, it has also been postulated that ionizing radiation increases the activity of VEGFR2 in the endothelium, resulting in protection from cell death

(Brieger et al. 2005). On irradiated HBMEC-60 (10 Gy), surface expression of VEGFR2 was up-regulated but not on HUVEC (**Figs. 3.4-3.5**). Kermani et al. demonstrated that even after exposure to a high dose of 10 Gy, the proangiogenic effect of ionizing radiation on human coronary artery endothelial cells was correlated with up-regulation of VEGFR2 and suggests that VEGFR2 up-regulation seems to be important in the survival of radiation-damaged endothelium and regulation of reendothelization in blood vessels *in vivo*, playing a radioprotective role (Kermani et al. 2001). Furthermore, radiation may promote immunosuppressive reactions in several ways, such as up-regulation of co-regulatory molecules PD-L1 and PD-L2 (Morisada et al. 2017; Song et al. 2018), which was confirmed, for PD-L1 and, by tendency, also for PD-L2 expression by HBMEC-6, but not HUVEC cells, after 10 Gy of γ-irradiation (**Figs. 3.4-3.5**). Primary HUVEC cells appear to be much more radiation-insensitive than the immortalized HBMEC-60 cell line.

Regarding cytokine treatment, the results were much more promising (**Figs. 3.6-3.7**). EC activation via pro-inflammatory cytokines is known as type II activation, which is a delayed but sustained response with de novo gene expression in endothelial cells (Pober and Sessa 2007). HUVEC showed increased expression of adhesion molecules, VEGFR2 and PD-L2. E-selectin expression was significantly induced by combination treatment of both pro-inflammatory cytokines, IL-1β and TNF-α. VCAM1 induction was mainly TNF-α dependent, and PD-L2 was also up-regulated by TNF-α. ICAM1 was strongly up-regulated by IL-1β and/or TNF-α. VEGFR2 was up-regulated by a combination of IL-1β and TNF-α, and the same tendency was noted for TIE2.

On HBMEC-60 cells, E-selectin expression was strongly up-regulated by both pro-inflammatory cytokines (IL-1β and TNF-α), alone or in combination, but predominantly by IL-1β, and ICAM1 only by combination treatment (or by tendency with IL-1β alone). VCAM1 was not influenced by cytokine-stimulation as well as VEGFR2, PD-L1, and PD-L2. For that reason, HBMEC-60 cells were considered a suboptimal model for transwell assays, so only HUVECs were used in future experiments. Rood et al. described that E-selectin and VCAM1 were not expressed on unstimulated HBMEC and stimulation with IL-1β up-regulated ICAM1 and VCAM1 (Rood et al. 2000). These previous results could not be confirmed for VCAM1.

4.3 VEGFR2 ANTIBODY-CYTOKINE FUSION PROTEINS IMPROVE BINDING OF ACTIVATED T CELLS TO EC

Tumor endothelium *in vivo* can be surrounded by an immunosuppressive microenvironment, inhibiting expression of adhesion molecules and hampering T cell infiltration (Peske et al. 2015b). Thus, the use of bispecific fusion proteins carrying pro-inflammatory cytokines (IL-1β and TNF-α) might represent a promising strategy to stimulate tumor EC directly *in situ*.

Moreover, the tumor microenvironment is also characterized by an excess of proangiogenic factors, like VEGF, creating an imbalance of pro- and anti-angiogenic signaling feeding tumor progression and reducing the efficacy of cancer therapies such as chemotherapy, radiotherapy, and immunotherapy (Datta et al. 2019; Goel et al. 2011; Yu and Cui 2018). Therefore, targeting the angiogenesis process can positively impact tumor regression, improve the efficacy of cancer treatments, and potentiate infiltration of effector immune cells.

Therefore, antibodies bearing cytokine fusion proteins (IL-1β and TNF-α) and targeting VEGFR2/TIE2 might represent a promising therapeutic approach since the tumor endothelium highly express these receptors due to deregulated angiogenesis (Lian et al. 2019; Mazzieri et al. 2011; Smith et al. 2010; Willam et al. 2000).

Self-produced αVEGFR2 scFv-Fc-cytokine fusion proteins bound efficiently to HUVEC and up-regulated activation markers in a dose-dependent way. The activation profile of HUVEC with αVEGFR2 scFv-Fc-cytokine fusion proteins was comparable with commercial cytokines (**Fig. 3.6 and Fig. 3.9**). E-selectin expression increased in the presence of both produced constructs, while VCAM1 was mainly modulated by αVEGFR2 scFv-Fc-TNF-α (**Fig. 3.9)**. ICAM1 expression was up-regulated by αVEGFR2 scFv-Fc-TNF-α alone or in combination with αVEGFR2 scFv-Fc-IL-1β.

Since αVEGFR2 scFv-Fc-cytokine fusion proteins induced EC activation and up-regulation of adhesion molecules, it could be expected that binding of activated T cell increases, which was confirmed, as shown in **Fig. 3.10.A**, reaching around 60% of $CD3^+$ bound cells to αVEGFR2 scFv-Fc-cytokine fusion proteins-stimulated HUVEC.

Blocking these angiogenic receptors (VEGFR2 or TIE2) can have a substantial impact on tumor growth. Although HUVEC activation results with αVEGFR2 scFv-Fc-cytokine fusion proteins successfully activated endothelial cells, systemically administered IL-1β and TNF-α fusion proteins can also bind to their receptor on many other cell types, which is likely to cause adverse side effects. In principle, intratumoral injection of anti-VEGFR2 cytokine fusions could circumvent these problems, or incorporation of these cytokines in liposomes which are coated with VEGFR2 antibodies.

4.4 DIRECT TARGETING OF T CELLS TO TUMOR ENDOTHELIUM USING BISPECIFIC ANTIBODIES INDUCES T CELL ACTIVATION AND SUBSEQUENT EC ACTIVATION

In this work, bispecific antibodies were investigated that could improve T cell targeting to tumor endothelium, mediate T cell activation *in situ*, and simultaneously deliver an anti-angiogenic effect. In a previous report αVEGFR2-MICA fusion proteins that activate NK and $CD8^+$ T cells

in the tumor microenvironment were studied (Xu et al. 2019), as well as bispecific T-cell engager (BiTE) antibody that targets human endoglin and CD3 (hEND-CD3/BiTE) (Zhong et al. 2021). Kopacek et al. first published bispecific αCD3–αVEGFR2 antibodies in di-scFv as well as diabody format but did not study functional properties of the antibodies (Kopacek et al. 2013). This is the first study to utilize αVEGFR2–αCD3ε bispecific antibodies to redirect T cells towards endothelial cells, to combine them with co-stimulatory EC-targeting antibodies and study activation and transmigration of T cells. Alternative vascular targeting approaches involve the use of VEGFR2-reactive CAR T cells (Hajari Taheri et al. 2019; Lanitis et al. 2021) or αCD16–αVEGFR2 bispecific single-domain antibodies (Xianglei Liu et al. 2020) that aim to attract $CD16^+$ NK cells and myeloid cells towards tumor endothelium.

For this research work, bispecific antibodies were produced in the tetravalent format $(scFv1\text{-}FcKO\text{-}scFv2)_2$, and mutations were introduced to silence the Fc domain to avoid Fc receptor engagement and bystander T cell activation, as previously developed by our lab (Warwas et al. 2021; Quitt et al. 2021). Therefore, the activity of produced bispecific agents is independent of FcγR binding, which is relevant for this study since endothelial cells can express Fcγ receptors (Tuijnman et al. 1993). T cell activation by αVEGFR2-Fc-αCD3ε exclusively relied on the presence of $VEGFR^+$ EC mediating cross-linking between targeted cells (**Fig. 3.13**). Importantly, αTIE2-Fc-αCD28 and αPD-L1-Fc-αCD28 had no activity as single agents in the absence of TCR complex triggering but drastically enhanced the magnitude of T cell activation and further boosted T cell activation in combination with the anti-CD3ε bispecific construct (**Fig. 3.13**). αVEGFR2-Fc-αCD28 was also tested as co-stimulatory treatment (data not shown), but T cell activation was not as high as with the other co-stimulatory tested BiMAbs. Since VEGFR2 is not expressed in high levels on resting HUVEC (**Fig. 3.6**), the competition between both αVEGFR2 constructs may limit αVEGFR2-Fc-αCD28 efficacy. Because of this fact, further experiments were performed with αTIE2-Fc-αCD28 and αPD-L1-Fc-αCD28.

These findings show an essential safety aspect diminishing T cell activation in the absence of EC. According to a titration experiment (**Fig. 3.13**), the best activation profile on both T cell subpopulations was achieved in the presence of 0.5 nM stimulatory αCD3ε BiMAb in combination with 1 nM co-stimulatory αCD28 of the BiMAb. As noted above, T cell co-stimulation could also be achieved by targeting TIE2 with two BiMAbs harboring αCD3ε scFv and αCD28 scFv, respectively, but showed less T cell activation capacity (data not shown). This finding might be explained by antigenic competition between the stimulatory and the co-stimulatory BiMAb in the presence of limiting quantities of EC-associated antigens.

To quantify the activation status of T cells, isolated $CD3^+$ cells were kept in culture alone or co-culture with HUVEC, in the presence of αVEGFR2-Fc-αCD3ε alone or together with αTIE2-

Fc-αCD28 or with αPD-L1-Fc-αCD28 for 24 h (**Fig. 3.14**). αVEGFR2-Fc-αCD3ε induced T cell activation which was boosted to a significant extent by co-stimulatory BiMAbs. Augmented T cell activation was confirmed by the increased surface expression of activation markers like 4-1BB, CD69, and CD25 on $CD4^+$ and $CD8^+$ T cells. αVEGFR2-Fc-αCD3ε in combination with αPD-L1-Fc-αCD28 restored CD3 expression levels (**Fig. 3.14C**). The expression of adhesion molecules on activated T cells is also an important point that should be studied in future experiments. TNF-α secretion was only induced in co-cultures in the presence of stimulatory and co-stimulatory BiMAbs simultaneously (**Fig. 3.15**). IFN-γ levels in the co-culture supernatant were up-regulated by αVEGFR2-Fc-αCD3ε and increased by co-stimulation with the αTIE2-Fc-αCD28 construct (**Fig. 3.15**). Together, these observations proved the capacity of self-produced bispecific antibodies αVEGFR2-Fc-αCD3ε, αTIE2-Fc-αCD28, and αPD-L1-Fc-αCD28 to elicit a successful T cell activation upon EC cross-linking and to induce TNF-α and IFN-γ secretion. Further experiments need to be performed with αPD-L1-Fc-αCD28 to compare both co-stimulatory BiMAbs regarding cytokine secretion. All T cell–EC co-cultures in the presence of self-produced BiMAbs were carefully monitored under the microscope after 24 h, and no significant killing was observed (data not shown).

Additionally, HUVECs from the co-culture were analyzed (**Fig. 3.16**). The percentage of E-$selectin^+$ and $VCAM1^+$ expressing cells was significantly higher when stimulation was combined with co-stimulation, in particular with αTIE2-Fc-αCD28. This fact could be explained by the increased secretion TNF-α by $CD3^+$ T cells in the presence co-stimulation. ICAM1 expression was more sensitive, showing significant up-regulation after αCD3 treatment, that was further increased by co-stimulation, particularly with the αPD-L1 BiMAb.

To better understand if HUVEC activation was induced by cell-cell contact or through secreted factors from activated T cells, supernatants from T-cell/HUVEC co-cultures with αCD3 BiMAbs (24 h) were collected and transferred to pre-seeded HUVEC (**Fig. 3.17B**). Supernatants from co-cultures (48 h) with the activating anti-CD3ε OKT3 antibodies were used for comparison. Analysis of HUVEC activation by FACS showed a similar up-regulation of E-selectin, VCAM1, and ICAM1 in the presence of αVEGFR2-Fc-αCD3ε plus αTIE2-Fc-αCD28 or OKT3 stimulation (**Fig. 3.17A**). Indeed, as shown in **Fig.3.17B**, the expression of VCAM1 and ICAM1 was increased by the supernatants from the co-cultures that underwent both stimulatory treatments (BiMAbs or OKT3) contrasting with E-selectin that was only inducible by supernatants OKT3-treated T cells. Since E-selectin induction on HUVEC cells depended on IL-1β (Fig. 3.6.A), secretion of sufficient quantities of IL-1β, whose primary source will be improperly depleted blood monocytes, B cells, and NK cells triggered by TNF-α (Dinarello

2009), may have required the comparatively more potent activation stimulus of OKT3 antibody inducing cross-talk between T cells and non-T cells.

The fact that HUVEC activation was inducible by soluble factors is an important finding that can be crucial to improve T cell transendothelial migration towards tumors with low levels of T cell infiltrates. Furthermore, once HUVEC activation is achieved, induced EC markers like E-selectin, VCAM1, or ICAM1 could also be used as targets to augment the migration of cytotoxic T cells towards tumor endothelium. In future studies the supernatants from T cell–EC co-cultures should be analyzed to better define soluble factors directly influencing HUVEC activation, and cytokine-neutralizing antibodies should be included.

4.5 T CELL TRANSENDOTHELIAL MIGRATION IS INCREASED BY THE PRESENCE OF STIMULATORY BISPECIFIC ANTIBODIES

As discussed above, self-produced bispecific antibodies effectively induced T cell activation and, consequently, EC activation. The αVEGFR2-Fc-αCD3ε BiMAb alone was capable of up-regulating CD69 and CD25 on the surface of $CD4^+$ and $CD8^+$ T cells and pro-inflammatory cytokine secretion (**Figs. 3.14, 3.15**), however, when combined with co-stimulatory bispecific constructs, αTIE2-Fc-αCD28 and αPD-L1-Fc-αCD28, the effect was even more pronounced, and significant increases in 4-1BB expression were detected. This co-stimulatory effect was reflected by enhanced HUVEC activation.

Further studies were focused on the dynamic interaction between T cells and EC and how self-produced bispecific antibodies could influence T cell transendothelial migration. For this purpose, a transwell assay was used, allowing T cell migration quantification. $2.5x10^4$ HUVEC were seeded that reached a tight monolayer after 48 h, as confirmed by the FITC-dextran permeabilization assay. The optimal cell number for HUVEC seeding was determined by comparing different seeding cell numbers (**Fig. 3.18**). Seeding $1x10^4$ cells or $5x10^4$ HUVEC was either too less or too much to form a healthy and tight monolayer. Isolated $CD3^+$ T cells were added to the upper chamber in a ratio of 1 EC to 10 T cells, together with 0.5 nM αVEGFR2-Fc-αCD3ε ± 1 nM αTIE2-Fc-αCD28 or ± 1 nM αPD-L1-Fc-αCD28 with the respective controls. Migrated $CD3^+$ cells were collected from the lower well and quantified by flow cytometry using counting beads (**Fig. 3.20**).

Results from the transwell assay (**Fig. 3.20**) show that 10% of T cells could migrate through HUVEC in the presence of Fc control antibodies, maybe due to gravity and lack of flow, which can result in prolonged T cell-HUVEC contact independent of the presence of bispecific constructs. Unexpectedly, αVEGFR2-Fc-αCD3ε was as effective alone as combined with co-

stimulatory bispecific constructs leading to ~2x more transmigrated T cells than the respective monospecific scFv-Fc control. Indeed, the addition of a co-stimulatory CD28 commercial antibody to the OKT3 treatment did not increase T cell adhesion molecules' expression, as shown in **Fig. 3.1-3.2**, although in EC binding assays (**Fig. 3.14**) the T cell activation status was positively influenced by co-stimulatory self-produced BiMAbs and the same was the case for EC activation. Future experiments need to be performed to understand whether adhesion molecules benefitted or not from co-stimulation in binding and transwell assays. The lack of augmented transmigration in the presence of co-stimulation could also have been a consequence of more stickiness between T cells and EC due to more cross-linking events in the presence of a second co-stimulatory construct, or the diffusion of solutes between the upper and lower chambers during the 24 h incubation time, “hiding” co-stimulatory effects related to more cytokine secretion (**Fig. 3.15**).

The activation of migrated T cells was evaluated by the expression of activation markers (**Fig. 3.21**). αVEGFR2-Fc-αCD3ε significantly induced CD69 on $CD8^+$ and $CD4^+$ T cell subpopulations after 24h and did not require co-stimulation. CD69 was the quickest marker to be up-regulated after activation compared to CD25 and 4-1BB, the significant up-regulation of which required co-stimulation. On $CD8^+$ T cells, CD25 modulation was only slightly induced in the presence of αVEGFR2-Fc-αCD3ε alone or together with αTIE2-Fc-αCD28, though maybe more incubation time is necessary to achieve significant expression values of this late activation marker.

HUVECs were also collected from the transwell membrane, and a preliminary cytofluorimetric analysis of surface markers was performed (**Fig. 3.22**). The expression of E-selectin on HUVEC after transmigration assay was poorly affected, although in the presence of both bispecific antibodies, stimulatory and co-stimulatory, showed a slight increase. VCAM1 expression showed the same regulation as E-selectin, but in the presence of αVEGFR2-Fc-αCD3ε with αPD-L1-Fc-αCD28, VCAM1 expression levels were significantly higher compared to the controls. Analysis of EC activation upon T cell transmigration needs to be repeated to confirm the preliminary data.

The activation of T cells and HUVECs were not as efficient in the transwell system as compared to the static co-culture system (**Fig. 3.14 and Fig.3.16**), especially in the presence of co-stimulatory BiMAbs. However, αVEGFR2-Fc-αCD3ε was still sufficient to improve T cell migration through HUVEC monolayer, as suggested by **Fig. 3.20.**

4.6 USING αCD8 BISPECIFIC ANTIBODIES TO PRIORITIZE CYTOTOXIC T CELL MIGRATION

The recruitment of T cells to endothelial cells via the CD3ε chain has advantages and disadvantages at the same time. The main advantage is recruiting a considerable number of T cells regardless of antigen specificity or T cell subtypes. Therefore, many T cells would be available at the tumor site to trigger an anti-tumor response. However, in addition to effector T cells, irrelevant T cells and regulatory T cells could also be recruited to the tumor site.

In an attempt to overcome this problem and take advantage of the fact that bispecific antibodies in the transmigration assay were inducing VCAM1 expression on HUVEC surface, other bispecific antibodies incorporating the scFv of the anti-CD8 antibody OKT8 together with αE-selectin, αVCAM1, and αTIE2 scFv antibodies were produced.

The binding efficiency of αCD8-BiMAbs to cytotoxic $CD8^+$ T cells was confirmed by flow cytometry as well as their binding to EC expressing E-selectin, VCAM1 and TIE2, respectively **(Fig. 3.23** and **3.24)**. αCD8-BiMAbs were incorporated in EC-T cell co-cultures under static conditions and in transwell assays together with self-made stimulatory and co-stimulatory antibodies (αVEGFR2-Fc-αCD3ε, αTIE2-Fc-αCD28, and αPD-L1-Fc-αCD28). αTIE2-Fc-αCD8 BiMAb was used as a positive control for binding since TIE2 is constitutively expressed by EC, whereas E-selectin and VCAM1 expression on EC were only induced after activation.

In the static co-culture system, αVEGFR2-Fc-αCD3ε and αTIE2-Fc-αCD28 enhanced the binding of $CD3^+$ T cells and, consequently, the binding of $CD8^+$ T cells (**Fig. 3.25A.2**). However, CD8-binding BiMAbs (αE-selectin, αVCAM1, and αTIE2) were unable to enhance this result. Unfortunately, targeting $CD8^+$ T cells through the CD8 molecule was also not successful with respect to the migration of this T cell subpopulation **(Fig. 3.26)**.

The expression levels of E-selectin and /or VCAM1 due to poor EC activation in the transwell assay could have obscured a beneficial effect of αE-selectin-Fc-αCD8 and αVCAM1-Fc-αCD8 BiMAbs. However, αTIE2-Fc-αCD8, which targets TIE2, a constitutively expressed molecule, also did not have any effect on improving $CD8^+$ T cell migration. Another contradictory fact is that EC activation after co-culture with T cell and BiMAbs was achieved, resulting in increased E-selectin and VCAM1 expression levels, so αE-selectin-Fc-αCD8 and αVCAM1-Fc-αCD8 should have been able to increase $CD8^+$ T cell binding. Increasing the amount of CD8-binding BiMAbs is one possible solution that will be tested in the future, and increasing the stimulatory and co-stimulatory BiMAbs to increase EC activation in the transwell experiments. A pre-activation of EC by αVEGFR2 or αTIE2 cytokine fusion proteins is another possibility to generate an environment that supports enhanced $CD8^+$ T cell migration by αCD8 BiMAbs.

Theoretically, this could also be done when T cells reach the tumor microenvironment, using a bispecific antibody that cross-links $CD8^+$ T cells and tumor-associated antigens simultaneously to promote directed tumor cell killing. However, CD3 engagement will be required in the first place since T cells cannot properly be activated via CD8. Furthermore, this treatment can also be combined with other therapies like CAR-T cells or checkpoint inhibition improving tumor targeting and killing.

4.7 CYTOTOXIC CAPACITY OF MIGRATED BIMAB-TREATED T CELLS TOWARDS TUMOR CELLS

One final important feature was to prove the functional capacity of BiMAb-activated migrated T cells killing the tumor in the presence of BiMAb targeting solid tumor-associated antigens (TAA). Pre-treated and migrated T cells were transferred onto an MCF-7 monolayer and incubated with 1 nM αHERxhIgG1xαCD3ε for 24 h. The cytotoxic capacity was evaluated by lactate dehydrogenase (LDH) quantification of supernatants from the co-culture.

As expected, migrated $CD3^+$ T cells after αVEGFR2-Fc-αCD3ε ± αTIE2-Fc-αCD28 or ± αPD-L1-Fc-αCD28 stimulation before transmigration does not show the ability to kill MCF-7 since there is no TAA antibody to directly target MCF-7 cells. Still, the induction of cytotoxicity by αHER2-Fc-αCD3ε was not compromised by VEGFR2-Fc-αCD3ε treatment. In fact, the cytotoxic effect of an αHER-Fc-αCD3ε BiMAb effect was further improved when transmigrated cells were used that had already encountered VEGFR2-Fc-αCD3ε and αPD-L1-Fc-αCD28 proving that it is possible to use this treatment in combination with TAA-binding BiMAb which subsequently induce tumor cell killing.

In summary, αVEGFR2-Fc-αCD3ε successfully increased T cell transendothelial migration after 24 h that was, however, not improved by simultaneous co-stimulation with αTIE2-Fc-αCD28 or αPD-L1-Fc-αCD28. The T cell early activation status did not benefit from co-stimulation on the transwell assay, while T cell late activation was dependent on co-stimulation as well as EC activation. Results from the transwell assay differed from the binding assays with regard to T cell activation and especially EC activation. HUVEC activation seems to be a secondary event mainly triggered by secreted cytokines from local activated T cells by the presence of αVEGFR2-Fc-αCD3ε and αTIE2-Fc-αCD28. Since the activation status of migrated T cells was lower as compared to T cells from the co-culture and secreted soluble factors were likely diluted in the transwell system, HUVEC activation was possibly compromised.

Since HUVEC activation was not wholly achieved on transwell assay, E-selectin and VCAM1 were not up-regulated, which possibly hampered the prioritization of cytotoxic by αE-selectin-

Fc-αCD8 and αVCAM1-Fc-αCD8. Besides increasing BiMAbs concentration for the transmigration assay, one could also combine stimulatory and co-stimulatory BiMAbs that target tumor endothelium and T cells with different adoptive T cell transfer therapies (CAR-T cells) or with other bispecific constructs that target tumor antigens, directly improving tumor cell killing (e.g., αEpCAM1-Fc-αCD8).

Future experiments will mainly focus on the regulation of adhesion molecules on activated T cells after EC-T cell co-cultures and transwell assays to understand their role in the migration of BiMAb-activated T cells. Additionally, complementary studies with αPD-L1-Fc-αCD28 need to be performed to support some of the findings.

Some limitations of this research work also need to be taken into account that mainly linked to the restrictions of the model. A central issue is that endothelial cell phenotype and function are modulated *in vivo* by shear stress resulting from blood pressure and flow (Zhou et al. 2014). Mechanical stimuli activate mechanosensors, signaling pathways, and gene/protein expressions on EC as a feedback control mechanism to maintain vascular homeostasis (Chien 2007). Biomolecules like integrins (Jalali et al. 2001; Schwartz 2001), tyrosine kinase receptors (like VEGFR2)(Wang et al. 2002), among others (Kuchan et al. 1994; Tzima et al. 2005), are the initial responders to the changes in the mechanical environment. For these reasons, a pump system from ibidi GmbH will be used to study T cell adhesion to EC in the presence of produced BiMAbs. In the pump system is possible to apply a controlled flow, which is an advantage. Unfortunately, the pump system still does not provide inserts that allow to study transmigration. *In vivo* models could also be a possible alternative, although all BiMAbs need to be reformulated to target mouse endothelium.

Nevertheless, it can be concluded that the project's main aim was achieved as T cell transmigration was increased by self-produced αVEGFR2-Fc-αCD3ε, a novel bispecific antibody.

5 SUMMARY

The migration of effector lymphocytes from the blood stream into the tumor microenvironment is believed to be a crucial step for the anti-tumor defense of the immune system. A high density of infiltrating $CD8^+$ T cells in the tumor bed has been correlated with a better prognosis in a variety of malignancies. Poorly infiltrated tumors often show an abnormal and dysfunctional vasculature with reduced expression of adhesion molecules such as E-selectin, ICAM1/2 and VCAM1 that are involved in the extravasation of immune cells.

Therefore, it seems desirable to develop new strategies leading to tumor vessel activation that consequently can increase the transendothelial migration of effector T cells into the tumor. We hypothesized that tumor endothelial cell activation could be facilitated either by direct activation through soluble factors or indirectly by T cell activation in contact with endothelial cells.

In the direct activation approach, recombinant bifunctional VEGFR2-binding fusion proteins were used to deliver activating cytokines to vascular endothelial cells. This targeted delivery of cytokines, that could be useful for future *in vivo* approaches, successfully achieved up-regulation of adhesion molecules, E-selectin, ICAM1 and VCAM1, and consequently increased $CD3^+$ T cell binding to activated human umbilical vein endothelial cells (HUVEC).

In the T cell activation approach, as an indirect means to activate vascular endothelium, tetravalent bispecific monoclonal antibodies (BiMAb) in the $(scFv\text{-}Fc\text{-}scFv)_2$ format were used. These BiMAb bind VEGFR2 or TIE2 endothelial cell (EC) growth factor receptors with the N-terminal single-chain variable fragment (scFv) antibodies, and the stimulatory/co-stimulatory T cell molecules CD3ε or CD28 with the C-terminal scFv antibodies. Local CD3ε-mediated T cell activation is expected to result in the release of cytokines (e.g., TNF-α and IFN-γ) that in turn induce the expression of adhesion molecules in endothelial cells. Antibody-mediated blocking of VEGF binding to VEGFR2 could concomitantly exert anti-angiogenic effects. Also this approach could allow the *in situ* activation of endothelial cells within tumor tissues.

To assess the activation capacity of self-produced bispecific antibodies, $CD3^+$ T cells were co-cultured with HUVEC in the presence of BiMAbs for 24 h. The treatment with αVEGFR2–αCD3 BiMAb resulted in a strong T cell activation as well as up-regulation of adhesion molecules on endothelial cells, as detected by cell surface staining and cytokine ELISA. This effect was slightly enhanced by the addition of an αTIE2–αCD28 BiMAb.

A transwell assay was established to assess the migration capacity of T cells through an EC monolayer in the presence or absence of BiMAbs. Compared to a monospecific αVEGFR2 scFv-Fc control antibody that elicited no EC or T cell activation, the migration of T cells was significantly increased in the presence of αVEGFR2–αCD3 BiMAb. Although additional treatment with the co-stimulatory αTIE2–αCD28 BiMAb augmented T cell activation, the

migration rate of T cells was not increased. In order to prioritize $CD8^+$ T cell transmigration αEC antigen–αCD8 BiMAbs were tested in combination with stimulatory and/or co-stimulatory BiMAbs mentioned above, however, without significant changes in the migration rate of cytotoxic T cells.

To study the killing capacity of transmigrated T cells against tumor cells, transmigrated T cells were transferred onto a monolayer of MCF-7 breast cancer cells in the presence or absence of BiMAbs mediating tumor cell targeting. Tumor cell killing was quantified using an LDH release assay. We observed that T cells that had been pre-activated with αVEGFR2–αCD3 and subsequently traversed an EC monolayer, still required the subsequent addition of tumor-reactive αHER2–αCD3 BiMAb in order to become cytotoxic. Killing was more prominent if migrated cells were pre-treated with a combination of stimulatory and co-stimulatory BiMAbs, αVEGFR2–αCD3 and αPD-L1–αCD28.

In conclusion, T cells activated by αVEGFR2–αCD3 BiMAb can indirectly activate EC *in situ* resulting in a better T cell migration. This treatment can be combined with other BiMAbs that target T cells towards tumor cells and induce tumor cell killing.

6 ZUSAMMENFASSUNG

Die Migration von Effektorlymphozyten aus dem zirkulierendem Blut in das Mikromilieu von Tumoren wird als ein wesentlicher Schritt der Tumorabwehr durch das Immunsystem betrachtet. Eine hohe Dichte infiltrierender $CD8^+$ T-Zellen im Tumorbett ist bei zahlreichen Tumorentitäten mit einer besseren Prognose korreliert. Schwach infiltrierte Tumoren zeigen häufig eine abnormale und dysfunktionale Vaskularisierung mit reduzierter Expression von Adhäsionsmolekülen wie E-Selectin, ICAM1/2 und VCAM1, die an der Extravasation von Immunzellen beteiligt sind.

Es erscheint daher wünschenswert, neue Strategien zu entwickeln, die eine Aktivierung der Tumor-Mikrovaskulatur bewirken, welche dann eine verstärkte transendotheliale Migration von Effektor-T-Zellen in den Tumor erlauben würde. Wir verfolgten die Arbeitshypothese, dass eine Aktivierung von Tumorendothelzellen entweder direkt durch lösliche Faktoren bewirkt werden kann oder indirekt infolge einer T-Zell-Aktivierung in Kontakt mit Endothelzellen.

Im Ansatz der direkten Endothelzellaktivierung wurden rekombinante bifunktionale VEGFR2-bindende Fusionsproteine verwendet, um vaskuläre Endothelzellen mit aktivierenden Zytokinen zu beliefern. Diese zielgerichtete Bereitstellung von aktivierenden Zytokinen, die für spätere In-vivo-Ansätze nützlich sein könnte, erzielte erfolgreich eine Hochregulation der Endothelzell-Adhäsionsmoleküle E-Selectin, ICAM1 und VCAM1 und bewirkte eine verstärkte Bindung von $CD3^+$ T-Zellen an aktivierte humane Nabelschnurvenen-Endothelzellen (HUVEC).

Im T-Zell-Aktivierungsansatz, der einen indirekten Weg zur Aktivierung von Gefäßendothel darstellt, wurden tetravalente bispezifische monoklonale Antikörper (BiMAk) im (scFv1-Fc-scFv1)$_2$-Format verwendet. Diese BiMAk binden die Endothelzell-Wachstumsfaktorrezeptoren VEGFR2 bzw. TIE2 mit den N-terminalen V_H–V_L Einzelketten-Antikörpern (scFv) und die stimulatorischen/kostimulatorischen T-Zell-Moleküle CD3ε bzw. CD28 mit den C-terminalen scFv-Antikörpern. Lokale CD3ε-vermittelte T-Zellaktivierung sollte zu der Freisetzung von Zytokinen führen (z.B. TNF-α oder IFN-γ), die wiederum bei Endothelzellen die Expression von Adhäsionsmolekülen induzieren. Eine antikörpervermittelte Blockade der VEGF-Bindung kann gleichzeitig antiangiogene Effekte haben. Dieser Ansatz könnte ebenfalls die In-situ-Aktivierung von Endothelzellen im Tumorgewebe ermöglichen.

Um die Aktivierungsfähigkeit von eigenen bispezifischen Antikörpern zu ermitteln, wurden $CD3^+$ T-Zellen mit HUVEC für 24 h in Gegenwart von bispezifischen Antikörpern kokultiviert. Die Behandlung mit αVEGFR2–αCD3 BiMAk resultierte in einer starken T-Zell-Aktivierung sowie einer Hochregulation von Adhäsionsmolekülen auf Endothelzellen, die durch Zelloberflächenfärbungen sowie Zytokin-ELISAs nachgewiesen wurde. Dieser Effekt wurde leicht verstärkt durch die zusätzliche Anwendung eines αTIE2–αCD28 BiMAk.

Ein Transwell-Testsystem wurde etabliert, um die Migrationsfähigkeit von T-Zellen durch einen einschichtigen Endothelzellverband (Monolayer) in Gegenwart und Abwesenheit von BiMAk zu messen. Verglichen mit einem monospezifischen αVEGFR2 scFv-Fc Kontrollantikörper, der keine Endothelzell- oder T-Zellaktivierung vermittelte, war die Migration von T-Zellen in Gegenwart des αVEGFR2–αCD3 BiMAk signifikant verstärkt. Obwohl die T-Zellaktivierung durch eine zusätzliche Behandlung mit dem kostimulatorischen αTIE2–αCD28 BiMAk verstärkt wurde, wurde die Migrationsrate von T-Zellen nicht erhöht. Mit dem Ziel die Migration von $CD8^+$ T-Zellen zu favorisieren, wurden verschiedene αEC-Antigen–αCD8 BiMAks zusammen mit den erwähnten (ko)stimulatorischen BiMAk getestet. Es wurden jedoch keine signifikanten Veränderungen in der Migrationsrate von zytotoxischen T-Zellen beobachtet.

Um die zytotoxische Kapazität von transmigrierten T-Zellen gegenüber Tumorzellen zu analysieren, wurden transmigrierte T-Zellen in Gegenwart oder Abwesenheit von tumorzellbindenden BiMAk auf einen Monolayer von MCF-7 Brustkrebszellen gesetzt. Die Abtötung von Tumorzellen wurden durch einen LDH-Freisetzungstest gemessen. Wir beobachteten, dass T-Zellen, die mit dem αVEGFR2–αCD3 BiMAk aktiviert worden waren und einen Endothelzell-Monolayer durchwandert hatten, für eine zytotoxische Aktivität einen zusätzlichen tumorreaktiven αHER2–αCD3 BiMAk benötigten. Die Zytotoxizität war verstärkt, wenn die transmigrierten T-Zellen mit einer Kombination der (ko)stimulatorischen BiMAk αVEGFR2–αCD3 und αPD-L1–αCD28 vorbehandelt worden waren.

Es kann die Schlussfolgerung gezogen werden, dass T-Zellen, die durch αVEGFR2–αCD3 BiMAk aktiviert wurden, Endothelzellen *in situ* indirekt aktivieren können, was zu einer verbesserten T-Zell-Migration führt. Diese Behandlung kann mit anderen BiMAk kombiniert werden, die eine zielgerichtete T-Zell–Tumorzellbindung vermitteln und eine Tumorzellabtötung induzieren.

7 REFERENCES

Abdollahi, A., Hlatky, L. and Huber, P. E. (2005). **Endostatin: The logic of antiangiogenic therapy**. Drug Resist Updat *8*(1–2), 59–74, doi:10.1016/j.drup.2005.03.001.

Abramsson, A., Berlin, Ö., Papayan, H., Paulin, D., Shani, M. and Betsholtz, C. (2002). **Analysis of mural cell recruitment to tumor vessels**. Circulation *105*(1), 112–117, doi:10.1161/hc0102.101437.

Afanasiev, O. K., Nagase, K., Simonson, W., Vandeven, N., Blom, A., Koelle, D. M., Clark, R. and Nghiem, P. (2013). **Vascular E-selectin expression correlates with CD8 lymphocyte infiltration and improved outcome in merkel cell carcinoma**. J Invest Dermatol *133*(8), 2065–2073, doi:10.1038/jid.2013.36.

Ahn, J. B., Rha, S. Y., Shin, S. J., Jeung, H. C., Kim, T. S., Zhang, X., Park, K. H., Noh, S. H., Roh, J. K. and Chung, H. C. (2010). **Circulating endothelial progenitor cells (EPC) for tumor vasculogenesis in gastric cancer patients**. Cancer Lett *288*(1), 124–132, doi:10.1016/j.canlet.2009.06.031.

Ahsmann, E., Lokhorst, H., Dekker, A. and Bloem, A. (1992). **Lymphocyte function-associated antigen-1 expression on plasma cells correlates with tumor growth in multiple myeloma**. Blood *79*(8), 2068–2075, doi:10.1182/blood.V79.8.2068.2068.

Al-Abd, A. M., Alamoudi, A. J., Abdel-Naim, A. B., Neamatallah, T. A. and Ashour, O. M. (2017). **Anti-angiogenic agents for the treatment of solid tumors: Potential pathways, therapy and current strategies - A review.** J Adv Res *8*(6), 591–605.

Al-Halafi, A. M. (2014). **Vascular endothelial growth factor trap-eye and trap technology: Aflibercept from bench to bedside**, *Oman J Ophthalmol* 7 (3) pp.112–115, doi:10.4103/0974-620X.142591.

Alvero, A. B., Fu, H. H., Holmberg, J., Visintin, I., Mor, L., Marquina, C. C., Oidtman, J., Silasi, D. A. and Mor, G. (2009). **Stem-like ovarian cancer cells can serve as tumor vascular progenitors**. Stem Cells *27*(10), 2405–2413, doi:10.1002/stem.191.

Angara, K., Rashid, M. H., Shankar, A., Ara, R., Iskander, A., Borin, T. F., Jain, M., Achyut, B. R. and Arbab, A. S. (2017). **Vascular mimicry in glioblastoma following anti-angiogenic and anti-20-HETE therapies**. Histol Histopathol *32*(9), 917–928, doi:10.14670/HH-11-856.

Anraku, M., Cunningham, K. S., Yun, Z., Tsao, M. S., Zhang, L., Keshavjee, S., Johnston, M. R. and de Perrot, M. (2008). **Impact of tumor-infiltrating T cells on survival in patients with malignant pleural mesothelioma**. J Thorac Cardiovasc Surg *135*(4), 823–829, doi:10.1016/j.jtcvs.2007.10.026.

Ansell, S. M., Lesokhin, A. M., Borrello, I., Halwani, A., Scott, E. C., Gutierrez, M., Schuster, S. J., Millenson, M. M., Cattry, D., Freeman, G. J., Rodig, S. J., Chapuy, B., Ligon, A. H., Zhu, L., Grosso, J. F., Kim, S. Y., Timmerman, J. M., Shipp, M. A. and Armand, P. (2015). **PD-1 Blockade with Nivolumab in Relapsed or Refractory Hodgkin's Lymphoma**. N Engl J Med *372*(4), 311–319, doi:10.1056/nejmoa1411087.

Apte, R. S., Chen, D. S. and Ferrara, N. (2019). **VEGF in Signaling and Disease: Beyond Discovery and Development**, *Cell* 176 (6) pp.1248–1264, doi:10.1016/j.cell.2019.01.021.

Arnaout, M. (1990). **Structure and function of the leukocyte adhesion molecules CD11/CD18**. Blood *75*(5), 1037–1050, doi:10.1182/blood.V75.5.1037.bloodjournal7551037.

Arrieta, O., Zatarain-Barrón, Z. L., Cardona, A. F., Carmona, A. and Lopez-Mejia, M. (2017). **Ramucirumab in the treatment of non-small cell lung cancer**, *Expert Opin Drug Saf* 16 (5) pp.637–644, doi:10.1080/14740338.2017.1313226.

Asahara, T., Murohara, T., Sullivan, A., Silver, M., Van Der Zee, R., Li, T., Witzenbichler, B., Schatteman, G. and Isner, J. M. (1997). **Isolation of putative progenitor endothelial cells for angiogenesis**. Science (80-) *275*(5302), 964–967, doi:10.1126/science.275.5302.964.

Baeten, C. I. M., Hillen, F., Pauwels, P., De Bruine, A. P. and Baeten, C. G. M. I. (2009). **Prognostic role of vasculogenic mimicry in colorectal cancer**. Dis Colon Rectum *52*(12), 2028–2035, doi:10.1007/DCR.0b013e3181beb4ff.

Baluk, P., Hashizume, H. and McDonald, D. M. (2005). **Cellular abnormalities of blood vessels as targets in cancer**, *Curr Opin Genet Dev* 15 (1) pp.102–111, doi:10.1016/j.gde.2004.12.005.

Baluk, P., Morikawa, S., Haskell, A., Mancuso, M. and McDonald, D. M. (2003). **Abnormalities of Basement Membrane on Blood Vessels and Endothelial Sprouts in Tumors**. Am J Pathol *163*(5), 1801–1815, doi:10.1016/S0002-9440(10)63540-7.

Bang, Y. J., Van Cutsem, E., Feyereislova, A., Chung, H. C., Shen, L., Sawaki, A., Lordick, F., Ohtsu, A., Omuro, Y., Satoh, T., Aprile, G., Kulikov, E., Hill, J., Lehle, M., Rüschoff, J. and Kang, Y. K. (2010). **Trastuzumab in combination with chemotherapy versus chemotherapy alone for treatment of HER2-positive advanced gastric or gastro-oesophageal junction cancer (ToGA): A phase 3, open-label, randomised controlled trial**. Lancet *376*(9742), 687–697, doi:10.1016/S0140-6736(10)61121-X.

Baselga, J., Bradbury, I., Eidtmann, H., Di Cosimo, S., De Azambuja, E., Aura, C., Gómez, H., Dinh, P., Fauria, K., Van Dooren, V., Aktan, G., Goldhirsch, A., Chang, T. W., Horváth, Z., Coccia-Portugal, M., Domont, J., Tseng, L. M., Kunz, G., Sohn, J. H., Semiglazov, V., Lerzo, G., Palacova, M., Probachai, V., Pusztai, L., Untch, M., Gelber, R. D. and Piccart-Gebhart, M. (2012). **Lapatinib with trastuzumab for HER2-positive early breast cancer (NeoALTTO): A randomised, open-label, multicentre, phase 3 trial**. In: **The Lancet**, 2012, Elsevier B.V., pp. 633–640, doi:10.1016/S0140-6736(11)61847-3.

Baskar, R., Dai, J., Wenlong, N., Yeo, R. and Yeoh, K. (2014). **Biological response of cancer cells to radiation treatment**. Front Mol Biosci *1*(NOV), doi:10.3389/FMOLB.2014.00024.

Bates, P. J., Laber, D. A., Miller, D. M., Thomas, S. D. and Trent, J. O. (2009). **Discovery and development of the G-rich oligonucleotide AS1411 as a novel treatment for cancer**, *Experimental and Molecular Pathology* 86 (3) pp.151–164, doi:10.1016/j.yexmp.2009.01.004.

Beaver, J. A., Tzou, A., Blumenthal, G. M., McKee, A. E., Kim, G., Pazdur, R. and Philip, R. (2017). **An FDA perspective on the regulatory implications of complex signatures to predict response to targeted therapies**, *Clin Cancer Res* 23 (6) pp.1368–1372, doi:10.1158/1078-0432.CCR-16-1098.

Behrends, U., Eißner, G., Bornkamm, G. W., Peter, R. U., Hintermeier-Knabe, R., Holler, E., Caughman, S. W. and Degitz, K. (1994). **Ionizing Radiation Induces Human Intercellular Adhesion Molecule-1 In Vitro**. J Invest Dermatol *103*(5), 726–730, doi:10.1111/1523-1747.ep12398607.

Bellone, M. and Elia, A. R. (2017). **Constitutive and acquired mechanisms of resistance to immune checkpoint blockade in human cancer**. Cytokine Growth Factor Rev *36*, 17–24, doi:10.1016/j.cytogfr.2017.06.002.

Bennewith, K. L. and Durand, R. E. (2004). **Quantifying transient hypoxia in human tumor xenografts by flow cytometry**. Cancer Res *64*(17), 6183–6189, doi:10.1158/0008-5472.CAN-04-0289.

Bergers, G. and Hanahan, D. (2008). **Modes of resistance to anti-angiogenic therapy**, *Nature Reviews Cancer* 8 (8) pp.592–603, doi:10.1038/nrc2442.

Berretta, M., Rinaldi, L., Di Benedetto, F., Lleshi, A., Re, V. De, Facchini, G., De Paoli, P. and Di Francia, R. (2016). **Angiogenesis inhibitors for the treatment of hepatocellular carcinoma**, *Frontiers in Pharmacology* 7 (NOV) p.428, doi:10.3389/fphar.2016.00428.

Blum, J. S., Wearsch, P. A. and Cresswell, P. (2013). **Pathways of antigen processing**, *Annual Review of Immunology* 31 pp.443–473, doi:10.1146/annurev-immunol-032712-095910.

Boghozian, R., Azizi, G. and Mirshafiey, A. (2013). **Molecular Pattern of Angiogenesis Phenomenon and Inflammatory Cytokines in Rheumatoid Arthritis**. Int Trends Immun *1*(3), 1–6, URL: http://www.researchpub.org/journal/iti/iti.html JULY.

Bonner, J. A., Harari, P. M., Giralt, J., Azarnia, N., Shin, D. M., Cohen, R. B., Jones, C. U., Sur, R., Raben, D., Jassem, J., Ove, R., Kies, M. S., Baselga, J., Youssoufian, H., Amellal, N., Rowinsky, E. K. and Ang, K. K. (2006). **Radiotherapy plus Cetuximab for Squamous-Cell Carcinoma of the Head and Neck**. N Engl J Med *354*(6), 567–578, doi:10.1056/NEJMoa053422.

Boomer, J. S. and Green, J. M. (2010). **An enigmatic tail of CD28 signaling.**, *Cold Spring Harbor perspectives in biology* 2 (8), doi:10.1101/cshperspect.a002436.

Borst, J., Ahrends, T., Bąbała, N., Melief, C. J. M. and Kastenmüller, W. (2018). **CD4+ T cell help in cancer immunology and immunotherapy**, *Nature Reviews Immunology* 18 (10) pp.635–647, doi:10.1038/s41577-018-0044-0.

Bose, A., Taylor, J. L., Alber, S., Watkins, S. C., Garcia, J. A., Rini, B. I., Ko, J. S., Cohen, P. A., Finke, J. H. and Storkus, W. J. (2011). **Sunitinib facilitates the activation and recruitment of therapeutic anti-tumor immunity in concert with specific vaccination**. Int J Cancer *129*(9), 2158–2170, doi:10.1002/ijc.25863.

Bouzin, C., Brouet, A., De Vriese, J., DeWever, J. and Feron, O. (2007). **Effects of Vascular Endothelial Growth Factor on the Lymphocyte-Endothelium Interactions: Identification of Caveolin-1 and Nitric Oxide as Control Points of Endothelial Cell Anergy**. J Immunol *178*(3), 1505–1511, doi:10.4049/jimmunol.178.3.1505.

Brahmer, J., Reckamp, K. L., Baas, P., Crinò, L., Eberhardt, W. E. E., Poddubskaya, E., Antonia, S., Pluzanski, A., Vokes, E. E., Holgado, E., Waterhouse, D., Ready, N., Gainor, J., Arén Frontera, O., Havel, L., Steins, M., Garassino, M. C., Aerts, J. G., Domine, M., Paz-Ares, L., Reck, M., Baudelet, C., Harbison, C. T., Lestini, B. and Spigel, D. R. (2015). **Nivolumab versus Docetaxel in Advanced Squamous-Cell Non–Small-Cell Lung Cancer**. N Engl J Med *373*(2), 123–135, doi:10.1056/nejmoa1504627.

Brieger, J., Schroeder, P., Gosepath, J. and Mann, W. J. (2005). **VEGF-subtype specific protection of SCC and HUVECs from radiation induced cell death**. Int J Mol Med *15*(1), 145–151, doi:10.3892/IJMM.15.1.145.

Brinkman, C. C., Rouhani, S. J., Srinivasan, N. and Engelhard, V. H. (2013). **Peripheral Tissue Homing Receptors Enable T Cell Entry into Lymph Nodes and Affect the Anatomical Distribution of Memory Cells**. J Immunol *191*(5), 2412–2425, doi:10.4049/jimmunol.1300651.

Brinkmann, U. and Kontermann, R. E. (2017). **The making of bispecific antibodies**, *mAbs* 9 (2) pp.182–212, doi:10.1080/19420862.2016.1268307.

Brooks, P. C., Strömblad, S., Klemke, R., Visscher, D., Sarkar, F. H. and Cheresh, D. A. (1995). **Antiintegrin alpha v beta 3 blocks human breast cancer growth and angiogenesis in human skin.** J Clin Invest *96*(4), 1815–1822, doi:10.1172/JCI118227.

Brown, M. N., Fintushel, S. R., Lee, M. H., Jennrich, S., Geherin, S. A., Hay, J. B., Butcher, E. C. and Debes, G. F. (2010). **Chemoattractant Receptors and Lymphocyte Egress from Extralymphoid Tissue: Changing Requirements during the Course of Inflammation**. J Immunol *185*(8), 4873–4882, doi:10.4049/JIMMUNOL.1000676.

Buckanovich, R. J., Facciabene, A., Kim, S., Benencia, F., Sasaroli, D., Balint, K., Katsaros, D., O'Brien-Jenkins, A., Gimotty, P. A. and Coukos, G. (2008). **Endothelin B receptor mediates the endothelial barrier to T cell homing to tumors and disables immune therapy**. Nat Med *14*(1), 28–36, doi:10.1038/nm1699.

Burger, J. A. and Gribben, J. G. (2014). **The microenvironment in chronic lymphocytic leukemia (CLL) and other B cell malignancies: Insight into disease biology and new targeted therapies**. Semin Cancer Biol *24*, 71–81, doi:10.1016/j.semcancer.2013.08.011.

Burugu, S., Dancsok, A. R. and Nielsen, T. O. (2018). **Emerging targets in cancer immunotherapy**, *Seminars in Cancer Biology* 52 (Pt 2) pp.39–52, doi:10.1016/j.semcancer.2017.10.001.

Bussolati, B., Grange, C. and Camussi, G. (2011). **Tumor exploits alternative strategies to achieve vascularization**. FASEB J *25*(9), 2874–2882, doi:10.1096/fj.10-180323.

Bussolati, B., Grange, C., Sapino, A. and Camussi, G. (2009). **Endothelial cell differentiation of human breast tumour stem/progenitor cells**. J Cell Mol Med *13*(2), 309–319, doi:10.1111/j.1582-4934.2008.00338.x.

Byrne, A. T., Ross, L., Holash, J., Nakanishi, M., Hu, L., Hofmann, J. I., Yancopoulos, G. D. and Jaffe, R. B. (2003). **Vascular Endothelial Growth Factor-Trap Decreases Tumor Burden, Inhibits Ascites, and Causes Dramatic Vascular Remodeling in an Ovarian Cancer Model**. Clin Cancer Res *9*(15), 5721–5728.

Cambiaggi, C., Scupoli, M. T., Cestari, T., Gerosa, F., Carra, G., Tridente, G. and Accolla, R. S. (1992). **Constitutive expression of CD69 in interspecies T-cell hybrids and locus assignment to human chromosome 12**. Immunogenetics *36*(2), 117–120, doi:10.1007/BF00215288.

Carlow, D., Williams, M. and Ziltener, H. (2005). **Inducing P-selectin ligand formation in CD8 T cells: IL-2 and IL-12 are active in vitro but not required in vivo**. J Immunol *174*(7), 3959–3966, doi:10.4049/JIMMUNOL.174.7.3959.

Carmeliet, P. and Jain, R. K. (2011). **Principles and mechanisms of vessel normalization for cancer and other angiogenic diseases**, *Nature Reviews Drug Discovery* 10 (6) pp.417–427, doi:10.1038/nrd3455.

Chae, S. S., Kamoun, W. S., Farrar, C. T., Kirkpatrick, N. D., Niemeyer, E., De Graaf, A. M. A., Sorensen, A. G., Munn, L. L., Jain, R. K. and Fukumura, D. (2010). **Angiopoietin-2 interferes with anti-VEGFR2-induced vessel normalization and survival benefit in mice bearing gliomas**. Clin Cancer Res *16*(14), 3618–3627, doi:10.1158/1078-0432.CCR-09-3073.

Chames, P. and Baty, D. (2009). **Bispecific antibodies for cancer therapy: The light at the end of the tunnel?**, *mAbs* 1 (6) pp.539–547, doi:10.4161/mabs.1.6.10015.

Chang, Edward I., Chang, Eric I., Thangarajah, H., Hamou, C. and Gurtner, G. C. (2007). **Hypoxia, hormones, and endothelial progenitor cells in hemangioma**, *Lymphatic Research and Biology* 5 (4) pp.237–243, doi:10.1089/lrb.2007.1014.

Chen, D. S. and Mellman, I. (2013). **Oncology meets immunology: The cancer-immunity cycle**, *Immunity* 39 (1) pp.1–10, doi:10.1016/j.immuni.2013.07.012.

Chen, J., He, Q., Liu, J., Xiao, Y., Xiao, C., Chen, K., Xie, D. and Zhang, X. (2018). **CD8+ tumor-infiltrating lymphocytes as a novel prognostic biomarker in lung sarcomatoid carcinoma, a rare subtype of lung cancer**. Cancer Manag Res *10*, 3505–3511, doi:10.2147/CMAR.S169074.

Chen, J., Salas, A. and Springer, T. A. (2003). **Bistable regulation of integrin adhesiveness by a bipolar metal ion cluster**. Nat Struct Mol Biol *10*(12), 995–1001, doi:10.1038/nsb1011.

Chen, L. and Flies, D. B. (2013). **Molecular mechanisms of T cell co-stimulation and co-inhibition**, *Nature Reviews Immunology* 13 (4) pp.227–242, doi:10.1038/nri3405.

Cheng, L., Huang, Z., Zhou, W., Wu, Q., Donnola, S., Liu, J. K., Fang, X., Sloan, A. E., Mao, Y., Lathia, J. D., Min, W., McLendon, R. E., Rich, J. N. and Bao, S. (2013). **Glioblastoma stem cells generate vascular pericytes to support vessel function and tumor growth**. Cell *153*(1), 139–152, doi:10.1016/j.cell.2013.02.021.

Chien, S. (2007). **Mechanotransduction and endothelial cell homeostasis: the wisdom of the cell**. Am J Physiol Heart Circ Physiol *292*(3), doi:10.1152/AJPHEART.01047.2006.

Choi, B. D., Cai, M., Bigner, D. D., Mehta, A. I., Kuan, C. T. and Sampson, J. H. (2011). **Bispecific antibodies engage T cells for antitumor immunotherapy**, *Expert Opinion on Biological Therapy* 11 (7) pp.843–853, doi:10.1517/14712598.2011.572874.

Choi, H. J., Kim, Y. J., Lee, S. and Kim, Y. S. (2013). **A heterodimeric fc-Based bispecific antibody simultaneously targeting vegfr-2 and met exhibits potent antitumor activity**. Mol Cancer Ther *12*(12), 2748–2759, doi:10.1158/1535-7163.MCT-13-0628.

Chopra, H., Hung, M. K., Kwong, D. L., Zhang, C. F. and Pow, E. H. N. (2018). **Insights into endothelial progenitor cells: Origin, classification, potentials, and prospects**, *Stem Cells International* 2018, doi:10.1155/2018/9847015.

Chung, A. S., Lee, J. and Ferrara, N. (2010). **Targeting the tumour vasculature: Insights from physiological angiogenesis**, *Nature Reviews Cancer* 10 (7) pp.505–514, doi:10.1038/nrc2868.

Clark, R. A., Huang, S. J., Murphy, G. F., Mollet, I. G., Hijnen, D., Muthukuru, M., Schanbacher, C. F., Edwards, V., Miller, D. M., Kim, J. E., Lambert, J. and Kupper, T. S. (2008). **Human squamous cell carcinomas evade the immune response by down-regulation of vascular E-selectin and recruitment of regulatory T cells**. J Exp Med *205*(10), 2221–2234, doi:10.1084/jem.20071190.

Collins, N., Jiang, X., Zaid, A., Macleod, B. L., Li, J., Park, C. O., Haque, A., Bedoui, S., Heath, W. R., Mueller, S. N., Kupper, T. S., Gebhardt, T. and Carbone, F. R. (2016). **Skin CD4+ memory T cells exhibit combined cluster-mediated retention and equilibration with the circulation**. Nat Commun 2016 71 *7*(1), 1–13, doi:10.1038/ncomms11514.

Crivellato, E., Nico, B., Vacca, A., Djonov, V., Presta, M. and Ribatti, D. (2004). **Recombinant human erythropoietin induces intussusceptive microvascular growth in vivo**. Leukemia *18*(2), 331–336, doi:10.1038/sj.leu.2403246.

Crotzer, V. L. and Blum, J. S. (2010). **Autophagy and adaptive immunity**. Immunology *131*(1). doi:10.1111/j.1365-2567.2010.03321.x.

Curtsinger, J. M. and Mescher, M. F. (2010). **Inflammatory cytokines as a third signal for T cell activation**, *Current Opinion in Immunology* 22 (3) pp.333–340, doi:10.1016/j.coi.2010.02.013.

Dai, Y., Hawinkels, L., Jiao, H., Zhang, D., Bi, J., Liang, Q., Wang, S., Zhang, L., Han, F., Li, S., Qiu, B., Fan, X., Chen, W., Ye, Y. and Ding, Y. (2020). **VCAM1 Promotes Tumor Cell Invasion and Metastasis by Inducing EMT and Transendothelial Migration in Colorectal Cancer**. Front Oncol | wwwfrontiersinorg *1*, 1066, doi:10.3389/fonc.2020.01066.

Datta, M., Coussens, L. M., Nishikawa, H., Hodi, F. S. and Jain, R. K. (2019). **Reprogramming the Tumor Microenvironment to Improve Immunotherapy: Emerging Strategies and Combination Therapies**. https://doi.org/101200/EDBK_237987 (39), 165–174.

Davis, A. A. and Patel, V. G. (2019). **The role of PD-L1 expression as a predictive biomarker: An analysis of all US food and drug administration (FDA) approvals of immune checkpoint inhibitors**. J Immunother Cancer *7*(1), doi:10.1186/s40425-019-0768-9.

De Falco, S. (2012). **The discovery of placenta growth factor and its biological activity**. Exp Mol Med *44*(1), 1–9, doi:10.3858/emm.2012.44.1.025.

De Spiegelaere, W., Casteleyn, C., Van Den Broeck, W., Plendl, J., Bahramsoltani, M., Simoens, P., Djonov, V. and Cornillie, P. (2012). **Intussusceptive angiogenesis: A biologically relevant form of angiogenesis**, *Journal of Vascular Research* 49 (5) pp.390–404, doi:10.1159/000338278.

de Visser, K. and Coussens, L. (2006). **The inflammatory tumor microenvironment and its impact on cancer development**. Contrib Microbiol *13*, 118–137, doi:10.1159/000092969.

DeMatteo, R. P., Ballman, K. V., Antonescu, C. R., Maki, R. G., Pisters, P. W., Demetri, G. D., Blackstein, M. E., Blanke, C. D., von Mehren, M., Brennan, M. F., Patel, S., McCarter, M. D., Polikoff, J. A., Tan, B. R. and Owzar, K. (2009). **Adjuvant imatinib mesylate after resection of localised, primary gastrointestinal stromal tumour: a randomised, double-blind, placebo-controlled trial**. Lancet *373*(9669), 1097–1104, doi:10.1016/S0140-6736(09)60500-6.

Deng, L., Liang, H., Xu, M., Yang, X., Burnette, B., Arina, A., Li, X. D., Mauceri, H., Beckett, M., Darga, T., Huang, X., Gajewski, T. F., Chen, Z. J., Fu, Y. X. and Weichselbaum, R. R. (2014). **STING-dependent cytosolic DNA sensing promotes radiation-induced type I interferon-dependent antitumor immunity in immunogenic tumors**. Immunity *41*(5), 843–852, doi:10.1016/j.immuni.2014.10.019.

Desgrosellier, J. S., Barnes, L. A., Shields, D. J., Huang, M., Lau, S. K., Prévost, N., Tarin, D., Shattil, S. J. and Cheresh, D. A. (2009). **An integrin αvβ3–c-Src oncogenic unit promotes anchorage-independence and tumor progression**. Nat Med *15*(10), 1163–1169, doi:10.1038/nm.2009.

Desgrosellier, J. S. and Cheresh, D. A. (2010). **Integrins in cancer: Biological implications and therapeutic opportunities**, *Nature Reviews Cancer* 10 (1) pp.9–22, doi:10.1038/nrc2748.

Dhimolea, E. and Reichert, J. M. (2012). **World Bispecific Antibody Summit, September 27–28, 2011, Boston, MA**. MAbs *4*(1), 4–13.

Di Marzo, L., Desantis, V., Solimando, A. G., Ruggieri, S., Annese, T., Nico, B., Fumarulo, R., Vacca, A. and Frassanito, M. A. (2016). **Microenvironment drug resistance in multiple myeloma: Emerging new players**, *Oncotarget* 7 (37) pp.60698–60711, doi:10.18632/oncotarget.10849.

Dinarello, C. A. (2009). **Immunological and Inflammatory Functions of the Interleukin-1 Family**. Annu Rev Immunol *27*, 519–550, doi:10.1146/ANNUREV.IMMUNOL.021908.132612.

Dings, R. P. M., Vang, K. B., Castermans, K., Popescu, F., Zhang, Y., Oude Egbrink, M. G. A., Mescher, M. F., Farrar, M. A., Griffioen, A. W. and Mayo, K. H. (2011). **Enhancement of T-cell-mediated antitumor response: Angiostatic adjuvant to immunotherapy against cancer**. Clin Cancer Res *17*(10), 3134–3145, doi:10.1158/1078-0432.CCR-10-2443.

Dirkx, A. E. M., Egbrink, M. G. A. oude, Castermans, K., Schaft, D. W. J., Thijssen, V. L. J. L., Dings, R. P. M., Kwee, L., Mayo, K. H., Wagstaff, J., Steege, J. C. A. B. and Griffioen, A. W. (2006). **Anti-angiogenesis therapy can overcome endothelial cell anergy and promote leukocyte-endothelium interactions and infiltration in tumors**. FASEB J *20*(6), 621–630, doi:10.1096/fj.05-4493com.

Dirkx, A. E. M., oude Egbrink, M. G. A., Kuijpers, M. J. E., van der Niet, S. T., Heijnen, V. V. T., Bouma-ter Steege, J. C. A., Wagstaff, J., Griffioen, A. W., Steege, J. C. A. B., Wagstaff, J. and Griffioen, A. W. (2003). **Tumor Angiogenesis Modulates Leukocyte-Vessel Wall Interactions in Vivo by Reducing Endothelial Adhesion Molecule Expression**. Cancer Res *63*(9), 2322–2329.

Djonov, V., Högger, K., Sedlacek, R., Laissue, J. and Draeger, A. (2001). **MMP-19: Cellular localization of a novel metalloproteinase within normal breast tissue and mammary gland tumours**. J Pathol *195*(2), 147–155, doi:10.1002/path.927.

Domigan, C. K., Ziyad, S. and Luisa Iruela-Arispe, M. (2015). **Canonical and noncanonical vascular endothelial growth factor pathways: New developments in biology and signal transduction**, *Arteriosclerosis, Thrombosis, and Vascular Biology* 35 (1) pp.30–39, doi:10.1161/ATVBAHA.114.303215.

Dong, D., Zheng, L., Lin, J., Zhang, B., Zhu, Y., Li, N., Xie, S., Wang, Y., Gao, N. and Huang, Z. (2019). **Structural basis of assembly of the human T cell receptor–CD3 complex**. Nature *573*(7775), 546–552, doi:10.1038/s41586-019-1537-0.

Donini, C., D'Ambrosio, L., Grignani, G., Aglietta, M. and Sangiolo, D. (2018). **Next generation immune-checkpoints for cancer therapy**, *Journal of Thoracic Disease* 10 (Suppl 13) pp.S1581–S1601, doi:10.21037/jtd.2018.02.79.

Druker, B. J., Guilhot, F., O'Brien, S. G., Gathmann, I., Kantarjian, H., Gattermann, N., Deininger, M. W. N., Silver, R. T., Goldman, J. M., Stone, R. M., Cervantes, F., Hochhaus, A., Powell, B. L., Gabrilove, J. L., Rousselot, P., Reiffers, J., Cornelissen, J. J., Hughes, T., Agis, H., Fischer, T., Verhoef, G., Shepherd, J., Saglio, G., Gratwohl, A., Nielsen, J. L., Radich, J. P., Simonsson, B., Taylor, K., Baccarani, M., So, C., Letvak, L. and Larson, R. A. (2006). **Five-Year Follow-up of Patients Receiving Imatinib for Chronic Myeloid Leukemia**. N Engl J Med *355*(23), 2408–2417, doi:10.1056/nejmoa062867.

Dumont, D. J., Jussila, L., Taipale, J., Lymboussaki, A., Mustonen, T., Pajusola, K., Breitman, M. and Alitalo, K. (1998). **Cardiovascular failure in mouse embryos deficient in VEGF receptor-3**. Science (80-) *282*(5390), 946–949, doi:10.1126/science.282.5390.946.

Dumont, D. J., Yamaguchi, T. P., Conlon, R. A., Rossant, J. and Breitman, M. L. (1992). **Tek, a novel tyrosine kinase gene located on mouse chromosome 4, is expressed in endothelial cells and their presumptive precursors**. Oncogene *7*(8), 1471–1480.

Dustin, M. L. and Long, E. O. (2010). **Cytotoxic immunological synapses**, *Immunological Reviews* 235 (1) pp.24–34, doi:10.1111/j.0105-2896.2010.00904.x.

Ebos, J. M. L., Lee, C. R., Cruz-Munoz, W., Bjarnason, G. A., Christensen, J. G. and Kerbel, R. S. (2009). **Accelerated Metastasis after Short-Term Treatment with a Potent Inhibitor of Tumor Angiogenesis**. Cancer Cell *15*(3), 232–239, doi:10.1016/j.ccr.2009.01.021.

Eggermont, L. J., Paulis, L. E., Tel, J. and Figdor, C. G. (2014). **Towards efficient cancer immunotherapy: Advances in developing artificial antigen-presenting cells**, *Trends in Biotechnology* 32 (9) pp.456–465, doi:10.1016/j.tibtech.2014.06.007.

Enarsson, K., Johnsson, E., Lindholm, C., Lundgren, A., Pan-Hammarström, Q., Strömberg, E., Bergin, P., Baunge, E.-L., Svennerholm, A.-M. and Quiding-Järbrink, M. (2006). **Differential mechanisms for T lymphocyte recruitment in normal and neoplastic human gastric mucosa**. Clin Immunol *118*(1), 24–34, doi:10.1016/j.clim.2005.08.001.

Erber, R., Thurnher, A., Katsen, A. D., Groth, G., Kerger, H., Hammes, H. P., Menger, M. D., Ullrich, A. and Vajkoczy, P. (2004). **Combined inhibition of VEGF and PDGF signaling enforces tumor vessel regression by interfering with pericyte-mediated endothelial cell survival mechanisms.** FASEB J *18*(2), 338–340, doi:10.1096/fj.03-0271fje.

Erdag, G., Schaefer, J. T., Smolkin, M. E., Deacon, D. H., Shea, S. M., Dengel, L. T., Patterson, J. W. and Slingluff, C. L. (2012). **Immunotype and immunohistologic characteristics of tumor-infiltrating immune cells are associated with clinical outcome in metastatic melanoma**. Cancer Res *72*(5), 1070–1080, doi:10.1158/0008-5472.CAN-11-3218.

Escudier, B., Lougheed, J. C. and Albiges, L. (2016). **Cabozantinib for the treatment of renal cell carcinoma**. Expert Opin Pharmacother *17*(18), 2499–2504, doi:10.1080/14656566.2016.1258059.

Fala, L. (2015). **Ofev (Nintedanib): First Tyrosine Kinase Inhibitor Approved for the Treatment of Patients with Idiopathic Pulmonary Fibrosis.** Am Heal Drug Benefits *8*(Spec Feature), 101–104.

Fan, G., Wang, Z., Hao, M. and Li, J. (2015). **Bispecific antibodies and their applications**. J Hematol Oncol *8*(1), doi:10.1186/s13045-015-0227-0.

Farber, D. L., Yudanin, N. A. and Restifo, N. P. (2014). **Human memory T cells: Generation, compartmentalization and homeostasis**, *Nature Reviews Immunology* 14 (1) pp.24–35, doi:10.1038/nri3567.

Ferguson, A. R. and Engelhard, V. H. (2010). **CD8 T Cells Activated in Distinct Lymphoid Organs Differentially Express Adhesion Proteins and Coexpress Multiple Chemokine Receptors**. J Immunol *184*(8), 4079–4086, doi:10.4049/jimmunol.0901903.

Ferrara, N. (2004). **Vascular endothelial growth factor: Basic science and clinical progress**, *Endocrine Reviews* 25 (4) pp.581–611, doi:10.1210/er.2003-0027.

Ferrara, N., Damico, L., Shams, N., Lowman, H. and Kim, R. (2006). **Development of ranibizumab, an anti-vascular endothelial growth factor antigen binding fragment, as therapy for neovascular age-related macular degeneration**, *Retina* 26 (8) pp.859–870, doi:10.1097/01.iae.0000242842.14624.e7.

Ferrara, N., Gerber, H. P. and LeCouter, J. (2003). **The biology of VEGF and its receptors**. Nat Med *9*(6), 669–676, doi:10.1038/nm0603-669.

Fielding, A. K., Rowe, J. M., Buck, G., Foroni, L., Gerrard, G., Litzow, M. R., Lazarus, H., Luger, S. M., Marks, D. I., McMillan, A. K., Moorman, A. V., Patel, B., Paietta, E., Tallman, M. S. and Goldstone, A. H. (2014). **UKALLXII/ECOG2993: Addition of imatinib to a standard treatment regimen enhances long-term outcomes in Philadelphia positive acute lymphoblastic leukemia**. Blood *123*(6), 843–850, doi:10.1182/blood-2013-09-529008.

Finetti, F. and Baldari, C. T. (2018). **The immunological synapse as a pharmacological target**, *Pharmacological Research* 134 pp.118–133,.

Finke, J. H., Rini, B., Ireland, J., Rayman, P., Richmond, A., Golshayan, A., Wood, L., Elson, P., Garcia, J., Dreicer, R. and Bukowski, R. (2008). **Sunitinib reverses type-1 immune suppression and decreases T-regulatory cells in renal cell carcinoma patients**. Clin Cancer Res *14*(20), 6674–6682, doi:10.1158/1078-0432.CCR-07-5212.

Fong, G. H. (2009). **Regulation of angiogenesis by oxygen sensing mechanisms**. J Mol Med *87*(6), 549–560, doi:10.1007/s00109-009-0458-z.

Forsythe, J. A., Jiang, B. H., Iyer, N. V, Agani, F., Leung, S. W., Koos, R. D. and Semenza, G. L. (1996). **Activation of vascular endothelial growth factor gene transcription by hypoxia-inducible factor 1.** Mol Cell Biol *16*(9), 4604–4613, doi:10.1128/mcb.16.9.4604.

Fridman, W. H., Pagès, F., Sautès-Fridman, C. and Galon, J. J. (2012). *The immune contexture in human tumours: impact on clinical outcome. 12*(4), 298–306, doi:10.1038/nrc3245.

Fuchs, C. S., Tomasek, J., Yong, C. J., Dumitru, F., Passalacqua, R., Goswami, C., Safran, H., Dos Santos, L. V., Aprile, G., Ferry, D. R., Melichar, B., Tehfe, M., Topuzov, E., Zalcberg, J. R., Chau, I., Campbell, W., Sivanandan, C., Pikiel, J., Koshiji, M., Hsu, Y., Liepa, A. M., Gao, L., Schwartz, J. D. and Tabernero, J. (2014). **Ramucirumab monotherapy for previously treated advanced gastric or gastro-oesophageal junction adenocarcinoma (REGARD): An international, randomised, multicentre, placebo-controlled, phase 3 trial**. Lancet *383*(9911), 31–39, doi:10.1016/S0140-6736(13)61719-5.

Gabrusiewicz, K., Liu, D., Cortes-Santiago, N., Hossain, M. B., Conrad, C. A., Aldape, K. D., Fuller, G. N., Marini, F. C., Alonso, M. M., Idoate, M. A., Gilbert, M. R., Fueyo, J. and Gomez-Manzano, C. (2014). **Anti-vascular endothelial growth factor therapy-induced glioma invasion is associated with accumulation of Tie2-expressing monocytes**. Oncotarget *5*(8), 2208–2220, doi:10.18632/oncotarget.1893.

Gahmberg, C. G., Fagerholm, S. C., Nurmi, S. M., Chavakis, T., Marchesan, S. and Grönholm, M. (2009). **Regulation of integrin activity and signalling**. Biochim Biophys Acta - Gen Subj *1790*(6), 431–444, doi:10.1016/j.bbagen.2009.03.007.

Galon, J., Angell, H. K., Bedognetti, D. and Marincola, F. M. (2013). **The Continuum of Cancer Immunosurveillance: Prognostic, Predictive, and Mechanistic Signatures**, *Immunity* 39 (1) pp.11–26, doi:10.1016/j.immuni.2013.07.008.

Galon, J., Costes, A., Sanchez-Cabo, F., Kirilovsky, A., Mlecnik, B., Lagorce-Pagès, C., Tosolini, M., Camus, M., Berger, A., Wind, P., Zinzindohoué, F., Bruneval, P., Cugnenc, P. H., Trajanoski, Z., Fridman, W. H. and Pagès, F. (2006). **Type, density, and location of immune cells within human colorectal tumors predict clinical outcome**. Science (80-) *313*(5795), 1960–1964, doi:10.1126/science.1129139.

Gao, D., Nolan, D. J., Mellick, A. S., Bambino, K., McDonnell, K. and Mittal, V. (2008). **Endothelial progenitor cells control the angiogenic switch in mouse lung metastasis**. Science (80-) *319*(5860), 195–198, doi:10.1126/science.1150224.

Gao, G., Wang, Z., Qu, X. and Zhang, Z. (2020). **Prognostic value of tumor-infiltrating lymphocytes in patients with triple-negative breast cancer: A systematic review and meta-analysis**. BMC Cancer *20*(1), 179, doi:10.1186/s12885-020-6668-z.

Garon, E. B., Ciuleanu, T. E., Arrieta, O., Prabhash, K., Syrigos, K. N., Goksel, T., Park, K., Gorbunova, V., Kowalyszyn, R. D., Pikiel, J., Czyzewicz, G., Orlov, S. V., Lewanski, C. R., Thomas, M., Bidoli, P., Dakhil, S., Gans, S., Kim, J. H., Grigorescu, A., Karaseva, N., Reck, M., Cappuzzo, F., Alexandris, E., Sashegyi, A., Yurasov, S. and Pérol, M. (2014). **Ramucirumab plus docetaxel versus placebo plus docetaxel for second-line treatment of stage IV non-small-cell lung cancer after disease progression on platinum-based therapy (REVEL): A multicentre, double-blind, randomised phase 3 trial**. Lancet *384*(9944), 665–673, doi:10.1016/S0140-6736(14)60845-X.

Gattei, V., Bulian, P., Del Principe, M. I., Zucchetto, A., Maurillo, L., Buccisano, F., Bomben, R., Dal-Bo, M., Luciano, F., Rossi, F. M., Degan, M., Amadori, S. and Del Poeta, G. (2008). **Relevance of CD49d protein expression as overall survival and progressive disease prognosticator in chronic lymphocytic leukemia**. Blood *111*(2), 865–873, doi:10.1182/blood-2007-05-092486.

Gaugler, M. H., Squiban, C., Van Der Meeren, A., Bertho, J. M., Vandamme, M. and Mouthon, M. A. (1997). **Late and persistent up-regulation of intercellular adhesion molecule-1 (ICAM-1) expression by ionizing radiation in human endothelial cells in vitro**. Int J Radiat Biol *72*(2), 201–209, doi:10.1080/095530097143428.

Gebhardt, T., Whitney, P. G., Zaid, A., Mackay, L. K., Brooks, A. G., Heath, W. R., Carbone, F. R. and Mueller, S. N. (2011). **Different patterns of peripheral migration by memory CD4+ and CD8+ T cells**. Nat 2011 4777363 *477*(7363), 216–219, doi:10.1038/nature10339.

Gehad, A. E., Lichtman, M. K., Schmults, C. D., Teague, J. E., Calarese, A. W., Jiang, Y., Watanabe, R. and Clark, R. A. (2012). **Nitric oxide-producing myeloid-derived suppressor cells inhibit vascular e-selectin expression in human squamous cell carcinomas**. J Invest Dermatol *132*(11), 2642–2651, doi:10.1038/jid.2012.190.

Gianni, L., Eiermann, W., Semiglazov, V., Lluch, A., Tjulandin, S., Zambetti, M., Moliterni, A., Vazquez, F., Byakhov, M. J., Lichinitser, M., Climent, M. A., Ciruelos, E., Ojeda, B., Mansutti, M., Bozhok, A., Magazzù, D., Heinzmann, D., Steinseifer, J., Valagussa, P. and Baselga, J. (2014). **Neoadjuvant and adjuvant trastuzumab in patients with HER2-positive locally advanced breast cancer (NOAH): Follow-up of a randomised controlled superiority trial with a parallel HER2-negative cohort**. Lancet Oncol *15*(6), 640–647, doi:10.1016/S1470-2045(14)70080-4.

Goel, S., Duda, D. G., Xu, L., Munn, L. L., Boucher, Y., Fukumura, D. and Jain, R. K. (2011). **Normalization of the Vasculature for Treatment of Cancer and Other Diseases**. Physiol Rev *91*(3), 1071–1121, doi:10.1152/physrev.00038.2010.

Gooden, M. J. M., De Bock, G. H., Leffers, N., Daemen, T. and Nijman, H. W. (2011). **The prognostic influence of tumour-infiltrating lymphocytes in cancer: A systematic review with meta-analysis**, *British Journal of Cancer* 105 (1) pp.93–103, doi:10.1038/bjc.2011.189.

Gotink, K. J. and Verheul, H. M. W. (2010). **Anti-angiogenic tyrosine kinase inhibitors: What is their mechanism of action?**, *Angiogenesis* 13 (1) pp.1–14, doi:10.1007/s10456-009-9160-6.

Greenfield, J. P., Cobb, W. S. and Lyden, D. (2010). **Resisting arrest: A switch from angiogenesis to vasculogenesis in recurrent malignant gliomas**, *Journal of Clinical Investigation* 120 (3) pp.663–667, doi:10.1172/JCI42345.

Greer, S. N., Metcalf, J. L., Wang, Y. and Ohh, M. (2012). **The updated biology of hypoxia-inducible factor**, *EMBO Journal* 31 (11) pp.2448–2460, doi:10.1038/emboj.2012.125.

Griffioen, A. W., Damen, C. A., Martinotti, S., Blijham, G. H. and Groenewegen, G. (1996). **Endothelial Intercellular Adhesion Molecule-1 Expression Is Suppressed in Human Malignancies: The Role of Angiogenic Factors**. Cancer Res *56*(5), 1111–1117.

Griffioen, A. W., Damen, C. A., Mayo, K. H., Barendsz-Janson, A. F., Martinotti, S., Blijham, G. H. and Groenewegen, G. (1999). **Angiogenesis inhibitors overcome tumor induced endothelial cell anergy**. Int J Cancer *80*(2), 315–319.

Groom, J. R. and Luster, A. D. (2011). **CXCR3 in T cell function**, *Experimental Cell Research* 317 (5) pp.620–631, doi:10.1016/j.yexcr.2010.12.017.

Grülich, C. (2014). **Cabozantinib: A MET, RET, and VEGFR2 tyrosine kinase inhibitor**. Recent Results Cancer Res *201*, 207–214, doi:10.1007/978-3-642-54490-3_12.

Haasken, S., Auger, J. L. and Binstadt, B. A. (2011). **Absence of β 2 Integrins Impairs Regulatory T Cells and Exacerbates CD4 + T Cell-Dependent Autoimmune Carditis** . J Immunol *187*(5), 2702–2710, doi:10.4049/jimmunol.1000967.

Hajari Taheri, F., Hassani, M., Sharifzadeh, Z., Behdani, M., Arashkia, A. and Abolhassani, M. (2019). **T cell engineered with a novel nanobody-based chimeric antigen receptor against VEGFR2 as a candidate for tumor immunotherapy**. IUBMB Life *71*(9), 1259–1267.

Hallahan, D., Kuchibhotla, J. and Wyble, C. (1996). **Cell adhesion molecules mediate radiation-induced leukocyte adhesion to the vascular endothelium**. Cancer Res *56*(22), 5150–5155.

Halle, S., Halle, O. and Förster, R. (2017). **Mechanisms and Dynamics of T Cell-Mediated Cytotoxicity In Vivo**. Trends Immunol *38*(6), 432–443, doi:10.1016/j.it.2017.04.002.

Hanahan, D. and Weinberg, R. A. (2011). **Hallmarks of cancer: The next generation**, *Cell* 144 (5) pp.646–674,.

Harjunpää, H., Asens, M. L., Guenther, C. and Fagerholm, S. C. (2019). **Cell Adhesion Molecules and Their Roles and Regulation in the Immune and Tumor Microenvironment**. Front Immunol *10*, 1078, doi:10.3389/fimmu.2019.01078.

Hartmann, T. N., Grabovsky, V., Wang, W., Desch, P., Rubenzer, G., Wollner, S., Binsky, I., Vallon-Eberhard, A., Sapoznikov, A., Burger, M., Shachar, I., Haran, M., Honczarenko, M., Greil, R. and Alon, R. (2009). **Circulating B-cell chronic lymphocytic leukemia cells display impaired migration to lymph nodes and bone marrow**. Cancer Res *69*(7), 3121–3130, doi:10.1158/0008-5472.CAN-08-4136.

Hashizume, H., Baluk, P., Morikawa, S., McLean, J. W., Thurston, G., Roberge, S., Jain, R. K. and McDonald, D. M. (2000). **Openings between defective endothelial cells explain tumor vessel leakiness**. Am J Pathol *156*(4), 1363–1380, doi:10.1016/S0002-9440(10)65006-7.

Heinemann, V., von Weikersthal, L., Decker, T., Kiani, A., Vehling-Kaiser, U., Al-Batran, S., Heintges, T., Lerchenmüller, C., Kahl, C., Seipelt, G., Kullmann, F., Stauch, M., Scheithauer, W., Hielscher, J., Scholz, M., Müller, S., Link, H., Niederle, N., Rost, A., Höffkes, H., Moehler, M., Lindig, R., Modest, D., Rossius, L., Kirchner, T., Jung, A. and Stintzing, S. (2014). **FOLFIRI plus cetuximab versus FOLFIRI plus bevacizumab as first-line treatment for patients with metastatic colorectal cancer (FIRE-3): A randomised, open-label, phase 3 trial**. Lancet Oncol *15*(10), 1065–1075, doi:10.1016/S1470-2045(14)70330-4.

Hellström, M., Kalén, M., Lindahl, P., Abramsson, A. and Betsholtz, C. (1999). **Role of PDGF-B and PDGFR-β in recruitment of vascular smooth muscle cells and pericytes during embryonic blood vessel formation in the mouse**. Development *126*(14), 3047–3055.

Hellström, M., Phng, L.-K., Hofmann, J. J., Wallgard, E., Coultas, L., Lindblom, P., Alva, J., Nilsson, A.-K., Karlsson, L., Gaiano, N., Yoon, K., Rossant, J., Luisa Iruela-Arispe, M., Kalén, M., Gerhardt, H. and Betsholtz, C. (n.d.). *LETTERS Dll4 signalling through Notch1 regulates formation of tip cells during angiogenesis*.

Hewett, Y., Ghimire, S., Farooqi, B. and Shah, B. K. (2018). **Lenvatinib – A multikinase inhibitor for radioiodine-refractory differentiated thyroid cancer**, *Journal of Oncology Pharmacy Practice* 24 (1) pp.28–32, doi:10.1177/1078155216680119.

Himburg, H. A., Sasine, J., Yan, X., Kan, J., Dressman, H., Chute, J. P., HA, H., J, S., X, Y., J, K., H, D. and JP, C. (2016). **A Molecular Profile of the Endothelial Cell Response to Ionizing Radiation**. Radiat Res *186*(2), 141–152, doi:10.1667/RR14444.1.

Hodi, F. S., Lawrence, D., Lezcano, C., Wu, X., Zhou, J., Sasada, T., Zeng, W., Giobbie-Hurder, A., Atkins, M. B., Ibrahim, N., Friedlander, P., Flaherty, K. T., Murphy, G. F., Rodig, S., Velazquez, E. F., Mihm, M. C., Russell, S., Di Piro, P. J., Yap, J. T., Ramaiya, N., Van Den Abbeele, A. D., Gargano, M. and McDermott, D. (2014). **Bevacizumab plus Ipilimumab in Patients with Metastatic Melanoma**. Cancer Immunol Res *2*(7), 632–642, doi:10.1158/2326-6066.CIR-14-0053.

Hodi, F. S., O'Day, S. J., McDermott, D. F., Weber, R. W., Sosman, J. A., Haanen, J. B., Gonzalez, R., Robert, C., Schadendorf, D., Hassel, J. C., Akerley, W., van den Eertwegh, A. J. M. J., Lutzky, J., Lorigan, P., Vaubel, J. M., Linette, G. P., Hogg, D., Ottensmeier, C. H., Lebbé, C., Peschel, C., Quirt, I., Clark, J. I., Wolchok, J. D., Weber, J. S., Tian, J., Yellin, M. J., Nichol, G. M., Hoos, A. and Urba, W. J. (2010). **Improved Survival with Ipilimumab in Patients with Metastatic Melanoma**. N Engl J Med *363*(8), 713–723, doi:10.1056/NEJMoa1003466.

Holling, T. M., Schooten, E. and Van Den Elsen, P. J. (2004). **Function and regulation of MHC class II molecules in T-lymphocytes: Of mice and men**. Hum Immunol *65*(4), 282–290, doi:10.1016/j.humimm.2004.01.005.

Hu-Lowe, D. D., Zou, H. Y., Grazzini, M. L., Hallin, M. E., Wickman, G. R., Amundson, K., Chen, J. H., Rewolinski, D. A., Yamazaki, S., Wu, E. Y., McTigue, M. A., Murray, B. W., Kania, R. S., O'Connor, P., Shalinsky, D. R. and Bender, S. L. (2008). **Nonclinical antiangiogenesis and antitumor activities of axitinib (AG-013736), an oral, potent, and selective inhibitor of vascular endothelial growth factor receptor tyrosine kinases 1, 2, 3**. Clin Cancer Res *14*(22), 7272–7283, doi:10.1158/1078-0432.CCR-08-0652.

Huang, H., Bhat, A., Woodnutt, G. and Lappe, R. (2010). **Targeting the ANGPT-TIE2 pathway in malignancy**, *Nature Reviews Cancer* 10 (8) pp.575–585, doi:10.1038/nrc2894.

Huang, Y., Stylianopoulos, T., Duda, D. G., Fukumura, D. and Jain, R. K. (2013). **Benefits of vascular normalization are dose and time dependent - Letter**, *Cancer Research* 73 (23) pp.7144–7146, doi:10.1158/0008-5472.CAN-13-1989.

Hurvitz, S. A., Martin, M., Symmans, W. F., Jung, K. H., Huang, C. S., Thompson, A. M., Harbeck, N., Valero, V., Stroyakovskiy, D., Wildiers, H., Campone, M., Boileau, J. F., Beckmann, M. W., Afenjar, K., Fresco, R., Helms, H. J., Xu, J., Lin, Y. G., Sparano, J. and Slamon, D. (2018). **Neoadjuvant trastuzumab, pertuzumab, and chemotherapy versus trastuzumab emtansine plus pertuzumab in patients with HER2-positive breast cancer (KRISTINE): a randomised, open-label, multicentre, phase 3 trial**. Lancet Oncol *19*(1), 115–126, doi:10.1016/S1470-2045(17)30716-7.

Huveneers, S., van den Bout, I., Sonneveld, P., Sancho, A., Sonnenberg, A. and Danen, E. H. J. (2007). **Integrin alpha v beta 3 controls activity and oncogenic potential of primed c-Src.** Cancer Res *67*(6), 2693–2700.

Hwang, W. T., Adams, S. F., Tahirovic, E., Hagemann, I. S. and Coukos, G. (2012). **Prognostic significance of tumor-infiltrating T cells in ovarian cancer: A meta-analysis**. Gynecol Oncol *124*(2), 192–198, doi:10.1016/j.ygyno.2011.09.039.

Hynes, R. O. (1992). **Integrins: Versatility, modulation, and signaling in cell adhesion**. Cell *69*(1), 11–25.

Idos, G. E., Kwok, J., Bonthala, N., Kysh, L., Gruber, S. B. and Qu, C. (2020). **The Prognostic Implications of Tumor Infiltrating Lymphocytes in Colorectal Cancer: A Systematic Review and Meta-Analysis**. Sci Rep *10*(1), 3360, doi:10.1038/s41598-020-60255-4.

Jackson, A. L., Matsumoto, H., Janszen, M., Maino, V., Blidy, A. and Shye, S. (1990). **Restricted expression of p55 interleukin 2 receptor (CD25) on normal T cells**. Clin Immunol Immunopathol *54*(1), 126–133.

Jain, P., Kantarjian, H., Jabbour, E., Gonzalez, G. N., Borthakur, G., Pemmaraju, N., Daver, N., Gachimova, E., Ferrajoli, A., Kornblau, S., Ravandi, F., O'Brien, S. and Cortes, J. (2015). **Ponatinib as first-line treatment for patients with chronic myeloid leukaemia in chronic phase: A phase 2 study**. Lancet Haematol *2*(9), e376–e383, doi:10.1016/S2352-3026(15)00127-1.

Jain, R. K. (2005). **Normalization of tumor vasculature: An emerging concept in antiangiogenic therapy**, *Science* 307 (5706) pp.58–62, doi:10.1126/science.1104819.

Jalali, S., del Pozo, M., Chen, K., Miao, H., Li, Y., Schwartz, M., Shyy, J. and Chien, S. (2001). **Integrin-mediated mechanotransduction requires its dynamic interaction with specific extracellular matrix (ECM) ligands**. Proc Natl Acad Sci U S A *98*(3), 1042–1046, doi:10.1073/PNAS.031562998.

Jass, J. R. (1986). **Lymphocytic infiltration and survival in rectal cancer**. J Clin Pathol *39*, 585–589, doi:10.1136/jcp.39.6.585.

Jayson, G. C., Hicklin, D. J. and Ellis, L. M. (2012). **Antiangiogenic therapy-evolving view based on clinical trial results**, *Nature Reviews Clinical Oncology* 9 (5) pp.297–303, doi:10.1038/nrclinonc.2012.8.

Jayson, G. C., Kerbel, R., Ellis, L. M. and Harris, A. L. (2016). **Antiangiogenic therapy in oncology: current status and future directions**. Lancet *388*(10043), 518–529, doi:10.1016/S0140-6736(15)01088-0.

Jiang, B. H. and Liu, L. Z. (2009). **Chapter 2 PI3K/PTEN Signaling in Angiogenesis and Tumorigenesis**, *Advances in Cancer Research* 102 pp.19–65, doi:10.1016/S0065-230X(09)02002-8.

Jiang, S. and Dong, C. (2013). A complex issue on CD4 + T-cell subsets, URL: www.chinatregs.com [Accessed May 2021].

Jin, H., Su, J., Garmy-Susini, B., Kleeman, J. and Varner, J. (2006). **Integrin alpha4beta1 promotes monocyte trafficking and angiogenesis in tumors.** Cancer Res *66*(4), 2146–2152.

Johnson, J. P., Stade, B. G., Holzmann, B., Schwäble, W., Riethmüller, G., Schwable, W. and Riethmuller, G. (1989). **De novo expression of intercellular-adhesion molecule 1 in melanoma correlates with increased risk of metastasis.** Proc Natl Acad Sci U S A *86*(2), 641–644, doi:10.1073/pnas.86.2.641.

Kang, S. A., Blache, C. A., Bajana, S., Hasan, N., Kamal, M., Morita, Y., Gupta, V., Tsolmon, B., Suh, S. K., Gorenstein, D. G., Razaq, W., Rui, H. and Tanaka, T. (2016). **The effect of soluble E-selectin on tumor progression and metastasis**. BMC Cancer *16*(1), 1–13, doi:10.1186/s12885-016-2366-2.

Kappelmayer, J. and Nagy, B. (2017). **The interaction of selectins and PSGL-1 as a key component in thrombus formation and cancer progression**, *BioMed Research International* 2017,.

Kawalec, P., Malinowska-Lipień, I., Brzostek, T. and Kózka, M. (2016). **Lenvatinib for the treatment of radioiodine-refractory differentiated thyroid carcinoma: a systematic review and indirect comparison with sorafenib**, *Expert Review of Anticancer Therapy* 16 (12) pp.1303–1309, doi:10.1080/14737140.2016.1247697.

Kazazi-Hyseni, F., Beijnen, J. H. and Schellens, J. H. M. (2010). **Bevacizumab**. Oncologist *15*(8), 819–825, doi:10.1634/theoncologist.2009-0317.

Keir, M., Butte, M., Freeman, G. and Sharpe, A. (2008). **PD-1 and its ligands in tolerance and immunity**. Annu Rev Immunol *26*, 677–704, doi:10.1146/ANNUREV.IMMUNOL.26.021607.090331.

Kenyon, N. J., Liu, R., O'Roark, E. M., Huang, W., Peng, L. and Lam, K. S. (2009). **An α4β1 integrin antagonist decreases airway inflammation in ovalbumin-exposed mice**. Eur J Pharmacol *603*(1–3), 138–146, doi:10.1016/j.ejphar.2008.11.063.

Kermani, P., Leclerc, G., Martel, R. and Fareh, J. (2001). **Effect of ionizing radiation on thymidine uptake, differentiation, and VEGFR2 receptor expression in endothelial cells: the role of VEGF(165)**. Int J Radiat Oncol Biol Phys *50*(1), 213–220, doi:10.1016/S0360-3016(01)01445-6.

Kershaw, M. H., Westwood, J. A. and Darcy, P. K. (2013). **Gene-engineered T cells for cancer therapy**, *Nature Reviews Cancer* 13 (8) pp.525–541, doi:10.1038/nrc3565.

Kim, E. S., Hirsh, V., Mok, T., Socinski, M. A., Gervais, R., Wu, Y. L., Li, L. Y., Watkins, C. L., Sellers, M. V., Lowe, E. S., Sun, Y., Liao, M. L., Østerlind, K., Reck, M., Armour, A. A., Shepherd, F. A., Lippman, S. M. and Douillard, J. Y. (2008). **Gefitinib versus docetaxel in previously treated non-small-cell lung cancer (INTEREST): a randomised phase III trial**. Lancet *372*(9652), 1809–1818, doi:10.1016/S0140-6736(08)61758-4.

Kim, J. M. and Chen, D. S. (2016). **Immune escape to PD-L1/PD-1 blockade: Seven steps to success (or failure)**, *Annals of Oncology* 27 (8) pp.1492–1504, doi:10.1093/annonc/mdw217.

Kim, P. S. and Ahmed, R. (2010). **Features of responding T cells in cancer and chronic infection**, *Current Opinion in Immunology* 22 (2) pp.223–230, doi:10.1016/j.coi.2010.02.005.

Kim, S. D., Yi, J. M. and Park, M.-T. (2019). **Irradiated endothelial cells modulate the malignancy of liver cancer cells**. Oncol Lett *17*(2), 2187, doi:10.3892/OL.2018.9833.

Kioi, M., Vogel, H., Schultz, G., Hoffman, R. M., Harsh, G. R., Brown, J. M., M, K., H, V., G, S., RM, H., GR, H. and JM, B. (2010). **Inhibition of vasculogenesis, but not angiogenesis, prevents the recurrence of glioblastoma after irradiation in mice**. J Clin Invest *120*(3), 694–705, doi:10.1172/JCI40283.

Klein, D. (2018). **The tumor vascular endothelium as decision maker in cancer therapy**, *Frontiers in Oncology* 8 (SEP) p.367, doi:10.3389/fonc.2018.00367.

Kloepper, J., Riedemann, L., Amoozgar, Z., Seano, G., Susek, K., Yu, V., Dalvie, N., Amelung, R. L., Datta, M., Song, J. W., Askoxylakis, V., Taylor, J. W., Lu-Emerson, C., Batista, A., Kirkpatrick, N. D., Jung, K., Snuderl, M., Muzikansky, A., Stubenrauch, K. G., Krieter, O., Wakimoto, H., Xu, L., Munn, L. L., Duda, D. G., Fukumura, D., Batchelor, T. T. and Jain, R. K. (2016). **Ang-2/VEGF bispecific antibody reprograms macrophages and resident microglia to anti-tumor phenotype and prolongs glioblastoma survival**. Proc Natl Acad Sci U S A *113*(16), 4476–4481, doi:10.1073/pnas.1525360113.

Kmiecik, J., Poli, A., Brons, N. H. C., Waha, A., Eide, G. E., Enger, P. Ø., Zimmer, J. and Chekenya, M. (2013). **Elevated CD3+ and CD8+ tumor-infiltrating immune cells correlate with prolonged survival in glioblastoma patients despite integrated immunosuppressive mechanisms in the tumor microenvironment and at the systemic level**. J Neuroimmunol *264*(1–2), 71–83, doi:10.1016/j.jneuroim.2013.08.013.

Ko, J. S., Zea, A. H., Rini, B. I., Ireland, J. L., Elson, P., Cohen, P., Golshayan, A., Rayman, P. A., Wood, L., Garcia, J., Dreicer, R., Bukowski, R. and Finke, J. H. (2009). **Sunitinib mediates reversal of myeloid-derived suppressor cell accumulation in renal cell carcinoma patients**. Clin Cancer Res *15*(6), 2148–2157, doi:10.1158/1078-0432.CCR-08-1332.

Koch, S. and Claesson-Welsh, L. (2012). **Signal transduction by vascular endothelial growth factor receptors**, *Cold Spring Harbor Perspectives in Medicine* 2 (7), doi:10.1101/cshperspect.a006502.

Koh, Y. J., Kim, H. Z. H., Hwang, S. I., Lee, J. E., Oh, N., Jung, K., Kim, M., Kim, K. E., Kim, H. Z. H., Lim, N. K., Jeon, C. J., Lee, G. M., Jeon, B. H., Nam, D. H., Sung, H. K., Nagy, A., Yoo, O. J. and Koh, G. Y. (2010). **Double antiangiogenic protein, DAAP, targeting VEGF-A and angiopoietins in tumor angiogenesis, metastasis, and vascular leakage**. Cancer Cell *18*(2), 171–184, doi:10.1016/j.ccr.2010.07.001.

Kohm, A. P., Carpentier, P. A., Anger, H. A. and Miller, S. D. (2002). **Cutting edge: CD4+CD25+ regulatory T cells suppress antigen-specific autoreactive immune responses and central nervous system inflammation during active experimental autoimmune encephalomyelitis.** J Immunol *169*(9), 4712–4716, doi:10.4049/jimmunol.169.9.4712.

Kontermann, R. E. (2012). **Dual targeting strategies with bispecific antibodies**, *mAbs* 4 (2) pp.182–197, doi:10.4161/mabs.4.2.19000.

Kontermann, R. E. and Brinkmann, U. (2015). **Bispecific antibodies**, *Drug Discovery Today* 20 (7) pp.838–847, doi:10.1016/j.drudis.2015.02.008.

Kopacek, A., Böldicke, T., Lergenmüller, S., Berthold, F., Jensen, M., Müller, P. P. and Grosse-Hovest, L. (2013). **Construction, expression and binding specificity of bispecific CD3 x VEGFR-2 and CD3 x NCAM antibodies in the single chain and diabody format**. Adv Biosci Biotechnol *04*(05), 654–664.

Kreiter, S., Vormehr, M., van de Roemer, N., Diken, M., Löwer, M., Diekmann, J., Boegel, S., Schrörs, B., Vascotto, F., Castle, J. C., Tadmor, A. D., Schoenberger, S. P., Huber, C., Türeci, O., Sahin, U., Türeci, Ö. and Sahin, U. (2015). **Mutant MHC class II epitopes drive therapeutic immune responses to cancer**. Nature *520*(7549), 692–696, doi:10.1038/nature14426.

Kuchan, M., Jo, H. and Frangos, J. (1994). **Role of G proteins in shear stress-mediated nitric oxide production by endothelial cells**. Am J Physiol *267*(3 Pt 1), doi:10.1152/AJPCELL.1994.267.3.C753.

Kulla, A., Burkhardt, K., Meyer-Puttlitz, B., Teesalu, T., Asser, T., Wiestler, O. D. and Becker, A. J. (2003). **Analysis of the TP53 gene in laser-microdissected glioblastoma vasculature**. Acta Neuropathol *105*(4), 328–332, doi:10.1007/s00401-003-0681-6.

Kupper, T. S. and Fuhlbrigge, R. C. (2004). **Immune surveillance in the skin: Mechanisms and clinical consequences**, *Nature Reviews Immunology* 4 (3) pp.211–222, doi:10.1038/nri1310.

Kurts, C., Robinson, B. W. S. and Knolle, P. A. (2010). **Cross-priming in health and disease**. Nat Rev Immunol *10*(6), 403–414.

Laffón, A., García-Vicuña, R., Humbría, A., Postigo, A., Corbí, A., de Landázuri, M. and Sánchez-Madrid, F. (1991). **Upregulated expression and function of VLA-4 fibronectin receptors on human activated T cells in rheumatoid arthritis**. J Clin Invest *88*(2), 546–552, doi:10.1172/JCI115338.

Lanitis, E., Kosti, P., Ronet, C., Cribioli, E., Rota, G., Spill, A., Reichenbach, P., Zoete, V., Laniti, D. D., Coukos, G. and Irving, M. (2021). **VEGFR-2 redirected CAR-T cells are functionally impaired by soluble VEGF-A competition for receptor binding**. J Immunother Cancer *9*, 2151, doi:10.1136/jitc-2020-002151.

Le, D. T., Uram, J. N., Wang, H., Bartlett, B. R., Kemberling, H., Eyring, A. D., Skora, A. D., Luber, B. S., Azad, N. S., Laheru, D., Biedrzycki, B., Donehower, R. C., Zaheer, A., Fisher, G. A., Crocenzi, T. S., Lee, J. J., Duffy, S. M., Goldberg, R. M., de la Chapelle, A., Koshiji, M., Bhaijee, F., Huebner, T., Hruban, R. H., Wood, L. D., Cuka, N., Pardoll, D. M., Papadopoulos, N., Kinzler, K. W., Zhou, S., Cornish, T. C., Taube, J. M., Anders, R. A., Eshleman, J. R., Vogelstein, B. and Diaz, L. A. (2015). **PD-1 Blockade in Tumors with Mismatch-Repair Deficiency**. N Engl J Med *372*(26), 2509–2520, doi:10.1056/nejmoa1500596.

Lee, H. G., Cho, M. Z. and Choi, J. M. (2020). **Bystander CD4+ T cells: crossroads between innate and adaptive immunity**, *Experimental and Molecular Medicine* 52 (8) pp.1255–1263,.

Lee, O. H., Xu, J., Fueyo, J., Fuller, G. N., Aldape, K. D., Alonso, M. M., Piao, Y., Liu, T. J., Lang, F. F., Bekele, B. N. and Gomez-Manzano, C. (2006). **Expression of the receptor tyrosine kinase Tie2 in neoplastic glial cells is associated with integrin β1-dependent adhesion to the extracellular matrix**. Mol Cancer Res *4*(12), 915–926, doi:10.1158/1541-7786.MCR-06-0184.

Lee, S. M., Khan, I., Upadhyay, S., Lewanski, C., Falk, S., Skailes, G., Marshall, E., Woll, P. J., Hatton, M., Lal, R., Jones, R., Toy, E., Chao, D., Middleton, G., Bulley, S., Ngai, Y., Rudd, R., Hackshaw, A. and Boshoff, C. (2012). **First-line erlotinib in patients with advanced non-small-cell lung cancer unsuitable for chemotherapy (TOPICAL): A double-blind, placebo-controlled, phase 3 trial**. Lancet Oncol *13*(11), 1161–1170, doi:10.1016/S1470-2045(12)70412-6.

Ley, K. and Reutershan, J. (2006). **Leucocyte-Endothelial Interactions in Health and Disease**. In: **The Vascular Endothelium II**, Eds Moncada, S. and Higgs, A. Springer Berlin Heidelberg, Berlin, Heidelberg, pp. 97–133, doi:10.1007/3-540-36028-X_4.

Li, M., Gu, Y., Zhang, Z., Zhang, S., Zhang, D., Saleem, A. F., Zhao, X. and Sun, B. (2010). **Vasculogenic mimicry: A new prognostic sign of gastric adenocarcinoma**. Pathol Oncol Res *16*(2), 259–266, doi:10.1007/s12253-009-9220-7.

Lian, L., Li, X.-L., Xu, M.-D., Li, X.-M., Wu, M.-Y., Zhang, Y., Tao, M., Li, W., Shen, X.-M., Zhou, C. and Jiang, M. (2019). **VEGFR2 promotes tumorigenesis and metastasis in a pro-angiogenic-independent way in gastric cancer**. BMC Cancer 2019 191 *19*(1), 1–15, doi:10.1186/S12885-019-5322-0.

Lim, M., Xia, Y., Bettegowda, C. and Weller, M. (2018). **Current state of immunotherapy for glioblastoma**, *Nature Reviews Clinical Oncology* 15 (7) pp.422–442, doi:10.1038/s41571-018-0003-5.

Lin, Y.-C. C., Shun, C.-T. T., Wu, M.-S. S. and Chen, C.-C. C. (2006). **A novel anticancer effect of thalidomide: inhibition of intercellular adhesion molecule-1-mediated cell invasion and metastasis through suppression of nuclear factor-kappaB.** Clin Cancer Res *12*(23), 7165–7173, doi:10.1158/1078-0432.CCR-06-1393.

Liu, L., Callahan, M. K., Huang, D. R. and Ransohoff, R. M. (2005). **Chemokine Receptor CXCR3: An Unexpected Enigma**, *Current Topics in Developmental Biology* 68 pp.149–181, doi:10.1016/S0070-2153(05)68006-4.

Liu, Xi, Guo, C. Y., Tou, F. F., Wen, X. M., Kuang, Y. K., Zhu, Q. and Hu, H. (2020). **Association of PD-L1 expression status with the efficacy of PD-1/PD-L1 inhibitors and overall survival in solid tumours: A systematic review and meta-analysis**. Int J Cancer *147*(1), 116–127, doi:10.1002/ijc.32744.

Liu, Xianglei, Sun, T., Ge, Q. and Zhu, J. (2020). **Construction of Novel Bispecific Single-Domain Antibodies (BiSdAbs) with Potent Antiangiogenic Activities**. Pharm Front *2*, 64–76, doi:10.1055/s-0040-1708527.

Löffler, A., Kufer, P., Lutterbüse, R., Zettl, F., Daniel, P. T., Schwenkenbecher, J. M., Riethmüller, G., Dörken, B. and Bargou, R. C. (2000). **A recombinant bispecific single-chain antibody, CD19 x CD3, induces rapid and high lymphoma-directed cytotoxicity by unstimulated T lymphocytes**. Blood *95*(6), 2098–2103.

López-Cabrera, M., Santis, A. G., Fernández-Ruiz, E., Blacher, R., Esch, F., Sánchez-Mateos, P. and Sánchez-Madrid, F. (1993). **Molecular clon;ng, expression, and chromosomal localization of the human earliest lymphocyte activation antigen AIM/CD69, a new member of the C-Type animal lectin superfamily of signal-transmitting receptors**. J Exp Med *178*(2), 537–548, doi:10.1084/jem.178.2.537.

Lúcio, P. J., Faria, M. T., Pinto, A. M., da Silva, M. R., Correia Júnior, M. E., da Costa, R. J. and Parreira, A. B. (1998). **Expression of adhesion molecules in chronic B-cell lymphoproliferative disorders.** Haematologica *83*(2), 104–111.

Lugano, R., Ramachandran, M. and Dimberg, A. (2020). **Tumor angiogenesis: causes, consequences, challenges and opportunities**. Cell Mol Life Sci *77*(9), 1745–1770, doi:10.1007/s00018-019-03351-7.

Madhavan, M., Srinivas, P., Abraham, E., Ahmed, I., Vijayalekshmi, N. R. and Balaram, P. (2002). **Down regulation of endothelial adhesion molecules in node positive breast cancer: Possible failure of host defence mechanism**. Pathol Oncol Res *8*(2), 125–128, doi:10.1007/BF03033721.

Maishi, N., Annan, D. A., Kikuchi, H., Hida, Y. and Hida, K. (2019). **Tumor endothelial heterogeneity in cancer progression**. Cancers (Basel) *11*(10), doi:10.3390/cancers11101511.

Manieri, N. A., Chiang, E. Y. and Grogan, J. L. (2017). **TIGIT: A Key Inhibitor of the Cancer Immunity Cycle**, *Trends in Immunology* 38 (1) pp.20–28, doi:10.1016/j.it.2016.10.002.

Maniotis, A. J., Folberg, R., Hess, A., Seftor, E. A., Gardner, L. M. G., Pe'er, J., Trent, J. M., Meltzer, P. S. and Hendrix, M. J. C. (1999). **Vascular channel formation by human melanoma cells in vivo and in vitro: Vasculogenic mimicry**. Am J Pathol *155*(3), 739–752, doi:10.1016/S0002-9440(10)65173-5.

Marin-Acevedo, J. A., Dholaria, B., Soyano, A. E., Knutson, K. L., Chumsri, S. and Lou, Y. (2018). **Next generation of immune checkpoint therapy in cancer: New developments and challenges**, *Journal of Hematology and Oncology* 11 (1), doi:10.1186/s13045-018-0582-8.

Marsal, J. and Agace, W. W. (2012). **Targeting T-cell migration in inflammatory bowel disease**. J Intern Med *272*(5), 411–429, doi:10.1111/j.1365-2796.2012.02588.x.

Marski, M., Kandula, S., Turner, J. R. and Abraham, C. (2005). **CD18 Is Required for Optimal Development and Function of CD4 + CD25 + T Regulatory Cells** . J Immunol *175*(12), 7889–7897, doi:10.4049/jimmunol.175.12.7889.

Martin, M., Holmes, F. A., Ejlertsen, B., Delaloge, S., Moy, B., Iwata, H., von Minckwitz, G., Chia, S. K. L., Mansi, J., Barrios, C. H., Gnant, M., Tomašević, Z., Denduluri, N., Šeparović, R., Gokmen, E., Bashford, A., Ruiz Borrego, M., Kim, S. B., Jakobsen, E. H., Ciceniene, A., Inoue, K., Overkamp, F., Heijns, J. B., Armstrong, A. C., Link, J. S., Joy, A. A., Bryce, R., Wong, A., Moran, S., Yao, B., Xu, F., Auerbach, A., Buyse, M., Chan, A., Harvey, V., Tomek, R., Robert, N. J., Gore, I., Smith, J. W., Masuda, N., Di Sean Kendall, S., Harker, W. G., Petrakova, K., Guerrero Zotano, A., Simon, A. R., Konstantinovic, Z. N., Iannotti, N. O., Tassone, P., Rodriguez, G. I., Jáñez Martinez, N., Crespo Massieu, C., Smickoska, S., Somali, I., Yilmaz, U., Alonso, M. G., Rosales, A. M., Cold, S., Knoop, A. S., Patt, D., Hellerstedt, B. A., Morales Murillo, S., Mayer, I. A., Means-Powell, J. A., Hui, R., Senecal, F. M., De Boer, R. H., Shen, Z., Luczak, A. A., Chui, J. W. Y., Tsang, J. W. hang, Lang, I., Rai, Y., Hozumi, Y., Ten Tije, A. J., Bhandari, M., Osborne, C. R. C., Ohtani, S., Higaki, K., Watanabe, K., Taguchi, K., Takahashi, M., Filipovic, S., Hansen, V. L., Rao, V. P., Gupta, M., Petrov, P., Coudert, B., Vojnovic, Z., Polya, Z., Miyaki, T., Yamamoto, N., Brincat, S., Lesniewski-Kmak, K., Chmielowska, E., Birhiray, R. E., Citron, M. L., Papish, S. W., Berry, W. R., Langkjer, S. T., Garcia Sáenz, J. A., Arance, A. M., Efrat, N., Sarosiek, T., Grzeda, L., Manalo, Y., Smith, J. C., Vaziri, I., Healey, T., Rahim, Y., Luk, C., Dingle, B., Franco, S., Sorensen, P. G., Anand, A., Khan, S., Fountzilas, G., Aogi, K., Shimizu, S., Mikulova, M., Spanik, S., Somer, R. A., Flynn, P. J., Coward, J., Mainwaring, P., Jerusalem, G., Segura-Ojezzar, C., Levy, C., Delozier, T., Khayat, D., Coleman, R. E., Rolles, M. J., Maisano, R., Nardi, M., Ito, Y., Yumuk, P. F., Basaran, G., Serdar Turhal, N., Wilkinson, M. J., Green, N. B., Sidrys, A. P., Hallmeyer, S., Testori, D. J., Sridhar, S., Chang, J., Sun, Q., Jara-Sanchez, C., Rubio, X., Garrido, M. L., De La Haba Rodriguez, J. R., Perello Martorell, A., Avelia Mestre, A., Rifa Ferrer, J., del Barco Berron, S., Nagy, Z., Tanaka, M., Im, Y. H., Carroll, R. R., Dickerson, L. C., Mace, J. R., Rivera, R., Klein, L. M., Ruxer, R., Wilks, S. T., Kotasek, D., Popov, V., Taskova, V., Marinova-Venkova, V., Timcheva, C., Desbiens, C., Ayoub, J. P., Grenier, D., Marschner, N., Tesch, H., Lueck, H. J., Janssen, J., Schwaner, I., Wahlstrom, S., Brix, E. H., Vallentin, S., Kristensen, D., Andreeva, A., Glavicic, V., Calvo Plaza, I., Anton Torres, A., Veyret, C., Bergerat, J. P., Bourbouloux, E., Ella, W. A., Algurafi, H., Robinson, A., Kim, S. J., Taguchi, T., Juozaityte, E., Madretsma, S., Radema, S., Czerniawska-Meier, M., Rogowski, W., Wagnerova, M., Richards, D. A., Tan-Chiu, E., Vasileios, A., Henderson, C. A., Holden, V. R., Wang, X., Tong, Z., Yang, J., Gonzalez, M. E., Rezai, M., Hackmann, J., de Dueñas, E. M., de las Heras, B. B., Dourthe, L. M., Chocteau-Bouju, D., Bougnoux, P., Kakolyris, S., Kalofonos, H., Pectasidis, D., Ng, T. Y., Pajkos, G., Somogyine, E. E., Tonini, G., Giuffrida, D., Takao, S., Ishitobi, M., Inaji, H., Tokuda, Y., Wozniak, K., Lungulescu, D., Lu, Y. S., Chang, K. J., Hill, J., Croot, C. C., Dekker, A., Belman, N. D., Conde, M., Michaelson, R. A., Kemmer, K., Chui, S., Luoh, S. W., Nahum, K., Greenspan, A. R., Nichols, J. C., Encarnacion, C. A., Niederman, T. M. J., Lee, T., Alexander, R., Gordon, R., Tomova, A., Rauch, D., Popescu, R. A., Rojas, G. A., Vanasek, J., Neunhoeffer, T., Barinoff, J., Graffunder, G., Wolfgang, A., Bojko, P., Heinrich, B., von der Assen, A., Antonovic, B. J., Adrian, L., Ramos Vazquez, M., Gonzalez Santiago, S., Dieras, V., Bishop, J. M., Perren, T. J., Varthalitis, I., Mavroudis, D., Georgoulias, V.,

Chow, L. W. C., Yau, C. C. T., Liang, R. H. S., Pikó, B., Wéber, A., Kaufman, B., Drumea, K., Nuzzo, F., De Matteis, A., Nuzzo, F., Carteni, G., Tokunaga, E., Ishida, M., Ohno, S., Sato, N., Kuroi, K., Nishimura, R., Watanabe, J., Choi, Y. J., Park, K. H., Wojtukiewicz, M., Jassem, J., Loman, N., Askoy, S., Altundag, M. K., Saip, P., Ali, M. A., Wade, J. L., Chien, A. J., Brandt, D., Novik, Y., Jani, C., Rice, R. L., Gaffar, Y. A. R., Keaton, M. R., Bajaj, R., Kimmick, G., Campbell, D., De Boer, R. H., Turnquest, T., Lucas, S., Dube, P., Xu, B., Schilling, J., Apel, K., Sorensen, P. G., Vestlev, P. M., Jensen, B. B., Haahr, V., Lescure, A. R., Grana Suarez, B., Saura Manich, C., Jacquin, J. P., Samreen, A., Boiangiu, I., Dank, M., Falci, C., Jirillo, A., Cinieri, S., Ueno, T., Sato, F., Yamashiro, H., Sugie, T., Lee, K. S., Ro, J. S., Park, I. H., Bustam, A. Z., Suszko-Kazarnowicz, M., Piktel, A., Krzemieniecki, K., Iorga, P. G., Yap, Y. S., Kakalejcik, M., Sevinc, A., Ozguroglu, M., Chen, S. C., Greenberg, R. H., Eisemann, A. D., Droder, R., Abbasi, M. R., Vaysburd, M., Caldera, H. J., Haley, B. B., Robin, E., Inhorn, R. C., Hufnagel, D., Kenyon, P. D., Spremulli, E., Silverman, P., Jain, S., Weigand, R., Mebis, J., Koynova, T., Lesperance, B., Prausova, J., Kohne, C. H., Schneeweiss, A., Jackisch, C., Fuxius, S., Cubedo Cervera, R., Urruticoechea Ribate, A., Pernas Simon, S., Valero Gallego, J., Arcusa Lanza, A., del Pilar Alvarez, M., Florian Gerico, J., Cany, L., Stebbing, J., Labudovic, D., Gugic, D., Vrbanec, D., Roila, F., Barni, S., Bidoli, P., Mukai, H., Bermudez, V., Eniu, A., Mirtsching, B. C., Ibrahim, E., Trey, J., Hergenroeder, P. F., Mahmood, A., Gonzalez, A., Kaplan, E. H., Ban, S., Patel, D., Clowney, B., Hoelzer, K., Schwartz, G. H., Salkeni, M., Abraham, J., Narula, S., Jabboury, K., Mocharnuk, R. S., McDonough, R. H., Sikes, D. H., Kawanchi, R. H., Schlabach, L., McCachren, S. S., Cosgriff, T. M., Dreisbach, L., DeMichele, A., Pawl, L., Lucas, J., Shinn, L. C., Alkhouri, N., Monga, M., Lindquist, D. L., Anderson, T. C., Khurshid, H., Witherby, S., Erickson, N., Traynor, A., Bose, R., Pluard, T. J., Jones, M. C., Prakash, S., Volterra, F., Capo, G., Flaherty, L. E., Gartner, E., Baidas, S., Okazaki, I., Nguyen, B., Rakowski, T., Oliff, I., Leach, J. W., Anderson, D., Kubiak, K., Tsai, M., Vroman, P., Deleu, I., Lybaert, W., Borms, M., Couture, F., Wilson, J. J., Hunt, G., Holland, D. R., Mingrone, W., Wang, S., Liu, D., Jiang, Z., Benesova, V., Smakal, M., Garnolova, P., Vesper, A. S., Neumann, M., Janni, W., Liedtke, C., Fischer, D., Grischke, E. M., Seeger, D., Moebus, V., Prechtl, A., Carlos Camara Toral, J., Sanchez Munoz, A., Gonzalez Jimenez, S., Cassinello Espinosa, J., Cirauqui, B., Margeli Vila, M., Batista Lopez, N., Chacon Lopez-Muniz, J. I., de la Cruz Mora, M. A., Mailliez, A., Vanlemmens, L., Pouessel, D., Espie, M., Conibear, J., Roylance, R., Harnett, A., Geffen, D., Ruggeri, E. M., Gamucci, T., Van Groeningen, C. J., Banas, R., Alkis, N., Hou, M. F., Krie, A. K., Vrindavanam, N. S., Howard, O. M., Citrin, D., Morginstin, M. S., Desai, A., Sanchez, I. J., Nixon, D. A., Beatty, P. G., Edmiston, K., McLaughlin, M., Eneman, J. D., Lynch, C. A., O'Brien, E., Call, J. A., Lanier, K. S., Conlin, A., Brooks, D. J., McIntyre, K., Saltzman, M. A., Castine, M. J., Ortega, G. L., Choi, Y. M., Reynolds, C. H., Brescia, F. A., Kramer, R., Kohn, A. D., Micha, J. P., Rhee, J. M., Shah, S., Riseberg, D. A., Patterson, W. K., Salmon, J. P., Andre, C., Bols, A., D'hondt, R., Luce, S., Nouwynck, C., Pelgrims, G., Richard, V., Verschuere, J., Geldhof, K., Caspar, C., Luo, R., Bednarik, O., Schwedler, K., Schmidt, M., Neumeister, R., Bischoff, J., Rack, B., Repp, R., Fries, S., Adrion, R., Schulz, V., Klare, P., Danei, M., Ossenbuhl, D., Kusche, J. M., Griesinger, F., Baena Canada, J. M., Martinez del Prado, P., Machover, D., Mayeur, D., Trufflandier, N., Delecroix, V., Mousseau, M., Mouret-Reynier, M. A., Nabholtz, J. M., Chetiyawardana, A. D., Papandreou, C., Hornyak, L., Faluhelyi, Z., Simo, E., Di Palma, M., Cognetti, F., Gorzegno, G., Dogliotti, L., Gridelli, C., Falcone, A., Soto Parra, H., Buscarino, C., Im, S. A., Sanchez Llamas, B., Dercksen, W., Erdkamp, F., Ruit, J. B., Braun, H., Portielje, J. E. A., Ciltas, A., Buyukberber, S., Benekli, M., Zahalsky, A. J., Jaslow, R., Thomas, G. W., Maini, A., Wiznitzer, I., Khojasteh, A., Francisco Gonzalez, M., Kong, L. R., Padmanabhan, A., Conkright, W. A., Swain, S. M., Faig, D. E., Jain, K., Yanagihara, R. H., Ottaviano, Y., Delmas, A., Steele, H. A., Rainey, G. K., Harris, P. J., Burris, J. K., Rupard, E. J., Tan, E., Whitworth, P. W., Bova, A. R., Anderson, I. C., Shirinian, M., Tin-u, C., O'Rourke, T. J., Roberts, M. S., Francisco, M., Pierson, A. S., Byeff, P. D., Kovach, P. A., Caton, J. R., Rarick, M. U., Schimidt, W. G., Stopeck, A. T., Swart, R., Carrillo Flores, M. R., Alemany, C. A., Lozada, B., Weinstein, P. L., Wang, W., Porubcin, M., Ellison, D. M., Geils, G. F., Rivera, E. and Charif, M. (2017). **Neratinib after trastuzumab-based adjuvant therapy in HER2-positive breast cancer (ExteNET): 5-year analysis of a randomised, double-blind, placebo-controlled, phase 3 trial**. Lancet Oncol *18*(12), 1688–1700, doi:10.1016/S1470-2045(17)30717-9.

Martin, V., Liu, D., Fueyo, J. and Gomez-Manzano, C. (2008). **Tie2: A journey from normal angiogenesis to cancer and beyond**, *Histology and Histopathology* 23 (6) pp.773–780, doi:10.14670/HH-23.773.

Masopust, D. and Schenkel, J. M. (2013). **The integration of T cell migration, differentiation and function**, *Nature Reviews Immunology* 13 (5) pp.309–320, doi:10.1038/nri3442.

Mauge, L., Terme, M., Tartour, E. and Helley, D. (2014). **Control of the adaptive immune response by tumor vasculature**, *Frontiers in Oncology* 4 MAR p.61, doi:10.3389/fonc.2014.00061.

May, M. B. and Glode, A. (2016). **Blinatumomab: A novel, bispecific, T-cell engaging antibody**, *American Journal of Health-System Pharmacy* 73 (1) pp.e6–e13, doi:10.2146/ajhp150134.

Mazzieri, R., Pucci, F., Moi, D., Zonari, E., Ranghetti, A., Berti, A., Politi, L. S., Gentner, B., Brown, J. L., Naldini, L. and De Palma, M. (2011). **Targeting the ANG2/TIE2 Axis Inhibits Tumor Growth and Metastasis by Impairing Angiogenesis and Disabling Rebounds of Proangiogenic Myeloid Cells**. Cancer Cell *19*(4), 512–526, doi:10.1016/J.CCR.2011.02.005.

Mazzone, M., Dettori, D., Leite de Oliveira, R., Loges, S., Schmidt, T., Jonckx, B., Tian, Y. M., Lanahan, A. A., Pollard, P., Ruiz de Almodovar, C., De Smet, F., Vinckier, S., Aragonés, J., Debackere, K., Luttun, A., Wyns, S., Jordan, B., Pisacane, A., Gallez, B., Lampugnani, M. G., Dejana, E., Simons, M., Ratcliffe, P., Maxwell, P. and Carmeliet, P. (2009). **Heterozygous Deficiency of PHD2 Restores Tumor Oxygenation and Inhibits Metastasis via Endothelial Normalization**. Cell *136*(5), 839–851, doi:10.1016/j.cell.2009.01.020.

McCabe, N. P., De, S., Vasanji, A., Brainard, J. and Byzova, T. V (2007). **Prostate cancer specific integrin alphavbeta3 modulates bone metastatic growth and tissue remodeling.** Oncogene *26*(42), 6238–6243.

McDonald, D. M. and Baluk, P. (2005). **Imaging of angiogenesis in inflamed airways and tumors: Newly formed blood vessels are not alike and may be wildly abnormal. Parker B. Francis lecture**. In: **Chest**, 2005, American College of Chest Physicians, pp. 602S-608S, doi:10.1378/chest.128.6_suppl.602S-a.

Mei, X., Chen, Y. S., Chen, F. R., Xi, S. Y. and Chen, Z. P. (2017). **Glioblastoma stem cell differentiation into endothelial cells evidenced through live-cell imaging**. Neuro Oncol *19*(8), 1109–1118, doi:10.1093/neuonc/nox016.

Mitragotri, S., Burke, P. A. and Langer, R. (2014). **Overcoming the challenges in administering biopharmaceuticals: Formulation and delivery strategies**, *Nature Reviews Drug Discovery* 13 (9) pp.655–672, doi:10.1038/nrd4363.

Moore, M. J., Goldstein, D., Hamm, J., Figer, A., Hecht, J. R., Gallinger, S., Au, H. J., Murawa, P., Walde, D., Wolff, R. A., Campos, D., Lim, R., Ding, K., Clark, G., Voskoglou-Nomikos, T., Ptasynski, M. and Parulekar, W. (2007). **Erlotinib plus gemcitabine compared with gemcitabine alone in patients with advanced pancreatic cancer: A phase III trial of the National Cancer Institute of Canada Clinical Trials Group**. J Clin Oncol *25*(15), 1960–1966, doi:10.1200/JCO.2006.07.9525.

Morgan, M. M., Labno, C. M., Seventer, G. A. Van, Denny, M. F., Straus, D. B. and Burkhardt, J. K. (2001). **Superantigen-Induced T Cell:B Cell Conjugation Is Mediated by LFA-1 and Requires Signaling Through Lck, But Not ZAP-70**. J Immunol *167*(10), 5708–5718, doi:10.4049/JIMMUNOL.167.10.5708.

Morikawa, S., Baluk, P., Kaidoh, T., Haskell, A., Jain, R. K. and McDonald, D. M. (2002). **Abnormalities in pericytes on blood vessels and endothelial sprouts in tumors**. Am J Pathol *160*(3), 985–1000, doi:10.1016/S0002-9440(10)64920-6.

Morisada, M., Clavijo, P., Moore, E., Sun, L., Chamberlin, M., Van Waes, C., Hodge, J., Mitchell, J., Friedman, J. and Allen, C. (2017). **PD-1 blockade reverses adaptive immune resistance induced by high-dose hypofractionated but not low-dose daily fractionated radiation**. Oncoimmunology *7*(3), doi:10.1080/2162402X.2017.1395996.

Moserle, L., Jiménez-Valerio, G. and Casanovas, O. (2014). **Antiangiogenic Therapies: Going beyond Their Limits**. Cancer Discov *4*(1), 31–41, doi:10.1158/2159-8290.CD-13-0199.

Motz, G. T. and Coukos, G. (2013). **Deciphering and Reversing Tumor Immune Suppression**, *Immunity* 39 (1) pp.61–73, doi:10.1016/j.immuni.2013.07.005.

Motzer, R. J., Escudier, B., McDermott, D. F., George, S., Hammers, H. J., Srinivas, S., Tykodi, S. S., Sosman, J. A., Procopio, G., Plimack, E. R., Castellano, D., Choueiri, T. K., Gurney, H., Donskov, F., Bono, P., Wagstaff, J., Gauler, T. C., Ueda, T., Tomita, Y., Schutz, F. A., Kollmannsberger, C., Larkin, J., Ravaud, A., Simon, J. S., Xu, L.-A., Waxman, I. M. and Sharma, P. (2015). **Nivolumab versus Everolimus in Advanced Renal-Cell Carcinoma**. N Engl J Med *373*(19), 1803–1813, doi:10.1056/nejmoa1510665.

Motzer, R. J., Escudier, B., Oudard, S., Hutson, T. E., Porta, C., Bracarda, S., Grünwald, V., Thompson, J. A., Figlin, R. A., Hollaender, N., Urbanowitz, G., Berg, W. J., Kay, A., Lebwohl, D. and Ravaud, A. (2008). **Efficacy of everolimus in advanced renal cell carcinoma: a double-blind, randomised, placebo-controlled phase III trial**. Lancet *372*(9637), 449–456, doi:10.1016/S0140-6736(08)61039-9.

Murdoch, C., Muthana, M., Coffelt, S. B. and Lewis, C. E. (2008). **The role of myeloid cells in the promotion of tumour angiogenesis**, *Nature Reviews Cancer* 8 (8) pp.618–631, doi:10.1038/nrc2444.

Nagl, L., Horvath, L., Pircher, A. and Wolf, D. (2020). **Tumor Endothelial Cells (TECs) as Potential Immune Directors of the Tumor Microenvironment – New Findings and Future Perspectives**. Front Cell Dev Biol *8*, doi:10.3389/FCELL.2020.00766.

Nakamura, N., Naruse, K., Matsuki, T., Hamada, Y., Nakashima, E., Kamiya, H., Matsubara, T., Enomoto, A., Takahashi, M., Oiso, Y. and Nakamura, J. (2009). **Adiponectin promotes migration activities of endothelial progenitor cells via Cdc42/Rac1**. FEBS Lett *583*(15), 2457–2463, doi:10.1016/j.febslet.2009.07.011.

Nath, S. and Mukherjee, P. (2014). **MUC1: a multifaceted oncoprotein with a key role in cancer progression.** Trends Mol Med *20*(6), 332–342.

Nico, B., Crivellato, E., Guidolin, D., Annese, T., Longo, V., Finato, N., Vacca, A. and Ribatti, D. (2010). **Intussusceptive microvascular growth in human glioma**. Clin Exp Med *10*(2), 93–98, doi:10.1007/s10238-009-0076-7.

Omata, M., Cheng, A. L., Kokudo, N., Kudo, M., Lee, J. M., Jia, J., Tateishi, R., Han, K. H., Chawla, Y. K., Shiina, S., Jafri, W., Payawal, D. A., Ohki, T., Ogasawara, S., Chen, P. J., Lesmana, C. R. A., Lesmana, L. A., Gani, R. A., Obi, S., Dokmeci, A. K. and Sarin, S. K. (2017). **Asia–Pacific clinical practice guidelines on the management of hepatocellular carcinoma: a 2017 update**, *Hepatology International* 11 (4) pp.317–370, doi:10.1007/s12072-017-9799-9.

Padera, T. P., Stoll, B. R., Tooredman, J. B., Capen, D., Di Tomaso, E. and Jain, R. K. (2004). **Cancer cells compress intratumour vessels**. Nature *427*(6976), 695, doi:10.1038/427695a.

Pàez-Ribes, M., Allen, E., Hudock, J., Takeda, T., Okuyama, H., Viñals, F., Inoue, M., Bergers, G., Hanahan, D. and Casanovas, O. (2009). **Antiangiogenic Therapy Elicits Malignant Progression of Tumors to Increased Local Invasion and Distant Metastasis**. Cancer Cell *15*(3), 220–231, doi:10.1016/j.ccr.2009.01.027.

Palmen, M. J., Dijkstra, C. D., van der Ende, M. B., Peña, A. S. and van Rees, E. P. (1995). **Anti-CD11b/CD18 antibodies reduce inflammation in acute colitis in rats.** Clin Exp Immunol *101*(2), 351–356.

Park, S. W., Royal, W., Semba, R. D., Wiegand, G. W. and Griffin, D. E. (1998). **Expression of adhesion molecules and CD28 on T lymphocytes during human immunodeficiency virus infection**. Clin Diagn Lab Immunol *5*(4), 583–587, doi:10.1128/CDLI.5.4.583-587.1998.

Patan, S., Munn, L. L. and Jain, R. K. (1996). **Intussusceptive microvascular growth in a human colon adenocarcinoma xenograft: A novel mechanism of tumor angiogenesis**. Microvasc Res *51*(2), 260–272, doi:10.1006/mvre.1996.0025.

Peske, J. D., Thompson, E. D., Gemta, L., Baylis, R. A., Fu, Y. X. and Engelhard, V. H. (2015a). **Effector lymphocyte-induced lymph node-like vasculature enables naive T-cell entry into tumours and enhanced anti-tumour immunity**. Nat Commun *6*(1), 1–15, doi:10.1038/ncomms8114.

Peske, J. D., Woods, A. B. and Engelhard, V. H. (2015b). **Control of CD8 T-Cell Infiltration into Tumors by Vasculature and Microenvironment**. In: **Advances in Cancer Research**, Academic Press Inc., pp. 263–307, doi:10.1016/bs.acr.2015.05.001.

Peterson, T. E., Kirkpatrick, N. D., Huang, Y., Farrar, C. T., Marijt, K. A., Kloepper, J., Datta, M., Amoozgar, Z., Seano, G., Jung, K., Kamoun, W. S., Vardam, T., Snuderl, M., Goveia, J., Chatterjee, S., Batista, A., Muzikansky, A., Leow, C. C., Xu, L., Batchelor, T. T., Duda, D. G., Fukumura, D. and Jain, R. K. (2016). **Dual inhibition of Ang-2 and VEGF receptors normalizes tumor vasculature and prolongs survival in glioblastoma by altering macrophages**. Proc Natl Acad Sci U S A *113*(16), 4470–4475, doi:10.1073/pnas.1525349113.

Petrylak, D., de Wit, R., Chi, K. N., Drakaki, A., Sternberg, C. N., Nishiyama, H., Castellano, D., Hussain, S., Fléchon, A., Bamias, A., Yu, E. Y., van der Heijden, M. S., Matsubara, N., Alekseev, B., Necchi, A., Géczi, L., Ou, Y. C., Coskun, H. S., Su, W. P., Hegemann, M., Percent, I., Lee, J. L., Tucci, M., Semenov, A., Laestadius, F., Peer, A., Tortora, G., Safina, S. Z., Del Muro, F. X. G., Rodriguez-Vida, A., Cicin, I., Harputluoglu, H., Widau, R. C., Liepa, A. M., Walgren, R. A., Hamid, O., Zimmermann, A. H., Bell-McGuinn, K. M., Powles, T., Wong, S. L. S., Tan, T. H., Hovey, E. J., Clay, T. D., Ng, S. S. W., Rutten, A., Machiels, J. P., Dumez, H., Cheng, S. Y. S., Ferrario, C., Sengeloev, L., Jensen, N. V., Thibault, C., Laguerre, B., Joly, F., Flechon, A., Culine, S., Becht, C., Niegisch, G., Stöckle, M., Grimm, M. O., Gakis, G., Schultze-Seemann, W., Kalofonos, H., Mavroudis, D., Papandreou, C., Karavasilis, V., Révész, J., Geczi, L., Rosenbaum, E., Leibowitz-Amit, R., Kejzman, D., Sarid, D., Scagliotti, G. V., Bracarda, S., Massari, F., Osawa, T., Miyajima, N., Shinohara, N., Fukuta, F., Ohyama, C., Obara, W., Yamashita, S., Tomita, Y., Kawai, K., Fukasawa, S., Oyama, M., Yonese, J., Nagata, M., Uemura, M., Nishimura, K., Kawakita, M., Tsunemori, H., Hashine, K., Inokuchi, J., Yokomizo, A., Nagamori, S., Lee, H. J., Park, S. H., Rha, S. Y., Kim, Y. J., Lee, Y. G., Cortés, L. V., Flores, C. L. U., Blaisse, R. J. B., Erdkamp, F. L. G., Aarts, M. J. B., Wojcik-Tomaszewska, J., Tomczak, P., Sikora-Kupis, B., Schenker, M., Herzal, A. A., Udrea, A. A., Karlov, P., Fomkin, R., Pulido, E. G., Mignorance, J. I. D., Gauna,

D. C., Rodríguez-Vida, A., Su, Y. L., Lin, C. L., Lin, C. C., Yeh, S. P., Çiçin, I., Erman, M., Urun, Y., Golovko, Y., Bondarenko, I., Sinielnikov, I., Crabb, S., Syndikus, I., Huddart, R., Sundar, S., Chowdhury, S., Sarwar, N., Flaig, T., Pan, C. X., Schwarz, J., Cultrera, J., Hainsworth, J., Herms, B., Lawler, W., Lowe, T., Tagawa, S., Aragon-Ching, J. and Vaishampayan, U. (2017). **Ramucirumab plus docetaxel versus placebo plus docetaxel in patients with locally advanced or metastatic urothelial carcinoma after platinum-based therapy (RANGE): a randomised, double-blind, phase 3 trial**. Lancet *390*(10109), 2266–2277, doi:10.1016/S0140-6736(17)32365-6.

Piali, L., Fichtd, A., Terpe, H. J., Imhof, B. A. and Gisler, R. H. (1995). **Endothelial vascular cell adhesion molecule 1 expression is suppressed by melanoma and carcinoma**. J Exp Med *181*(2), 811–816, doi:10.1084/jem.181.2.811.

Pober, J. S. and Sessa, W. C. (2007). **Evolving functions of endothelial cells in inflammation**, *Nature Reviews Immunology* 7 (10) pp.803–815, doi:10.1038/nri2171.

Potente, M., Gerhardt, H. and Carmeliet, P. (2011). **Basic and therapeutic aspects of angiogenesis**, *Cell* 146 (6) pp.873–887, doi:10.1016/j.cell.2011.08.039.

Powles, T., Eder, J. P., Fine, G. D., Braiteh, F. S., Loriot, Y., Cruz, C., Bellmunt, J., Burris, H. A., Petrylak, D. P., Teng, S. L., Shen, X., Boyd, Z., Hegde, P. S., Chen, D. S. and Vogelzang, N. J. (2014). **MPDL3280A (anti-PD-L1) treatment leads to clinical activity in metastatic bladder cancer**. Nature *515*(7528), 558–562, doi:10.1038/nature13904.

Price, T. J., Peeters, M., Kim, T. W., Li, J., Cascinu, S., Ruff, P., Suresh, A. S., Thomas, A., Tjulandin, S., Zhang, K., Murugappan, S. and Sidhu, R. (2014). **Panitumumab versus cetuximab in patients with chemotherapy-refractory wild-type KRAS exon 2 metastatic colorectal cancer (ASPECCT): A randomised, multicentre, open-label, non-inferiority phase 3 study**. Lancet Oncol *15*(6), 569–579, doi:10.1016/S1470-2045(14)70118-4.

Quezada, S. A., Simpson, T. R., Peggs, K. S., Merghoub, T., Vider, J., Fan, X., Blasberg, R., Yagita, H., Muranski, P., Antony, P. A., Restifo, N. P. and Allison, J. P. (2010). **Tumor-reactive CD4+ T cells develop cytotoxic activity and eradicate large established melanoma after transfer into lymphopenic hosts**. J Exp Med *207*(3), 637–650, doi:10.1084/jem.20091918.

Quitt, O., Luo, S., Meyer, M., Xie, Z., Golsaz-Shirazi, F., Loffredo-Verde, E., Festag, J., Bockmann, J. H., Zhao, L., Stadler, D., Chou, W.-M., Tedjokusumo, R., Wettengel, J. M., Ko, C., Noeßner, E., Bulbuc, N., Shokri, F., Lüttgau, S., Heikenwälder, M., Bohne, F., Moldenhauer, G., Momburg, F. and Protzer, U. (2021). **T-cell engager antibodies enable T cells to control HBV infection and to target HBsAg-positive hepatoma in mice**. J Hepatol, doi:10.1016/j.jhep.2021.06.022.

Rajendra, Y., Kiseljak, D., Baldi, L., Hacker, D. L. and Wurm, F. M. (2011). **A simple high-yielding process for transient gene expression in CHO cells**. J Biotechnol *153*(1–2), 22–26.

Rajendra, Y., Kiseljak, D., Baldi, L., Hacker, D. L. and Wurm, F. M. (2012). **Reduced glutamine concentration improves protein production in growth-arrested CHO-DG44 and HEK-293E cells**. Biotechnol Lett *34*(4), 619–626.

Rajkumar, S. V., Hayman, S., Gertz, M. A., Dispenzieri, A., Lacy, M. Q., Greipp, P. R., Geyer, S., Iturria, N., Fonseca, R., Lust, J. A., Kyle, R. A. and Witzig, T. E. (2002). **Combination therapy with thalidomide plus dexamethasone for newly diagnosed myeloma**. J Clin Oncol *20*(21), 4319–4323, doi:10.1200/JCO.2002.02.116.

Rajkumar, S. V., Jacobus, S., Callander, N. S., Fonseca, R., Vesole, D. H., Williams, M. E., Abonour, R., Siegel, D. S., Katz, M. and Greipp, P. R. (2010). **Lenalidomide plus high-dose dexamethasone versus lenalidomide plus low-dose dexamethasone as initial therapy for newly diagnosed multiple myeloma: an open-label randomised controlled trial**. Lancet Oncol *11*(1), 29–37, doi:10.1016/S1470-2045(09)70284-0.

Ramjiawan, R. R., Griffioen, A. W. and Duda, D. G. (2017). **Anti-angiogenesis for cancer revisited: Is there a role for combinations with immunotherapy?**, *Angiogenesis* 20 (2) pp.185–204, doi:10.1007/s10456-017-9552-y.

Reale, A., Melaccio, A., Lamanuzzi, A., Saltarella, I., Dammacco, F., Vacca, A. and Ria, R. (2016). **Functional and biological role of endothelial precursor cells in tumour progression: A new potential therapeutic target in haematological malignancies**, *Stem Cells International* 2016, doi:10.1155/2016/7954580.

Reddy, M., Eirikis, E., Davis, C., Davis, H. M. and Prabhakar, U. (2004). **Comparative analysis of lymphocyte activation marker expression and cytokine secretion profile in stimulated human peripheral blood mononuclear cell cultures: An in vitro model to monitor cellular immune function**. J Immunol Methods *293*(1–2), 127–142.

Reinacher-Schick, A., Pohl, M. and Schmiegel, W. (2008). **Drug Insight: Antiangiogenic therapies for gastrointestinal cancers - Focus on monoclonal antibodies**, *Nature Clinical Practice Gastroenterology and Hepatology* 5 (5) pp.250–267, doi:10.1038/ncpgasthep1097.

Reiss, Y., Knedla, A., Tal, A. O., Schmidt, M. H. H., Jugold, M., Kiessling, F., Burger, A. M., Wolburg, H., Deutsch, U. and Plate, K. H. (2009). **Switching of vascular phenotypes within a murine breast cancer model induced by angiopoietin-2**. J Pathol *217*(4), 571–580, doi:10.1002/path.2484.

Restifo, N. P., Dudley, M. E. and Rosenberg, S. A. (2012). **Adoptive immunotherapy for cancer: harnessing the T cell response**. Nat Publ Gr, doi:10.1038/nri3191.

Rey, J. B., Launay-Vacher, V. and Tournigand, C. (2015). **Regorafenib as a single-agent in the treatment of patients with gastrointestinal tumors: an overview for pharmacists**, *Targeted Oncology* 10 (2) pp.199–213, doi:10.1007/s11523-014-0333-x.

Ribatti, D., Nico, B., Floris, C., Mangieri, D., Piras, F., Ennas, M. G., Vacca, A. and Sirigu, P. (2005). **Microvascular density, vascularendothelial growth factor immunoreactivity in tumor cells, vessel diameter and intussusceptive microvascular growth in primary melanoma**. Oncol Rep *14*(1), 81–84, doi:10.3892/or.14.1.81.

Ricci-Vitiani, L., Pallini, R., Biffoni, M., Todaro, M., Invernici, G., Cenci, T., Maira, G., Parati, E. A., Stassi, G., Larocca, L. M. and De Maria, R. (2010). **Tumour vascularization via endothelial differentiation of glioblastoma stem-like cells**. Nature *468*(7325), 824–830, doi:10.1038/nature09557.

Riches, J. C., O'Donovan, C. J., Kingdon, S. J., McClanahan, F., Clear, A. J., Neuberg, D. S., Werner, L., Croce, C. M., Ramsay, A. G., Rassenti, L. Z., Kipps, T. J. and Gribben, J. G. (2014). **Trisomy 12 chronic lymphocytic leukemia cells exhibit upregulation of integrin signaling that is modulated by NOTCH1 mutations**. Blood *123*(26), 4101–4110, doi:10.1182/blood-2014-01-552307.

Risau, W. (1997). **Mechanisms of angiogenesis**, *Nature* 386 (6626) pp.671–674, doi:10.1038/386671a0.

Risau, W. and Lemmon, V. (1988). **Changes in the vascular extracellular matrix during embryonic vasculogenesis and angiogenesis**. Dev Biol *125*(2), 441–450, doi:10.1016/0012-1606(88)90225-4.

Risau, W., Sariola, H., Zerwes, H. G., Sasse, J., Ekblom, P., Kemler, R. and Doetschman, T. (1988). **Vasculogenesis and angiogenesis in embryonic-stem-cell-derived embryoid bodies**. Development *102*(3), 471–478.

Roche, P. A. and Furuta, K. (2015). **The ins and outs of MHC class II-mediated antigen processing and presentation**, *Nature Reviews Immunology* 15 (4) pp.203–216, doi:10.1038/nri3818.

Rodriguez, E., Chevalier, J., Ghoul, H. El, Voldum-Clausen, K., Mundy, J. and Petersen, M. (2018). **DNA damage as a consequence of NLR activation**. PLOS Genet *14*(2), e1007235, doi:10.1371/JOURNAL.PGEN.1007235.

Rodriguez, F. J., Orr, B. A., Ligon, K. L. and Eberhart, C. G. (2012). **Neoplastic cells are a rare component in human glioblastoma microvasculature**. Oncotarget *3*(1), 98–106, doi:10.18632/oncotarget.427.

Roland, C. L., Harken, A. H., Sarr, M. G. and Barnett, C. C. J. (2007). **ICAM-1 expression determines malignant potential of cancer.** Surgery *141*(6), 705–707.

Roland, C. L., Lynn, K. D., Toombs, J. E., Dineen, S. P., Udugamasooriya, D. G. and Brekken, R. A. (2009). **Cytokine levels correlate with immune cell infiltration after anti-VEGF therapy in preclinical mouse models of breast cancer**. PLoS One *4*(11), doi:10.1371/journal.pone.0007669.

Rolston, K. V. I. (2017). **Infections in Cancer Patients with Solid Tumors: A Review**. Infect Dis Ther *6*, 69–83, doi:10.1007/s40121-017-0146-1.

Rondaij, M. G., Bierings, R., Kragt, A., Van Mourik, J. A. and Voorberg, J. (2006). **Dynamics and plasticity of Weibel-Palade bodies in endothelial cells**, *Arteriosclerosis, Thrombosis, and Vascular Biology* 26 (5) pp.1002–1007, doi:10.1161/01.ATV.0000209501.56852.6c.

Rood, P. M. L., Calafat, J., Von Dem Borne, A. E. G. K., Gerritsen, W. R. and Van Der Schoot, C. E. (2000). **Immortalisation of human bone marrow endothelial cells: Characterisation of new cell lines**. Eur J Clin Invest *30*(7), 618–629.

Rose, D. M., Han, J. and Ginsberg, M. H. (2002). **α4 integrins and the immune response**. Immunol Rev *186*(1), 118–124, doi:10.1034/j.1600-065X.2002.18611.x.

Rosenberg, S. A. and Restifo, N. P. *Adoptive cell transfer as personalized immunotherapy for human cancer. Science*. (2015)., doi:10.1126/science.aaa4967.

Rosenberg, S. A., Yang, J. C., Sherry, R. M., Kammula, U. S., Hughes, M. S., Phan, G. Q., Citrin, D. E., Restifo, N. P., Robbins, P. F., Wunderlich, J. R., Morton, K. E., Laurencot, C. M., Steinberg, S. M., White, D. E. and Dudley, M. E. (2011). *Cancer Therapy: Clinical Durable Complete Responses in Heavily Pretreated Patients with Metastatic Melanoma Using T-Cell Transfer Immunotherapy*., doi:10.1158/1078-0432.CCR-11-0116.

Roskoski, R. (2007). **Sunitinib: A VEGF and PDGF receptor protein kinase and angiogenesis inhibitor**, *Biochemical and Biophysical Research Communications* 356 (2) pp.323–328,.

Sahin, U. and Türeci, Ö. (2018). **Personalized vaccines for cancer immunotherapy**, *Science* 359 (6382) pp.1355–1360, doi:10.1126/science.aar7112.

Scheuer, W., Thomas, M., Hanke, P., Sam, J., Osl, F., Weininger, D., Baehner, M., Seeber, S., Kettenberger, H., Schanzer, J., Brinkmann, U., Weidner, K. M., Regula, J. and Klein, C. (2016). **Anti-tumoral, anti-angiogenic and anti-metastatic efficacy of a tetravalent bispecific antibody (TAvi6) targeting VEGF-A and angiopoietin-2**. MAbs *8*(3), 562–573, doi:10.1080/19420862.2016.1147640.

Schlesinger, M. and Bendas, G. (2015). **Vascular cell adhesion molecule-1 (VCAM-1) - An increasing insight into its role in tumorigenicity and metastasis**, *International Journal of Cancer* 136 (11) pp.2504–2514, doi:10.1002/ijc.28927.

Schmidt, T. and Carmeliet, P. (2011). **Angiogenesis: A Target in Solid Tumors, Also in Leukemia?** Am Soc Hematol Educ Progr *2011*, 1–8, doi:10.1182/asheducation-2011.1.1.

Schmittnaegel, M., Rigamonti, N., Kadioglu, E., Cassará, A., Rmili, C. W., Kiialainen, A., Kienast, Y., Mueller, H. J., Ooi, C. H., Laoui, D. and De Palma, M. (2017). **Dual angiopoietin-2 and VEGFA inhibition elicits antitumor immunity that is enhanced by PD-1 checkpoint blockade**. Sci Transl Med *9*(385), doi:10.1126/scitranslmed.aak9670.

Schröder, C., Witzel, I., Müller, V., Krenkel, S., Wirtz, R. M., Jänicke, F., Schumacher, U. and Milde-Langosch, K. (2011). **Prognostic value of intercellular adhesion molecule (ICAM)-1 expression in breast cancer.** J Cancer Res Clin Oncol *137*(8), 1193–1201, doi:10.1007/s00432-011-0984-2.

Schroder, K. and Tschopp, J. (2010). **The inflammasomes**. Cell *140*(6), 821–832, doi:10.1016/J.CELL.2010.01.040.

Schumacher, T., Bunse, L., Pusch, S., Sahm, F., Wiestler, B., Quandt, J., Menn, O., Osswald, M., Oezen, I., Ott, M., Keil, M., Balß, J., Rauschenbach, K., Grabowska, A. K., Vogler, I., Diekmann, J., Trautwein, N., Eichmüller, S. B., Okun, J., Stevanović, S., Riemer, A. B., Sahin, U., Friese, M. a., Beckhove, P., von Deimling, A., Wick, W. and Platten, M. (2014). **A vaccine targeting mutant IDH1 induces antitumour immunity.** Nature.

Schwartz, M. (2001). **Integrin signaling revisited**. Trends Cell Biol *11*(12), 466–470, doi:10.1016/S0962-8924(01)02152-3.

Scotney, P. D., MacKenzie, A., Maccarone, P., Fabri, L. J., Scrofani, S. D. B., Gooley, P. R. and Nash, A. D. (2002). **Human vascular endothelial growth factor B: Characterization of recombinant isoforms and generation of neutralizing monoclonal antibodies**. In: **Clinical and Experimental Pharmacology and Physiology**, 2002, Clin Exp Pharmacol Physiol, pp. 1024–1029, doi:10.1046/j.1440-1681.2002.03769.x.

Scott, A. M., Wolchok, J. D. and Old, L. J. (2012). **Antibody therapy of cancer**, *Nature Reviews Cancer* 12 (4) pp.278–287, doi:10.1038/nrc3236.

Selvaraj, S., Raundhal, M., Patidar, A. and Saha, B. (2014). **Anti-VEGF antibody enhances the antitumor effect of CD40**. Int J Cancer *135*(8), 1983–1988, doi:10.1002/ijc.28833.

Sepesi, B., Cuentes, E. P., Canales, J. R., Behrens, C., Correa, A., Antonoff, M., Gibbons, D. L., Heymach, J., Hofstetter, W., Mehran, R., Rice, D. C., Roth, J., Vaporciyan, A. A., Walsh, G., Weissferdt, A., Kalhor, N., Moran, C., Swisher, S. G. and Wistuba, I. (2017). **Tumor-Infiltrating Lymphocytes and Overall Survival in Surgically Resected Stage II and III Non–Small Cell Lung Cancer**. Int J Radiat Oncol *98*(1), 223, doi:10.1016/j.ijrobp.2017.01.060.

Sequist, L. V., Yang, J. C. H., Yamamoto, N., O'Byrne, K., Hirsh, V., Mok, T., Geater, S. L., Orlov, S., Tsai, C. M., Boyer, M., Su, W. C., Bennouna, J., Kato, T., Gorbunova, V., Lee, K. H., Shah, R., Massey, D., Zazulina, V., Shahidi, M. and Schuler, M. (2013). **Phase III study of afatinib or cisplatin plus pemetrexed in patients with metastatic lung adenocarcinoma with EGFR mutations**. J Clin Oncol *31*(27), 3327–3334, doi:10.1200/JCO.2012.44.2806.

Shaik, F., Cuthbert, G. A., Homer-Vanniasinkam, S., Muench, S. P., Ponnambalam, S. and Harrison, M. A. (2020). **Structural basis for vascular endothelial growth factor receptor activation and implications for disease therapy**. Biomolecules *10*(12), 1–25.

Shanafelt, T. D., Geyer, S. M., Bone, N. D., Tschumper, R. C., Witzig, T. E., Nowakowski, G. S., Zent, C. S., Call, T. G., LaPlant, B., Dewald, G. W., Jelinek, D. F. and Kay, N. E. (2008). **CD49d expression is an independent predictor of overall survival in patients with chronic lymphocytic leukaemia: A prognostic parameter with therapeutic potential**. Br J Haematol *140*(5), 537–546, doi:10.1111/j.1365-2141.2007.06965.x.

Sharma, N., Seftor, R. E. B., Seftor, E. A., Gruman, L. M., Heidger, P. M., Cohen, M. B., Lubaroff, D. M. and Hendrix, M. J. C. (2002). **Prostatic tumor cell plasticity involves cooperative interactions of distinct phenotypic subpopulations: Role in vasculogenic mimicry**. Prostate *50*(3), 189–201, doi:10.1002/pros.10048.

Sherwood, L. M., Parris, E. E. and Folkman, J. (1971). **Tumor Angiogenesis: Therapeutic Implications**. N Engl J Med *285*(21), 1182–1186.

Shibuya, M. and Claesson-Welsh, L. (2006). **Signal transduction by VEGF receptors in regulation of angiogenesis and lymphangiogenesis**, *Experimental Cell Research* 312 (5) pp.549–560, doi:10.1016/j.yexcr.2005.11.012.

Shim, W. S. N., Ho, I. A. W. and Wong, P. E. H. (2007). **Angiopoietin: A TIE(d) balance in tumor angiogenesis**, *Molecular Cancer Research* 5 (7) pp.655–665, doi:10.1158/1541-7786.MCR-07-0072.

Shipkova, M. and Wieland, E. (2012). **Surface markers of lymphocyte activation and markers of cell proliferation**, *Clinica Chimica Acta* 413 (17–18) pp.1338–1349, doi:10.1016/j.cca.2011.11.006.

Shrimali, R. K., Yu, Z., Theoret, M. R., Chinnasamy, D., Restifo, N. P. and Rosenberg, S. A. (2010). **Antiangiogenic agents can increase lymphocyte infiltration into tumor and enhance the effectiveness of adoptive immunotherapy of cancer**. Cancer Res *70*(15), 6171–6180, doi:10.1158/0008-5472.CAN-10-0153.

Skoberne, M., Somersan, S., Almodovar, W., Truong, T., Petrova, K., Henson, P. M. and Bhardwaj, N. (2006). **The apoptotic-cell receptor CR3, but not alphavbeta5, is a regulator of human dendritic-cell immunostimulatory function.** Blood *108*(3), 947–955.

Slaney, C. Y., Kershaw, M. H. and Darcy, P. K. (2014). **Trafficking of T cells into tumors**, *Cancer Research* 74 (24) pp.7168–7174, doi:10.1158/0008-5472.CAN-14-2458.

Smith, N. R., Baker, D., James, N. H., Ratcliffe, K., Jenkins, M., Ashton, S. E., Sproat, G., Swann, R., Gray, N., Ryan, A., Jürgensmeier, J. M. and Womack, C. (2010). **Vascular endothelial growth factor receptors VEGFR-2 and VEGFR-3 are localized primarily to the vasculature in human primary solid cancers**. Clin Cancer Res *16*(14), 3548–3561, doi:10.1158/1078-0432.CCR-09-2797.

Snyder, A., Makarov, V., Merghoub, T., Yuan, J., Zaretsky, J. M., Desrichard, A., Walsh, L. A., Postow, M. A., Wong, P., Ho, T. S., Hollmann, T. J., Bruggeman, C., Kannan, K., Li, Y., Elipenahli, C., Liu, C., Harbison, C. T., Wang, L., Ribas, A., Wolchok, J. D. and Chan, T. A. (2014). **Genetic Basis for Clinical Response to CTLA-4 Blockade in Melanoma**. N Engl J Med *371*(23), 2189–2199, doi:10.1056/NEJMoa1406498.

Song, X., Shao, Y., Jiang, T., Ding, Y., Xu, B., Zheng, X., Wang, Q., Chen, X., Gu, W., Wu, C. and Jiang, J. (2018). **Radiotherapy Upregulates Programmed Death Ligand-1 through the Pathways Downstream of Epidermal Growth Factor Receptor in Glioma**. EBioMedicine *28*, 105–113, doi:10.1016/J.EBIOM.2018.01.027.

Sonpavde, G. and Hutson, T. E. (2007). **Pazopanib: A novel multitargeted tyrosine kinase inhibitor**, *Current Oncology Reports* 9 (2) pp.115–119, doi:10.1007/s11912-007-0007-2.

Span, P. N. and Bussink, J. (2015). **Biology of hypoxia**, *Seminars in Nuclear Medicine* 45 (2) pp.101–109, doi:10.1053/j.semnuclmed.2014.10.002.

Spring, H., Schüler, T., Arnold, B., Hämmerling, G. J. and Ganss, R. (2005). **Chemokines direct endothelial progenitors into tumor neovessels**. Proc Natl Acad Sci U S A *102*(50), 18111–18116, doi:10.1073/pnas.0507158102.

Stoecklein, V. M., Osuka, A., Ishikawa, S., Lederer, M. R., Wanke-Jellinek, L. and Lederer, J. A. (2015). **Radiation exposure induces inflammasome pathway activation in immune cells**. J Immunol *194*(3), 1178, doi:10.4049/JIMMUNOL.1303051.

Suri, C., Jones, P. F., Patan, S., Bartunkova, S., Maisonpierre, P. C., Davis, S., Sato, T. N. and Yancopoulos, G. D. (1996). **Requisite role of angiopoietin-1, a ligand for the TIE2 receptor, during embryonic angiogenesis**. Cell *87*(7), 1171–1180, doi:10.1016/S0092-8674(00)81813-9.

Suurs, F. V., Lub-de Hooge, M. N., de Vries, E. G. E. and de Groot, D. J. A. (2019). **A review of bispecific antibodies and antibody constructs in oncology and clinical challenges**, *Pharmacology and Therapeutics* 201 pp.103–119, doi:10.1016/j.pharmthera.2019.04.006.

Swift, M. R. and Weinstein, B. M. (2009). **Arterial-venous specification during development**, *Circulation Research* 104 (5) pp.576–588, doi:10.1161/CIRCRESAHA.108.188805.

Tabernero, J., Van Cutsem, E., Lakomý, R., Prausová, J., Ruff, P., Van Hazel, G. A., Moiseyenko, V. M., Ferry, D. R., McKendrick, J. J., Soussan-Lazard, K., Chevalier, S. and Allegra, C. J. (2014). **Aflibercept versus placebo in combination with fluorouracil, leucovorin and irinotecan in the treatment of previously treated metastatic colorectal cancer: Prespecified subgroup analyses from the VELOUR trial**. Eur J Cancer *50*(2), 320–331, doi:10.1016/j.ejca.2013.09.013.

Tada, Y., Togashi, Y., Kotani, D., Kuwata, T., Sato, E., Kawazoe, A., Doi, T., Wada, H., Nishikawa, H. and Shitara, K. (2018). **Targeting VEGFR2 with Ramucirumab strongly impacts effector/ activated regulatory T cells and CD8+ T cells in the tumor microenvironment**. J Immunother Cancer *6*(1), 1–14, doi:10.1186/s40425-018-0403-1.

Takayama, S., Ishii, S., Ikeda, T., Masamura, S., Doi, M. and Kitajima, M. (2005). **The relationship between bone metastasis from human breast cancer and integrin alpha(v)beta3 expression.** Anticancer Res *25*(1A), 79–83.

Tan, J. and Zhou, G. (2005). Chemokine Receptors and Transplantation.

Tatsumi, T., Shimazaki, C., Goto, H., Araki, S. I., Sudo, Y., Yamagata, N., Ashihara, E., Inaba, T., Fujita, N. and Nakagawa, M. (1996). **Expression of adhesion molecules on myeloma cells**. Japanese J Cancer Res *87*(8), 837–842, doi:10.1111/j.1349-7006.1996.tb02108.x.

Terme, M., Pernot, S., Marcheteau, E., Sandoval, F., Benhamouda, N., Colussi, O., Dubreuil, O., Carpentier, A. F., Tartour, E. and Taieb, J. (2013). **VEGFA-VEGFR pathway blockade inhibits tumor-induced regulatory T-cell proliferation in colorectal cancer**. Cancer Res *73*(2), 539–549, doi:10.1158/0008-5472.CAN-12-2325.

Tetreault, J., Chintharlapalli, S., Leung, D., Gerald, D., Lee, L., Almonte-Baldonado, R., Huber, L., Xu, J., Ramamurthy, B., Pereira, J., Croy, J., Lu, J. and Liu, L. (2017). **Abstract 3090: LY3207447, a tetravalent bispecific antibody targeting VEGFR2 and angiopoietin-2, provides a more efficient anti-angiogenic therapy and an alternative for combination**. In: **Cancer Research**, 1 July 2017, American Association for Cancer Research (AACR), pp. 3090–3090, doi:10.1158/1538-7445.am2017-3090.

Thatcher, N., Hirsch, F. R., Luft, A. V., Szczesna, A., Ciuleanu, T. E., Dediu, M., Ramlau, R., Galiulin, R. K., Bálint, B., Losonczy, G., Kazarnowicz, A., Park, K., Schumann, C., Reck, M., Depenbrock, H., Nanda, S., Kruljac-Letunic, A., Kurek, R., Paz-Ares, L. and Socinski, M. A. (2015). **Necitumumab plus gemcitabine and cisplatin versus gemcitabine and cisplatin alone as first-line therapy in patients with stage IV squamous non-small-cell lung cancer (SQUIRE): An open-label, randomised, controlled phase 3 trial**. Lancet Oncol *16*(7), 763–774, doi:10.1016/S1470-2045(15)00021-2.

Tinoco, R., Otero, D. C., Takahashi, A. A. and Bradley, L. M. (2017). **PSGL-1: A New Player in the Immune Checkpoint Landscape**. Trends Immunol *38*(5), 323–335.

Ton, G. T. N., Banaszynski, M. E. and Kolesar, J. M. (2013). **Vandetanib: a novel targeted therapy for the treatment of metastatic or locally advanced medullary thyroid cancer.**, *American journal of health-system pharmacy : AJHP : official journal of the American Society of Health-System Pharmacists* 70 (10) pp.849–855,

doi:10.2146/ajhp120253.

Tong, R. T., Boucher, Y., Kozin, S. V., Winkler, F., Hicklin, D. J. and Jain, R. K. (2004). **Vascular normalization by vascular endothelial growth factor receptor 2 blockade induces a pressure gradient across the vasculature and improves drug penetration in tumors**. Cancer Res *64*(11), 3731–3736, doi:10.1158/0008-5472.CAN-04-0074.

Tromp, S. C., Oude Egbrink, M. G. A., Dings, R. P. M., Van Velzen, S., Slaaf, D. W., Hillen, H. F. P., Tangelder, G. J., Reneman, R. S. and Griffioen, A. W. (2000). **Tumor angiogenesis factors reduce leukocyte adhesion in vivo**. Int Immunol *12*(5), 671–676.

Tsai, S.-C., Lin, S.-J., Lin, C.-J., Chou, Y.-C., Lin, J.-H., Yeh, T.-H., Chen, M.-R., Huang, L.-M., Lu, M.-Y., Huang, Y.-C., Chen, H.-Y. and Tsai, C.-H. (2013). **Autocrine CCL3 and CCL4 Induced by the Oncoprotein LMP1 Promote Epstein-Barr Virus-Triggered B Cell Proliferation**. J Virol *87*(16), 9041–9052, doi:10.1128/jvi.00541-13.

Tuijnman, W. B., Wichen, D. F. VAN and Schuurman, H.-J. (1993). **Tissue distribution of human IgG Fc receptors CD16, CD32 and CD64: An immunohistochemical study**. APMIS *101*(1–6), 319–329, doi:10.1111/J.1699-0463.1993.TB00117.X.

Tumeh, P. C., Harview, C. L., Yearley, J. H., Shintaku, I. P., Taylor, E. J. M., Robert, L., Chmielowski, B., Spasic, M., Henry, G., Ciobanu, V., West, A. N., Carmona, M., Kivork, C., Seja, E., Cherry, G., Gutierrez, A. J., Grogan, T. R., Mateus, C., Tomasic, G., Glaspy, J. A., Emerson, R. O., Robins, H., Pierce, R. H., Elashoff, D. A., Robert, C. and Ribas, A. (2014). **PD-1 blockade induces responses by inhibiting adaptive immune resistance**. Nature *515*(7528), 568–571, doi:10.1038/nature13954.

Twomey, J. D. and Zhang, B. (2021). **Cancer Immunotherapy Update: FDA-Approved Checkpoint Inhibitors and Companion Diagnostics**, *AAPS Journal* 23 (2) pp.1–11, doi:10.1208/s12248-021-00574-0.

Tysome, J. R., Lemoine, N. R. and Wang, Y. (2013). **Update on oncolytic viral therapy - Targeting angiogenesis**, *OncoTargets and Therapy* 6 pp.1031–1040, doi:10.2147/OTT.S46974.

Tzima, E., Irani-Tehrani, M., Kiosses, W., Dejana, E., Schultz, D., Engelhardt, B., Cao, G., DeLisser, H. and Schwartz, M. (2005). **A mechanosensory complex that mediates the endothelial cell response to fluid shear stress**. Nature *437*(7057), 426–431, doi:10.1038/NATURE03952.

Uhm, J. H., Dooley, N. P., Kyritsis, A. P., Rao, J. S. and Gladson, C. L. (1999). **Vitronectin, a glioma-derived extracellular matrix protein, protects tumor cells from apoptotic death.** Clin cancer Res an Off J Am Assoc Cancer Res *5*(6), 1587–1594.

Upile, T., Jerjes, W., Radhi, H., Al-Khawalde, M., Kafas, P., Nouraei, S. and Sudhoff, H. (2011). **Vascular mimicry in cultured head and neck tumour cell lines**. Head Neck Oncol *3*(1), 55, doi:10.1186/1758-3284-3-55.

Urbich, C. and Dimmeler, S. (2004). **Endothelial progenitor cells: Characterization and role in vascular biology**, *Circulation Research* 95 (4) pp.343–353, doi:10.1161/01.RES.0000137877.89448.78.

Usami, Y., Ishida, K., Sato, S., Kishino, M., Kiryu, M., Ogawa, Y., Okura, M., Fukuda, Y. and Toyosawa, S. (2013). **Intercellular adhesion molecule-1 (ICAM-1) expression correlates with oral cancer progression and induces macrophage/cancer cell adhesion.** Int J cancer *133*(3), 568–578, doi:10.1002/ijc.28066.

Vacca, A., Loreto, M. Di, Ribatti, D., Stefano, R. Di, Gadaleta-Caldarola, G., Iodice, G., Caloro, D. and Dammacco, F. (1995). **Bone marrow of patients with active multiple myeloma: Angiogenesis and plasma cell adhesion molecules LFA-1, VLA-4, LAM-1, and CD44**. Am J Hematol *50*(1), 9–14, doi:10.1002/ajh.2830500103.

Van Cutsem, E., Tabernero, J., Lakomy, R., Prenen, H., Prausová, J., Macarulla, T., Ruff, P., Van Hazel, G. A., Moiseyenko, V., Ferry, D., McKendrick, J., Polikoff, J., Tellier, A., Castan, R. and Allegra, C. (2012). **Addition of aflibercept to fluorouracil, leucovorin, and irinotecan improves survival in a phase III randomized trial in patients with metastatic colorectal cancer previously treated with an oxaliplatin-based regimen**. J Clin Oncol *30*(28), 3499–3506, doi:10.1200/JCO.2012.42.8201.

Van Hinsbergh, V. W. M. and Koolwijk, P. (2008). **Endothelial sprouting and angiogenesis: Matrix metalloproteinases in the lead**, *Cardiovascular Research* 78 (2) pp.203–212, doi:10.1093/cvr/cvm102.

Van Meter, M. E. M. and Kim, E. S. (2010). **Bevacizumab: Current updates in treatment**, *Current Opinion in Oncology* 22 (6) pp.586–591, doi:10.1097/CCO.0b013e32833edc0c.

Vassilopoulos, D., Kovacs, B. and Tsokos, G. C. (1995). **TCR/CD3 complex-mediated signal transduction pathway in T cells and T cell lines from patients with systemic lupus erythematosus.** J Immunol *155*(4).

Vasudev, N. S. and Reynolds, A. R. (2014). **Anti-angiogenic therapy for cancer: Current progress, unresolved questions and future directions**, *Angiogenesis* 17 (3) pp.471–494, doi:10.1007/s10456-014-9420-y.

Verbovetski, I., Bychkov, H., Trahtemberg, U., Shapira, I., Hareuveni, M., Ben-Tal, O., Kutikov, I., Gill, O. and Mevorach, D. (2002). **Opsonization of apoptotic cells by autologous iC3b facilitates clearance by immature dendritic cells, down-regulates DR and CD86, and up-regulates CC chemokine receptor 7.** J Exp Med *196*(12), 1553–1561.

Voron, T., Colussi, O., Marcheteau, E., Pernot, S., Nizard, M., Pointet, A. L., Latreche, S., Bergaya, S., Benhamouda, N., Tanchot, C., Stockmann, C., Combe, P., Berger, A., Zinzindohoue, F., Yagita, H., Tartour, E., Taieb, J. and Terme, M. (2015). **VEGF-A modulates expression of inhibitory checkpoints on CD8++ T cells in tumors**. J Exp Med *212*(2), 139–148, doi:10.1084/jem.20140559.

Voron, T., Marcheteau, E., Pernot, S., Colussi, O., Tartour, E., Taieb, J. and Terme, M. (2014). **Control of the immune response by pro-angiogenic factors**, *Frontiers in Oncology* 4 APR p.70, doi:10.3389/fonc.2014.00070.

Wagner, S. C., Ichim, T. E., Ma, H., Szymanski, J., Perez, J. A., Lopez, J., Bogin, V., Patel, A. N., Marincola, F. M. and Kesari, S. (2015). **Cancer anti-angiogenesis vaccines: Is the tumor vasculature antigenically unique?**, *Journal of Translational Medicine* 13 (1) p.340, doi:10.1186/s12967-015-0688-5.

Wallin, J. J., Bendell, J. C., Funke, R., Sznol, M., Korski, K., Jones, S., Hernandez, G., Mier, J., He, X., Hodi, F. S., Denker, M., Leveque, V., Cañamero, M., Babitski, G., Koeppen, H., Ziai, J., Sharma, N., Gaire, F., Chen, D. S., Waterkamp, D., Hegde, P. S. and McDermott, D. F. (2016). **Atezolizumab in combination with bevacizumab enhances antigen-specific T-cell migration in metastatic renal cell carcinoma**. Nat Commun *7*(1), 1–8, doi:10.1038/ncomms12624.

Wang, H., Peters, T., Sindrilaru, A., Kess, D., Oreshkova, T., Yu, X. Z., Seier, A. M., Schreiber, H., Wlaschek, M., Blakytny, R., Röhrbein, J., Schulz, G., Weiss, J. M. and Scharffetter-Kochanek, K. (2008). **TGF-β-dependent suppressive function of Tregs requires wild-type levels of CD18 in a mouse model of psoriasis**. J Clin Invest *118*(7), 2629–2639, doi:10.1172/JCI34916.

Wang, J., Tian, S., Sun, J., Zhang, J., Lin, L. and Hu, C. (2020). **The presence of tumour-infiltrating lymphocytes (TILs) and the ratios between different subsets serve as prognostic factors in advanced hypopharyngeal squamous cell carcinoma**. BMC Cancer *20*(1), 731, doi:10.1186/s12885-020-07234-0.

Wang, R., Chadalavada, K., Wilshire, J., Kowalik, U., Hovinga, K. E., Geber, A., Fligelman, B., Leversha, M., Brennan, C. and Tabar, V. (2010). **Glioblastoma stem-like cells give rise to tumour endothelium**. Nature *468*(7325), 829–835, doi:10.1038/nature09624.

Wang, Y., Miao, H., Li, S., Chen, K., Li, Y., Yuan, S., Shyy, J. and Chien, S. (2002). **Interplay between integrins and FLK-1 in shear stress-induced signaling**. Am J Physiol Cell Physiol *283*(5), doi:10.1152/AJPCELL.00222.2002.

Ward-Kavanagh, L. K., Lin, W. W., Šedý, J. R. and Ware, C. F. (2016). **The TNF Receptor Superfamily in Co-stimulating and Co-inhibitory Responses**, *Immunity* 44 (5) pp.1005–1019, doi:10.1016/j.immuni.2016.04.019.

Warwas, K. M., Meyer, M., Gonçalves, M., Moldenhauer, G., Bulbuc, N., Knabe, S., Luckner-Minden, C., Ziegelmeier, C., Heussel, C. P., Zörnig, I., Jäger, D. and Momburg, F. (2021). **Co-Stimulatory Bispecific Antibodies Induce Enhanced T Cell Activation and Tumor Cell Killing in Breast Cancer Models**. Front Immunol *12*, 3240, doi:10.3389/fimmu.2021.719116.

Weishaupt, C., Munoz, K. N., Buzney, E., Kupper, T. S. and Fuhlbrigge, R. C. (2007). **T-cell distribution and adhesion receptor expression in metastatic melanoma**. Clin Cancer Res *13*(9), 2549–2556, doi:10.1158/1078-0432.CCR-06-2450.

West, C. and Barnett, G. (2011). **Genetics and genomics of radiotherapy toxicity: towards prediction**. Genome Med *3*(8), doi:10.1186/GM268.

Wettschureck, N., Strilic, B. and Offermanns, S. (2019). **Passing the vascular barrier: Endothelial signaling processes controlling extravasation**. Physiol Rev *99*(3), 1467–1525, doi:10.1152/physrev.00037.2018.

Wherry, E. J. (2011). **T cell exhaustion**, *Nature Immunology* 12 (6) pp.492–499, doi:10.1038/ni.2035.

Wilhelm, S. M., Carter, C., Tang, L. Y., Wilkie, D., McNabola, A., Rong, H., Chen, C., Zhang, X., Vincent, P., McHugh, M., Cao, Y., Shujath, J., Gawlak, S., Eveleigh, D., Rowley, B., Liu, L., Adnane, L., Lynch, M., Auclair, D., Taylor, I., Gedrich, R., Voznesensky, A., Riedl, B., Post, L. E., Bollag, G. and Trail, P. A. (2004). **BAY 43-9006 exhibits broad spectrum oral antitumor activity and targets the RAF/MEK/ERK pathway and receptor tyrosine kinases involved in tumor progression and angiogenesis**. Cancer Res *64*(19), 7099–7109, doi:10.1158/0008-5472.CAN-04-1443.

Wilke, H., Muro, K., Van Cutsem, E., Oh, S. C., Bodoky, G., Shimada, Y., Hironaka, S., Sugimoto, N., Lipatov, O., Kim, T. Y., Cunningham, D., Rougier, P., Komatsu, Y., Ajani, J., Emig, M., Carlesi, R., Ferry, D., Chandrawansa, K., Schwartz, J. D. and Ohtsu, A. (2014). **Ramucirumab plus paclitaxel versus placebo plus paclitaxel in patients with previously treated advanced gastric or gastro-oesophageal junction adenocarcinoma (RAINBOW): A double-blind, randomised phase 3 trial**. Lancet Oncol *15*(11), 1224–1235, doi:10.1016/S1470-2045(14)70420-6.

Willam, C., Koehne, P., Jürgensen, J. S., Gräfe, M., Wagner, K. D., Bachmann, S., Frei, U. and Eckardt, K.-U. (2000). **Tie2 Receptor Expression Is Stimulated by Hypoxia and Proinflammatory Cytokines in Human Endothelial Cells**. Circ Res *87*(5), 370–377, doi:10.1161/01.RES.87.5.370.

Williamson, S. C., Metcalf, R. L., Trapani, F., Mohan, S., Antonello, J., Abbott, B., Leong, H. S., Chester, C. P. E., Simms, N., Polanski, R., Nonaka, D., Priest, L., Fusi, A., Carlsson, F., Carlsson, A., Hendrix, M. J. C., Seftor, R. E. B., Seftor, E. A., Rothwell, D. G., Hughes, A., Hicks, J., Miller, C., Kuhn, P., Brady, G., Simpson, K. L., Blackhall, F. H. and Dive, C. (2016). **Vasculogenic mimicry in small cell lung cancer**. Nat Commun *7*(1), 1–14, doi:10.1038/ncomms13322.

Wilting, J., Birkenhäger, R., Eichmann, A., Kurz, H., Martiny-Baron, G., Marmé, D., McCarthy, J. E. G., Christ, B. and Weich, H. A. (1996). **VEGF121 induces proliferation of vascular endothelial cells and expression of flk-1 without affecting lymphatic vessels of the chorioallantoic membrane**. Dev Biol *176*(1), 76–85, doi:10.1006/dbio.1996.9993.

Winkler, F., Kozin, S. V., Tong, R. T., Chae, S. S., Booth, M. F., Garkavtsev, I., Xu, L., Hicklin, D. J., Fukumura, D., Di Tomaso, E., Munn, L. L. and Jain, R. K. (2004). **Kinetics of vascular normalization by VEGFR2 blockade governs brain tumor response to radiation: Role of oxygenation, angiopoietin-1, and matrix metalloproteinases**. Cancer Cell *6*(6), 553–563, doi:10.1016/j.ccr.2004.10.011.

Wohler, J., Bullard, D., Schoeb, T. and Barnum, S. (2009). **LFA-1 is critical for regulatory T cell homeostasis and function**. Mol Immunol *46*(11–12), 2424–2428, doi:10.1016/j.molimm.2009.04.004.

Woo, S. R., Fuertes, M. B., Corrales, L., Spranger, S., Furdyna, M. J., Leung, M. Y. K., Duggan, R., Wang, Y., Barber, G. N., Fitzgerald, K. A., Alegre, M. L. and Gajewski, T. F. (2014). **STING-dependent cytosolic DNA sensing mediates innate immune recognition of immunogenic tumors**. Immunity *41*(5), 830–842, doi:10.1016/j.immuni.2014.10.017.

Wu, A. A., Drake, V., Huang, H. S., Chiu, S. C. and Zheng, L. (2015). **Reprogramming the tumor microenvironment: tumor-induced immunosuppressive factors paralyze T cells**. Oncoimmunology *4*(7), 1–14, doi:10.1080/2162402X.2015.1016700.

Wu, F. T. H., Man, S., Xu, P., Chow, A., Paez-Ribes, M., Lee, C. R., Pirie-Shepherd, S. R., Emmenegger, U. and Kerbel, R. S. (2016). **Efficacy of cotargeting angiopoietin-2 and the VEGF pathway in the adjuvant postsurgical setting for early breast, colorectal, and renal cancers**. Cancer Res *76*(23), 6988–7000, doi:10.1158/0008-5472.CAN-16-0888.

Wu, T.-C. C. (2007). **The role of vascular cell adhesion molecule-1 in tumor immune evasion.** Cancer Res *67*(13), 6003–6006, doi:10.1158/0008-5472.CAN-07-1543.

Wulhfard, S., Baldi, L., Hacker, D. and Wurm, F. (2010). **Valproic acid enhances recombinant mRNA and protein levels in transiently transfected Chinese hamster ovary cells**. J Biotechnol *148*(2–3), 128–132.

Wulhfard, S., Bouchet, S., Cevey, J., Jesus, M. De, Hacker, D. L. and Wurm, F. M. (2008). **Mild Hypothermia Improves Transient Gene Expression Yields Several Fold in Chinese Hamster Ovary Cells**. Biotechnol Prog *24*(2), 458–465.

Xu, Y., Zhang, X., Wang, Y., Pan, M., Wang, M. and Zhang, J. (2019). **A VEGFR2–MICA bispecific antibody activates tumor-infiltrating lymphocytes and exhibits potent anti-tumor efficacy in mice**. Cancer Immunol Immunother *68*(9), 1429–1441, doi:10.1007/s00262-019-02379-9.

Yadav, L., Puri, N., Rastogi, V., Satpute, P. and Sharma, V. (2015). **Tumour angiogenesis and angiogenic inhibitors: A review**. J Clin Diagnostic Res *9*(6), XE01–XE05, doi:10.7860/JCDR/2015/12016.6135.

Yamada-Ohnishi, Y., Azuma, H., Urushibara, N., Yamaguchi, M., Fujihara, M., Kobata, T. and Ikeda, H. (2004). **Cytotoxic Difference of T Cells Expanded with Anti-CD3 Monoclonal Antibody in the Presence and Absence of Anti-CD28 Monoclonal Antibody**. Stem Cells Dev *13*, 315–322.

Yoong, K. F., McNab, G., Hübscher, S. G. and Adams, D. H. (1998). **Vascular Adhesion Protein-1 and ICAM-1 Support the Adhesion of Tumor-Infiltrating Lymphocytes to Tumor Endothelium in Human Hepatocellular Carcinoma**. J Immunol *160*(8), 3978 LP – 3988, URL: http://www.jimmunol.org/content/160/8/3978.abstract.

Yu, P., Lee, Y., Liu, W., Krausz, T., Chong, A., Schreiber, H. and Fu, Y. X. (2005). **Intratumor depletion of CD4+ cells unmasks tumor immunogenicity leading to the rejection of late-stage tumors**. J Exp Med *201*(5), 779–791, doi:10.1084/jem.20041684.

Yu, Y. and Cui, J. (2018). **Present and future of cancer immunotherapy: A tumor microenvironmental perspective (Review)**. Oncol Lett *16*(4), 4105–4113, doi:10.3892/OL.2018.9219.

Yuan, J., Zhou, J., Dong, Z., Tandon, S., Kuk, D., Panageas, K. S., Wong, P., Wu, X., Naidoo, J., Page, D. B., Wolchok, J. D. and Hodi, F. S. (2014). **Pretreatment serum VEGF is associated with clinical response and overall survival in advanced melanoma patients treated with ipilimumab**. Cancer Immunol Res *2*(2), 127–132, doi:10.1158/2326-6066.CIR-13-0163.

Zarbock, A., Ley, K., McEver, R. P. and Hidalgo, A. (2011). **Leukocyte ligands for endothelial selectins: Specialized glycoconjugates that mediate rolling and signaling under flow**, *Blood* 118 (26) pp.6743–6751, doi:10.1182/blood-2011-07-343566.

Zarrin, B., Zarifi, F., Vaseghi, G. and Javanmard, S. H. (2017). **Acquired tumor resistance to antiangiogenic therapy: Mechanisms at a glance**, *Journal of Research in Medical Sciences* 22 (10), doi:10.4103/jrms.JRMS_182_17.

Zhang, L., Conejo-Garcia, J. R., Gimotty, P. A., Massobrio, M., Regnani, G., Makrigiannakis, A., Gray, H., Schlienger, K., Liebman, M. N., Rubin, S. C. and Coukos, G. (2003). Intratumoral T Cells, Recurrence, and Survival in Epithelial Ovarian Cancer, URL: http://www.nejm.org.

Zhang, N. and Bevan, M. J. (2011). **CD8+ T Cells: Foot Soldiers of the Immune System**, *Immunity* 35 (2) pp.161–168, doi:10.1016/j.immuni.2011.07.010.

Zhang, Q.-Q., Hu, X.-W., Liu, Y.-L., Ye, Z.-J., Gui, Y.-H., Zhou, D.-L., Qi, C.-L., He, X.-D., Wang, H. and Wang, L.-J. (2015). **CD11b deficiency suppresses intestinal tumor growth by reducing myeloid cell recruitment.** Sci Rep *5*, 15948.

Zhong, L., Shi, W., Gan, L., Liu, X., Huo, Y., Wu, P., Zhang, Z., Wu, T., Peng, H., Huang, Y., Zhao, Y., Yuan, Y., Deng, Z. and Tang, H. (2021). **Human endoglin-CD3 bispecific T cell engager antibody induces anti-tumor effect in vivo**. Theranostics *11*(13), 6393–6406, doi:10.7150/THNO.53121.

Zhong, L., Simoneau, B., Tremblay, P.-L., Gout, S., Simard, M. J. and Huot, J. (2014). **E-Selectin-Mediated Adhesion and Extravasation in Cancer**. In: **Encyclopedia of Cancer**, Springer Berlin Heidelberg, pp. 1618–1624, doi:10.1007/978-3-662-46875-3_1781.

Zhou, J., Li, Y.-S. and Chien, S. (2014). **Shear stress-initiated signaling and its regulation of endothelial function**. Arterioscler Thromb Vasc Biol *34*(10), 2191, doi:10.1161/ATVBAHA.114.303422.

Zhu, J., Yamane, H. and Paul, W. E. (2010). **Differentiation of effector CD4+ T cell populations**, *Annual Review of Immunology* 28 pp.445–489, doi:10.1146/annurev-immunol-030409-101212.

Zhu, Y., Feng, Y., Liu, H., Ye, H., Guo, C., Feng, J., Dai, S. and Zheng, X. (2015). **CD4+CD29+T cells are blamed for the persistent inflammatory response in ulcerative colitis**. Int J Clin Exp Pathol *8*(3), 2627, URL: /pmc/articles/PMC4440077/ [Accessed August 2021].

Zonneville, J., Safina, A., Truskinovsky, A. M., Arteaga, C. L. and Bakin, A. V. (2018). **TGF-β signaling promotes tumor vasculature by enhancing the pericyte-endothelium association**. BMC Cancer *18*(1), doi:10.1186/S12885-018-4587-Z.

8 PERSONAL CONTRIBUTIONS

Poster presentations

Gonçalves, M., Schwartz-Albiez, R., Momburg, F. (2018). Role of E-selectin ligands for endothelial cell binding of lymphocyte subsets. IMMUNOSHAPE International Symposium on Glycoimmunology, San Sebastian, Spain

Gonçalves, M., Schwartz-Albiez, R., Momburg, F. (2018). Use of cell surface receptors on activated tumor endothelial cells to improve tumor targeting of effector lymphocytes. Frontiers in Cancer Research (FCR), Heidelberg, Germany

Gonçalves, M., Meyer, M., Knabe, S., Bulbuc, N., Schwartz-Albiez, R., Momburg, F. (2019). Improving tumor endothelium targeting of effector lymphocytes by bispecific constructs. NCT retreat, Heidelberg, Germany.

APPENDIX - PROTEIN SEQUENCES OF PRODUCED RECOMBINANT PROTEINS AND BISPECIFIC ANTIBODIE

I) Recombinant proteins

Construct ID	Anti-EC	Anti-T cells	Structure
9289.1	VEGFR2	x	αVEGFR2 x mIgG2aFc
9617.1		IL-1β	αVEGFR2 x mIgG2aFc x IL-1β
9757.1		TNF-α	αVEGFR2 x mIgG2aFc x TNF-α

Legend:

ER signal sequence
scFv anti-VEGFR2
Glycine-serine-rich linker sequence
mIgG2a-Fc[C224S,N297Q]
WSHPQFEK StrepTag II
IEGR Factor X cleavage site
IL-1β, TNF-α

9289.1 - Theoretical pI/Mw monomer: 8.23 / 54465.15 Da

pcDNA3.1–SS_{IL-2}^anti-VEGFR2 scFv (KDR-1121)^*GSL*^mIgG2a-Fc[C224S,N297Q]^StrepTag

MYRMQLLSCIALSLALVT*NS*EVQLVQSGGGLVKPGGSLRLSCAASGFTFSSYSMNWVRQAPGKGLEWVSSISSSS
SYIYYADSVKGRFTISRDNAKNSLYLQMNSLRAEDTAVYYCARVTDAFDIWGQGTMVTVSSGGGGSGGGGSGGGG
SDIQMTQSPSSVSASIGDRVTITCRASQGIDNWLGWYQQKPGKAPKLLIYDASNLDTGVPSRFSGSGSGTYFTLT
ISSLQAEDFAVYFCQQAKAFPPTFGGGTKVDIK*GNS*GGGGSGGGGSGGGGS*AS*EPRGPTIKP***S***PPCKCPAPNLLG
GPSVFIFPPKIKDVLMISLSPMVTCVVVDVSEDDPDVQISWFVNNVEVLTAQTQTHREDY***Q***STLRVVSALPIQHQ
DWMSGKEFKCKVNNKALPAPIERTISKPKGSVRAPQVYVLPPPEEEMTKKQVTLTCMVTDFMPEDIYVEWTNNGK
TELNYKNTEPVLDSDGSYFMYSKLRVEKKNWVERNSYSCSVVHEGLHNHHTTKSFSRTPGK*DPG***WSHPQFEK***SRG**
*PV**

9617.1 - Theoretical pI/Mw monomer: 7.92 / 72026.22 Da

pcDNA3.1–SS_{IL-2}^anti-VEGFR2 scFv (KDR-1121)^mIgG2a-Fc[C224S,N297Q]^StrepTag^FX_{CS}-hIL-1β

MYRMQLLSCIALSLALVT*NS*EVQLVQSGGGLVKPGGSLRLSCAASGFTFSSYSMNWVRQAPGKGLEWVSSISSSS
SYIYYADSVKGRFTISRDNAKNSLYLQMNSLRAEDTAVYYCARVTDAFDIWGQGTMVTVSSGGGGSGGGGSGGGG
SDIQMTQSPSSVSASIGDRVTITCRASQGIDNWLGWYQQKPGKAPKLLIYDASNLDTGVPSRFSGSGSGTYFTLT
ISSLQAEDFAVYFCQQAKAFPPTFGGGTKVDIK*GNS*GGGGSGGGGSGGGGS*AS*EPRGPTIKP***S***PPCKCPAPNLLG
GPSVFIFPPKIKDVLMISLSPMVTCVVVDVSEDDPDVQISWFVNNVEVLTAQTQTHREDY***Q***STLRVVSALPIQHQ
DWMSGKEFKCKVNNKALPAPIERTISKPKGSVRAPQVYVLPPPEEEMTKKQVTLTCMVTDFMPEDIYVEWTNNGK
TELNYKNTEPVLDSDGSYFMYSKLRVEKKNWVERNSYSCSVVHEGLHNHHTTKSFSRTPGK*DPG***WSHPQFEK***SRI**
EGRAPVRSLNCTLRDSQQKSLVMSGPYELKALHLQGQDMEQQVVFSMSFVQGEESNDKIPVALGLKEKNLYLSCV
LKDDKPTLQLESVDPKNYPKKKMEKRFVFNKIEINNKLEFESAQFPNWYISTSQAENMPVFLGGTKGGQDITDFT
MQFVSS*

9757.1 - Theoretical pI/Mw monomer: 8.15 / 72002.07 Da

pcDNA3.1–SS_{IL-2}^anti-VEGFR2 scFv (KDR-1121)^*GSL*^mIgG2a-Fc[C224S, N297Q]-StrepTag^FX_{CS}-hTNF-α

MYRMQLLSCIALSLALVT*NS*EVQLVQSGGGLVKPGGSLRLSCAASGFTFSSYSMNWVRQAPGKGLEWVSSISSSS
SYIYYADSVKGRFTISRDNAKNSLYLQMNSLRAEDTAVYYCARVTDAFDIWGQGTMVTVSSGGGGSGGGGSGGGG
SDIQMTQSPSSVSASIGDRVTITCRASQGIDNWLGWYQQKPGKAPKLLIYDASNLDTGVPSRFSGSGSGTYFTLT
ISSLQAEDFAVYFCQQAKAFPPTFGGGTKVDIK*GNS*GGGGSGGGGSGGGGS*AS*EPRGPTIKP***S***PPCKCPAPNLLG
GPSVFIFPPKIKDVLMISLSPMVTCVVVDVSEDDPDVQISWFVNNVEVLTAQTQTHREDY***Q***STLRVVSALPIQHQ
DWMSGKEFKCKVNNKALPAPIERTISKPKGSVRAPQVYVLPPPEEEMTKKQVTLTCMVTDFMPEDIYVEWTNNGK
TELNYKNTEPVLDSDGSYFMYSKLRVEKKNWVERNSYSCSVVHEGLHNHHTTKSFSRTPGK*DPG***WSHPQFEK***SRI*
EGRVRSSSRTPSDKPVAHVVANPQAEGQLQWLNRRANALLANGVELRDNQLVVPSEGLYLIYSQVLFKGQGCPST
HVLLTHTISRIAVSYQTKVNLLSAIKSPCQRETPEGAEAKPWYEPIYLGGVFQLEKGDRLSAEINRPDYLDFAES
GQVYFGIIAL*

II) Bispecific antibodies (BiMAbs)

Construct ID	Anti-EC	Anti-T cells	Structure
11335.1	VEGFR2	x	αVEGFR2 x hIgG1Fc
10444.3		CD3	αVEGFR2 x hIgG1Fc x αCD3ε
10709.2		CD28	αVEGFR2 x hIgG1Fc x αCD28
11286.3	TIE2	X	αTIE2 x hIgG1Fc
11151.1		CD28	αTIE2 x hIgG1Fc x αCD28
11381.1		CD8	αTIE2 x hIgG1Fc x αCD8
11282.2	PD-L1	X	αPD-L1 x hIgG1Fc
11020.1		CD28	αPD-L1 x hIgG1Fc x αCD28
9052.1	E-selectin	X	αE-selectin x hIgG1Fc
11367.1		CD8	αE-selectin x hIgG1Fc x αCD8
11285.3	VCAM1	X	αVCAM1 x hIgG1Fc
11368.1		CD8	αVCAM1 x hIgG1Fc x αCD8
10403.1	HER2	CD3	aHER2 x hIgG1Fc x αCD3ε
11009.1		CD28	aHER2 x hIgG1Fc x aCD28

Legend:

ER signal sequence
scFv #1 (anti-EC)
Glycine-serine-rich linker sequence
hIgG2a-Fc[C220S,E233P,L234A,L235A,ΔG236,N297Q,K322A,A327G,P329A,A330S,P331S]
hIgG2a-Fc[C220S,N297Q]
N *N*-glycan attachment site
WSHPQFEK StrepTag II
scFv#2 (anti-CD3ε, anti-CD28, anti-CD8)

11335.1 - Theoretical pI/Mw monomer: 8.22 / 53689.81 Da + 1 *N*-glycan (~3 kDa)

pcDNA3.1– SS_{IL-2}^anti-VEGFR2 scFv (KDR-1121)^*GSL*^hIgG1-Fc[ΔADCC/ΔCDC]^StrepTag

MYRMQLLSCIALSLALVT*NS*EVQLVQSGGGLVKPGGSLRLSCAASGFTFSSYSMNWVRQAPGKGLEWVSSISSSS
SYIYYADSVKGRFTISRDNAKNSLYLQMNSLRAEDTAVYYCARVTDAFDIWGQGTMVTVSSGGGGSGGGGSGGGG
SDIQMTQSPSSVSASIGDRVTITCRASQGIDNWLGWYQQKPGKAPKLLIYDASNLDTGVPSRFSGSGSGTYFTLT
ISSLQAEDFAVYFCQQAKAFPPTFGGGTKVDIK*GNS*GGGGSGGGGSGGGGS*AS*EPKS***S***DKTHTCPPCPAP***PAAG***P
SVFLFPPKPKDTLMISRTPEVTCVVVDVSHEDPEVKFNWYVDGVEVHNAKTKPREEQYNSTYRVVSVLTVLHQDW
LNGKEYKC***A***VSNK***G***L***ASS***IEKTISKAKGQPREPQVYTLPPSRDELTKNQVSLTCLVKGFYPSDIAVEWESNGQPE
NNYKTTPPVLDSDGSFFLYSKLTVDKSRWQQGNVFSCSVMHEALHNHYTQKSLSLSPGK*DPG***WSHPQFEK***.*SR**

10444.3 - Theoretical pI/Mw monomer: 8.51 / 80405.12 Da + 1 *N*-glycan (~3 kDa)

pcDNA3.1– SS_{IL-2}^anti-VEGFR2 scFv (KDR-1121)^*GSL*^hIgG1-Fc[ΔADCC/ΔCDC]^StrepTag^anti-CD3ε (OKT3) scFv

MYRMQLLSCIALSLALVT*NS*EVQLVQSGGGLVKPGGSLRLSCAASGFTFSSYSMNWVRQAPGKGLEWVSSISSSS
SYIYYADSVKGRFTISRDNAKNSLYLQMNSLRAEDTAVYYCARVTDAFDIWGQGTMVTVSSGGGGSGGGGSGGGG
SDIQMTQSPSSVSASIGDRVTITCRASQGIDNWLGWYQQKPGKAPKLLIYDASNLDTGVPSRFSGSGSGTYFTLT
ISSLQAEDFAVYFCQQAKAFPPTFGGGTKVDIK*GNS*GGGGSGGGGSGGGGS*AS*EPKS***S***DKTHTCPPCPAP***PAAG***P
SVFLFPPKPKDTLMISRTPEVTCVVVDVSHEDPEVKFNWYVDGVEVHNAKTKPREEQYNSTYRVVSVLTVLHQDW
LNGKEYKC***A***VSNK***G***L***ASS***IEKTISKAKGQPREPQVYTLPPSRDELTKNQVSLTCLVKGFYPSDIAVEWESNGQPE
NNYKTTPPVLDSDGSFFLYSKLTVDKSRWQQGNVFSCSVMHEALHNHYTQKSLSLSPGK*DPG***WSHPQFEK***.*SR*GGG
GQVQLQQSGAELARPGASVKMSCKASGYTFTRYTMHWVKQRPGQGLEWIGYINPSRGYTNYNQKFKDKATLTTDK
SSSTAYMQLSSLTSEDSAVYYCARYYDDHYCLDYWGQGTTLTVSS*GNS*GGGGSGGGGSGGGGS*AS*QIVLTQSPAI
MSASPGEKVTMTCSASSSVSYMNWYQQKSGTSPKRWIYDTSKLASGVPAHFRGSGSGTSYSLTISGMEAEDAATY
YCQQWSSNPFTFGSGTKLEIN*GNS**

10709.2 - Theoretical pI/Mw monomer: 8.08 / 80227.22 + 1 N-glycan (~3 kDa)

pcDNA3.1– SS_{IL-2}^anti-VEGFR2 scFv (KDR-1121)^*GSL*^hIgG1-Fc[ΔADCC/ΔCDC]^StrepTag ^anti-CD28 (9.3) scFv

MYRMQLLSCIALSLALVT*NS*EVQLVQSGGGLVKPGGSLRLSCAASGFTFSSYSMNWVRQAPGKGLEWVSSISSSS
SYIYYADSVKGRFTISRDNAKNSLYLQMNSLRAEDTAVYYCARVTDAFDIWGQGTMVTVSSGGGGSGGGGSGGGG
SDIQMTQSPSSVSASIGDRVTITCRASQGIDNWLGWYQQKPGKAPKLLIYDASNLDTGVPSRFSGSGSGTYFTLT
ISSLQAEDFAVYFCQQAKAFPPTFGGGTKVDIK*GNS*GGGGSGGGGSGGGGS*AS*EPKS***S***DKTHTCPPCPAP***PAAG***P
SVFLFPPKPKDTLMISRTPEVTCVVVDVSHEDPEVKFNWYVDGVEVHNAKTKPREEQYNSTYRVVSVLTVLHQDW
LNGKEYKC***A***VSNK***G***L***ASS***IEKTISKAKGQPREPQVYTLPPSRDELTKNQVSLTCLVKGFYPSDIAVEWESNGQPE
NNYKTTPPVLDSDGSFFLYSKLTVDKSRWQQGNVFSCSVMHEALHNHYTQKSLSLSPGK*DPG***WSHPQFEK***.*SS*GGG
GQVQLQESGPGLVTPSQSLSITCTVSGFSLSDYGVHWVRQSPGQGLEWLGVIWAGGGTNYNSALMSRKSISKDNS
KSQVFLKMNSLQADDTAVYYCARDKGYSYYYSMDYWGQGTTVTVSSRGGGSGGGGSGGGGSDIELTQSPASLAVS
LGQRATISCRASESVEYYVTSLMQWYQQKPGQPPKLLIFAASNVESGVPARFSGSGSGTNFSLNIHPVDEDDVAM
YFCQQSRKVPYTFGGGTKLEIKR

11286.3 - Theoretical pI/Mw monomer: 7.10 / 54710.86 Da + 1 *N*-glycan (~3 kDa)

pcDNA3.1– SS$_{mIgVH}$^anti-TIE2 (12H8) scFv^*GSL*^hIgG1-Fc[ΔADCC/ΔCDC]^StrepTag

*le*atMGWSYIILFLLATATCVHS*TS*EVQLVESGGGLVKPGGSLKLSCAASGFTFSDYGMHWVRQAPEKGLEWVAY
INSGSSTITYADTVKGRFTISRDNAKNTLFLQMTSLRSEDTAIYYCARGYYGPYYFDYWGQGTALTVSSGGGGSG
GGGSGGGGSDIVMTQSHKFMSTSVGDRVSFTCKASQNVGTAVAWYQQKPGQSPKLLIYWASSRHTGVPDRFTGSG
SGTDFTLTITNVQSEDLADYFCQEYSSYPLTFGVGTKLELK*GNS*GGGGSGGGGSGGGGS*AS*EPKS***S***DKTHTCPPC
PAP***PAAG***PSVFLFPPKPKDTLMISRTPEVTCVVVDVSHEDPEVKFNWYVDGVEVHNAKTKPREEQYNSTYRVVSV
LTVLHQDWLNGKEYKC***A***VSNK***G***L***ASS***IEKTISKAKGQPREPQVYTLPPSRDELTKNQVSLTCLVKGFYPSDIAVE
WESNGQPENNYKTTPPVLDSDGSFFLYSKLTVDKSRWQQGNVFSCSVMHEALHNHYTQKSLSLSPGK*DPG***WSHPQ
FEK***SR**

11151.1 - Theoretical pI/Mw monomer: 7.13 / 81248.27 Da + 1 *N*-glycan (~3 kDa)

pcDNA3.1– SS$_{mIgVH}$^anti-TIE2 (12H8) scFv^*GSL*^hIgG1-Fc[ΔADCC/ΔCDC]^StrepTag^anti-CD28(9.3) scFv

MGWSYIILFLLATATCVHS*TS*EVQLVESGGGLVKPGGSLKLSCAASGFTFSDYGMHWVRQAPEKGLEWVAYINSG
SSTITYADTVKGRFTISRDNAKNTLFLQMTSLRSEDTAIYYCARGYYGPYYFDYWGQGTALTVSSGGGGSGGGGS
GGGGSDIVMTQSHKFMSTSVGDRVSFTCKASQNVGTAVAWYQQKPGQSPKLLIYWASSRHTGVPDRFTGSGSGTD
FTLTITNVQSEDLADYFCQEYSSYPLTFGVGTKLELK*GNS*GGGGSGGGGSGGGGS*AS*EPKS***S***DKTHTCPPCPAP***P***
AAGPSVFLFPPKPKDTLMISRTPEVTCVVVDVSHEDPEVKFNWYVDGVEVHNAKTKPREEQYNSTYRVVSVLTVL
HQDWLNGKEYKC***A***VSNK***G***L***ASS***IEKTISKAKGQPREPQVYTLPPSRDELTKNQVSLTCLVKGFYPSDIAVEWESN
GQPENNYKTTPPVLDSDGSFFLYSKLTVDKSRWQQGNVFSCSVMHEALHNHYTQKSLSLSPGK*DPG***WSHPQFEK***S***
*S*GGGGQVQLQESGPGLVTPSQSLSITCTVSGFSLSDYGVHWVRQSPGQGLEWLGVIWAGGGTNYNSALMSRKSIS
KDNSKSQVFLKMNSLQADDTAVYYCARDKGYSYYYSMDYWGQGTTVTVSSRGGGSGGGGSGGGGSDIELTQSPAS
LAVSLGQRATISCRASESVEYYVTSLMQWYQQKPGQPPKLLIFAASNVESGVPARFSGSGSGTNFSLNIHPVDED
DVAMYFCQQSRKVPYTFGGGTKLEIKR*

11381.1 - Theoretical pI/Mw monomer: 6.60 / 83164.85 + 1 *N*-glycan (~3 kDa)

pcDNA3.1– SS$_{mIgVH}$^anti-TIE2 (12H8) scFv^*GSL*^hIgG1-Fc[ΔADCC/ΔCDC]^StrepTag^anti-CD8 (OKT8) scFv

MGWSYIILFLLATATCVHS*TS*EVQLVESGGGLVKPGGSLKLSCAASGFTFSDYGMHWVRQAPEKGLEWVAYINSG
SSTITYADTVKGRFTISRDNAKNTLFLQMTSLRSEDTAIYYCARGYYGPYYFDYWGQGTALTVSSGGGGSGGGGS
GGGGSDIVMTQSHKFMSTSVGDRVSFTCKASQNVGTAVAWYQQKPGQSPKLLIYWASSRHTGVPDRFTGSGSGTD
FTLTITNVQSEDLADYFCQEYSSYPLTFGVGTKLELK*GNS*GGGGSGGGGSGGGGS*AS*EPKS***S***DKTHTCPPCPAP***P***
AAGPSVFLFPPKPKDTLMISRTPEVTCVVVDVSHEDPEVKFNWYVDGVEVHNAKTKPREEQYNSTYRVVSVLTVL
HQDWLNGKEYKC***A***VSNK***G***L***ASS***IEKTISKAKGQPREPQVYTLPPSRDELTKNQVSLTCLVKGFYPSDIAVEWESN
GQPENNYKTTPPVLDSDGSFFLYSKLTVDKSRWQQGNVFSCSVMHEALHNHYTQKSLSLSPGK*DPG***WSHPQFEK***S***
*S*GGGGSGGGGSGGGGG*SS***WSHPQFEK***SS***EVQLQQSGAELVKPGASVKLSCTASGFNIKDTYIHFVRQRPEQGLEW
IGRIDPANDNTLYASKFQGKATITADTSSNTAYMHLSSLTSGDTAVYYCGRGYGYYVFDHWGQGTTLTVSSGSTS
GGGSGGGSGGGGSSDVQINQSPSFLAASPGETITINCRTSRSISQYLAWYQEKPGKTNKLLIYSGSTLQSGIPSR
FSGSGSGTDFTLTISGLEPEDFAMYYCQQHNENPLTFGAGTKLELK*GNSAS**

11282.2 - Theoretical pI/Mw monomer: 8.18 / 54479.51 + 1 *N*-glycan (~3 kDa)

pcDNA3.1– SS_{mIgVH}^anti-PD-L1 (*Avelumab*) scFv^*GSL*^hIgG1-Fc[ΔADCC/ΔCDC]-StrepTag

MGWSYIILFLLATATCVHS*TS*EVQLLESGGGLVQPGGSLRLSCAASGFTFSSYIMMWVRQAPGKGLEWVSSIYPS
GGITFYADTVKGRFTISRDNSKNTLYLQMNSLRAEDTAVYYCARIKLGTVTTVDYWGQGTLVTVSSGGGGSGGGG
SGGGGSQSALTQPASVSGSPGQSITISCTGTSSDVGGYNYVSWYQQHPGKAPKLMIYDVSNRPSGVSNRFSGSKS
GNTASLTISGLQAEDEADYYCSSYTSSSTRVFGTGTKVTV*GNS*GGGGSGGGGSGGGGS*AS*EPKS***S***DKTHTCPPCP
AP***PAAG***PSVFLFPPKPKDTLMISRTPEVTCVVVDVSHEDPEVKFNWYVDGVEVHNAKTKPREEQYNSTYRVVSVL
TVLHQDWLNGKEYKC***A***VSNK***G***L***ASS***IEKTISKAKGQPREPQVYTLPPSRDELTKNQVSLTCLVKGFYPSDIAVEW
ESNGQPENNYKTTPPVLDSDGSFFLYSKLTVDKSRWQQGNVFSCSVMHEALHNHYTQKSLSLSPGK*DPG***WSHPQF***
EK*SRGPV**

11020.1 - Theoretical pI/Mw monomer: 8.03 / 80763.63 Da + 1 N-glycan (~3 kDa)

pcDNA3.1– SS_{mIgVH}^anti-PD-L1 (*Avelumab*) scFv^*GSL*^hIgG1-Fc[ΔADCC/ΔCDC]-StrepTag^anti-CD28 (9.3) scFv

MGWSYIILFLLATATCVHS*TS*EVQLLESGGGLVQPGGSLRLSCAASGFTFSSYIMMWVRQAPGKGLEWVSSIYPS
GGITFYADTVKGRFTISRDNSKNTLYLQMNSLRAEDTAVYYCARIKLGTVTTVDYWGQGTLVTVSSGGGGSGGGG
SGGGGSQSALTQPASVSGSPGQSITISCTGTSSDVGGYNYVSWYQQHPGKAPKLMIYDVSNRPSGVSNRFSGSKS
GNTASLTISGLQAEDEADYYCSSYTSSSTRVFGTGTKVTV*GNS*GGGGSGGGGSGGGGS*AS*EPKS***S***DKTHTCPPCP
AP***PAAG***PSVFLFPPKPKDTLMISRTPEVTCVVVDVSHEDPEVKFNWYVDGVEVHNAKTKPREEQYNSTYRVVSVL
TVLHQDWLNGKEYKC***A***VSNK***G***L***ASS***IEKTISKAKGQPREPQVYTLPPSRDELTKNQVSLTCLVKGFYPSDIAVEW
ESNGQPENNYKTTPPVLDSDGSFFLYSKLTVDKSRWQQGNVFSCSVMHEALHNHYTQKSLSLSPGK*DPG***WSHPQF***
EK*SS*GGGGQVQLQESGPGLVTPSQSLSITCTVSGFSLSDYGVHWVRQSPGQGLEWLGVIWAGGGTNYNSALMSRK
SISKDNSKSQVFLKMNSLQADDTAVYYCARDKGYSYYYSMDYWGQGTTVTVSSRGGGSGGGGSGGGGSDIELTQS
PASLAVSLGQRATISCRASESVEYYVTSLMQWYQQKPGQPPKLLIFAASNVESGVPARFSGSGSGTNFSLNIHPV
DEDDVAMYFCQQSRKVPYTFGGGTKLEIKR*

9052.1 - Theoretical pI/Mw monomer: 7.07 / 55462.65 Da

pcDNA3.1–$SS_{IL\text{-}2}$^anti-E-selectin scFv (huENA-2)^*GSL*^hIgG1-Fc[C220S, N297Q]-StrepTag

MYRMQLLSCIALSLALV*TNS**TS*QVQLVQSGAEVKKPGSSVKVSCKASGYTFTDHEMHWVRQAPGQGLEWIGTIDP
ETGGTAYNQKFKGRATLTADKSTNTAYMELSSLRSEDTAVYYCTVLRMDYWGQGTLVTVSSGGGGSGGGGSGGGG
SDIQMTQSPSTLSASVGDRVTITCKSSQSLLNSGNQQNYLTWYQQKPGKAPKLLIYWASTRESGVPDRFTGSGSG
TDFTLTISSLQPDDFATYYCQNDYDYPLTFGQGTKVEIKR*GNS*GGGGSGGGGSSGGGGS*ASSS*EPKS***S***DKTHTCPP
CPAPELLGGPSVFLFPPKPKDTLMISRTPEVTCVVVDVSHEDPEVKFNWYVDGVEVHNAKTKPREEQY***Q***STYRVV
SVLTVLHQDWLNGKEYKCKVSNKALPAPIEKTISKAKGQPREPQVYTLPPSRDELTKNQVSLTCLVKGFYPSDIA
VEWESNGQPENNYKTTPPVLDSDGSFFLYSKLTVDKSRWQQGNVFSCSVMHEALHNHYTQKSLSLSPGK*DPG***WSH***
PQFEK*SR**

11367.1 - Theoretical pI/Mw monomer: 6.57 / 83916.64 Da

pcDNA3.1–SS_{IL-2}^anti-E-selectin scFv (huENA-2)^*GSL*^hIgG1-Fc[C220S, N297Q]-StrepTag^-anti-CD8 (OKT8) scFv

MYRMQLLSCIALSLALV*TNSTS*QVQLVQSGAEVKKPGSSVKVSCKASGYTFTDHEMHWVRQAPGQGLEWIGTIDP
ETGGTAYNQKFKGRATLTADKSTNTAYMELSSLRSEDTAVYYCTVLRMDYWGQGTLVTVSSGGGGSGGGGSGGGG
SDIQMTQSPSTLSASVGDRVTITCKSSQSLLNSGNQQNYLTWYQQKPGKAPKLLIYWASTRESGVPDRFTGSGSG
TDFTLTISSLQPDDFATYYCQNDYDYPLTFGQGTKVEIKR*GNS*GGGGSGGGGSSGGGGS*ASS*EPKS***S***DKTHTCPP
CPAPELLGGPSVFLFPPKPKDTLMISRTPEVTCVVVDVSHEDPEVKFNWYVDGVEVHNAKTKPREEQY***Q***STYRVV
SVLTVLHQDWLNGKEYKCKVSNKALPAPIEKTISKAKGQPREPQVYTLPPSRDELTKNQVSLTCLVKGFYPSDIA
VEWESNGQPENNYKTTPPVLDSDGSFFLYSKLTVDKSRWQQGNVFSCSVMHEALHNHYTQKSLSLSPGK*DPG***WSH**
PQFEK*SS*GGGGSGGGGSGGGGGS*S***WSHPQFEK***SS*EVQLQQSGAELVKPGASVKLSCTASGFNIKDTYIHFVRQRP
EQGLEWIGRIDPANDNTLYASKFQGKATITADTSSNTAYMHLSSLTSGDTAVYYCGRGYGYYVFDHWGQGTTLTV
SSGGSTSGGGSGGGSGGGGSSDVQINQSPSFLAASPGETITINCRTSRSISQYLAWYQEKPGKTNKLLIYSGSTLQ
SGIPSRFSGSGSGTDFTLTISGLEPEDFAMYYCQQHNENPLTFGAGTKLELK*GNSAS**

11285.3 - Theoretical pI/Mw monomer: 8.51 / 54513.40 Da + 1 *N*-glycan (~3 kDa)

pcDNA3.1– SS_{mIgVH}^anti-VCAM1 scFv (H6)^*GSL*^hIgG1-Fc[ΔADCC/ΔCDC]-StrepTag

MGWSYIILFLLATATCVHS*TS*EVQLLESGGGLVQPGGSLRLSCAASGFTFSSYDMSWVRQAPGKGLEWVSGISYS
GGSTYYADSVKGRFTISRDNSKNTLYLQMNSLRAEDTAVYYCAKGPFRMRFRSFDYWGQGTTVTVSSGGGGSGGG
GSSGGGSQSVLTQPPSASGTPGQRATISCTGSSSNIGSNSVSWYQQLPGTAPKLLIYANSNRPSGVPDRFSGSKS
GTSASLAISGLRSEDEADYYCGTWDASLSAYVFGGGTKLTVL*RNS*GGGGSGGGGSGGGGS*AS*EPKS***S***DKTHTCPP
CPAP***PAAG***PSVFLFPPKPKDTLMISRTPEVTCVVVDVSHEDPEVKFNWYVDGVEVHNAKTKPREEQY*N*STYRVVS
VLTVLHQDWLNGKEYKC***A***VSNK***G***L***ASS***IEKTISKAKGQPREPQVYTLPPSRDELTKNQVSLTCLVKGFYPSDIAV
EWESNGQPENNYKTTPPVLDSDGSFFLYSKLTVDKSRWQQGNVFSCSVMHEALHNHYTQKSLSLSPGK*DPG***WSHP**
QFEK*SR**

11368.1 - Theoretical pI/Mw monomer: 7.80 / 83419.98 Da

pcDNA3.1– SS_{mIgVH}^anti-VCAM1 scFv (H6)^*GSL*^hIgG1-Fc[ΔADCC/ΔCDC]-StrepTag^anti-CD8 (OKT8) scFv

MGWSYIILFLLATATCVHS*TS*EVQLLESGGGLVQPGGSLRLSCAASGFTFSSYDMSWVRQAPGKGLEWVSGISYS
GGSTYYADSVKGRFTISRDNSKNTLYLQMNSLRAEDTAVYYCAKGPFRMRFRSFDYWGQGTTVTVSSGGGGSGGG
GSSGGGSQSVLTQPPSASGTPGQRATISCTGSSSNIGSNSVSWYQQLPGTAPKLLIYANSNRPSGVPDRFSGSKS
GTSASLAISGLRSEDEADYYCGTWDASLSAYVFGGGTKLTVL*RNS*GGGGSGGGGSGGGGS*ASS*EPKS***S***DKTHTC
PPCPAPELLGGPSVFLFPPKPKDTLMISRTPEVTCVVVDVSHEDPEVKFNWYVDGVEVHNAKTKPREEQY***Q***STYR
VVSVLTVLHQDWLNGKEYKCKVSNKALPAPIEKTISKAKGQPREPQVYTLPPSRDELTKNQVSLTCLVKGFYPSD
IAVEWESNGQPENNYKTTPPVLDSDGSFFLYSKLTVDKSRWQQGNVFSCSVMHEALHNHYTQKSLSLSPGK*DPG***W**
SHPQFEK*SS*GGGGSGGGGSGGGGGS*S***WSHPQFEK***SS*EVQLQQSGAELVKPGASVKLSCTASGFNIKDTYIHFVRQ
RPEQGLEWIGRIDPANDNTLYASKFQGKATITADTSSNTAYMHLSSLTSGDTAVYYCGRGYGYYVFDHWGQGTTL
TVSSGSTSGGGSGGGSGGGGSSDVQINQSPSFLAASPGETITINCRTSRSISQYLAWYQEKPGKTNKLLIYSGST
LQSGIPSRFSGSGSGTDFTLTISGLEPEDFAMYYCQQHNENPLTFGAGTKLELK*GNSAS**

10403.1 - Theoretical pI/Mw monomer: 8.50 / 81212.93 + 1 *N*-glycan (~3 kDa)

pcDNA3.1– SS_{mIgVH}^anti-HER2/neu (*Trastuzumab*) scFv^*GSL*^hIgG1-Fc[ΔADCC/ΔCDC]-StrepTag ^anti-CD3ε (OKT3) scFv

MYRMQLLSCIALSLALVTNSEVQLVESGGGLVQPGGSLRLSCAASGFNIKDTYIHWVRQAPGKGLEWVARIYPTN
GYTRYADSVKGRFTISADTSKNTAYLQMNSLRAEDTAVYYCSRWGGDGFYAMDYWGQGTLVTVSSGGGGSGGGGS
GGGGSDIQMTQSPSSLSASVGDRVTITCRASQDVNTAVAWYQQKPGKAPKLLIYSASFLYSGVPSRFSGSRSGTD
FTLTISSLQPEDFATYYCQQHYTTPPTFGQGTKVEIKGNSGGGGSGGGGSGGGGSASEPKSSDKTHTCPPCPAPP
AAGPSVFLFPPKPKDTLMISRTPEVTCVVVDVSHEDPEVKFNWYVDGVEVHNAKTKPREEQYNSTYRVVSVLTVL
HQDWLNGKEYKCAVSNKGLASSIEKTISKAKGQPREPQVYTLPPSRDELTKNQVSLTCLVKGFYPSDIAVEWESN
GQPENNYKTTPPVLDSDGSFFLYSKLTVDKSRWQQGNVFSCSVMHEALHNHYTQKSLSLSPGKDPGWSHPQFEKS
RGGGGQVQLQQSGAELARPGASVKMSCKASGYTFTRYTMHWVKQRPGQGLEWIGYINPSRGYTNYNQKFKDKATL
TTDKSSSTAYMQLSSLTSEDSAVYYCARYYDDHYCLDYWGQGTTLTVSSGNSGGGGSGGGGSGGGGSASQIVLTQ
SPAIMSASPGEKVTMTCSASSSVSYMNWYQQKSGTSPKRWIYDTSKLASGVPAHFRGSGSGTSYSLTISGMEAED
AATYYCQQWSSNPFTFGSGTKLEINGNS*

11009.1 - Theoretical pI/Mw monomer: 8.07 / 81035.03 + 1 *N*-glycan (~3 kDa)

pcDNA3.1– SS_{mIgVH}^anti-HER2/neu (*Trastuzumab*) scFv^*GSL*^hIgG1-Fc[ΔADCC/ΔCDC]-StrepTag ^anti-CD28 (9.3) scFv

MYRMQLLSCIALSLALVTNSEVQLVESGGGLVQPGGSLRLSCAASGFNIKDTYIHWVRQAPGKGLEWVARIYPTN
GYTRYADSVKGRFTISADTSKNTAYLQMNSLRAEDTAVYYCSRWGGDGFYAMDYWGQGTLVTVSSGGGGSGGGGS
GGGGSDIQMTQSPSSLSASVGDRVTITCRASQDVNTAVAWYQQKPGKAPKLLIYSASFLYSGVPSRFSGSRSGTD
FTLTISSLQPEDFATYYCQQHYTTPPTFGQGTKVEIKGNSGGGGSGGGGSGGGGSASEPKSSDKTHTCPPCPAPP
AAGPSVFLFPPKPKDTLMISRTPEVTCVVVDVSHEDPEVKFNWYVDGVEVHNAKTKPREEQYNSTYRVVSVLTVL
HQDWLNGKEYKCAVSNKGLASSIEKTISKAKGQPREPQVYTLPPSRDELTKNQVSLTCLVKGFYPSDIAVEWESN
GQPENNYKTTPPVLDSDGSFFLYSKLTVDKSRWQQGNVFSCSVMHEALHNHYTQKSLSLSPGKDPGWSHPQFEKS
SGGGGQVQLQESGPGLVTPSQSLSITCTVSGFSLSDYGVHWVRQSPGQGLEWLGVIWAGGGTNYNSALMSRKSIS
KDNSKSQVFLKMNSLQADDTAVYYCARDKGYSYYYSMDYWGQGTTVTVSSRGGGSGGGGSGGGGSDIELTQSPAS
LAVSLGQRATISCRASESVEYYVTSLMQWYQQKPGQPPKLLIFAASNVESGVPARFSGSGSGTNFSLNIHPVDED
DVAMYFCQQSRKVPYTFGGGTKLEIKR*

CURRICULUM VITAE

Personal Data

Name	Márcia Figueiredo Goncalves
Date of birth	August 6th, 1991
Place of Birth	Quiaios, Portugal
Nationality	Portuguese
Address	Jägerpfad, 13 | 69118 Heidelberg, Germany
Mobile Phone	0173 4927647
email	marciafgoncalves6@gmail.com

Education

July 2016 - present
PhD Immunology
German Cancer Research Center (DKFZ), Heidelberg, Germany

September 2013 - November 2015
MSc Biochemistry for Health
Faculdade de Ciências e Tecnologia, ITQB and NOVA Medical School, Universidade Nova de Lisboa, Portugal

September 2009 - July 2013
BSc Biochemistry
Faculdade de Ciências e Tecnologia, Universidade Nova de Lisboa, Portugal

Research Experience

July 2016 – present
PhD student at German Cancer Research Center (DKFZ), Heidelberg, Germany
Project: Use of bispecific antibodies to improve transendothelial migration of T cells towards tumor cells

September 2014 –April 2015
Master student at Vrije Universiteit Amsterdam / VU, The Netherlands
Project: Understanding how dendritic cell glycans affect antitumor immune responses

April 2015 –September 2015
Master student at CEDOC – NOVA Medical School, Universidade Nova de Lisboa, Portugal
Project: Understanding how dendritic cell glycans affect antitumor immune responses

February 2013 – June 2013
Bachelor student at Grupo de Biologia da Reprodução e células estaminais, Centro de Neurociências e Biologia Celular da Universidade de Coimbra, Portugal.
Project: Estudo de subpopulações de espermatozoides migrados e não migrados

Fellowships

2016/2019

Early-Stage Researcher funded by Marie Skłodwska-Curie Initial Training Network Immunoshape at German Cancer Research Center (DKFZ), Heidelberg, Germany
Project: Use of bispecific antibodies to improve transendothelial migration of T cells towards tumor cells

2014/2015

European Mobility – Erasmus programe (SMT) at Vrije Universiteit Amsterdam / VU, The Netherlands
Project: Understanding how dendritic cell glycans affect antitumor immune responses

Courses

October 2018
Laboratory Animal Science Course (FELASA category B) at Interfacultary Biomedical Faculty (IBF), University of Heidelberg, Germany

November 2016
Cell Culture under perfusion (ibidi system) at ibidi GmbH, Martinsried, Germany

ACKNOWLEDGEMENTS

The first two years and a half of this study were financed by European Union's Horizon 2020 research and innovation program under the Marie Skłodowska-Curie grant agreement No. 642870 (IMMUNOSHAPE Network).

Last but far from least, I want to thank everyone who taught me, encouraged me and supported me on my way.

First of all, I would like to express my profound gratitude to PD Dr. Frank Momburg for giving me the opportunity to be part of his group "Antigen Presentation and T/NK Cell Activation Group" within the Clinical Cooperation Unit "Applied Tumor Immunity" (Head of Department: Prof. Dr. Dirk Jäger) at the German Cancer Research Center (Deutsches Krebsforschungszentrum (DKFZ)), Heidelberg, for the support, trust and patience through all these years, for always believing in me. I am very thankful for all your effort in designing all the protein constructs essential for this project.

Furthermore, I want to express my genuine gratitude to Nadja Bulbuc, who carried out the majority of construct cloning procedures, to Dr. Marten Meyer for his efforts setting up and optimizing the protein production system, to Susanne Knabe, who did the production and purification of all recombinant proteins and BiMAbs and to Karsten Warwas for helping with PBMC preparation and T cell isolation. Likewise, I would like to thank my former student Alina Siebenmorgen, Annkathrin Teschner, who helped to build a productive and pleasant working atmosphere, and my co-supervisor PD Dr. Reinhard Schwartz-Albiez for sharing his knowledge, and to the IMMUNOSHAPE family for sharing such good moments with me. Moreover, a special thank you goes to Nadja for her friendship, support, and love, as well as to Karsten for his friendship, for listening, and always giving me good advice.

I want to express my sincere appreciation to Margareta for everything you did for me. I am very grateful for all your scientific input, support and especially for your unconditional friendship.

My earnest acknowledgment goes to my friends for always encouraging me and contributing to making this journey more effortless, especially Eliana, Joana, Verónica, and Inês.

Finally, my most profound appreciation goes to my family, in particular to my parents, Mário and Beatriz, and my fiancé, Manuel Traveira, for all the motivation, patience, and unconditional support. Without them, everything would have been much harder. Thank you for always believing in me.

EIDESSTATTLICHE VERSICHERUNG

1. Bei der eingereichten Dissertation zu dem Thema **„Use of bispecific antibodies to improve transendothelial migration of T cells towards tumor cells“** handelt es sich um meine eigenständig erbrachte Leistung.

2. Ich habe nur die angegebenen Quellen und Hilfsmittel benutzt und mich keiner unzulässigen Hilfe Dritter bedient. Insbesondere habe ich wörtlich oder sinngemäß aus anderen Werken übernommene Inhalte als solche kenntlich gemacht.

3. Die Arbeit oder Teile davon habe ich bislang nicht an einer Hochschule des In- oder Auslands als Bestandteil einer Prüfungs- oder Qualifikationsleistung vorgelegt.

4. Die Richtigkeit der vorstehenden Erklärungen bestätige ich.

5. Die Bedeutung der eidesstattlichen Versicherung und die strafrechtlichen Folgen einer unrichtigen oder unvollständigen eidesstattlichen Versicherung sind mir bekannt. Ich versichere an Eides statt, dass ich nach bestem Wissen die reine Wahrheit erklärt und nichts verschwiegen habe.